

**FINAL REPORT:  
ASSESSING POST-FIRE RECOVERY OF SAGEBRUSH-STEPPE  
RANGELANDS IN SOUTHEASTERN IDAHO  
(NNX08AO90G)**

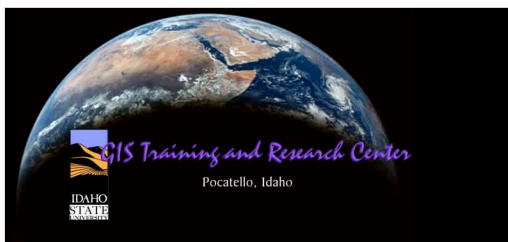
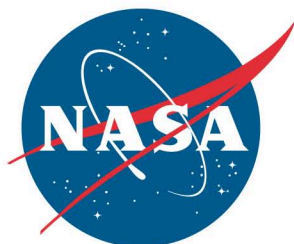
**Keith T. Weber and Kerynn Davis, editors**

**Idaho State University  
GIS Training and Research Center  
921 S. 8th Ave., Stop 8104  
Pocatello, Idaho 83209-8104**

**CD-ROM included!**



- Full-color PDF version of the report.
- GIS data and models.
- Easy HTML directory.



**FINAL REPORT:  
ASSESSING POST-FIRE RECOVERY OF SAGEBRUSH-STEPPE  
RANGELANDS IN SOUTHEASTERN IDAHO (NNX08AO90G)**

---

**Keith T. Weber and Kerynn Davis, editors**

**Contributing Investigators**

Keith T. Weber, Principal Investigator ([webekeit@isu.edu](mailto:webekeit@isu.edu)), Idaho State University, GIS Training and Research Center, 921 S. 8th Ave., stop 8104, Pocatello, ID 83209-8104.

Project web-site: [http://giscenter.isu.edu/research/Techpg/nasa\\_postfire/template.htm](http://giscenter.isu.edu/research/Techpg/nasa_postfire/template.htm)

---

*All rights reserved. No part of this publication may be reproduced, stored in a retrieval system or transmitted, in any form or by any means without the prior permission of the editor.*

#### **ACKNOWLEDGEMENTS**

This study was made possible by a grant from the National Aeronautics and Space Administration Goddard Space Flight Center (NNX08AO90G). ISU would like to acknowledge the Idaho Delegation for their assistance in obtaining this grant.

#### **Recommended citation style:**

Davis, K. and K. T. Weber, 2011. 2009 Rangeland Vegetation Assessment at the O'Neal Ecological Reserve, Idaho. Pages 3-9 in K. T. Weber and K. Davis (Eds.), Final Report: Assessing Post-Fire Recovery of Sagebrush-Steppe Rangelands in Southeastern Idaho (NNX08AO90G). 252pp.

## Table of Contents

Chapter	Title (author)	Page
	<i>Executive Summary</i>	1
1	2009 Rangeland Vegetation Assessment at the O'Neal Ecological Reserve, Idaho (Davis and Weber)	3
2	2009 Range Vegetation Assessment in the Big Desert, Upper Snake River Plain, Idaho (Studley and Weber)	11
3	2010 Rangeland Vegetation Assessment at the O'Neal Ecological Reserve, Idaho (Davis et al.)	21
4	2010 Field Spectrometry Collection of Sagebrush at the O'Neal Ecological Reserve, Idaho (Hanson and Weber)	29
5	Intercalibration and Evaluation of ResourceSat-1 and Landsat-5 NDVI (Anderson et al.)	37
6	Assessing the Susceptibility of Semiarid Rangelands to Wildfires using Terra MODIS and Landsat Thematic Mapper Data (Chen et al.)	47
7	Comparison of MODIS fPAR Products with Landsat-5 TM Derived fPAR over Semiarid Rangelands of Idaho (Chen et al.)	69
8	Herbaceous Biomass Estimation from SPOT-5 Imagery in Semiarid Rangelands of Idaho (Chen et al.)	89
9	NDVI Changes over a Calendar Year in the Rangelands of Southeast Idaho (Tedrow and Weber)	105
10	Diurnal NDVI Fluctuations in Semiarid Rangelands (Weber and Chen)	117
11	Detection Thresholds for Rare, Spectrally Unique Targets within Semiarid Rangelands (Weber and Chen)	129
12	Comparison of Atmospheric Correction Algorithms for Multispectral Satellite Imagery (Weber)	143
13	Comparing Two Ground-Cover Measurement Methodologies for Semiarid Rangelands (Weber et al.)	149
14	Evaluating Land Degradation Indicators in Semiarid Ecosystems Relative to Wildfire (Weber and Chen)	161
15	Comparison of Image Resampling Techniques for Satellite Imagery (Studley and Weber)	185
16	Applying Indigenous Pastoralist Experiences to Western Range Management (Weber and Horst)	197
17	Detecting Dead Shrub Patches Using Remote Sensing Techniques in Southeast Idaho (Hanson and Weber)	211
18	Quantifying Habitat Fragmentation in the Big Desert, Idaho (Hanson and Weber)	235

# ASSESSING POST-FIRE RECOVERY OF SAGEBRUSH STEPPE RANGELANDS IN SOUTHEASTERN IDAHO

## Executive Summary Significant Findings and Achievements

- Two primary objectives were addressed in this study, 1) determine the ability of geospatial technologies to reliably capture and characterize changes in the vegetation community following wildfire and 2) determine if the Big Desert study area in southeast Idaho is moving toward a state of desertification as a consequence of the 2006 Crystal fire disturbance.
- Characterizing changes in the vegetation community following a wildfire disturbance was examined using MODIS, Landsat, and SPOT satellite imagery. In each case specific abilities of each sensor were revealed including the ability of MODIS fPAR data to reliably describe changes in primary productivity within semiarid savanna ecosystems (cf. chapters 6-8).
- Semiarid savanna ecosystems are paradoxical. At first glance the untrained eye may be led to believe the sagebrush-steppe is a stagnant sea of unchanging shrubs. In reality however, these ecosystems exhibit tremendous changes throughout each year and each growing season (cf. chapter 9). Furthermore, the C3 plants found throughout the study area exhibit distinct diurnal patterns of respiration and photosynthesis (cf. chapter 10). A consequence of these research findings have direct implication for primary productivity modeling and suggest current primary productivity values may underestimate actual productivity of semiarid savanna ecosystems.
- Assessing changes in land cover over extended temporal periods requires the use of a correspondingly lengthy dataset. Making valid comparisons across time further requires the use of complimentary datasets. Based upon these statements and suppositions it becomes clear that the Landsat data archive is arguably the most important dataset available to geospatial scientists. However, current Landsat satellites are experiencing difficulties and it is uncertain whether Landsat imagery will remain continuous through the successful launch of Landsat 8 in December of 2012.
- An investigation into the complementary nature of Landsat and ResourceSat --a recommended interim alternative platform-- was conducted as part of this study. Results suggest with proper site-specific intercalibration, ResourceSat could serve adequately as an interim replacement for Landsat (cf. chapter 5).
- The development of a long-term Landsat dataset (1984-2010) was initiated as part of this project. Using data from 2000-2009 an evaluation of various primary productivity indicators was conducted to assess the status of sagebrush-steppe rangelands prior to and following the 250,000 acre Crystal fire of 2006. Specific indicators used in this study include composite-NDVI, rain-use efficiency, water-use efficiency, and local net primary productivity scaling. Results suggest that while primary productivity is *estimated* to be relatively low across the Big Desert, it is also fairly stable when viewed from a long-term, decadal perspective. Results also underscore the importance of using long-term data (10 years longer) for this and other assessments as short-term (2-4 years) snapshots of change could be misleading (cf. chapter 14).

- The detection of landscape or regional land cover change is ultimately tied to fine-scale changes in bare ground, plant community species/structure, and current phenological-status at the time of data capture. Issues related to phenology can be effectively resolved through the use of composite-NDVI, but properly scaling data from plant scale (fine-scale) to landscape scale is very difficult. To address scaling issues we examined the ability of remote sensing technologies to detect various fine-scale landscape features such as small patches of dead shrubs (cf. chapters 4 and 17) and randomly located, rare and spectrally unique targets (cf. chapter 11). Results demonstrate various limitations of current remote sensing capabilities due to mixed pixels and the signal-to-noise ratio of the sensor.
- Eight of the chapters included in this final report have been published (five) or are in review for publication (three) in a peer-reviewed professional journal.
- Five graduate students were supported in whole or in part through this grant (Bhushan Gokhale [cf. chapters 5-8, and 13], Darci Hanson [cf. chapters 3, 4, 17, and 18], Mansoor Raza [cf. chapter 13], Heather Studley [cf. chapters 2 and 15]), and Linda Tedrow [cf. chapter 9]) as well as one undergraduate student (Kerynn Davis [cf. chapters 1 and 3]). Each of these students have completed their studies at Idaho State University and have graduated.

## **2009 Rangeland Vegetation Assessment at the O'Neal Ecological Reserve, Idaho**

Kerynn Davis, Idaho State University. GIS Training and Research Center, 921 S. 8<sup>th</sup> Ave., Stop 8104, Pocatello, ID 83209-8104

Keith T. Weber, GISP. GIS Director, Idaho State University. GIS Training and Research Center, 921 S. 8<sup>th</sup> Ave., Stop 8104, Pocatello, ID 83209-8104. [webekeit@isu.edu](mailto:webekeit@isu.edu)

### **ABSTRACT**

Vegetation data were collected at 30 randomly located sample points during June 2009. Data were collected using both ocular estimation and line-point intercept transects each describing fuel load and percent cover of grasses, forbs, shrubs, litter, microbial crust, bare ground, and weeds respectively. In the SHPG (Simulated Holistic Planned Grazing) grazing treatment of the O'Neal, percent cover of grass (2009=24.66%, 2008=13.84%), forbs (7%, 5.82%), and shrubs (12.33%, 11.1%) increased from 2008. The Rest-Rotation grazing allotment also saw increased percentage cover in grasses (22.66%, 8.96%), forbs (9.16%, 6.34%) and shrubs (13.83%, 11.26%). In the Total Rest grazing allotment, percent cover increased in grasses (28.33%, 12.27%), forbs (10.33%, 4.1%), and weeds (13.6%, 12.33%). Much of the changes observed are likely attributable to the increase in precipitation in 2009 (106.8 mm) relative to 2008 (9.2 mm).

*KEYWORDS: Vegetation, sampling, GIS, remote sensing, GPS, grazing treatment, land management*

## INTRODUCTION

There are many factors that influence land cover changes. Wildfire has been, and will always be, a primary source of broad scale land cover change. In addition, grazing management decisions and practices have also been linked to land cover change. With wildfire or grazing, a change in plant community composition, plant structure, or ecosystem function may result in increases in bare ground and decreases in land productivity. The introduction of non-native vegetation can lead to a degraded system due to the competition placed upon native plant life and the change in plant community composition. An increase in non-native vegetation may reduce the rangeland's ability to support livestock and wildlife, and may reduce its resiliency to larger, catastrophic events. Cheatgrass (*Bromus tectorum*) is an example of a non-native species that has greatly affected rangeland ecosystems throughout the Intermountain West.

This paper describes the vegetation/land cover sampling performed during the summer of 2009 which was performed to support on-going rangeland research at Idaho State University's GIS Training and Research Center (Anderson et al, 2008; Gregory et al., 2008; Russell and Weber, 2003; Sander and Weber, 2004; Tedrow, Davis, and Weber, 2008; Underwood et al, 2008; Weber and McMahan, 2005). In this study, land cover was estimated using line-point intercept transects and these data were used to foster a better understanding of the effect of grazing management practices at the O'Neal Ecological Reserve, with potential application to other semiarid rangelands around the world.

## METHODS

### Study Area

Research at the O'Neal Ecological Reserve is being conducted to A) determine if Simulated Holistic Planned Grazing can be used to effectively decrease bare ground exposure, B) determine if soil moisture changes relative to bare ground exposure and treatment, and C) examine the ecological effects of livestock grazing. The approximate location of the study area is shown below (Figure 1).

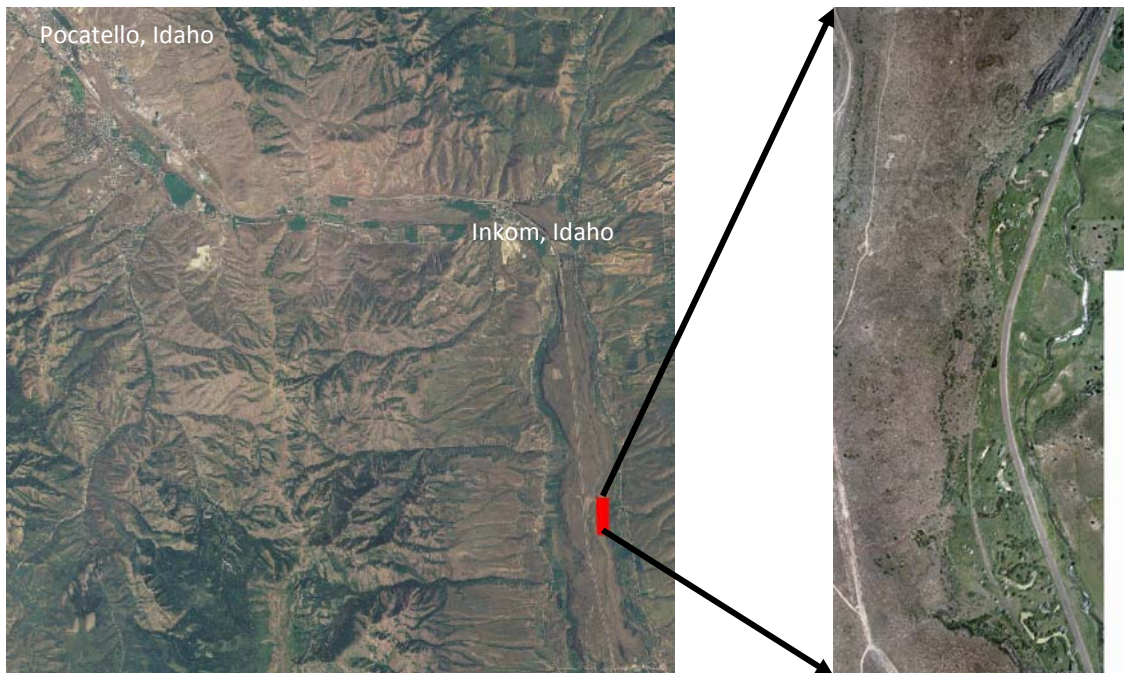


Figure 1. Research study area. The O'Neal Ecological Reserve, represented by red rectangle, is located near McCammon, Idaho.

Three different grazing treatments were sampled; Simulated Planned Holistic Grazing (SHPG), rest-rotation (RESTROT), and total rest (TREST). After comparing several metrics for each of these areas we infer various generalizations which may shed light on relationships between the measured variables and aid range managers in making decisions about prescribed and targeted grazing management.

#### *Field data collection*

Sample points for this study were randomly generated based on criteria determined prior to collecting the data. These criteria include: all points must be 1) >70 meters from an edge (road, trail, or fence line) and 2) <750 meters from a road. There were 30 points generated in total throughout the three O'Neal grazing pastures. The three grazing treatments were: 1) Simulated Holistic Planned Grazing (SHPG) 2) rest-rotation (RESTROT) and 3) total rest (TREST). A new criterion considered for the 2009 study included placing an east or west bearing on each sample point depending on its location in reference to the flight line of a concurrently acquired high-resolution (0.05m) aerial photography mission. If the random sample point was located to the west of the flight line path, then the point would be marked with an E to indicate the transect would be read to the east of the sample point (plot center), in contrast, if the random sample point was located to the east of the flight line path, then the transect would read directly to the west of plot center. This was done to ensure the entire transect would be acquired by the aerial photography mission.

Sample points were navigated to using a Trimble GeoXH GPS receiver. A 20 m flexible tape was laid out on the ground from the starting point (plot center) and in the designated direction (directly east or west) with the aid of a compass. Photographs were taken using a Sony digital camera in each cardinal direction, starting at north and proceeding to photographs viewing east, south, and west. Land cover type was determined by looking straight down at the transect tape and recording the land cover feature in the upper most canopy directly above the designated observation point. Observation points began at 10 cm from the sample point (observation point one) and continued every 20 cm thereafter (observation points 2-100). Land cover at each observation point was classified as either shrub, rock (if the rock was over 7.5 cm in surface diameter), bare soil, invasive weed, grass, forb, litter, standing dead herbaceous material, standing dead woody material (e.g., a dead tree or sagebrush shrub still intact at the ground), or microbial crust. A total of 100 point observations were made and recorded in the GPS-based field form.

The Trimble GeoXH GPS receiver ( $\pm 0.20$  m @ 95% CI after post processing) using latitude-longitude (WGS 84) was used to record the location of each sample point (Serr et al., 2006). Points were occupied until a minimum of 60 points were acquired and WAAS was used whenever available. All points were post-process differentially corrected using a constellation of GPS base stations each located <80km from the study area. This technique used Trimble's H-star technology to achieve improved horizontal positional accuracy. The sample points were projected into Idaho Transverse Mercator NAD 83 using ESRI's ArcGIS 9.3.1 for datum transformation and projection (Gneiting, et al., 2005).

Fuel load was determined by visually estimating the vegetation type and quantity in the immediate vicinity (approximately 20 meters) of the sample point. Anderson's (1982) fuel load classes were used (Table 1).

**Table 1. Fuel load classes used in this study**

Fuel Load Class	(Tons/Acre)	Description
1	0.74	Almost bare ground, very little vegetation
2	1.00	Grasses, some bare ground, few shrubs
3	2.00	Mixture of shrubs and grasses
4	4.00	Predominantly shrubs
5	>6.00	Shrubs to trees

**RESULTS**

Based upon land cover estimates, maximum bare ground was 26%, maximum weed cover was 25%, maximum grass cover was 46%, maximum shrub cover was 33%, and maximum forb cover was 24%.

Each grazing treatment was independently analyzed in order to better understand how land cover responded in relation to each grazing treatments. The mean cover of each cover type were separated by grazing treatment and summarized in Table 2.

**Table 2. Mean cover of each land cover type by grazing treatment (2009).**

Land cover class	Mean cover (%)		
	SHPG ( <i>n</i> =3)	Rest-rotation ( <i>n</i> =24)	Total rest ( <i>n</i> =3)
Bare Ground	15.33	8.12	2.00
Shrub	12.33	13.83	13.00
Grass	24.66	22.66	28.33
Litter	9.33	9.04	7.60
Weed	3.00	8.25	13.60
Forb	7.00	9.16	10.33

Compared to a similar sampling campaign during the summer of 2008 (*n*= 150), 2009 showed a decrease in bare ground and litter across all treatment pastures as well as a decrease in weed cover in both the SHPG and rest-rotation pastures. In contrast, there was an increase in grass and forb cover found across all treatment pastures which is most probably the result of increased precipitation in 2009 relative to that in 2008. In June of 2008 the total rainfall was 9.2 mm with the monthly average at 0.025 mm. This differs greatly from June 2009 which had a total rainfall of 106.8 mm and a daily average of 0.296 mm. Similarly, there was an increase in shrub cover in both the SHPG and rest-rotation pastures as well as an increase in weed cover in the total rest pasture. The latter change may be due to the absence of grazing which in turn may favor the establishment of invasive annual weeds such as cheatgrass (Table 3). It is noted however, that these changes are observations based upon absolute values and not the result of a statistical comparison of inter-annual differences within each pasture. Statistical analyses were not performed as the number of samples was not sufficient.

**Table 3. Mean cover of each land cover type by grazing treatment (2008).**

Land cover class	Mean cover (%)		
	SHPG ( <i>n</i> =50)	Rest-rotation ( <i>n</i> =50)	Total rest ( <i>n</i> =50)
Bare Ground	17.52	10.36	5.47
Shrub	11.1	11.26	13.86
Grass	13.84	8.96	12.27
Litter	18.68	12.14	8.47
Weed	4.5	12.04	12.33
Forb	5.82	6.34	4.10

In 2009, the SHPG was not grazed, which may be a factor explaining the increased grasses and forbs compared to the summer of 2008 when the allotment had been grazed. The RESTROT pasture was grazed in 2009 and 2008, and in this case an increase similar to that found in the SHPG treatment area was observed. This suggests the changes observed in the SHPG pasture is attributable more to the increase in precipitation (environmental effects) than grazing (anthropic effects). The small number of samples in both the SHPG (*n*=3) and TREST (*n*=3) pastures in 2009 compared with the number of samples taken from the RESTROT (*n*=24) pasture could also be a factor affecting the reported results.

### CONCLUSIONS

The results from 2009 field season saw some dramatic changes when compared with the results from 2008. There was an increase in both grass and forb cover classes across all three grazing treatments (Tables 2 and 3). In addition, there was also a decrease in bare ground and litter in each pasture.

Higher percentages of grass cover are very important to provide a healthy environment for both livestock and wildlife and in 2009 there was a substantial increase in grass cover. Each allotment increased from 2008 by an average of 13.5%. The differences observed could be due to more effective grazing treatments, but observational bias as well as environmental factors should be noted as possible influences to changes reported from the previous year. During June of 2009, rain fell consistently at the O'Neal site, resulting in an increase in precipitation from 2008 by 97.6 mm. This is most probably the principle factor in the increased growth of grasses and forbs. However, further comparisons would help to better analyze whether there were any grazing treatments effects as well.

Bare ground decreased by an average of 2.63% while litter decreased by an average of 4.44%. Comparing the 2008 results with the summer of 2007 shows a similar trend of decreasing bare ground and litter. The RESTROT pasture and TREST pasture both exhibited a decrease in bare ground while the SHPG allotment maintained the same average percent bare ground from 2007 to 2008. It should be noted, however, that not as many sample points were taken within the SHPG pasture (*n*=3) and TREST pasture (*n*=3) as compared with the sample size from the RESTROT pasture (*n*=24). This could be a factor affecting the reported results, but the general trend towards a decrease in bare ground suggests an overall improvement. Further sampling and monitoring will more definitively indicate if these trends will continue towards a reduction in bare ground.

## **ACKNOWLEDGEMENTS**

This study was made possible by a grant from the National Aeronautics and Space Administration Goddard Space Flight Center (NNX08AO90G). ISU would like to acknowledge the Idaho Delegation for their assistance in obtaining this grant.

## **LITERATURE CITED**

Anderson, J., J Tibbitts, and K. T. Weber, 2008. Range Vegetation Assessment in the Big Desert, Upper Snake River Plain, Idaho 2007. Pages 16-26 in K.T. Weber (Ed.), Final Report: Impact of Temporal Landcover Changes in Southeastern Idaho Rangelands (NNG05GB05G). 345pp.

Gnieting, P., J. Gregory, and K.T. Weber, 2005. Datum Transforms Involving WGS84. URL = [http://giscenter.isu.edu/research/techpg/nasa\\_tlcc/to\\_pdf/wgs84\\_nad83-27\\_datumtransform.pdf](http://giscenter.isu.edu/research/techpg/nasa_tlcc/to_pdf/wgs84_nad83-27_datumtransform.pdf) visited 7-Dec-2009

Gregory, J., L. Sander, and K. T. Weber, 2008. Range Vegetation Assessment in the Big Desert, Upper Snake River Plain, Idaho 2005. Pages 3-8 in K.T. Weber (Ed.), Final Report: Impact of Temporal Landcover Changes in Southeastern Idaho Rangelands (NNG05GB05G). 345pp.

Russell, G. and K. T. Weber, 2003. Field Collection of Fuel Load, Vegetation Characteristics, and Forage Measurements on Rangelands of the Upper Snake River Plain, ID for Wildfire Fuel and Risk Assessment Models. Pages 4-11 in K. Weber (Ed.), Final Report: Wildfire Effects on Rangeland Ecosystems and Livestock Grazing in Idaho. 209pp. URL = [http://giscenter.isu.edu/research/techpg/nasa\\_wildfire/Final\\_Report/Documents/Chapter1.pdf](http://giscenter.isu.edu/research/techpg/nasa_wildfire/Final_Report/Documents/Chapter1.pdf) visited 7-Dec-2009

Sander L. and K. T. Weber, 2005. Range Vegetation Assessment in the Big Desert, Upper Snake River Plain, Idaho. Pages 85-90 in K. T. Weber (Ed.) Final Report: Detection, Prediction, Impact, and Management of Invasive Plants Using GIS. 196pp. URL = [http://giscenter.isu.edu/Research/techpg/nasa\\_weeds/to\\_pdf/fieldreport\\_2003-2004.pdf](http://giscenter.isu.edu/Research/techpg/nasa_weeds/to_pdf/fieldreport_2003-2004.pdf) visited 7-Dec-2009

Serr, K., T. Windholz, and K.T. Weber, 2006. Comparing GPS Receivers: A Field Study. *Journal of the Urban and Regional Information Systems Association*. 18(2):19-23

Tedrow, L., K. Davis, K.T. Weber, 2008. Range Vegetation Assessment in the Big Desert Upper Snake River Plain, Idaho 2008. Pages 41-50 in K.T. Weber and K. Davis (Eds.), Final Report: Comparing Effects of Management Practices on Rangeland Health with Geospatial Technologies. 170 pp.

Underwood, J., J Tibbitts, and K. T. Weber, 2008. Range Vegetation Assessment in the Big Desert, Upper Snake River Plain, Idaho 2006. Pages 9-15 in K.T. Weber (Ed.), Final Report: Impact of Temporal Land cover Changes in Southeastern Idaho Rangelands (NNG05GB05G). 345pp.

Weber, K. T. and J. B. McMahan. 2003. Field Collection of Fuel Load and Vegetation Characteristics for Wildfire Risk Assessment Modeling: 2002 Field Sampling Report. Pages 12-17 in K. T. Weber (Ed.) Final report: Wildfire Effects on Rangeland Ecosystems and Livestock Grazing in Idaho. 209 pp. URL = [http://giscenter.isu.edu/research/techpg/nasa\\_wildfire/Final\\_Report/Documents/Chapter2.pdf](http://giscenter.isu.edu/research/techpg/nasa_wildfire/Final_Report/Documents/Chapter2.pdf) visited 7-Dec-2009

**Recommended citation style:**

Davis, K. and K. T. Weber, 2011. 2009 Rangeland Vegetation Assessment at the O'Neal Ecological Reserve, Idaho. Pages 3-9 in K. T. Weber and K. Davis (Eds.), Final Report: Assessing Post-Fire Recovery of Sagebrush-Steppe Rangelands in Southeastern Idaho (NNX08AO90G). 252pp.

[THIS PAGE LEFT BLANK INTENTIONALLY]

## **2009 Range Vegetation Assessment in the Big Desert, Upper Snake River Plain, Idaho**

Heather Studley, Idaho State University. GIS Training and Research Center, 921 S. 8th Ave., Stop 8104, Pocatello, ID 83209-8104

Keith T. Weber, GISP. GIS Director, Idaho State University. GIS Training and Research Center, 921 S. 8th Ave., Stop 8104, Pocatello, ID 83209-8104. [webekeit@isu.edu](mailto:webekeit@isu.edu)

### **ABSTRACT**

Vegetation data were collected at 60 randomly located sample points during June 2009. Data were collected using both ocular estimation, line-point intercept transects, and hoop sampling to describe fuel load, percent cover of grasses, forbs, shrubs, litter, microbial crust, bare ground, and weeds, and to assess forage availability. Due to the increased precipitation that fell in 2009, percent bare ground was reduced in comparison to all other years while forage availability increased substantially. Precipitation is the limiting factor in semiarid rangelands and the relationship between forage availability and precipitation was never illustrated better than it was in 2009. Linear regression analysis using precipitation as the independent variable and forage (kg/ha) as the dependent variable resulted in a strong coefficient of determination ( $R^2 = 0.93$ ). Additional data will be collected in subsequent years to continue monitoring the condition of the Big Desert.

*KEYWORDS: vegetation, transects, land cover*

## INTRODUCTION

The study area, known as the Big Desert (Figure 1), is located in southeast Idaho, northwest of the American Falls Reservoir, and bordered on the west by the Craters of the Moon National Monument. The area is managed by the Bureau of Land Management (BLM), with current and historic livestock grazing.

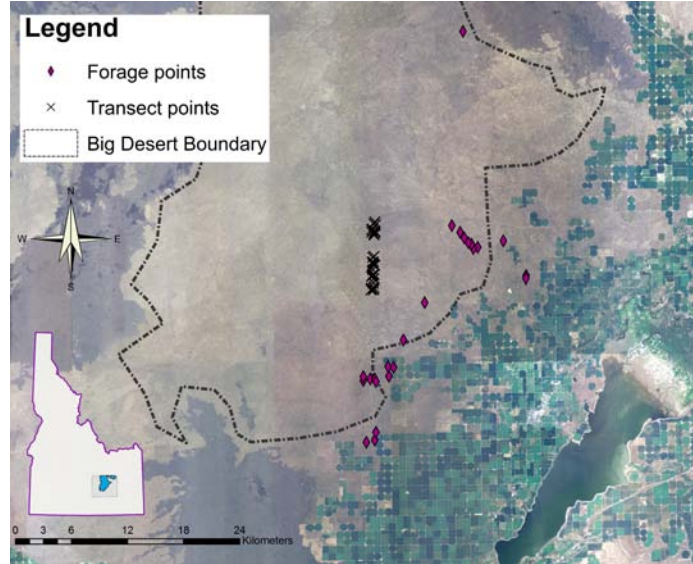


**Figure 1. The Big Desert region of southeastern Idaho. The boundary of the Big Desert is shown, as are the collection points for both forage and land cover sample sites.**

The Big Desert is a semiarid sagebrush-steppe ecosystem, surrounded to the north, south, and east by agricultural lands. The dominant shrub is sagebrush, with big sagebrush (*Artemisia tridentata*) and three-tip sagebrush (*A. tripartita*) being the most common. The herbaceous understory is comprised mostly of a mixture of grasses such as Cheatgrass (*Bromus tectorum*), native grasses, and forbs. Cheatgrass is an invasive weed that contributes to a decreased fire return interval and increased fire severity. Areas dominated by Cheatgrass tend to show decreased species diversity and increased susceptibility to severe soil erosion (Knapp, 1996).

The purpose of data collection at the Big Desert was to support the continued studies of the area (2000 to 2008) for use in the rangeland research program at Idaho State University's GIS Training and Research Center (Anderson et al, 2008; Gregory et al., 2008; Russell and Weber, 2003; Sander and Weber, 2004; Tedrow, Davis, and Weber, 2008; Underwood et al, 2008; Weber and McMahan, 2005). In this study, land cover was estimated using line transects. and forage biomass was measured using hoop sampling.

## MATERIALS AND METHODS

### *Land Cover Estimation*

Thirty random points were generated for line transect data collection using Hawth's Analysis Tools within ArcGIS 9.3.1. Parameters constraining the location of the random points included being 1) within the flight line of a concurrently acquired 0.05 m aerial photography mission (located within WRS path 39 and row 30), 2) at least 70 m from anything that could be defined as an "edge" (fences, roads, permanent trails, etc), and 3) within 750 m of a road to aid in access. Transects were designated as either running to the east or to the west from the plot center point, based upon which side of the flight line each point was

located (e.g., if a random sample point was located to the east of the center of the flight line then the transect would be read directly to the west). This was done to ensure the entire transect would be acquired by the aerial photography mission.

Sample points were navigated to using a Trimble GeoXH GPS receiver. A 20 m flexible tape was laid out on the ground from the starting point and in the designated direction (directly east or west) with the aid of a compass. Photographs were taken using a Sony digital camera in each cardinal direction, starting at north and proceeding to photographs viewing east, south, and west. Land cover type was determined by looking straight down at the transect tape and recording the land cover feature in the upper most canopy and directly above the designated observation point. Observation points began at 10 cm from the sample point (observation point one) and continued every 20 cm thereafter (observation points 2-100). Land cover at each observation point was classified as either shrub, rock (if the rock was over 7.5 cm in surface diameter), bare ground, invasive weed (e.g., Cheatgrass or Canadian thistle (*Cirsium arvense*)), grass, forb, litter, standing dead herbaceous material, standing dead woody material (e.g., a dead tree or sagebrush shrub still intact at the ground), or microbial crust. A total of 100 point observations were made and recorded in the GPS-based field form.

Fuel load was determined by visually estimating the vegetation type and quantity in the immediate vicinity (approximately 20 meters) of the sample point. Anderson’s (1982) fuel load classes were used (Table 1).

**Table 1. Fuel load classes used in this study.**

Fuel Load Class	(Tons/Acre)	Description
1	0.74	Almost bare ground, very little vegetation
2	1.00	Grasses, some bare ground, few shrubs
3	2.00	Mixture of shrubs and grasses
4	4.00	Predominantly shrubs
5	>6.00	Shrubs to trees

*Forage Biomass Estimation*

Forage biomass was estimated at 30 sample points. These data were collected to support an herbaceous biomass study using remotely-sensed imagery. That study required entire pixels (20m x 20m) be covered by herbaceous vegetation and so a directed method of sampling involving travelling across the Big Desert study area to locate suitable collection sites was employed. Sites needed to be at least 20 x 20 meters in size, more than 70 meters from “edges” (roads, fences, powerlines, etc), and with less than 20% shrub cover. Adjacent sites also needed to be located at least 100 meters between site perimeters, with preference given to locations where perimeters were >250 meters apart.

Once a suitable site had been located, a Trimble GeoXH GPS receiver was used to record the approximate perimeter of the site. A location near the center of each site was chosen from which forage biomass data were collected as well as photographs which followed the protocol described above. Forage was measured following methods described by Sheley et al. (1995) and entailed the use of a hoop with a circumference of 2.36 meters (0.44 m<sup>2</sup>) which was randomly tossed into each of four quadrants

(northeast, southeast, southwest, and northwest) from the plot center location. All herbaceous plant material rooted within the hoop was clipped as close to the ground as possible (approximately 6 mm), placed in an ordinary paper bag, and weighed using a Pesola scale (+/- 1g) tared to the weight of the bag. The phenological stage of grasses within each quadrant was noted as either “Before initial growth-boot stage”, “Headed-out boot stage to flowering”, “Seed ripe/leaf tips drying”, “Leaves dry/ stems partly dry”, or “Apparent dormancy” (Sheley et al., 1995). Sample bags were noted with sample ID, date, and quadrant information and retained for further processing.

Forage biomass was dried in an oven for 48 hours at 75° C and re-weighed. The total, dry-weight of forage at each sample point was converted to an estimate of forage expressed in kg/ha by multiplying the forage weight (in grams) by 5.0262 to arrive at an estimate in lbs/acre (note: the value of 5.0262 was derived from Sheley's "AUM Analyzer" software and is considered accurate for grasses in this region and for the phenological stages observed during this sampling period). This value was then converted to kg/ha by multiplying lbs/acre by 1.121 (Equation 1).

$$\text{kg/ha} = 1.121 * (5.0262 * (\text{g})) \quad (\text{Eq. 1})$$

A Trimble GeoXH GPS receiver (+/-0.20 m @ 95% CI after post processing) was used to record the location of each sample point (Serr et al., 2006) in latitude-longitude (WGS 84). Points were occupied until a minimum of 60 positions were acquired and WAAS was used whenever available. All points were post-process differentially corrected using a constellation of GPS base stations each located <80 km from the Big Desert study area. This technique used Trimble's H-star technology to achieve improved horizontal positional accuracy. The sample points were projected into Idaho Transverse Mercator NAD 83 using ESRI's ArcGIS 9.3.1 for datum transformation and projection (Gneiting, et al., 2005).

## RESULTS AND DISCUSSION

### *Land Cover*

Transect data were collected June 23-24, 2009. On average, grass was the most common cover type, being found 22% of the time. Grass was also one of only four cover types to be found at every site; the others being forbs, litter, or patches of bare ground with no cover. Areas of bare ground with no other cover composed about 18% of the area in the Big Desert. Weeds comprised about 16% of the land cover. Shrubs, litter, and forbs were commonly encountered as well. The least common cover type was microbotic crust, which was found to cover an average of 0.2% of the Big Desert study area (Table 2).

**Table 2. Percent cover by cover type. All values are the percent total across all sites (n=30). “Dead herb.” and “Dead wood” refer to standing dead herbaceous material and standing dead wood, respectively. “Missing” refers to the number of times a cover type was not found in any of the transects.**

	Shrub	Bare ground	Weed	Grass	Forb	Rock	Dead herb.	Dead wood	Micro crust	
Min	0	1	0	6	1	0	4	0	0	0
Max	47	37	52	42	30	7	25	6	4	1
Mean	14.5	17.8	16.2	22.0	10.8	1.7	14.4	1.8	0.6	0.2
Missing	4	14	7	0	0	14	0	11	20	25

Land cover data from 2009 were compared with cover data from previous years by cover type. Data for all cover types were not available for all years, so focus was placed on weed, grass, bare ground, and shrub cover types, as data for these cover types were available over the past several years.

Based upon results from 2009 transect data ( $n=30$ ) weed cover has increased since 2002. Data collected from 2002 through 2006 showed that approximately half of the time, weeds contributed < 5% of total cover. In 2007 and 2008, more instances of weeds covering up to 25% of the landscape were reported. In 2009 very few sites had <5% weed cover, and approximately one fifth of the sites had weeds contributing 26-35% of total cover. This suggests that weeds are becoming more common in the Big Desert study area (Figure 2).

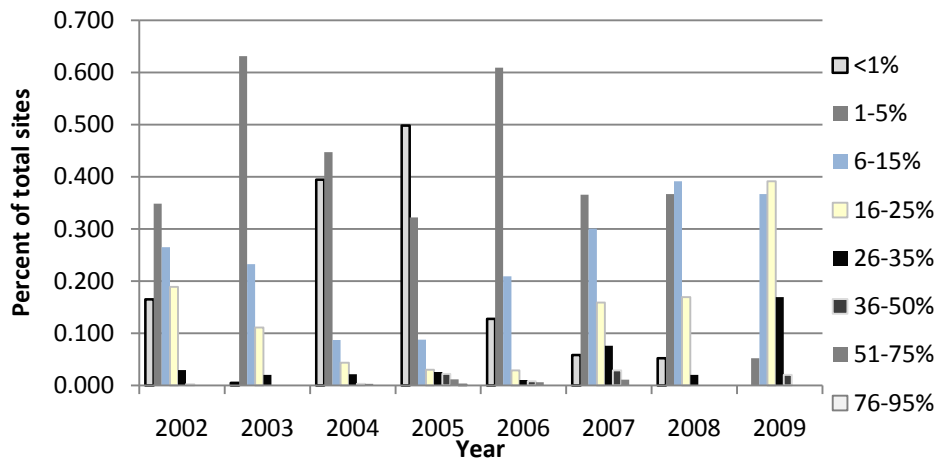


**Figure 2. Percent cover of weeds from 2002 to 2009, divided into percent cover categories to better enable comparison with other years.**

Bare ground was lower in 2009 than in previous years, with most sites having <25% bare ground. In previous years bare ground had contributed 25-75% of total land cover (Figure 3).

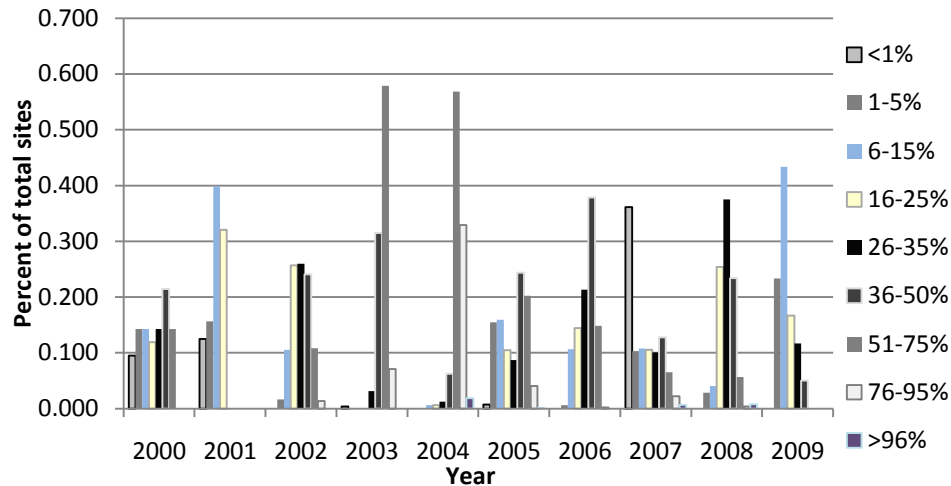


**Figure 3. Percentage of bare ground from 2000 to 2009, divided into percent cover categories to better enable comparison with other years.**

Both grass and shrub cover in 2009 appeared similar to past years, with grass averaging between 6-35% cover and shrubs contributing to 1-25% cover. A slight, negative correlation existed between shrub cover and weed cover, suggesting areas with higher percentages of shrub cover have less weed cover. While the correlation was weak ( $R^2 = 0.525$ ), it is supported by research reported by Anderson and Inouye (2001) from the nearby US DOE Idaho National Laboratory.

### Forage

Forage biomass samples were collected July 1-9, 2009. These data were collected later in the season because unusually heavy June rains made road travel hazardous in the study area. Most sites (60%) found to be suitable for forage collection were dominated by Crested wheatgrass (*Agropyron cristatum*). Most of these sites appeared to have been reclaimed farm land, though some were the result of reseeding following wildfire. One-third of the sites were dominated by Cheatgrass (*Bromus tectorum*) and/or tumbling mustard (*Sisymbrium altissimum*) while only one site was dominated by a native grass, western wheatgrass (*Pascoyprum smithii*).

Average forage weight in 2009 (1386 kg/ha) was very different compared to previous years (Table 3). This may be attributed to a variety of interrelated factors. First, southeast Idaho experienced an unusually high amount of rain in June of 2009. According to the Western Regional Climate Center (WRCC), the total monthly precipitation for June at the Craters of the Moon National Monument was 16.8 cm, almost 10 times the average of the previous eight years (WRCC 2009). Another factor was how forage data was collected in 2009. In previous years, collection points were selected randomly. In 2009, forage sample sites were selected using a directed method with sites selected because they had high percent cover of homogeneous grasses and low percent cover of shrubs. As a result, higher forage weights were anticipated. Finally, forage collections this year included forbs such as tumbling mustard, where as in past years it was principally composed of grasses.

**Table 3. Comparison of mean forage weight (kg/ha) with total precipitation for the month of June by year (note: 2002 was omitted as no forage data was collected for that year).**

Year	Mean Forage Weight (kg/ha)	June Precipitation (cm)
2000	290	0.2
2001	320	0.3
2002	unk	unk
2003	191	0.9
2004	290	2.2
2005	488	3.6
2006	263	1.5
2007	590	2.1
2008	365	2.2
2009	1386	16.8

*Note: Other factors besides precipitation, such as forage collection methodology, may have contributed to the high forage weights collected in 2009.*

When forage weights were compared with June precipitation from 2000 to 2008, only a slight correlation was found to exist ( $R^2 = 0.34$ ) (Figure 4). Based upon this relationship, the actual precipitation recorded for June, 2009 was applied to the linear regression equation derived for the line of best fit ( $y = 67.698x + 239.59$ ). The result of this computation predicted that the forage weight for 2009 would be 1,377 kg/ha, which is very close to the actual weight of 1,386 kg/ha. This relationship illustrates the import role precipitation plays in the vegetation characteristics of semiarid rangelands. The resulting coefficient of determination ( $R^2$ ) for the relationship between precipitation (2000-2009) and mean weight of forage was 0.93.

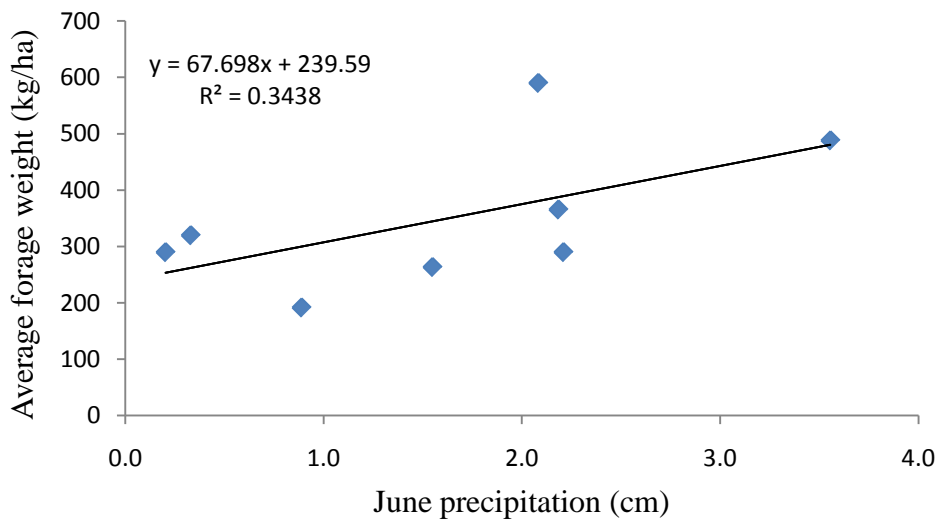


**Figure 4. Comparison of June precipitation (cm) with forage weight (kg/ha) 2000-2008 (2002 was omitted as no forage data were collected in that year).**

## **CONCLUSIONS**

Transect data collected for the Big Desert study area showed that grass was the most common land cover type. Comparisons with previous years' data show an overall increase in weed cover, as well as a decrease in bare ground. A slight negative correlation between shrub cover and weed cover was observed and suggests an area of future research. Most sites used for forage collection were dominated by Crested wheatgrass, although Cheatgrass and tumbling mustards also contributed to overall forage availability in 2009. High June rains may have had an impact on available forage in the Big Desert study area, with weights being the highest recorded since 2000. While changes in forage collection methodology made it difficult to directly compare 2009 results with those collected in the past, a strong relationship ( $R^2 = 0.93$ ) between forage availability (dependent variable) and precipitation (independent, driver variable) was observed and validated, suggesting the primary factor controlling vegetation characteristics in the Big Desert study area is precipitation. This relationship is likely true of all semiarid rangeland ecosystems as similar results have been reported in other studies (Niamir-Fuller and Turner 1999; Gregory et al. 2008).

## **ACKNOWLEDGEMENTS**

This study was made possible by a grant from the National Aeronautics and Space Administration Goddard Space Flight Center (NNX08AO90G). Idaho State University would also like to acknowledge the Idaho Delegation for their assistance in obtaining this grant.

## **LITERATURE CITED**

- Anderson, H. E., 1982. Aids to Determining Fuel Models for Estimating Fire Behavior. USDA For. Serv. Gen. Tech. Rep. INT-122. Ogden, UT
- Anderson, J., and R. Inouye, 2001. Landscape-scale Changes in Plant Species Abundance and Biodiversity of a Sagebrush Steppe over 45 Years. *Ecological Monographs* 71(4): 531-556
- Anderson, J., J. Tibbits, and K. T. Weber, 2008. Range Vegetation Assessment in the Big Desert, Upper Snake River Plain, Idaho 2007. Pages 16-26 in K.T. Weber (ED), Final Report: Impact of Temporal Landcover Changes in Southeastern Idaho Rangelands (NNG05GB05G). 345pp.
- Beyer, H. L. 2004. Hawth's Analysis Tools for ArcGIS. URL = <http://www.spataleecology.com/htools> visited May 2009
- Gnieting, P., J. Gregory, and K. T. Weber, 2005. Datum Transforms Involving WGS84. Idaho State University, GIS Training and Research Center. URL = [http://giscenter.isu.edu/research/techpg/nasa\\_tlcc/to\\_pdf/wgs84\\_nad83-27\\_datumtransform.pdf](http://giscenter.isu.edu/research/techpg/nasa_tlcc/to_pdf/wgs84_nad83-27_datumtransform.pdf) visited October 29, 2008
- Gregory, J., L. Sander, and K. T. Weber, 2008. Range Vegetation Assessment in the Big Desert, Upper Snake River Plain, Idaho 2005. Pages 3-8 in K.T. Weber (ED), Final Report: Impact of Temporal Landcover Changes in Southeastern Idaho Rangelands (NNG05GB05G). 345pp.
- Knapp, P. 1996. Cheatgrass (*Bromus tectorum* L) Dominance in the Great Basin Desert: History, Persistence, and Influences to Human Activities. *Global Environmental Change*. 6(1):37-52

- Niamir-Fuller, M. and M. D. Turner, 1999. A Review of Recent Literature on Pastoralism and Transhumance in Africa. Pages 18-46 in M. Niamir-Fuller (Eds.), Managing Mobility in African Rangelands: The Legitimization of Transhumance. FAO: IT Publications. 314 pp.
- Russell, G. and K. T. Weber, 2003. Field Collection of Fuel Load, Vegetation Characteristics, and Forage Measurements on Rangelands of the Upper Snake River Plain, ID for Wildfire Fuel and Risk Assessment Models. Pages 4-11 in K. Weber (Ed.), Final Report: Wildfire Effects on Rangeland Ecosystems and Livestock Grazing in Idaho. Idaho State University. URL = [http://giscenter.isu.edu/research/techpg/nasa\\_wildfire/template.htm](http://giscenter.isu.edu/research/techpg/nasa_wildfire/template.htm) visited October 29, 2008
- Sander L. and K. T. Weber, 2005. Range Vegetation Assessment in the Big Desert, Upper Snake River Plain, Idaho. GIS Training and Research Center. URL = [http://giscenter.isu.edu/Research/techpg/nasa\\_weeds/to\\_pdf/fieldreport\\_2003-2004.pdf](http://giscenter.isu.edu/Research/techpg/nasa_weeds/to_pdf/fieldreport_2003-2004.pdf) visited October 29, 2008
- Sheley, R., S. Saunders, and S. Henry, 1995. AUM Analyzer: A Tool to Determine Forage and Production and Stocking Rates as a Result of Managing Rangeland Weeds or Making Other Improvements. Montana State University Extension Service, EB 133
- Serr, K., T. Windholz, and K. T. Weber, 2006. Comparing GPS Receivers: A Field Study. Journal of the Urban and Regional Information Systems Association. 18(2):19-23
- Tedrow, L., K. Davis, and K.T. Weber, 2008. Range Vegetation Assessment in the Big Desert Upper Snake River Plain, Idaho 2008. Pages 41-50 in K. T. Weber (Ed.), Final Report: Comparing Effects of Management Practices on Rangeland Health with Geospatial Technologies
- Underwood, J., J Tibbits, and K. T. Weber, 2008. Range Vegetation Assessment in the Big Desert, Upper Snake River Plain, Idaho 2006. Pages 9-15 in K.T. Weber (Ed.), Final Report: Impact of Temporal Landcover Changes in Southeastern Idaho Rangelands (NNG05GB05G). 345pp.
- Weber, K. T. and J. B. McMahan, 2003. Field Collection of Fuel Load and Vegetation Characteristics for Wildfire Risk Assessment Modeling: 2002 Field Sampling Report. In: K. T. Weber [Ed.]. Final report: Wildfire Effects on Rangeland Ecosystems and Livestock Grazing in Idaho. 209 p. URL = [http://giscenter.isu.edu/research/techpg/nasa\\_wildfire/Final\\_Report/Documents/Chapter2.pdf](http://giscenter.isu.edu/research/techpg/nasa_wildfire/Final_Report/Documents/Chapter2.pdf) visited October 29, 2008
- Western Regional Climate Center (WRCC). 2009. URL = <http://www.wrcc.dri.edu/cgi-bin/cliMONtpre.pl?id2260> visited September 3, 2009

**Recommended Citation Style:**

Studley, H. and K. T. Weber, 2011. 2009 Range Vegetation Assessment in the Big Desert, Upper Snake River Plain, Idaho. Pages 11-20 in K. T. Weber and K. Davis (Eds.), Final Report: Assessing Post-Fire Recovery of Sagebrush-Steppe Rangelands in Southeastern Idaho (NNX08AO90G). 252 pp.

[THIS PAGE LEFT BLANK INTENTIONALLY]

## **2010 Rangeland Vegetation Assessment at the O'Neal Ecological Reserve, Idaho**

Kerynn Davis, Idaho State University. GIS Training and Research Center, 921 S. 8<sup>th</sup> Ave., Stop 8104, Pocatello, ID 83209-8104

Keith T. Weber, GISP Director, Idaho State University. GIS Training and Research Center, 921 S. 8<sup>th</sup> Ave., Stop 8104, Pocatello, ID 83209-8104 [webekeit@isu.edu](mailto:webekeit@isu.edu)

Darci Hanson, Idaho State University. GIS Training and Research Center, 921 S. 8th Ave., Stop 8104, Pocatello, ID 83209-8104

### **ABSTRACT**

To better understand long term post-fire effects in sagebrush steppe ecosystems, vegetation data were collected and analyzed during the months of June and July, 2010. The study was conducted at the O'Neal Ecological Reserve in southeast Idaho on rangelands managed under rest-rotation grazing. Twig samples of both dead and live sagebrush were collected as part of this study to investigate subsequent areas of sagebrush die-off. Twig wet weights were acquired on-site, and again after the twig samples had been dried. Results showed a large difference between the wet and dry weights of the live sagebrush ( $n = 10.4\text{g}$ ) while samples from dead shrubs did not show a significant difference between wet and dry weights ( $n = 0.6\text{ g}$ ). Data describing the state of sagebrush plants were collected using ocular estimation (live or dead). In addition, the stem diameter of sagebrush plants was collected to estimate plant age. Average age estimations were used to compare the recovery rate of sagebrush following a 1992 wildfire. The average age of sagebrush plants within the fire perimeter ( $n = 78$ ) was compared to the age of plants outside the fire perimeter ( $n = 370$ ). Mean sagebrush age showed no difference between these areas (17.8 and 17.7 within the fire perimeter and outside the fire perimeter, respectively) indicating the sagebrush-steppe ecosystem of the O'Neal Ecological Reserve effectively shows no indications of the 18 year-old fire in the age stratification of sagebrush plants. This result concurs with observations from other studies suggesting sagebrush steppe rangelands often return to a pre-fire condition within 6-10 years of the disturbance.

*KEYWORDS: Age estimation, sampling, GIS, remote sensing, GPS, grazing treatment, land management*

## INTRODUCTION

There are many factors that influence land cover change. Wildfire has been, and will always be, a primary source of broad scale land cover change. In addition, grazing management decisions and practices have also been linked to land cover change. With wildfire or grazing, a change in plant community composition, plant structure, or ecosystem function may result in increases in bare ground and decreases in land productivity. The introduction of non-native vegetation can also lead to a degraded or disturbed system due to the competition placed upon native plant life and the change in plant community composition.

This paper describes the vegetation/land cover sampling performed during the summer of 2010 to support on-going rangeland research at Idaho State University's GIS Training and Research Center (Anderson et al, 2008; Gregory et al., 2008; Russell and Weber, 2003; Sander and Weber, 2004; Tedrow, Davis, and Weber 2008; Underwood et al, 2008; Weber and McMahan, 2005). Research was conducted using random and directed sampling techniques to collect various sagebrush plant characteristics including twig weight, plant height, and plant age. These data were used to foster a better understanding of the effect of an 18 year-old fire (1992) at the O'Neal Ecological Reserve (Figure 1) with potential application to other semiarid rangelands around the world.



**Figure 1. The focus of this study, the O'Neal Ecological Reserve, is located in eastern Idaho, just south of Pocatello.**

## **METHODS**

### *Study Area*

Research at the O'Neal Ecological Reserve was conducted to determine long-term post-fire effects upon the sagebrush shrub community. The majority of the study area is actively grazed in the early summer (May), however the stocking density is very low (6 AUD ha<sup>-1</sup>). In 2010, two treatments were sampled; rest-rotation grazing (RESTROT) and total rest (TREST). After comparing several metrics from each of these areas we made various inferences which may shed light upon relationships between the measured variables and thereby aid range managers in making decisions about long term post-fire management as well as prescribed/ targeted grazing.

### *Field Data Collection*

Two sampling sessions were completed during the summer of 2010. The first session, consisted of randomly located sample points based on criteria determined prior to data collection and following protocols described at [http://giscenter.isu.edu/research/Techpg/nasa\\_postfire/results.htm](http://giscenter.isu.edu/research/Techpg/nasa_postfire/results.htm). This criteria ensured that all points were 10 meters from an edge (road, trail, or fence line). There were 60 random points generated throughout the O'Neal study area,

These sample points were navigated to using a Trimble GeoXH GPS receiver (< 1.0 m @ 95% CI). This point was considered plot center. Photographs were taken using a Sony digital camera in each cardinal direction, starting with a view to the north and proceeding to photograph the eastern, southern, and western horizons. The site was then classified as being representative of a homogeneous live-sagebrush stand or a homogeneous dead-shrub stand. This was determined by predetermined standards for homogeneity based on the Data Collection Protocol. If the site was considered a dead-shrub stand, then the spatial extent of the homogeneous area was determined using a tape measurements to accurately determine the corresponding homogeneous pixel size, for example if the area was approximately 30 m x 30 m or larger in size, it was considered consistent with a Landsat 5 TM pixel. Similarly, sites could be classified as consistent with SPOT 5 (10 m x10 m or larger), or Quickbird/Worldview2 (2 m x 2 m or larger) (Hanson, 2010). The largest area of homogeneous consistency was recorded for each site. In addition, sagebrush twig samples were clipped from up to four sagebrush plants at each site and weighed using a Pesola scale (+/- 1 g). Selected twigs were approximately 5 mm in diameter and approximately 250 mm in length. A total of 30 live-sagebrush twig samples were taken as well as 30 dead-shrub twig samples. These samples were placed in a bag, labeled with a unique ID consisting of the sample point ID, date, and sequence (1-4) and returned to the laboratory for further analysis.

Maximum stem diameter of sagebrush plants were measured and recorded to estimate sagebrush age. A maximum of four samples were collected at each sample site with one taken from the nearest sagebrush plant in each quadrant (NE, SE, SW, and SE) arranged over plot center. Sagebrush age was estimated by measuring the maximum basal stem diameter using calipers. Sagebrush age was estimated following Perryman and Olson (2000) and Narsavage and Weber (2002) (equation 1).

$$\text{Age} = 6.1003 + 0.5769(\text{diameter}) \quad (\text{Eq. 1})$$

An insufficient number of dead sagebrush sites were found during the initial sampling session ( $n = 13$ ) and as a result, a directed sampling approach was used in the second sampling session. The directed

sampling approach is one where field personnel use their knowledge of the study area to locate additional sample sites. While this approach introduced a bias into the sample dataset it was effective for locating uncommon targets such as homogeneous stands of dead shrubs. When a new site was located, the same sampling protocol as described above was followed. The goal of the field collection campaign was to collect a minimum of 60 live- and 60 dead-sagebrush sites, each of which was homogeneous at one of the following spatial scales: 5 m<sup>2</sup>, 100 m<sup>2</sup>, or 1000 m<sup>2</sup>. These spatial scales are equivalent to imagery collected by the WorldView2/Quickbird, SPOT 5, and Landsat satellites, respectively.

*Laboratory and Statistical Analysis*

All sagebrush twig samples ( $n = 60$ ) were oven-dried at 75° C for 48 hours and re-weighed. These data were recorded in a MS Excel spreadsheet along with the wet-weight of each individual twig. Percent water content was then calculated and analysis of variance (ANOVA) used to determine if a difference existed in moisture content of live- and dead-sagebrush plants.

**RESULTS**

A total of 119 sample sites were collected in this study. Twenty of these samples were located within the 1992 fire perimeter of the O’Neal Study Area and 99 were located outside of the fire perimeter. A maximum of four sagebrush stem diameter measurements were taken at each site to calculate sagebrush ages ( $n = 78$  and 370, respectively). Based upon sagebrush diameter measurements the mean age of all plants was 17.8 years. The oldest sagebrush plant recorded was located outside the 1992 fire perimeter and was 50.5 years while the youngest sagebrush plant recorded (7.8 years) was located within the 1992 fire perimeter (Table 1).

**Table 1. Sagebrush age estimates at the O’Neal Ecological Reserve based upon 2010 field sampling relative to the 1992 wildfire.**

	Within fire perimeter	Outside fire perimeter
<i>n</i>	78	370
Minimum age	7.8	8.4
Maximum age	41.8	50.5
Mean age	17.8	17.7

The mean age of sagebrush plants within the fire area did not differ greatly from mean sagebrush age outside the fire area ( $P = 0.048$ ;  $P_{critical} = 0.01$ ). The distribution of sagebrush plant age was concentrated largely among plants 10-20 years old both within the 1992 fire areas (Figure 2) and outside the fire area (Figure 3).

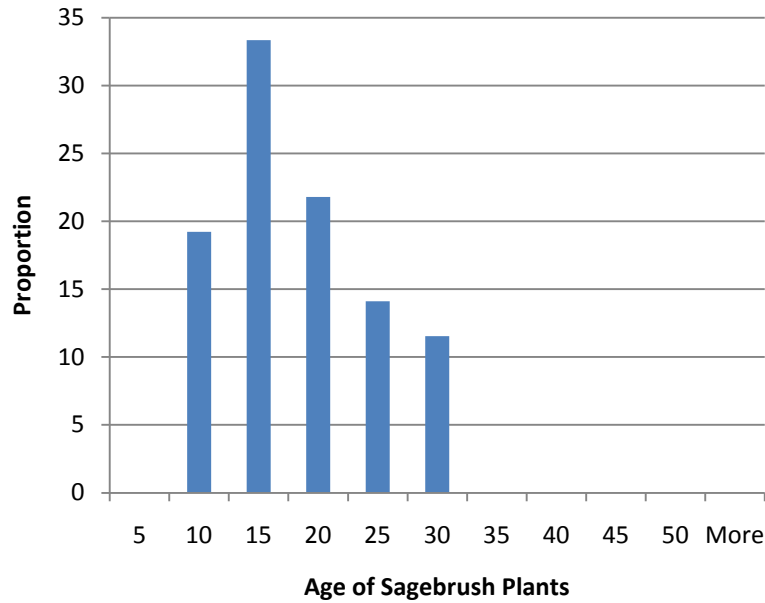


Figure 2. Age distribution of sagebrush plants within the 1992 wildfire area.

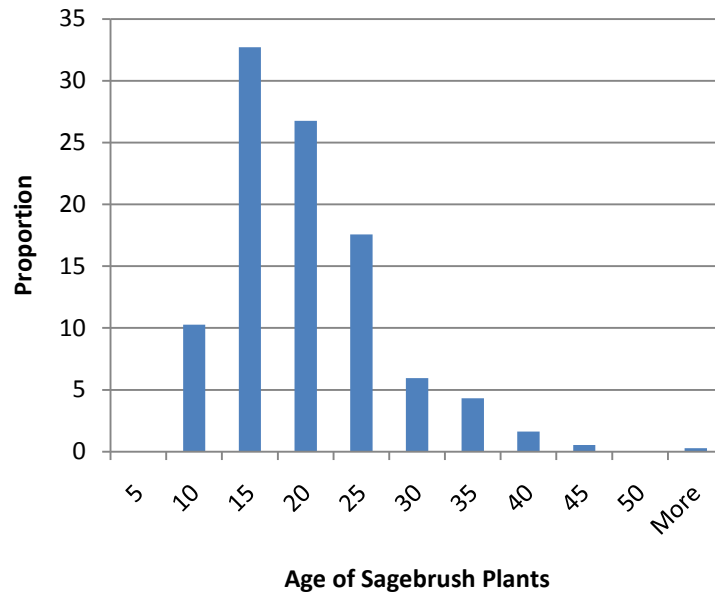


Figure 3. Age distribution of sagebrush plants outside the 1992 wildfire area.

Results of twig weight analysis showed a substantial difference between wet and dry weights of live sagebrush twig samples (Figure 4), but only a minor difference between wet and dry weights from dead shrub twig samples (Figure 5). Results of single-factor ANOVA tests indicate the wet weights between the two twig type groups (live and dead samples) were significantly different ( $P < 0.001$ ) as were the dry weight comparison between the two twig type groups ( $P < 0.001$ ). The results also showed a large difference between the average wet and dry weights of live sagebrush twigs ( $n = 10.4$  g) while dead shrub twig samples did not show a difference in mean weight ( $n = 0.6$  g).

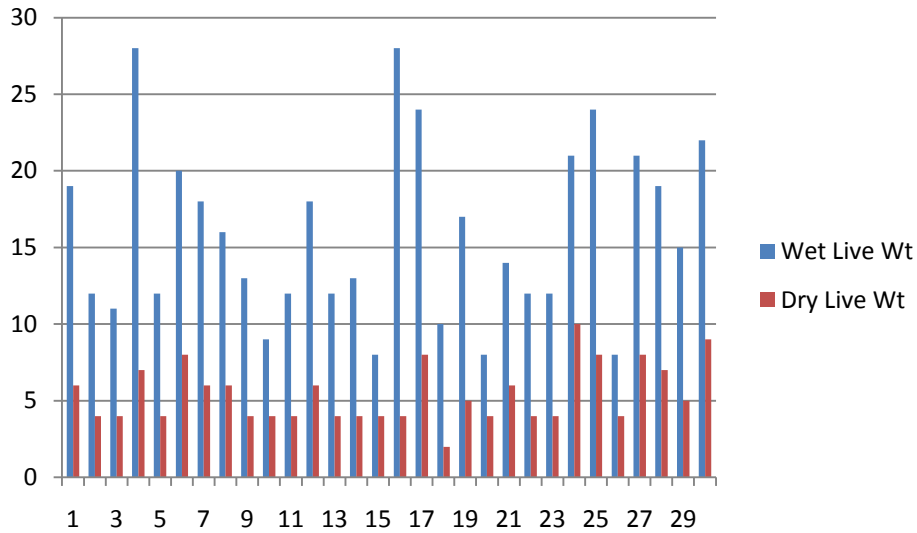


Figure 4. Comparison of wet and dry weights of live sagebrush twig samples (grams).

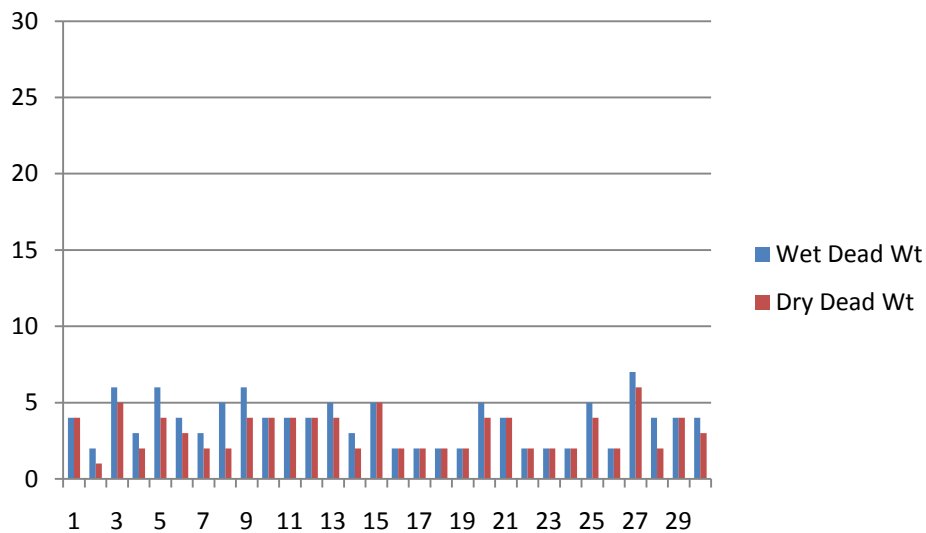


Figure 5. Comparison of wet and dry weights of dead sagebrush represented in grams.

### CONCLUSIONS

The results from the 2010 field season revealed no appreciable difference in sagebrush plant age within and outside the 1992 fire area. In essence it appears that after 18 years, the rangeland ecosystem has recovered to pre-fire conditions save for the absence of some old individual plants. Sagebrush twig weight analysis indicated a significant difference between live and dead shrub twig weights which is likely attributable to a much higher water-content present in the live sagebrush plants. This physical difference between living and dead sagebrush plants may provide a potential to differentiate stands of living and dead sagebrush plants by leveraging the water-sensitive short wave infrared portions satellite sensors like Landsat and SPOT5. Additional research is required to determine if this potential can be fulfilled.

## **ACKNOWLEDGMENTS**

This study was made possible by a grant from the National Aeronautics and Space Administration Goddard Space Flight Center (NNX08AO90G). ISU would like to acknowledge the Idaho Delegation for their assistance in obtaining this grant.

## **LITERATURE CITED**

- Anderson, J., J. Tibbits, and K.T. Weber, 2008. Range Vegetation Assessment in the Big Desert, Upper Snake River Plain, Idaho 2007. Pages 16-26 in K.T. Weber (Ed.), Final Report: Impact of Temporal Landcover Changes in Southeastern Idaho Rangelands (NNG05GB05G). 345 pp.
- Davis, K. and K.T. Weber, 2009. Rangeland Vegetation Assessment at the O'Neal Ecological Reserve, Idaho. Pages 41-48 in K.T. Weber (Ed.), Final Report: Forecasting Rangeland Condition with GIS in Southeastern Idaho (NNG06GD82G). 189pp.
- Gnieting, P., J. Gregory, and K.T. Weber, 2005. Datum Transforms Involving WGS84. URL = [http://giscenter.isu.edu/research/techpg/nasa\\_tlcc/template.htm](http://giscenter.isu.edu/research/techpg/nasa_tlcc/template.htm)
- Grazing in Idaho. Chapter 1. Pp. 4-11. Idaho State University. URL = [http://giscenter.isu.edu/research/techpg/nasa\\_wildfire/template.htm](http://giscenter.isu.edu/research/techpg/nasa_wildfire/template.htm) visited October 29, 2008
- Gregory, J., L. Sander, and K.T. Weber, 2008. Range Vegetation Assessment in the Big Desert, Upper Snake River Plain, Idaho, 2005. Pages 3-8 in K.T. Weber (Ed.), Final Report: Impact of Temporal Landcover Changes in Southeastern Idaho Rangelands (NNG05GB05G). 345 pp.
- Hanson, Darci, 2010. Data Collection Protocol: Dead and Live Sagebrush. 3pp.
- Narsavage, D. and K.T. Weber, 2002. Sagebrush Age Estimation in the Upper Snake River Plain, Idaho. URL = [http://giscenter.isu.edu/research/techpg/nasa\\_wildfire/Final\\_Report/Documents/Chapter5.pdf](http://giscenter.isu.edu/research/techpg/nasa_wildfire/Final_Report/Documents/Chapter5.pdf) visited August 16, 2010
- Perryman, B.L., and R.A. Olson, 2000. Age-Stem Diameter Relationships of Big Sagebrush and their Management Implications. *J Range Management*. 53: 342-346
- Russell, G. and K.T. Weber, 2003. Field Collection of Fuel Load, Vegetation Characteristics, and Forage Measurements on Rangelands of the Upper Snake River Plain, ID for Wildfire Fuel and Risk Assessment Models. In K.T. Weber (Ed.), Final Report: Wildfire Effects on Rangeland Ecosystems and Livestock
- Sander, L. and K.T. Weber, 2005. Range Vegetation Assessment in the Big Desert, Upper Snake River Plain, Idaho. GIS Training and Research Center. URL = [http://giscenter.isu.edu/Research/techpg/nasa\\_weeds/to\\_pdf/fieldreport\\_2003-2004.pdf](http://giscenter.isu.edu/Research/techpg/nasa_weeds/to_pdf/fieldreport_2003-2004.pdf) visited October 29, 2008
- Serr, K., T. Windholz, and K.T. Weber, 2006. Comparing GPS Receivers: A Field Study. *Journal of the Urban and Regional Information Systems Association*. 18(2): 19-23

Tedrow, L., K. Davis, K.T. Weber, 2008. Range Vegetation Assessment in the Big Desert, Upper Snake River Plain, Idaho 2008. Pages 41-50 in K.T. Weber (ED), Final Report: Comparing Effects of Management Practices on Rangeland Health with Geospatial Technologies

Underwood, J., J. Tibbits, and K.T. Weber, 2008. Range Vegetation Assessment in the Big Desert, Upper Snake River Plain, Idaho 2006. Pages 9-15 in K.T. Weber (ED), Final Report: Impact of Temporal Landcover Changes in Southeastern Idaho Rangelands (NNG05GB05G). 345pp.

Weber, K.T. and J.B. McMahan, 2003. Field Collection of Fuel Load and Vegetation Characteristics for Wildfire Risk Assessment Modeling: 2002 Field Sampling Report. In: K.T. Weber (ED). Final Report: Wildfire Effects on Rangeland Ecosystems and Livestock Grazing in Idaho. 209 pp. URL = [http://giscenter.isu.edu/research/techpg/nasa\\_wildfire/Final\\_Report/Documents/Chapter2.pdf](http://giscenter.isu.edu/research/techpg/nasa_wildfire/Final_Report/Documents/Chapter2.pdf) visited October 29, 2008

**Recommended Citation Style:**

Davis, K., K. T. Weber, and D. Hanson, 2011. 2010 Rangeland Vegetation Assessment at the O'Neal Ecological Reserve, Idaho. Pages 21-28 in K. T. Weber and K. Davis (Eds.), Final Report: Assessing Post-Fire Recovery of Sagebrush-Steppe Rangelands in Southeastern Idaho (NNX08AO90G). 252 pp.

## **2010 Field Spectrometry Collection of Sagebrush at the O’Neal Ecological Reserve, Idaho**

Darci Hanson, GIS Training and Research Center, Idaho State University, Pocatello, ID 83209-8104, (<http://giscenter.isu.edu>, e-mail: [giscenter@isu.edu](mailto:giscenter@isu.edu))

Keith T. Weber, GISP. GIS Director, Idaho State University. GIS Training and Research Center, 921 S. 8<sup>th</sup> Ave., Stop 8104, Pocatello, ID 83209-8104. [webekeit@isu.edu](mailto:webekeit@isu.edu)

### **ABSTRACT**

The spectral reflectance of a ground target can be greatly influenced by atmospheric conditions and airborne particles before reaching a satellite-based sensor. For this reason, compiling a spectral library characterizing target spectra can be useful in later classification of remotely sensed imagery. Spectral data were collected for five ground target classes (basalt, bare ground, grass, dead-shrub, and live-sagebrush) during July, 2010 ( $n = 2,565$ ). Data were collected using an Analytical Spectral Devices, Inc. (ASD) FieldSpec® Pro Spectroradiometer and imported into Microsoft Excel for further processing. Spectra were sorted by target type and wavelength. Descriptive statistics were calculated, and mean spectral reflectance values for each target were used to calculate a pairwise single-factor Analysis of Variance (ANOVA) comparing the spectra of dead shrubs to each of the other four targets types to determine if dead woody shrubs could be differentiate from the matrix of other rangeland features (e.g., basalt, bare ground, grass, and live-sagebrush). In each case a statistical difference was observed ( $P < 0.001$ ) between pairwise samples suggesting further differentiation with satellite sensors may be possible. Calculated variability of spectra within each target type is narrow providing additional supporting evidence that differentiation is possible.

*KEYWORDS: Sagebrush, sampling, GIS, remote sensing, field spectroscopy, shrub die-off, spectroradiometer*

## INTRODUCTION

Sage Grouse (*Centrocercus urophasianus*) are a sagebrush-obligate species requiring large, contiguous expanses of habitat. While the quantity or area of available habitat is important, so too is the quality of the available habitat. Recent land cover maps typically describe sagebrush dominated areas and treat all these areas as viable Sage Grouse habitat. However, large areas of dead sagebrush sometimes occur which may lead to an overestimation of total habitat available to the Sage Grouse. Sagebrush (shrub) die-off in semiarid rangelands was a widespread phenomenon in the salt-desert region of Utah between 1983 and 1988 due to extremely wet seasons (Wallace et al., 1989). Though this phenomenon is known to occur throughout the semiarid sagebrush-steppe, published reports pertaining to this phenomenon in southeast Idaho is limited. Shrub die-off affects the quality of Sage Grouse habitat as it impacts their primary food source and a source of shelter. The ability to differentiate dead shrubs from other ground cover targets with remotely sensed satellite imagery would allow land managers to better assess the quality of Sage Grouse habitat across their range.

Aside from monitoring Sage Grouse habitat however, positive identification of dead shrub during image classification would provide new insight into the capabilities of remote sensing technologies. This study determined whether stands of dead shrubs can be accurately delineated using geospatial technologies beginning with the characterization of target spectra in the field.

Field spectrometry is the quantitative measurement of radiance, irradiance, reflectance or transmission in the field (Curtiss and Goetz, 1994). Field spectroradiometers have a wide range of useful applications from aiding understanding of how an object of interest (i.e., target) might be detected using remote sensing, to collecting data that will serve as a spectral library for more precise image analysis and interpretation.

Atmospheric scattering and the signal to noise ratio (SNR) of a sensor can interrupt or alter spectral reflectance of a target. Scattering occurs when reflected light strikes other particles in the atmosphere before reaching the satellite sensor. The type of scattering (Rayleigh, Mie, or Nonselective) is dependent upon the size of particles in the atmosphere, their abundance, the wavelength of the reflected light, and the depth of the atmosphere through which the energy is traveling (Campbell, 2008). Rayleigh scattering is attributed to atmospheric gas molecules and cause visible effects such as a blue sky. Mie scattering occurs when particles have diameters that are roughly equivalent to the wavelength of the scattered radiation, and is experienced primarily in the lower atmosphere through larger particles such as dust or pollen. Nonselective scattering accounts for what we observe as a whitish haze in the atmosphere, and refers to scattering that occurs from particles larger than the wavelength of the scattered light (Campbell, 2008). The SNR of a particular sensor can also influence the ability to discriminate field targets. The signal refers to differences in image brightness caused by actual variations in scene brightness whereas noise refers to variations unrelated to scene brightness, and more with errors inherent in the sensor itself. If the magnitude of noise is large relative to the signal, resulting imagery image will not provide a reliable representation of the target of interest (Campbell, 2008). For this study, *in situ* spectra were collected from five target types (basalt, bare ground, grass, dead shrub, and live sagebrush) to produce a spectral reference library of ground cover types throughout the O'Neal study area in southeast Idaho. These data were analyzed to determine feasibility of target differentiation between dead shrubs and the matrix of other sagebrush-steppe plants and landscape features present at the study area.

## METHODS

### Study area

The O'Neal Ecological Reserve (Figure 1) is located along the Portneuf River, approximately 30 km southeast of Pocatello, Idaho (42° 42' 25"N, 112° 13' 0" W). The O'Neal receives <0.38 m of precipitation annually with nearly 50 percent falling as snow in the winter months (October 1- March 31). An average of 0.15 m (SE = 55.4) of rainfall occurs during the growing season (April 1 – September 31). The topography is relatively flat with a mean elevation of approximately 1426 m (1400-1440 m).

The site is characterized by shallow, well drained soils over basalt flows originally formed from weathered basalt, loess, and silty alluvium that remain homogenous throughout the site (USDA NRCS 1987; Weber and Gokhale 2010). Dominant plant species include big sagebrush (*Artemisia tridentata*) with various native and non-native grasses, including Indian rice grass (*Oryzopsis hymenoides*) and needle-and-thread (***Hesperostipa comata***) (Weber et al. 2010). The O'Neal is managed by Idaho State University (ISU) while land immediately surrounding it is managed by the USDI BLM. This area has a history of rest-rotation cattle grazing (> 20 years) at low stocking rates (300 AU/ 1467 ha [6 AUD ha<sup>-1</sup>]). Prior to ISU management, no fences existed to restrict movement of cattle from the adjacent USDI BLM grazing allotment to the O'Neal study area. In 2005, the site was fenced providing areas of grazing and total rest. The last fire to occur within the O'Neal was in 1992.

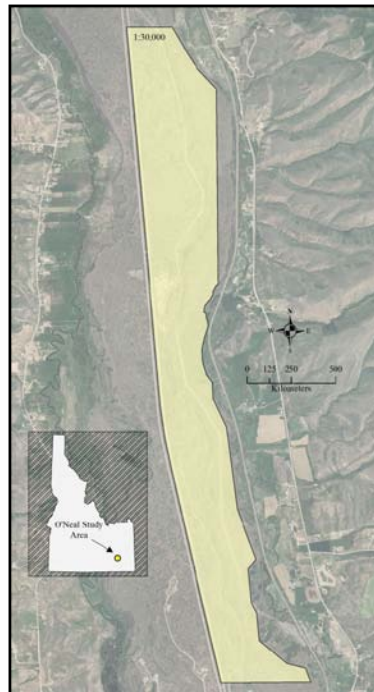


**Figure 1. Research study area: The O'Neal Ecological Reserve, represented by the polygon, is located near McCammon, Idaho.**

### Field Spectroradiometer

An ASD FieldSpec® Pro Spectroradiometer was used to collect target spectra in the field. The FieldSpec Pro model was used to record relative spectral reflectance at wavelengths ranging from 350 - 2500nm.

Spectral irradiance for targets was collected using a bare fiber optic sensor and then converted from raw digital number (DN) to relative reflectance values using ViewSpec®Pro software.

### *Field Sampling*

Thirty sample sites were visited for each of five target categories (basalt, bare ground, grass, dead shrub, and live sagebrush) representing the primary ground cover types found at the O'Neal study area. Directed sampling was used to locate representative targets and capture the variability in reflectance of these targets.

All spectra were collected  $\pm$  1 hour of solar noon from 9 July 2010 to 12 July 2010. A calibrated diffuse white reference panel was used to optimize the sensor to sky/weather conditions on each day of the collection. The pistol grip fiber optic cable sensor attached to the ASD was pointed approximately at nadir above targets at a distance of approximately 60 cm. The bare fiber optic cable used represented a field of view (FOV) of 60 cm. When nadir perspective was inaccessible (such as when we approached shrubs or rock faces that exceeded our own height), the sensor was pointed toward targets at an angle, however this angle never exceeded 90° from nadir. At each site, a minimum of 15 spectra were collected consecutively resulting in a total of 2565 spectra collected (a minimum of 450 spectra per target class). Data were downloaded and processed at ISU's GIS Center using Microsoft Excel to sort reflectance data according to target type and wavelength.

### *Analysis of Spectra*

Spikes in reflectance associated with atmospheric water absorption bands were removed from all further analysis of target reflectance. Absorption bands included wavelengths from 1300nm to 1550nm, 1750nm to 2080nm, and from 2350nm to 2500nm. Descriptive statistics were calculated for each target type describing mean reflectance and standard deviation among samples. Mean reflectance for each target were plotted on a line graph along with the variability in spectra (mean  $\pm$  2 S.E.) and used to interpret the spectra for potential differentiation.

### *Statistical Analysis*

To determine if differences exist between dead shrub and the other target spectra, pairwise single-factor ANOVA tests were used. The ANOVA is a statistical test which compares varying observations and describes how much the observations differ from the sample mean. Variability (@ 95% CI) within each target spectra was calculated by multiplying the standard error of each target spectra by 1.96 (or the z-score for a 95% confidence interval). These values were then applied to the calculated mean of each target type at each wavelength and plotted on a line graph. Targets were considered differentiable when separated by  $>$  1.96 standard errors.

## **RESULTS AND DISCUSSION**

Approximately 500 spectra were collected for each target type (bare soil [ $n = 525$ ], basalt [ $n = 525$ ], grass [ $n = 525$ ], live sagebrush [ $n = 495$ ], and dead shrub [ $n = 495$ ]). Using visual analysis of the spectra (Figure 2), it seems that wavelengths having the greatest potential for differentiation of dead shrubs from other target types occur between 700 and 2500nm. These observations suggest that optimal spectral differentiation between dead shrubs and the four other target types might occur within those wavelengths associated with the red and infrared portions of the electromagnetic spectrum.

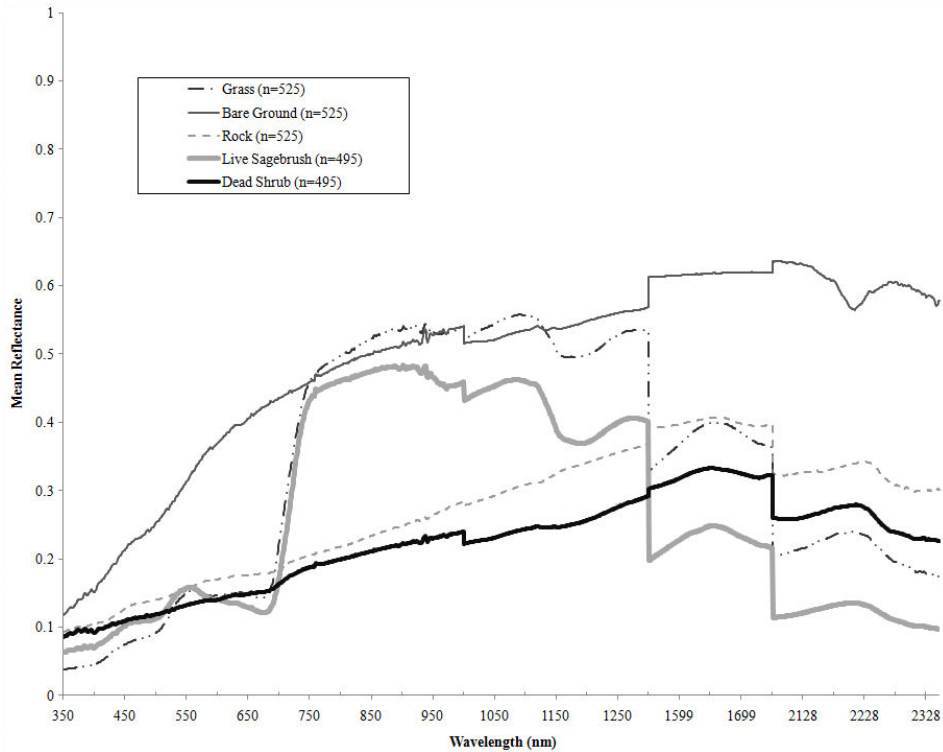


**Figure 2. Mean reflectance for basalt, bare ground, grass, dead shrub, and live sagebrush at the O’Neal Ecological Reserve.**

Pairwise ANOVA tests revealed statistical difference between mean spectral responses ( $P < 0.001$ ) (Table 1). This result suggests differentiation is possible between target types within the study area. Calculated variability for each target reveals that spectra are sufficiently separated to support the initial conclusion that differentiation between targets is possible (Figure 3).

**Table 1. Results of pairwise ANOVA tests between mean reflectance of dead shrub and four other common ground targets (basalt, bare ground, grass, and live sagebrush) (F-critical = 3.84)**

<b>Target</b>	<b>P-Value</b>	<b>F-Value</b>
Basalt	<0.001	269.39
Bare Ground	<0.001	4456.30
Grass	<0.001	519.49
Live Sagebrush	<0.001	95.71

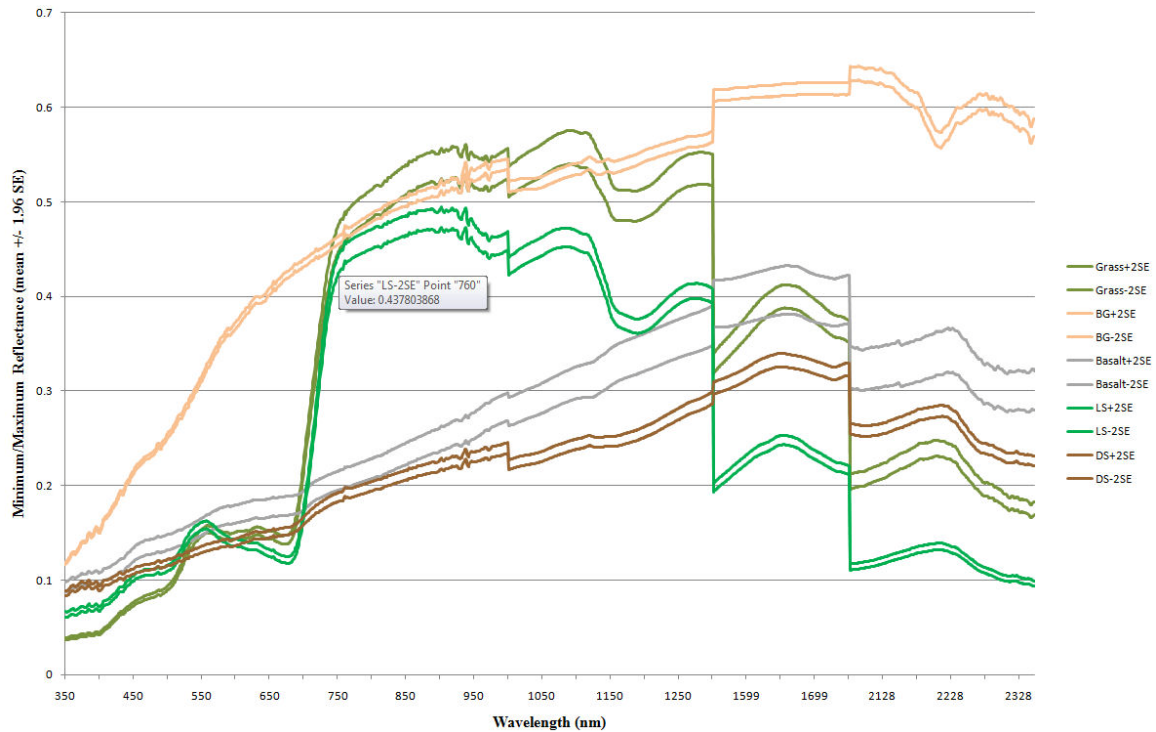


**Figure 3. Variability in target spectra are shown as the approximate minimum and maximum reflectance (@ 95% CI) based upon mean reflectance +/- 2 standard deviations.**

## CONCLUSIONS

Pairwise ANOVA results from the spectrometry data collected during the 2010 field season demonstrated statistical difference between mean reflectance of dead shrub and each of the other four target spectra ( $P < 0.001$ ). This suggests that differentiation of dead shrubs from the other ground target types was possible. The variability in spectral reflectance within each target type further supports the conclusion that separation is possible because there are specific wavelengths/ wavebands where dead shrub spectra are distinct among the other target spectra. However, influences such as atmospheric scattering (Rayleigh, Mie, Nonselective) and the signal to noise ratio (SNR) of a satellite sensor could make differentiation of dead shrubs extremely difficult. Aside from these potential influences, the greatest potential for differentiation appears to occur at approximately 950 nm to 1300 nm, 1550 nm to 1750 nm, and 2080 nm to 2350 nm wavelengths.

Field spectral data collected for ground targets with a handheld sensor may not correspond perfectly with spectral data collected by satellite sensors because reflectance values collected from a ground perspective do not undergo as much atmospheric influence. For many satellite sensors, there is a much larger FOV per pixel than for handheld spectroradiometers, so there is much more opportunity for adjacent objects, or underlying objects with stronger spectral reflectance characteristics to influence the overall reflectance received at the sensor. While a reference library for target spectral reflectance can be useful in isolating wavelengths where spectral differentiation seems likely, spectra collected with a handheld sensor should not be expected to perfectly correspond to a satellite sensor.

Field spectrometry can be very useful for aiding in understanding how an object of interest might be detected using remote sensing or serving as a spectral reference library for more precise image analysis and interpretation. This study represents only one part of a larger scientific analysis attempting to accurately classify dead shrubs using satellite imagery. Shrub die off is a phenomenon that affects the quality of Sage Grouse habitat and if it is possible to detect dead shrubs with remotely sensed imagery, this would represent an important management opportunity.

#### **ACKNOWLEDGEMENTS**

This study was made possible by a grant from the National Aeronautics and Space Administration Goddard Space Flight Center (NNX08AO90G). Idaho State University would also like to acknowledge the Idaho Delegation for their assistance in obtaining this grant.

#### **LITERATURE CITED**

- Campbell, J.B., 2008. Introduction to Remote Sensing. (4<sup>th</sup> ed.). New York: Guilford Press, 626 pp.
- Curtiss, B., and A.H. Goetz, 1994. Field Spectrometry: Techniques and Instrumentation. Proceedings: International Symposium on Spectral Sensing Research (ISSSR), 1, 195-203
- Davis, K. and K.T. Weber, 2010. 2008 Rangeland Vegetation Assessment at the O'Neal Ecological Reserve, Idaho. Pages 29-40 in K. T. Weber and K. Davis (Eds.), Final Report: Forecasting Rangeland Condition with GIS in Southeastern Idaho (NNG06GD82G). 189 pp.
- Wallace, A., and D.L. Nelson, 1989. Wildland Shrub Die-offs Following Excessively Wet Periods: A Synthesis. Pages 81-83 in E. D. McArthur, E. M. Romney, S. D. Smith, and P. T. Tueller (Eds.), Proceedings- Symposium on Cheatgrass Invasion, Shrub Die-off, and Other Aspects of Shrub Biology and Management. Ogden, UT: US Department of Agriculture, Forest Service, Intermountain Research Station General Technical Report INT-GTR-276. 351 pp.
- Weber, K.T. and B. Gokhale, 2010. Effect of Grazing Treatment on Soil Moisture in Semiarid Rangelands. Pages 161-174 in K. T. Weber and K. Davis (Eds.), Final Report: Forecasting Rangeland Condition with GIS in Southeastern Idaho (NNG06GD82G). 189 pp.

#### **Recommended citation style:**

Hanson, D. and K. T. Weber, 2011. 2010 Field Spectrometry Collection of Sagebrush at the O'Neal Ecological Reserve, Idaho. Pages 29-36 in K. T. Weber and K. Davis (Eds.), Final Report: Assessing Post-Fire Recovery of Sagebrush-Steppe Rangelands in Southeastern Idaho (NNX08AO90G). 252 pp.

[THIS PAGE LEFT BLANK INTENTIONALLY]

## **Intercalibration and Evaluation of ResourceSat-1 and Landsat-5 NDVI**

Jamey H. Anderson, Idaho State University. GIS Training and Research Center, 921 S. 8<sup>th</sup> Ave., Stop 8104, Pocatello, ID 83209-8104

Keith T. Weber, GISP Director, Idaho State University. GIS Training and Research Center, 921 S. 8<sup>th</sup> Ave., Stop 8104, Pocatello, ID 83209-8104 webekeit@isu.edu

Bhushan Gokhale, Idaho State University, GIS Training and Research Center, 921 S. 8<sup>th</sup> Ave., Stop 8104, Pocatello, ID 83209-8104

Fang Chen, Idaho State University, GIS Training and Research Center, 921 S. 8<sup>th</sup> Ave., Stop 8104, Pocatello, ID 83209-8104

### **ABSTRACT**

ResourceSat-1 is a designated alternative to Landsat should the existing TM (Thematic Mapper) and ETM+ (Enhanced Thematic Mapper Plus) sensors fail prior to the successful launch of Landsat 8 in late 2012. However, to enable integration of ResourceSat-1 into the many existing long-term Landsat projects around the world, practicable similarity must be demonstrated. To quantify the potential for ResourceSat-1 to satisfy some of the needs of the remote sensing community, Normalized Difference Vegetation Index (NDVI) values derived from Landsat-5 were compared to NDVI values derived from ResourceSat-1. An intercalibration equation was derived which converts ResourceSat-1 NDVI values to equivalent Landsat-5 NDVI values thereby enabling direct comparison between the two sensors. Comparisons were made using imagery spanning a three-year time period. Prior to intercalibration, NDVI values were highly correlated (mean  $R^2 > 0.73$ ) but statistically different ( $P < 0.001$ ). Following intercalibration, the resulting indices were statistically inseparable (min  $P = 0.56$ ). The intercalibration technique described in this paper represents an easily repeatable process which demonstrates practicable similarity between ResourceSat-1 and Landsat-5 imagery.

## INTRODUCTION

Medium resolution earth imaging sensors have become an integral part of land cover analysis and change detection in many land management agencies and research institutions. Landsat imagery in particular has contributed to over 35 years of continuous earth imaging and still plays a prominent role in research and management (Cohen and Goward, 2004; Leimgruber et al., 2005; Williams et al., 2006). However, the National Research Council of the National Academies recently chronicled the dire condition of the United States' earth imaging satellite fleet as well as the political and financial challenges facing current and future earth imaging programs (National Research Council, 2007). An additional concern is the likelihood of the current Landsat satellites failing prior to the launch of Landsat 8, late in 2012 as both Landsat-5 and Landsat-7 have exceeded their mission lifetimes (USGS, 2004 and USGS, 2008). It is this situation which has spurred National Aeronautics and Space Administration (NASA) scientists to identify active earth imaging sensors that are comparable to Landsat, and able to fill the gap in earth imaging capabilities should the need arise (Chander et al., 2008; Wulder et al., 2008).

## LANDSAT PROGRAM STATUS

NASA started the Landsat program with the launch of Landsat 1 on July-23 1972. This and the subsequent launch of additional Landsat satellites have resulted in over 35 years of continuous earth imaging from these sensors. Landsat-5 was launched in 1984 with a design life of 3 years. It carried the Thematic Mapper (TM) sensor, which is comprised of seven operational bands including three in the visible portion of the electromagnetic spectrum (Table 1). Landsat-7 was launched in 1999 with a design life of 5 years. It carried the Enhanced Thematic Mapper Plus (ETM+) sensor, which is comprised of eight operational bands including three in the visible portion of the electromagnetic spectrum.

**Table 1. Landsat-5 Thematic Mapper (TM) and ResourceSat-1 LISS III spectral and spatial characteristics. Temporal resolution of Landsat-5 = 16 days, swath width = 185km, and 30 m spatial resolution on bands 1-5 and 7. ResourceSat-1 temporal resolution = 24 days, swath width = 141km, and 23.5 m spatial resolution on all bands.**

Band	Landsat-5 Spectral Resolution ( $\mu\text{m}$ )	ResourceSat-1 Spectral Resolution ( $\mu\text{m}$ )
1	0.45-0.52	-
2	0.52-0.60	0.52-0.59
3	0.63-0.69	0.62-0.68
4	0.76-0.90	0.77-0.86
5	1.55-1.75	1.55-1.70
6	10.40-12.50	-
7	2.08-2.35	-

In the joint opinion of NASA and the USGS, it is "likely and expected" that either Landsat-5 or Landsat-7 could fail at any moment (USGS Remote Sensing Technologies Project: Landsat Data Gap Studies, 2008) as indeed, neither satellite is functioning properly at this time. For example, the batteries on Landsat-5 run too low during its June, July, and August transits over the southern hemisphere resulting in only the far northern portions of Australia being imaged during those months (Geoscience Australia, 2008). In addition, the Enhanced Thematic Mapper Plus (ETM+) instrument onboard Landsat-7 has a Scan Line Corrector (SLC) failure (USGS, 2003) and has operated in "SLC off" mode since May of 2003. The result

of this failure is that some areas are imaged twice, while other areas are not imaged at all, leaving up to one fourth of a scene missing (Markham et al., 2004). While the resulting data gaps can be filled using data from other dates, this is not a satisfactory solution for many scientific applications as this introduces temporal inconsistencies (minimum 16 days) into the imagery.

### **LANDSAT DATA GAP STUDY TEAM**

NASA and the USGS have recognized the potential earth imaging data gap and in response, formed the joint Landsat Data Gap Study Team (LDGST) in 2005. The study team identified candidate platforms that would help reduce the impact of a data gap until the Landsat Data Continuity Mission (LDCM) (i.e., Landsat 8) would launch late in 2012 (Chander, 2007). In the LDGST study, two potential gap-fill sensors, the Indian ResourceSat-1 (Linear Imaging Self Scanning III [LISS-III]) and the China-Brazil Earth Resources Satellite (CBERS-2) were selected. Following this selection, an interagency Data Characterization Working Group (DCWG) was formed and tasked with assessing the potential of these sensors to mitigate a possible Landsat data gap.

Of the DCWG's two sensor recommendations, ResourceSat-1 (Table 1), was considered the sensor that provided the best combination of Landsat-5 like data, capabilities, spectral band characteristics, and data accessibility and hence, was considered best able to fulfill immediate data needs with minimal complication (Chander, 2007; Teillet, 2008). It is for this reason that the present study focuses upon ResourceSat-1 and specifically its LISS-III sensor.

### **NORMALIZED DIFFERENCE VEGETATION INDEX**

The Normalized Difference Vegetation Index (NDVI), derived from the red and near-infrared bands common to many sensors, is a widely used numeric indicator of photosynthetically active green vegetation used to estimate biomass, plant productivity, and vegetation cover (Tucker, 1979). It has been shown that NDVI values are not identical across sensors due to uncertainties related to viewing angle, atmospheric conditions, and spectral band difference effects (Teillet et al., 1997, 2006; Goetz, 1997; van Leeuwen, 2006). However, vegetation indices are relatively insensitive to uncertainties in atmospheric corrections and differences in satellite viewing angle and thereby provide the means for direct comparison between sensors (Steven et al, 1998, 2003). This elimination of several potentially confounding factors makes the use of NDVI ideal for intercalibration testing.

Landsat-5 and ResourceSat-1 share many spectral, spatial, and temporal characteristics (Table 1). Among the strongest similarities are near coincident spectral bandwidths in the red, near infrared (NIR), and short-wave infrared (SWIR) regions of the electromagnetic spectrum. Because NDVI is derived from red and near infrared bands only, much of the potential spectral band difference effects caused when using the green and blue bands in other vegetation indices such as atmospherically resistant vegetation index (ARVI) and modified triangular vegetation index 2 (MTVI2) are avoided (Teillet, 2008). The slight differences in swath width and spatial resolution of both sensors were not directly considered in this study, but might have practical effects regarding the extent and characteristics of targeted areas of interest. The eight-day difference in the temporal resolution of these two sensors is of practical concern as it limits the number of cloud free scenes available over the course of a growing season.

The main objective of this study was to compare Landsat-5 with ResourceSat-1 and determine an intercalibration correction between the sensors. Random point sampling of heterogeneous semiarid landscapes allowed for a full range of NDVI values to be used in the development of the intercalibration. In light of potential Landsat program data gaps and given the importance of NDVI in research and land management decisions, these techniques provide a simple but robust procedure for providing reliable intercalibration of NDVI from one sensor to the other.

## **METHODOLOGY**

### *Study Area*

Landsat-5 and ResourceSat-1 imagery was acquired for a study area covering approximately 17,000 km<sup>2</sup> in southeast Idaho, USA (112° 27' 44" W and 43° 00' 12" N) (Figure 1). All Landsat-5 scenes used in this study were acquired for path 39, row 30 with spatially coincident ResourceSat-1 scenes acquired for path 253, row 39. The landscape imaged in these scenes included semiarid sagebrush-steppe, active and fallow agricultural fields, high altitude coniferous forests, several large reservoirs, lava flows, and various towns and cities, resulting in a highly heterogeneous study area.

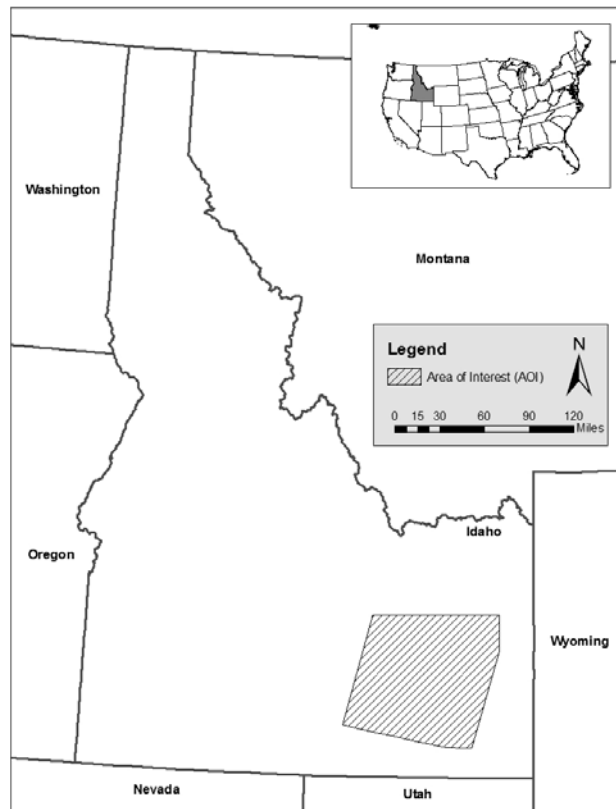


**Figure 1. Study area in Southeast Idaho, USA used to compare ResourceSat-1 and Landsat-5 NDVI values.**

## **DATA SOURCES AND PREPARATION**

Three Landsat-5 scenes were acquired for this study (August 13, 2005, July 15, 2006, and September 20, 2007) along with three ResourceSat-1 scenes (August 20, 2005, July 22, 2006, and September 3, 2007). These images formed the basis of the three annual cross-sensor comparisons used in this study.

All imagery were atmospherically corrected using the Cos(t) technique (Chavez, 1996) in Idrisi Andes. NDVI layers were created and subsequently georectified against 2004 National Agriculture Imagery Program (NAIP) natural color aerial imagery (1 m x 1 m pixels). Resulting RMSE was < 1/2 pixel (Weber, 2006) ( $\bar{x}$  RMSE = 8.2 m and 6.5 m for Landsat-5-derived NDVI layers and ResourceSat-1 derived NDVI layers, respectively). Each of the three image pairs (i.e., NDVI layers from 2005, 2006, and 2007) were then co-registered to each other with a resulting mean RMSE of 7.4 m. Paired Landsat-5/ResourceSat-1 layers were clipped to a coincident area and all cloud cover was removed by manually digitizing a cloud mask layer (Figure 2), resulting in an area of interest (AOI) used throughout this study.

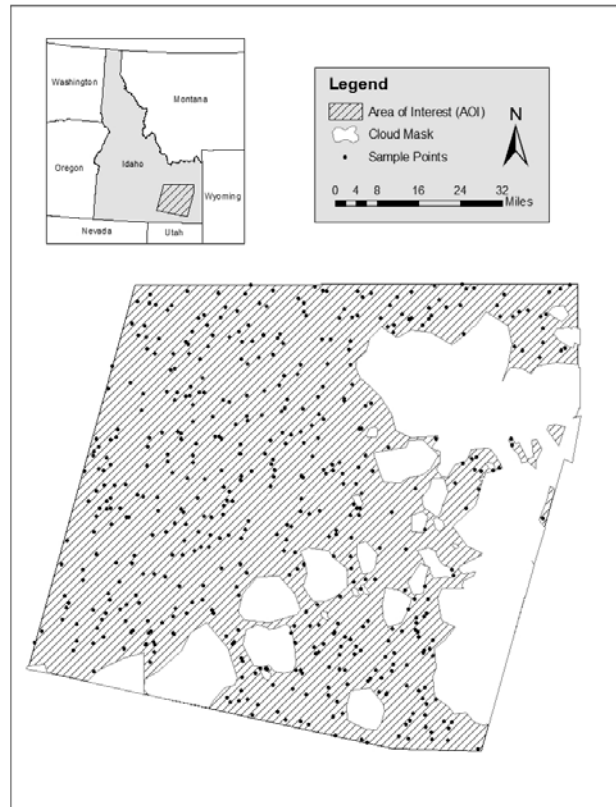


**Figure 2. Example of combined cloud mask, sample points and coincident area between 2005 Landsat-5 and ResourceSat-1 scenes.**

Weber (2006) reported the importance of identifying the same target pixel when comparing imagery and the need to evaluate co-registration error. Co-registration error between Landsat-5 and ResourceSat-1 image pairs was independently verified using the Georeferencing extension in ArcGIS 9.3. Using 20 well-defined and recognizable features with the image pairs ( $n = 10$  [2005],  $n = 5$  [2006], and  $n = 5$  [2007]), resulting mean RMSE was 8.67 m.

### **SAMPLING AND STATISTICAL ANALYSIS**

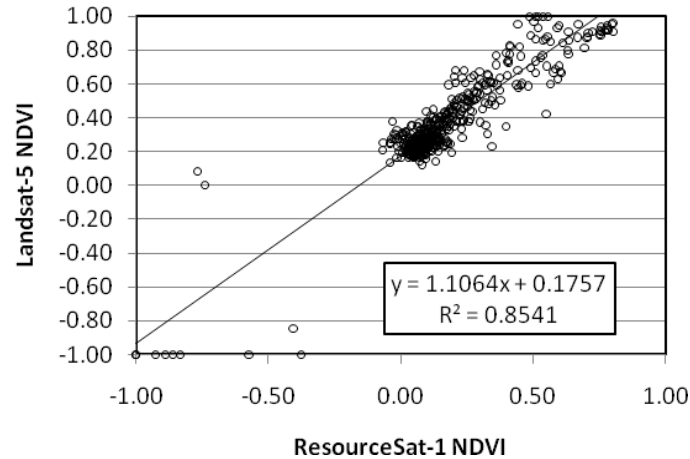
For each of the three annual image pairs, 500 development random sample points within the AOI of each image pair were generated using Hawth's Tools for ArcGIS 9.3. The pixel value at each sample point was extracted from both the Landsat-5-derived NDVI layers and the ResourceSat-1 derived NDVI layers using the "Sample" tool in ArcGIS 9.3, creating a table of NDVI values for statistical comparison

( $n=1500$  records). Linear regression analyses were used to calculate the coefficient of determination ( $R^2$ ) between NDVI values and find the slope and Y-intercept between each image pair. Mean slope and intercept of the three image pairs were calculated and the resulting regression equation was then used to intercalibrate ResourceSat-1 values to a Landsat-5 equivalent.

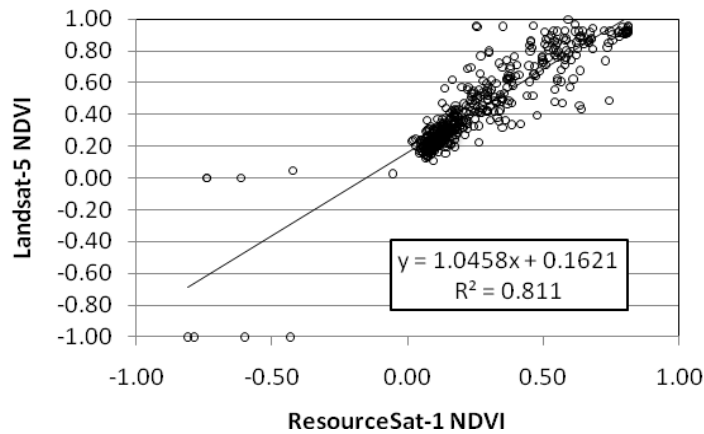
To test the intercalibration equation, NDVI values at 500 independent random sample points were extracted from each image pair using the sample tool in ArcGIS 9.3. The intercalibration equation was applied to ResourceSat-1 NDVI values and then compared to original Landsat-5 derived NDVI values. Linear regression analyses were used to determine the correlation coefficient and Analysis of Variance (ANOVA) was used to test for statistical difference between NDVI values both before and after intercalibration.

### RESULTS AND DISCUSSION

Scatter plots with correlation coefficients for 2005, 2006, and 2007 image pair comparisons demonstrate inherent similarity between Landsat-5 and Resource-1 NDVI values even when comparisons included 17-day differences between image acquisitions (Figure 3).



a.



b.

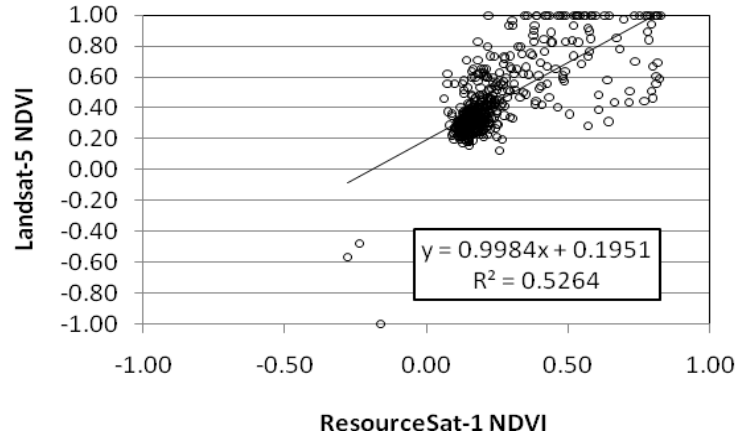


**Figure 3. Distribution and correlation of Landsat-5/ResourceSat-1 NDVI values for (a) 2005; (Landsat-5) – (ResourceSat-1) time difference = – 7 day, (b) 2006; (Landsat-5) – (ResourceSat-1) time difference = – 7 day, and (c) 2007; (Landsat-5) – (ResourceSat-1) time difference = + 17 day.**

In each, NDVI values extracted from ResourceSat-1 are shown on the X-axis with NDVI values extracted from Landsat-5 given on the Y-axis. Outliers in Figure 3 are largely the result of anthropogenic effects on the environment that occurred between the image pair dates, for example, reservoir drawdown for agricultural irrigation and agricultural harvest. From these data, the mean slope (1.0502; SE = 0.031) and Y-intercept (0.177633; SE = 0.009) and used to form an intercalibration equation (Equation 1).

$$\text{Intercalibrated NDVI}_{\text{Landsat-5}} = 1.0502 * \text{NDVI}_{\text{ResourceSat-1}} + 0.177633 \quad (1)$$

Prior to intercalibration NDVI values from Landsat-5 and ResourceSat-1 were highly correlated (minimum  $R^2 > 0.56$ ) but statistically different ( $P < 0.001$ ). As a result, the NDVI values from one sensor could not be compared directly to the values from the other sensor. Following intercalibration, the resulting NDVI values were statistically inseparable (minimum  $R^2 > 0.53$  and minimum  $P = 0.56$ ) (Table 2).

**Table 2. Coefficient of determination and probability values for pre- and post-intercalibrated NDVI values**

Year	$R^2$	<i>P-value</i>	
		Pre-intercalibration	Post-intercalibration
2005	0.83	< 0.001	0.61
2006	0.84	< 0.001	0.66
2007	0.58	< 0.001	0.56

This study demonstrated the ability to develop effective intercalibrations between Landsat-5 and ResourceSat-1 over large heterogeneous regions using imagery acquired over a 17 day interval. This study builds upon and broadens the application of other studies that derived intercalibrations under more homogeneous conditions. For instance, Chander et al. (2008) used near simultaneous image pairs to compare the average of paired homogeneous areas and reported  $R^2$  values between Landsat-5 and ResourceSat-1 of 0.99 for every band, with differences in reflectance across all bands of approximately 13%. The techniques described in this paper use only simple spatial and statistical tools to derive an

effective intercalibration equation that is easily repeated and does not require field spectroradiometer data (Steven et al., 2003).

Co-registration errors may lead to erroneous intercalibration of the imagery. Weber et al. (2008) highlight the importance of considering co-registration and independent verification of co-registration error performed in this study revealed the RMSE for 2005, 2006, and 2007 were 6.99, 10.62, and 10.10 m respectively, The weighted mean RMSE was 8.67. Consequently, it is highly probable that the pixel values used this study were extracted from pixels representing the same land features and locations on the earth's surface as the observed RMSE values imply precise co-registration between Landsat-5 and ResourceSat-1 image pairs.

## **CONCLUSIONS**

The importance of medium resolution earth imaging satellites for land cover analysis and change detection, combined with the tenuous status of active Landsat satellites, make studies such as the one presented in this paper timely and valuable. This study produced an easily repeatable and accurate region-specific intercalibration of ResourceSat-1 NDVI to its Landsat-5 equivalent ( $R^2 > 0.85$ ). The process described in this paper illustrates that intercalibrated NDVI is resilient to temporal variations (intercalibrations were based upon 7-17 day differences), as well as spectral band differences. Replication of this technique in other regions will aid scientists contending with the potential Landsat data gap or otherwise needing to compare values from one sensor to another.

## **ACKNOWLEDGEMENTS**

This study was made possible by a grant from the National Aeronautics and Space Administration Goddard Space Flight Center (NNX08AO90G). ISU would like to acknowledge the Idaho Delegation for their assistance in obtaining this grant.

## **LITERATURE CITED**

- Chander, G., 2007. Landsat Data Gap Study - Technical Report: Initial Data Characterization, Science Utility and Mission Capability Evaluation of Candidate Landsat Mission Data Gap Sensors. United States Geological Survey
- Chander, G., M.J. Coan, and P.L. Scaramuzza, 2008. Evaluation and Comparison of the IRS-P6 and the Landsat Sensors. *Ieee Transactions on Geoscience and Remote Sensing*, 46:209-221
- Chavez, P.S., 1996. Image-based Atmospheric Corrections Revisited and Improved. *Photogrammetric Engineering and Remote Sensing*, 62:1025-1036
- Cohen, W.B., and S.N. Goward, 2004. Landsat's Role in Ecological Applications of Remote Sensing. *Bioscience*, 54:535-545
- Geoscience Australia, 2008. New Satellite Imagery for Australia. In *Ausgeo News*: 91, 1. Commonwealth of Australia

- Goetz, S.J., 1997. Multi-Sensor Analysis of NDVI, Surface Temperature and Biophysical Variables at a Mixed grassland site. *International Journal of Remote Sensing*, 18:71-94
- Leimgruber, P., C.A. Christen, and A. Laborderie, 2005. The Impact of Landsat Satellite Monitoring on Conservation Biology. *Environmental Monitoring and Assessment*, 106: 81-101
- Markham, B.L., and J.L. Barker, 1985. Spectral Characterization of the Landsat Thematic Mapper Sensors. *International Journal of Remote Sensing*, 6:697-716
- National Research Council, 2007. *Earth Science and Applications from Space: National Imperative for the Next Decade and Beyond*. National Academies Press, Washington, D.C.
- Steven, M.D., 1998. The Sensitivity of the OSAVI Vegetation Index to Observational Parameters. *Remote Sensing of Environment*, 63:49-60
- Steven, M.D., Malthus, T.J., Baret, F., Xu, H., and Chopping, M.J. 2003. Intercalibration of Vegetation Indices from Different Sensor Systems. *Remote Sensing of Environment*, 88:412-422
- Teillet, P.M., and X.M. Ren, 2008. Spectral Band Difference Effects on Vegetation Indices Derived from Multiple Satellite Sensor Data. *Canadian Journal of Remote Sensing*, 34:159-173
- Teillet, P.M., B.L. Markham, and R.R. Irish, 2006b. Landsat Cross-calibration Based on Near Simultaneous Imaging of Common Ground Targets. *Remote Sensing of Environment*, 102: 264-270
- Teillet, P.M., K. Staenz, and D.J. Williams, 1997. Effects of Spectral, Spatial, and Radiometric Characteristics on Remote Sensing Vegetation Indices of Forested Regions. *Remote Sensing of Environment*, 61:139-149
- Tucker, C.J. 1979. Red and Photographic Infrared Linear Combinations for Monitoring Vegetation. *Remote Sensing of Environment*, 8:127-150
- United States Geological Survey. 2003. Landsat Monthly Update – June 2003, Online Newsletter, 1–3
- United States Geological Survey. 2004. Landsat Monthly Update – April 2004. Online Newsletter, 1–3
- United States Geological Survey. 2008. USGS remote sensing technologies project. Landsat Data Gap Studies. URL = <http://calval.cr.usgs.gov/LDGST.php> visited October 17, 2008
- van Leeuwen, W.J.D., B.J. Orr, S.E. Marsh, and S.M. Herrmann, 2006. Multi-sensor NDVI Data Continuity: Uncertainties and Implications for Vegetation Monitoring Applications. *Remote Sensing of Environment*, 100:67-81

Weber, K.T. 2006. Challenges of Integrating Geospatial Technologies into Rangeland Research and Management. *Rangeland Ecology & Management*, 59: 38-43

Weber, K.T., J. Théau, and K. Serr, 2008. Effect of Coregistration Error on Patchy Target Detection using High-resolution Imagery. *Remote Sensing of Environment*, 112:845-850

Williams, D.L., S. Goward, and T. Arvidson, 2006. Landsat: Yesterday, Today, and Tomorrow. *Photogrammetric Engineering and Remote Sensing*, 72:1171-1178

Wulder, M.A., J.C. White, S.N. Goward, J.G. Masek, J.R. Irons, M. Herold, W.B. Cohen, T.R. Loveland, and C.E. Woodcock, 2008b. Landsat continuity: Issues and opportunities for land cover monitoring. *Remote Sensing of Environment*, 112: 955-969

**Recommended Citation Style:**

Anderson, J.H., K.T. Weber, B. Gokhale, and F. Chen, 2011. Intercalibration and Evaluation of Resource Sat-1 and Landsat-5 NDVI. Pages 37-46 in K. T. Weber and K. Davis (Eds.), Final Report: Assessing Post-Fire Recovery of Sagebrush-Steppe Rangelands in Southeastern Idaho. 252 pp.

## **Assessing the Susceptibility of Semiarid Rangelands to Wildfires using Terra MODIS and Landsat Thematic Mapper Data**

Fang Chen, GIS Training and Research Center, Idaho State University, 921 S. 8<sup>th</sup> Ave, Stop 8104, Pocatello Idaho 83209-8104 [chenfang@isu.edu](mailto:chenfang@isu.edu)

Keith T. Weber, GISP, GIS Director, Idaho State University, GIS Training and Research Center, 921 S. 8th Ave., Stop 8104, Pocatello, ID 83209-8104. [webekeit@isu.edu](mailto:webekeit@isu.edu)

Jamey Anderson, GIS Training and Research Center, Idaho State University, 921 S. 8<sup>th</sup> Ave, Stop 8104, Pocatello Idaho 83209-8104

Bhushan Gokhale, GIS Training and Research Center, Idaho State University, 921 S. 8<sup>th</sup> Ave, Stop 8104, Pocatello Idaho 83209-8104

### **ABSTRACT**

In order to monitor wildfires at broad-spatial scales and with frequent periodicity, satellite remote sensing techniques have been used in many studies. Rangeland susceptibility to wildfires closely relates to accumulated fuel load. The normalized difference vegetation index (NDVI) and fraction of photosynthetically active radiation (fPAR) are key variables used by many ecological models to estimate biomass and vegetation productivity. Subsequently, both NDVI and fPAR data have become an indirect means of deriving fuel load information. For these reasons, NDVI and fPAR, derived from the Moderate Resolution Imaging Spectroradiometer (MODIS) onboard Terra and Landsat Thematic Mapper (TM) imagery, were used to represent pre-fire vegetation changes in fuel load preceding the Millennial and Crystal Fires of 2000 and 2006 in the rangelands of southeast Idaho, respectively. NDVI and fPAR change maps were calculated between active growth and late-summer senescence periods and compared with precipitation, temperature, forage biomass, and percent ground cover data. The results indicate that NDVI and fPAR change values two years prior to the fire were greater than those one-year prior to fire as an abundance of grasses existed two years prior to each wildfire based upon field forage biomass sampling. NDVI and fPAR have direct implication for the assessment of pre-fire vegetation change. Therefore, rangeland susceptibility to wildfire may be estimated using NDVI/fPAR change analysis. Furthermore, fPAR change data may be included as an input source for early fire warning models, and may increase the accuracy and efficiency of fire and fuel load management in semiarid rangelands.

**KEYWORDS:** *NDVI, fPAR, fuel loads, biomass burning, remote sensing, Idaho*

## **INTRODUCTION**

Rangelands refer to expansive, mostly non-cultivated, non-irrigated, and non-forested lands that include grasslands, savannas, and shrublands where livestock grazing is a common land use. Rangelands cover approximately 40% of the Earth's terrestrial surface and play an important role in global ecosystem productivity (Breman and de Wit 1983; Huntsinger and Hopkinson 1996). Wildfires are common in rangelands worldwide and have significant effects on rangeland ecosystem balance with the most obvious effect being direct impact on vegetation communities (Mutch 1970; Pierson *et al.* 2002; West and Yorks 2002; Taylor 2003). In a wild land fire, fuel is composed nearly entirely of vegetation and severe fires can leave entire landscapes devoid of vegetative cover, resulting in numerous significant climatic, ecological, and hydrologic hazards (Pierson *et al.* 2002; Hilty *et al.* 2004; Collins *et al.* 2006). In addition, biomass burning is recognized as an important source of trace gases to the atmosphere, such as carbon dioxide, methane, carbon monoxide, nitrogen dioxide and non-methane hydrocarbons (Crutzen *et al.* 1979; Greenberg *et al.* 1984). These trace gases' compounds may trap the heat radiated by the earth and contribute to the greenhouse effect (e.g. average annual CO<sub>2</sub> emissions from fires in the lower 48 states of U.S. are approximately 213 Tg CO<sub>2</sub> yr<sup>-1</sup> from 2002-2006) (Houghton 1992; Wiedinmyer and Neff 2007; EPA 2008). Furthermore, following a fire, vegetation communities may transition to a very different community type due to invasions by non-native species resulting in a variety of propagated indirect effects (Thomas and Davis 1989; Hilty *et al.* 2004).

Satellite remote sensing is an evolving technology providing regional and global imagery that has been used for many wildfire studies (Fernandez *et al.* 1997; Miller and Yool 2002; Wooster *et al.* 2003; Lentile *et al.* 2006; Weber *et al.* 2008b). These studies include both observational and modeled data and have been conducted on active fires and for detecting post-fire burn extent. For example, National Oceanic and Atmospheric Administration (NOAA) Advanced Very High Resolution Radiometer (AVHRR) imagery has been used to detect and map fire growth (Kennedy *et al.* 1994; Fernandez *et al.* 1997; Pozo *et al.* 1997; Siegert and Hoffmann 2000). MODIS imagery provides thermal anomalies/fire products to meet the requirements of understanding the timing and spatial distribution of fires at various regional and global scales (Wooster *et al.* 2003; Li *et al.* 2004; Morissette *et al.* 2005). In addition, Landsat-5 TM and Landsat-7 ETM+ have been used to determine fire perimeter and burn severity of the Cerro Grande Fire, New Mexico, USA. (Miller and Yool 2002). Similarly, post-fire field observations coupled with Satellite Pour l'Observation de la Terre 5 (SPOT 5) imagery have been used for fire severity modeling of sagebrush steppe rangelands in southeastern Idaho (Weber *et al.* 2008b).

Recently, satellite-based wildfire studies have focused upon post-fire factors (i.e., severity and perimeter mapping), with emphasis on forested ecosystems (Chuvienco and Congalton 1989; Fernandez *et al.* 1997; Fraser and Li 2002; Giglio *et al.* 2003). Many reflectance indicators derived from various remotely sensed data have been tested to assess forest fire effects including NDVI (Illera *et al.* 1996; Leblon *et al.* 2001; Aguado *et al.* 2003; Chuvienco *et al.* 2004), spectral indices retrieved by Tasseled Cap (Mbow *et al.*, 2004), and normalized difference water index (NDWI) (Verbesselt *et al.* 2006; Maki *et al.* 2004). In addition, in order to calculate burn severity, the Normalized Burn Ratio (NBR; Key and Benson 1999), which incorporates near- and mid-infrared bands, and the differenced Normalized Burn Ratio (dNBR), which is the result of differenced pre- and post-fire NBR models, have been widely applied (Epting *et al.* 2005; Escuin *et al.* 2008). NBR and dNBR are key indicators of burn severity and can be used to infer many post-fire effects such as fire extent (Holden *et al.* 2005), and fire severity classification (Brewer *et al.*

2005; Smith *et al.* 2005). For example, incorporating Classification Tree Analysis (CTA) techniques and post-fire field survey data, NBR along with various other band ratios was used to assess the severity of fire occurring in rangelands of Idaho (Weber *et al.* 2008b). Furthermore, these reflectance indicators derived from remotely sensed data were widely used for fire studies in savannahs and semiarid environments (Fisher *et al.* 2005; Smith *et al.* 2005; Weber *et al.* 2008a).

Many studies indicate that wildfire danger is directly linked to fuel properties (e.g., fuel load, fuel size, fuel moisture content, and fuel type) and many of these fuel properties can be assessed using remotely sensed data (West and Yorks 2002; Westerling *et al.* 2003). For example, estimates of forest biomass have been used to reveal changes in crown fuels (Nelson *et al.* 1988; Means *et al.* 1999; Franklin, *et al.* 2003). In addition, surface fuel type has been characterized using vegetation classification maps derived from various remotely sensed data (Keane *et al.* 2001; Riano *et al.* 2002; Van Wagtendonk and Root 2003) including various vegetation indices (e.g., NDVI) which have been related to fuel moisture content and fire potential (Paltridge and Barber, 1988; Chuvieco *et al.* 2002; Danson & Bowyer 2004; Dennison *et al.* 2008).

Fire danger conditions are related to, although not entirely attributable to accumulated fuel load which in turn, is related to vegetation cover, type, biomass, phenology, and various fuel properties such as moisture content. Rangeland susceptibility to wildfire is determined by the combined effect of these characteristics, many of which can be accurately estimated based upon empirical relationships with remotely sensed imagery. NDVI and fPAR are two important indicators of these vegetation variables, and global or regional scale NDVI and fPAR have been derived through satellite remote sensing (Chuvieco *et al.* 2002; Chen *et al.* 2008). Because NDVI and fPAR represent canopy greenness and are closely related to biomass, vegetation type, leaf area index (LAI), and primary productivity, they represent an indirect way to derive fuel load (Van Wagtendonk and Root 2003) in conjunction with field data. NDVI leverages the ratio of reflectance in the red band (where chlorophyll makes notable absorption of incoming sunlight) of a sensor to that of the near infra-red band (where considerable reflectance is made by a plant's spongy mesophyll leaf structure) of the sensor, and is closely related to the quantity of green vegetation on the landscape (Tucker, 1979). NDVI is easy to calculate and can be considered a basic index from which many subsequent vegetation variables can be calculated or deduced (i.e., LAI, vegetation cover, biomass) (Chen and Cihlar 1996; Boelman *et al.* 2003; Hill and Donald 2003). fPAR is the fraction of available radiation in specific photosynthetically active wavelengths of the electromagnetic spectrum (i.e., 0.4 - 0.7  $\mu\text{m}$ ) that a canopy absorbs (Chen 1996; Myneni *et al.* 1999; Chen *et al.* 2008). In many ecosystem models, fPAR has been used as a modeling input across several biomes (Bonan 1995; Hély *et al.* 2003). In addition, after accounting for atmospheric effects and background contributions to the signal, linear relationships have been established between fPAR and NDVI.

While both fPAR and NDVI respond to pixel heterogeneity, background noise, and atmospheric effects and exhibit similar responses to vegetation percent cover, leaf area, leaf orientation, solar zenith angle, and atmospheric optical depth, they respond differently to soil reflectance and leaf optical properties (Daughtry *et al.* 1983; Myneni and Williams 1994). In this study, both NDVI and fPAR were used as indicators to evaluate wildfire danger in semiarid rangelands. MODIS and TM derived fPAR and NDVI data were chosen to represent vegetation status and to detect changes in fuel load. Incorporating monthly precipitation, monthly mean temperature, field-based measurements of ground cover, and measures of

biomass at numerous sites, variation in fuel load across the semiarid rangelands of Idaho, USA was evaluated.

## MATERIALS AND METHODS

### Study Area

The Big Desert study area lies approximately 71 km northwest of Pocatello Idaho and the center of the study area is approximately 113° 4' 18.68" W and 43° 14' 27.88" N (Figure 1). The study area is located on the land managed by the United States Department of the Interior Bureau of Land Management (USDI BLM). The area is a semiarid sagebrush-steppe ecosystem with a high proportion of bare ground ( $\bar{x}$  bare ground > 17%), and the area consists primarily of native and non-native grasses, forbs, and many shrub species including sagebrush (*Artemisia tridentata*) and rabbit brush (*Chrysothamnus nauseosus*). The elevation of the study area ranges from 1349-2297 m above sea level, and annual precipitation is 230 mm with 40% of the precipitation falling from April through June (Yanskey *et al.* 1966). Cattle and sheep grazing is the primary anthropic disturbance to the study area with deferred, rest-rotation, and continuous/seasonal grazing systems used on allotments ranging in size from 1100 to over 125,000 ha. The stocking rate is low across the study area approximately 19 ha/animal unit [AU] and is considered a semi-extensive grazing regime. Wildfire is another common disturbance and 39% of the study area has burned in the past 10 years.

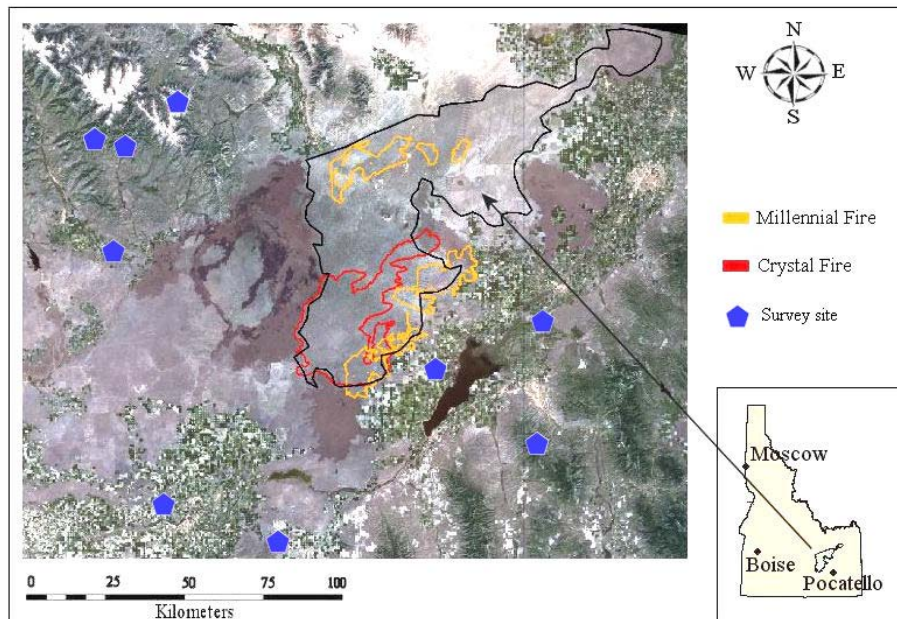


**Figure 1. Location and general characteristics of the Big Desert in southeastern, Idaho. The true color composite of Landsat-5 TM: band3=red, band2=green, band1=blue.**

### Sample Design and Field Measurements

Four hundred and seventeen sample points were randomly generated across the study area. Each point met the following criteria: 1) >70 meters from an edge (road, trail, or fence line), and 2) <750 meters from a road. Table 1 details four field campaigns from 2004-2006. Each plot center location was recorded using a Trimble GPS receiver and all points were post-processed differentially corrected (+/-1 m [2004],

+/-0.70 m [2005] and +/-0.20 m [2006] after post processing with a 95% CI). The sample points were then projected into Idaho Transverse Mercator NAD 83(Gneiting *et al.* 2005).

**Table 1. Dates and numbers of field sample plots used for validation**

Year	Sampling date	Number of sample plots
2004	01-June to 30-June	154
2005	01-June to 15-July	88
2006	05-June to 10-July	175

Ground vegetation cover and biomass are two variables which closely relate to wildfire fuel load. For this reason, ground cover and biomass were estimated in the field survey. This study sought to characterize vegetation cover and biomass at the time of maximum primary production in June, but was not intent on relating field measurements directly to pixel data. Ground cover estimations were made within 10m x 10m square plots centered over each sample point with the edges of the plots aligned in cardinal directions. The percent cover of five vegetation classes (bare ground, litter, grass, shrub, and weed) was estimated by walking the plot and estimating/generalizing a cover category for each class (Kercher *et al.* 2003). Percent cover was estimated using categorical breaks of 0%, 1-5%, 6-15%, 16-25%, 26-35%, 36-50%, 51-75%, 76-95%, and 96-100% .

Forage wet biomass was measured four times within each sample plot ( $n = 1668$ ). All green and senescent herbaceous biomass was clipped and weighed in an ordinary paper bag using a Pesola scale (+/- 1g) tared to the weight of the bag. All grass species were considered forage and these measurements were used to estimate forage availability, expressed as kilograms per hectare. Dry biomass would have preferable. However, there have been accumulated up to 10 years of database in the study area, all the previous field surveys collected wet biomass. The dry biomass data between 2004 and 2006 are not available for this study. Wet biomass could represent vegetation productivity as well, though dry biomass maybe better in this study.

In this study, monthly precipitation and monthly mean temperature data were provided by the United States Department of Agriculture (USDA) Natural Resources Conservation Service (NRCS) (<http://www.id.nrcs.usda.gov/snow/data/historic.html>) and the United States Bureau of Reclamation (USBR) AgriMet Program (<http://www.usbr.gov/pn/agrimet/>). While no weather station survey sites were available within the Big Desert study area, nine sites bounding the study area (< 70 km from the Big Desert study area) were located and used (Figure 1). Though some sites are in the mountains, the weather there has identical change trends compared to the Snake River Plain (Table 2).

**Table 2. Natural Resources Conservation Service (NRCS) and AgriMet survey site list and monthly precipitation (mm) and mean temperature (°C) data for this study**

Site name	Lat	Long	Year	Precipitation				Mean temperature			
				March	April	May	June	March	April	May	June
Garfield R.S.	43°36'	-113°55'	2004	10	36	74	33	1	5	7	12
			2005	53	58	198	74	0	3	7	9
			2006	76	130	43	15	-3	4	9	13
			2004	15	46	94	25	1	4	6	11

Swede Peak	43°37'	-113°58'	2005	81	61	188	86	-1	2	6	8
			2006	117	160	51	15	-4	2	7	13
			2004	20	46	102	30	0	1	4	8
Smiley Mountain	43°43'	-113°50'	2005	76	112	226	119	-3	0	4	6
			2006	130	208	51	25	-6	0	6	10
			2004	66	79	112	15	2	3	5	11
Howell Canyon	42°19'	-113°36'	2005	114	127	208	94	-1	2	6	9
			2006	168	145	74	38	-3	3	7	13
			2004	66	36	76	48	2	5	8	12
Wildhorse Divide	42°45'	-112°28'	2005	76	86	117	71	1	4	8	10
			2006	132	155	25	28	-1	4	9	13
			2004	7	19	30	26	5	9	12	17
Fort Hall	43°04'	-112°25'	2005	18	46	86	29	3	7	12	15
			2006	36	67	9	21	2	8	13	18
			2004	8	15	20	2	6	9	12	17
Rupert	42°35'	-113°52'	2005	19	71	124	22	5	7	12	14
			2006	26	54	37	8	2	8	14	19
			2004	5	17	46	16	3	9	11	17
Picabo	43°18'	-114°09'	2005	51	21	86	28	2	6	11	13
			2006	40	89	22	6	-1	7	12	18
			2004	5	23	33	7	4	9	12	16
Aberdeen	42°57'	-112°49'	2005	16	50	67	12	4	7	12	15
			2006	37	33	18	39	1	8	13	18

#### Landsat-5 TM NDVI and fPAR Calculation

Because Terra satellite launched in December 1999, there are no MODIS data available between 1998 and 1999. Therefore, four cloud-free TM scenes (path/row 039/030) captured on 10 August 1998, 25 May 1999, 29 August 1999, and 27 May 2000 were used to derive NDVI and fPAR prior to the Millennial Fire of August 2000. Digital Number (DN) values were converted into planetary reflectance using gain and offset coefficients, solar zenith angle, solar irradiances and the sun-earth distance factors from the metadata of the imagery (Chander and Markham 2003). The imagery was then processed to reflectance by performing an atmospheric correction using the dark object subtraction (DOS) method (Chavez 1996; Song *et al.* 2001). All imagery was projected into Idaho Transverse Mercator, NAD 83 and was georectified against 2004 National Agriculture Imagery Program (NAIP) natural color aerial imagery (1 m x 1 m pixels) (RMSE = 8.126).

TM NDVI values were calculated using equation 1. Because there were no ground-measured fPAR data available for this study, TM fPAR estimations were accomplished using the SR-fPAR algorithm, built on the remote sensing of vegetation and plant physiology described by Sellers *et al.* (1992). The simple ratio (SR) is the ratio of reflectance in the red band to that of the near infra-red band (Equation 2) and NDVI and SR are related functionally, as both represent slope-based spectral vegetation index band ratios designed to characterize photosynthetically active vegetation (Chen *et al.* 1996; Stenberg *et al.* 2004). The SR-fPAR algorithm is a straightforward fPAR retrieval approach and is considered applicable within a variety of biome types (e.g. broadleaf evergreen trees, needle leaf deciduous trees, and grasslands)

(Paruelo *et al.* 1997; Los *et al.* 2000; Hassan *et al.* 2006). A near linear relationship between fPAR and SR (Eq. 3) was assumed and followed Sellers *et al.* (1996): "The value of the 98 % NDVI for tall vegetation and agriculture is assumed to represent vegetation at full cover and maximum activity with fPAR values close to 1. The 98 % NDVI value of agriculture was used to represent all short vegetation types, while the 5 % desert value is assumed to represent no vegetation activity with an fPAR of 0.001 (Sellers *et al.* 1996, p.722) ". Once these two values were determined, the relationship between fPAR and SR can be described as shown in equation 3.

$$NDVI = \frac{NIR-RED}{NIR+RED} \quad (1)$$

$$SR = \frac{NIR}{RED} \quad (2)$$

$$fPAR = \frac{(SR-SR_{i,min})(fPAR_{max}-fPAR_{min})}{(SR_{i,max}-SR_{i,min})} + fPAR_{min} \quad (3)$$

*RED* and *NIR* stand for the spectral reflectance measurements acquired in the red and near-infrared regions, respectively.  $SR_{i,max}$  and  $SR_{i,min}$  are corresponding to the maximal and minimal NDVI data population for type *i* vegetation, and the maximum ( $fPAR_{max}=0.950$ ) and minimum ( $fPAR_{min}=0.001$ ) values of fPAR are independent of vegetation type (Sellers *et al.* 1996).

#### *MODIS NDVI and fPAR Product*

Collection 5 MODIS NDVI (MOD13A2) and fPAR (MOD15A2) products (1-km spatial resolution) were used in this study. The MODIS NDVI algorithm operates on a per-pixel basis and relies on multiple observations over a 16-day period to generate a composite NDVI (Huete *et al.* 2002; Tarnavsky *et al.* 2008). The MOD15A2 fPAR product represents a time interval of eight days and in the case of fPAR the values represent eight-day maxima. The theoretical basis of the MODIS fPAR algorithm is the three dimensional radiative transfer theory, and the inversion of the three dimensional radiative transfer problem is solved using a look up table method (Knyazikhin *et al.* 1998; Myneni *et al.* 1999). In this study, four MODIS NDVI and four MODIS fPAR scenes were used. MODIS fPAR imagery for the entire study area was captured between 12-19 August 2004, 10-17 June 2005, 13-20 August 2005, and 10-17 June 2006 prior to the Crystal fire. In addition NDVI imagery was also acquired on the basis of temporal coincidence with existing MODIS fPAR imagery.

Based on MODIS NDVI and fPAR quality control (QC) layers, NDVI and fPAR data were screened to reject all data of insufficient quality. Only pixels with the best possible quality (i.e., values on all bit fields are equal to zero) under the fPAR QC definition and pixels with the "use with confidence" under the vegetation indices QC definition were retained. The QC filter includes pixels with good quality and removes pixels which were not produced due to cloud or other reasons.

#### *Data Analysis*

Field work began in June, as this was considered optimal to characterize the phenological changes over the growing season through to late Fall. There were no field surveys conducted before 2000 and field data were only used in conjunction with MODIS image analysis. For these analyses, field data were collected between June and early July at the same time as the remotely sensed data were acquired. Imagery for the

August 2004 and 2005 time periods were also used to capture late-summer senescence and thereby better assess changes in fPAR over each growing season.

In the semiarid sagebrush-steppe rangelands of Idaho, plant growth rates dramatically decrease following the active growth period which typically ends in June (Figure 2). However, plant growth does continue and in some years exhibits a spike of activity when sufficient autumn precipitation is present. Therefore, the fPAR change layers, calculated by finding the difference between in fPAR between August 2004 and June 2005 (i.e., dotted line marked in figure 2), do not include vegetation changes that occurred between June and early August of 2005. Following this approach, the resultant change layers represent the amount of new green biomass available (e.g. actively growing grasses) as the difference between the total biomass during the Fall active growth period (i.e., actively growing grasses, accumulated litter, and residual plant matter) and the total biomass at the end of the spring growing season (i.e., accumulated litter and residual plant matter).

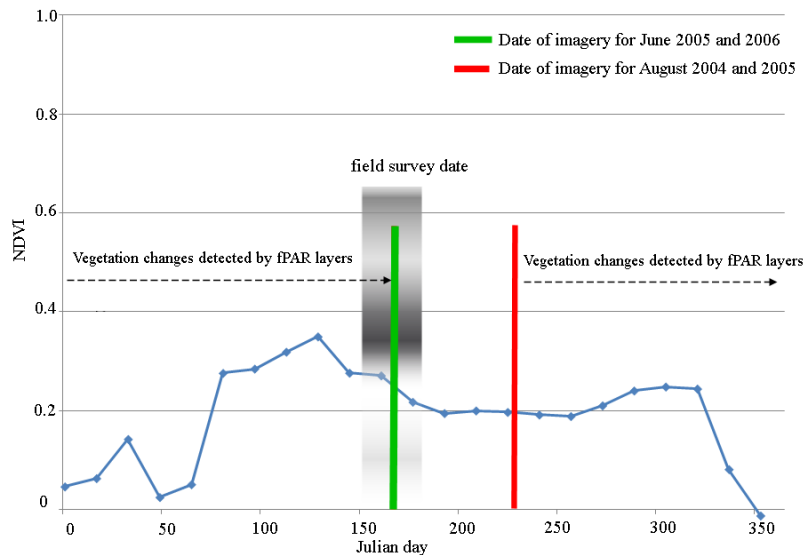


**Figure 2. Annual phenology as described using NDVI of 2007 in relation to the dates of imagery selected for the study.**

Using four years of field survey data, we note that grass, shrub, and dominant weeds tend to be green and actively growing, resulting in high fPAR values, during spring and early summer (i.e., June). In the late-summer senescence period, high temperatures hasten the desiccation of plants and in contrast to the active growing period, fPAR values are reduced and substantially different at this time. Therefore, we selected TM and MODIS imagery during these periods to optimally detect fPAR change and thereby better understand seasonal productivity within semiarid rangelands.

Two notable wildfires occurred in the Big Desert study area: one in August 2000 (Millennial Fire) and another in August 2006 (Crystal Fire). The Millennial Fire burned approximately 62,018 ha within the Big Desert study area. The Crystal fire burned approximately 90,528 ha of grasslands and sagebrush between August 15 and August 31, 2006, and more than 16,100 ha of grassland were burned in a single day.

### *Pre-fire Vegetation Change Distribution Monitoring*

Image differencing is a widely used change detection technique for remotely sensed data and change data are often thresholded (Singh 1989; Ridd and Liu 1998) or classified (Lyon *et al.* 1998). In this study image differencing was used to calculate pre-fire NDVI/fPAR changes in different years, however, image differencing is not used for setting thresholds to determine whether fPAR changed or not. TM NDVI/fPAR change layers were calculated by subtracting NDVI/fPAR values for 10 August 1998 from NDVI/fPAR values for 25 May 1999. Similarly, NDVI/fPAR values for 29 August 1999 were subtracted from NDVI/fPAR values for 27 May 2000. MODIS NDVI/fPAR change layers were calculated by subtracting August 2004 values from June 2005 values, and subtracting August 2005 values from June 2006 values. The historic fire perimeter database of Idaho maintained by USDI BLM (Collins R, BLM, Idaho State Office, <http://inside.uidaho.edu/geodata/BLM/index.htm>) was used to overlay wildfire perimeter layers upon Landsat-5 NDVI/fPAR change layers and MODIS NDVI/fPAR change layers for inspection. NDVI and fPAR change layers were compared with monthly precipitation, monthly mean temperature, and field-based measurements of forage biomass and percent ground cover within the Crystal Fire area. This was not done for the Millennial Fire area as detailed field data were not available within its fire perimeter. Lastly, a total of 500 independent randomly distributed test points were selected from NDVI/fPAR change layers. Of these, 207 points were retained for analysis within the Millennial Fire area and 238 points were retained within the Crystal fire area after removing all points falling in “no-data” areas of the imagery. Pixel values were extracted, and mean values of NDVI change and fPAR change at different years were summarized to assess the susceptibility of semiarid rangelands to wildfires.

## **RESULTS AND DISCUSSION**

Pre-fire TM NDVI/fPAR change layers illustrate an overall increase in NDVI and fPAR values ( $0.1 < \text{NDVI/fPAR change} < 0.5$ ) within the Millennial Fire area between 1998 and 1999 (i.e., two years prior to the fire, Figure 3 and Figure 4). Similarly, NDVI values increased 0.15 - 0.25 and fPAR values increased  $>0.20$  within the Crystal Fire area from 2004 to 2005 (i.e., two years prior to the fire). Compared to the "two years prior to the fire" period, where NDVI/fPAR change values showed an overall increase, there was a substantial difference with the "one year prior to fire" period (NDVI/fPAR change  $< 0.1$ ). In general, NDVI and fPAR values for both the Millennial and Crystal Fire areas experienced large increases two years prior to the fire period, with much lower increases in NDVI and fPAR values just one year prior to the fire. These changes likely correspond to a change in vegetation conditions (e.g., vegetation cover, and biomass) within the fire areas as the same overall trend of change was depicted in both the fPAR and NDVI change maps.

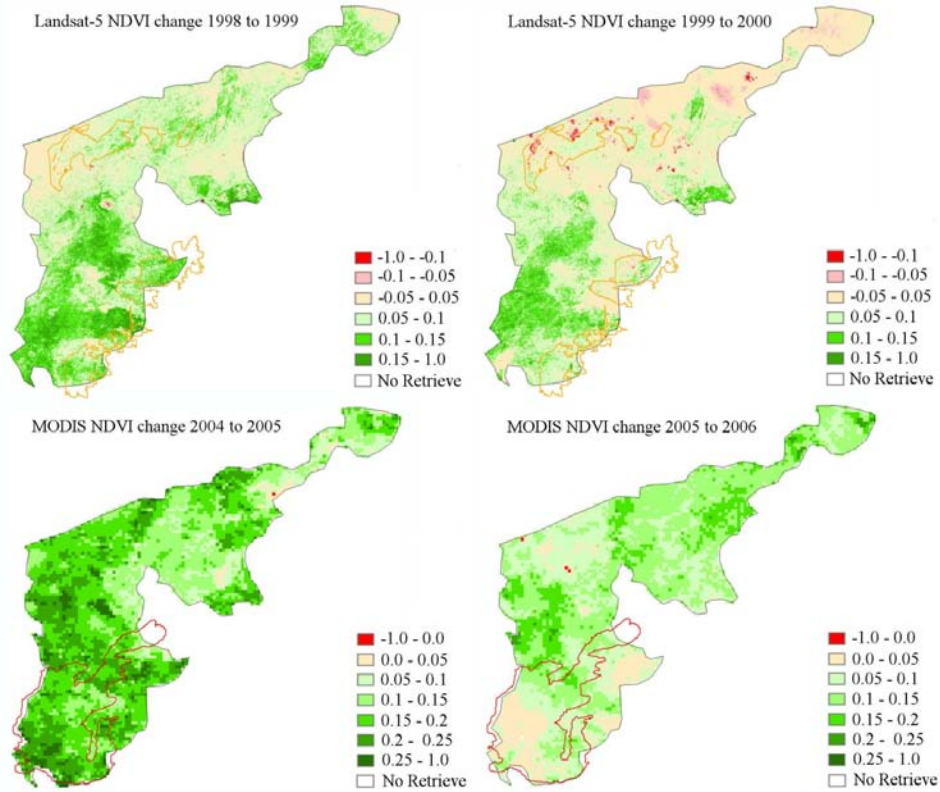


Figure 3. Pre-fire Landsat-5TM NDVI and MODIS NDVI change layers.

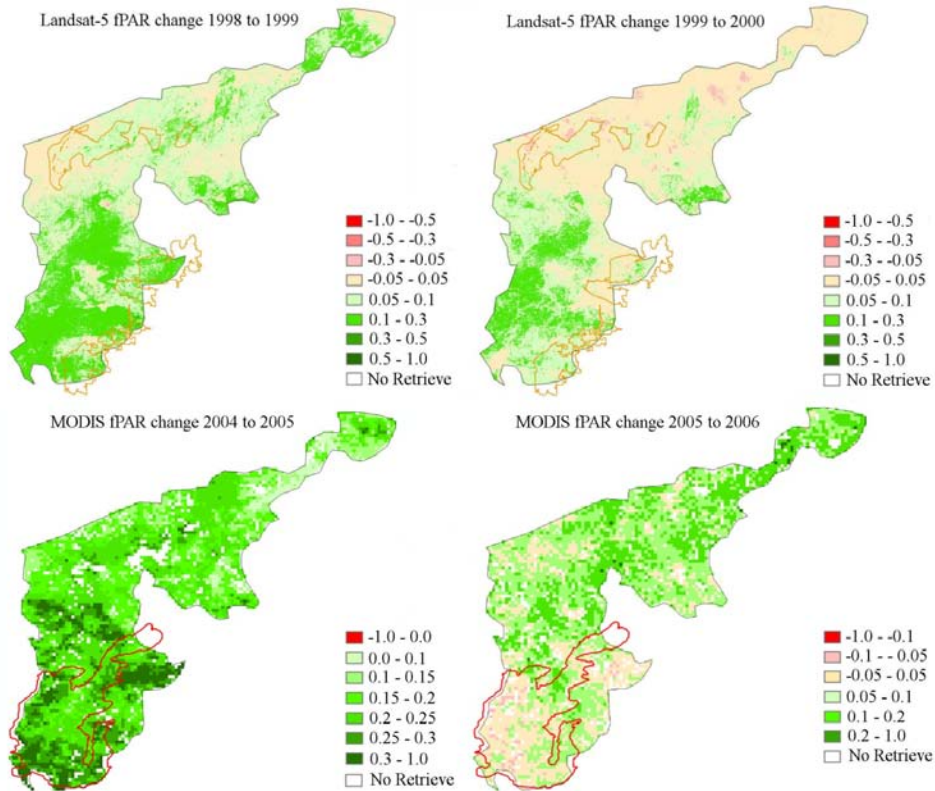


Figure 4. Pre-fire Landsat-5TM fPAR and MODIS fPAR change layers.

Grass is a common component of the fuel load in southeast Idaho, and accumulated fuel loads can burn intensely and severely. The development of fuel stockpiles and the prevalence of cheatgrass (*Bromus tectorum*), an invasive annual grass, have made the fuels on Idaho's rangelands increasingly problematic (Weber *et al.* 2008b). Historically, rangelands in southeast Idaho experienced wildfire throughout a 2-3 week period in late summer (Judd pers. comm.). However, with the introduction of cheatgrass, the wildfire "season" has been inadvertently extended to approximately 2-3 months as this non-native annual grass senesces early in the growing season and produces large contiguous areas of highly flammable fine fuels. Therefore, in rangeland ecosystems like these, ground vegetation conditions closely correlate with fuel load which in turn, can function as an early warning for rangeland wildfire.

The observed NDVI and fPAR changes are a function of changes in grasses as these are more ephemeral in nature than shrubs. In order to validate this observation, field-based measurements of forage biomass and percent cover of grasses in the Crystal Fire area were examined. Average grass cover in 2004 and 2005 were similar, however, forage biomass in 2004 (334 Kg/Ha) was less than in 2005 (583 Kg/Ha) (Table 3). While more grass was produced in 2005 than in 2004 this is most probably the result of increased precipitation during that same year (Le Houérou and Hoste, 1977; Fisher *et al.* 1988). Average precipitation between March and June of 2005, (a crucial part of the growing season in southeast Idaho rangelands), was 330 mm with 40% of the total falling in May while in 2004 there was only 145 mm of rainfall (SD= 57 mm) (Table 2; Table 4). From 2005 to 2006 average grass cover increased only 1-3%, and forage biomass reduced 300 Kg/Ha. Similarly, average precipitation between March and June of 2006 was reduced as well (259 mm) (SD= 73 mm) with most of this precipitation falling between March (85 mm) and April (116 mm).

**Table 3. Forage biomass and percent ground cover for fPAR change analysis**

	Forage Biomass (Kg/Ha)	Average ground percent cover (%)					Number of sample plots
		Shrub	Grass	Litter	Bare ground	Weed	
Fire areas 2004	334	5-12	5-12	6-15	53-78	1-5	47
Fire areas 2005	583	6-14	5-13	1-7	48-71	1-6	57
Fire areas 2006	283	17-26	6-16	18-29	15-23	5-11	24
Changes in fire areas 2004-2005	249	1-2	0-1	-(5-8)	-(5-6)	0-1	N/A
Changes in fire areas 2005-2006	-300	11-12	1-3	17-22	-(33-48)	-(1-5)	N/A

**Table 4. Analysis of precipitation (mm) and temperature (°C) on 2004, 2005 and 2006**

Year	Average precipitation				Average temperature				Average four months precipitation	Standard deviations
	March	April	May	June	March	April	May	June		
2004	22	35	65	22	3	6	9	13	145	57* 73**
2005	56	70	144	59	1	4	9	11	330	
2006	85	116	37	22	-1	5	10	15	259	

\*Standard deviation of precipitation for 2004 and 2005. \*\*Standard deviation of precipitation for 2005 and 2006.

The majority of grass growth activity occurs within a specific range of temperatures (Went 1953). Comparing average temperatures in May 2005 (9°C), which was the major precipitation period for 2005, with average temperatures in March (-1 °C) and April (5°C) of 2006 the effect on grass growth becomes apparent (Table 4) (Figure 5). Because temperature and precipitation act together to affect the biophysical and ecological status of grasses we conclude that monthly precipitation and mean temperature in the spring of 2005 were much better suited for grass growth than that seen in 2006, hence more grass was produced between 2004 and 2005 than between 2005 and 2006 (Figure 6). These differences in grass growth activity suggests a concomitant change in NDVI and fPAR should exist. Analysis of monthly precipitation, mean temperature, field-based measurements of ground cover, and measures of biomass suggest that the Crystal Fire area should have greater NDVI and fPAR change between 2004 and 2005 than between 2005 and 2006.

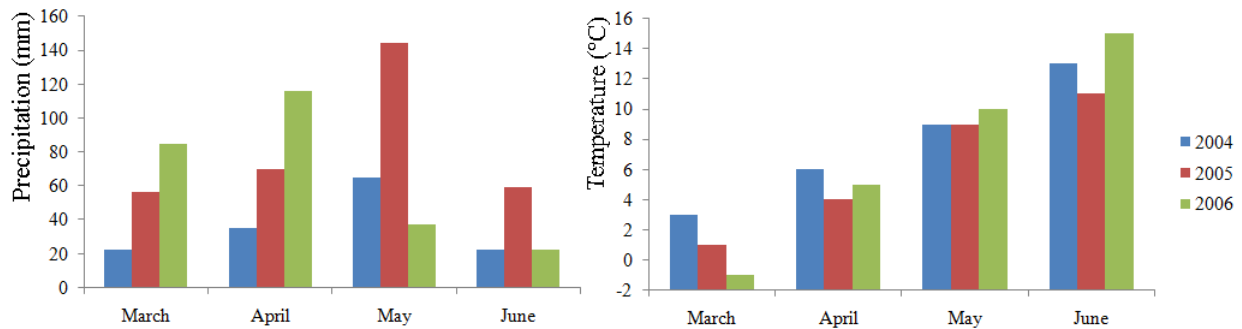


**Figure 5. Monthly precipitation and temperature for the study.**

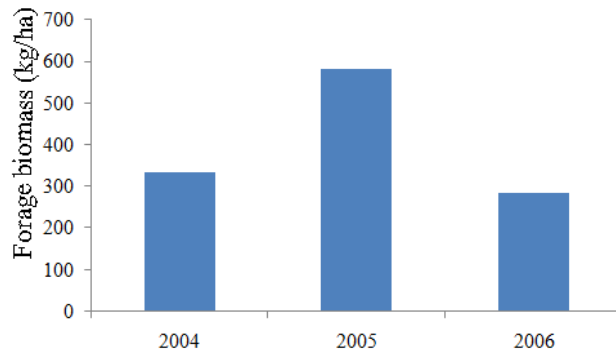


**Figure 6. Yearly forage biomass for the study.**

In order to validate this supposition, fPAR and NDVI annual changes showed in Figure 7. It is noted that either NDVI or fPAR, the change values two years prior to the fire (e.g., 2004 to 2005) were greater than those one-year prior to fire (e.g., 2005 to 2006). This suggested that there was the prevalence of grasses in two years prior to fire period for each wildfire. Thus, it is concluded that the information represented by field-based measurements follow the same trend as indicated in the NDVI and fPAR change maps. NDVI and fPAR have means for assessing pre-fires vegetation changes, and the susceptibility to wildfire can be estimated using in a NDVI/fPAR change analysis.

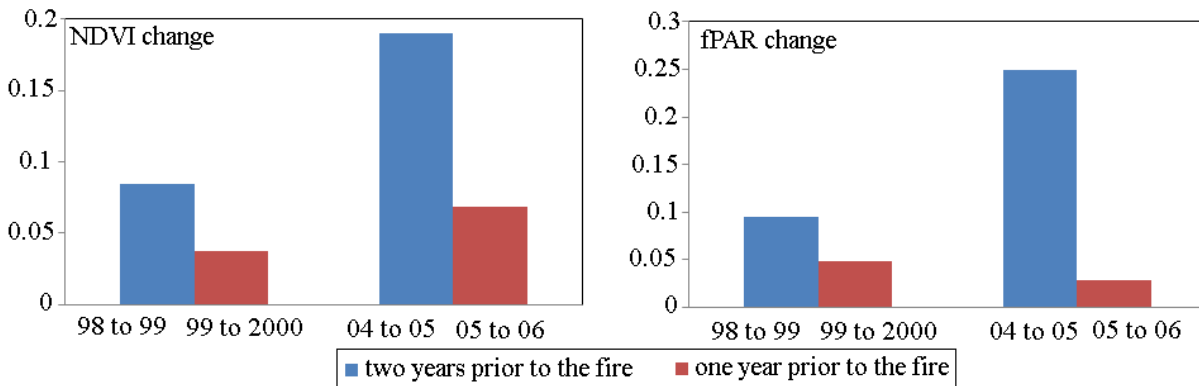


**Figure 7. Summary for NDVI and fPAR change in different years.**

Another important component of fine fuels in semiarid ecosystems is litter. Litter is senescent (dead or dry) plant material and in general, an abundance of grasses ultimately leads to an increase in litter (Nagler *et al.* 2000) unless herbivory, trampling by livestock (leading to accelerated rates of organic decomposition), or wildlife removes the litter. Although rangeland fuels are relatively simple compared to forest fuels, different species of rangeland plants generate different fire behavior characteristics depending on factors like moisture content and blade height (Sandberg *et al.* 2001; Agee *et al.* 2002). In comparison to green grass, litter and dry grass flashes much more quickly and burns easily. Therefore, an area covered by a continuous surface of litter and dry grass is more flammable than areas with less litter cover.

Average percent litter cover increased 17-22% (while forage biomass decreased 300 Kg/Ha) in the Crystal Fire area from 2005 to 2006 (Table 3). The mean litter cover class in 2005 was only 1-7%, however, mean litter cover increased to 18-29% in the following year. In light of these data, the following interpretation is offered: the prevalence of grasses reported from 2004 to 2005 was followed by a reduction in photosynthetically active grass productivity between 2005 to 2006 in the Crystal Fire area. Following two years of highly productive growth, many grasses died back (due to drier conditions) and contributed to an increase in litter (i.e., fine fuels).

The observed changes in grass productivity reported in this study were found to closely correlate (albeit with a lag interval) to a change in litter cover. As a result, the prevalence of litter in 2006 most likely had an effect on the size and severity of the Crystal Fire. These observations and trends were observed in both the NDVI and fPAR change layers which suggests the potential for these data to be used for future fire risk modeling. The absence of field data between 1998 and 1999 limited the susceptibility analysis to

Millennial Fire. However, interpretation of 2004-2006 field data offer insights into the patterns TM data represented.

A survey of current literature indicates that multi-sensor NDVI (thus, fPAR) those derived from AVHRR, MODIS, TM, ETM+, Spot-4 and QuickBird exhibit offsets (Goetz, 1997; Steven et al., 2003). Sensor spatial resolution, atmospheric calibration, and fPAR retrieval algorithm will have effect on the accuracy of NDVI/fPAR comparison. There is no comparison between TM and MODIS in this study, however, we would anticipate that the error caused by spatial resolution, reflectance calibration and the fPAR calculation method would have effect on the sensitivity of the change algorithm to actual changes on the ground. In addition, NDVI may not exhibit an immediate and direct response to changes in vegetation moisture and water content as high temperatures hasten the desiccation of grass during the late-summer senescence period (Ceccato *et al.* 2001). As a result, dry grasses and litter constitute part of any NDVI value and can range from 0.09 to 0.20 in areas entirely covered by litter in late summer (Nagler *et al.* 2000). In contrast, fPAR values of dry grass and litter reduce to 0.00, and are substantially different from those seen during the active growth period. For these reasons, fPAR change layers were considered sensitive to litter within semiarid rangeland ecosystems. Therefore, fPAR could be an input source for fire early warning models, and increase the efficiency of fire management in semiarid rangeland.

## **CONCLUSION**

Using MODIS NDVI/fPAR products and TM NDVI/fPAR algorithms, this study focused on assessing pre-fire vegetation characteristics and fuel load change. TM and MODIS NDVI/fPAR data were compared between active growth periods and late-summer senescence periods and interpreted using monthly precipitation, mean temperature, and field-based measurements of forage biomass and percent ground cover from 2004, 2005, and 2006. In general, fPAR exhibited a similar trend of change relative to NDVI, and the results of this study indicate that both NDVI and fPAR can be used to assess susceptibility of rangelands to wildfire. Used over long time periods, these data may also be applied to the determination of areas suitable for fuel load reduction, which may eliminate or reduce wildfire danger in many areas. In an ideal situation both MODIS and Landsat imagery would have been available for all parts of this study. In addition, it would have been useful to have extensive pre-fire vegetation data for all fire areas. These needs were very difficult to anticipate and future field campaigns are planned to address this issue. Furthermore, wildfire susceptibility predictions are very complicated and this study represents an incremental step toward improved wildfire susceptibility modeling research. We considering additional ecological and environmental parameters to improve future models and the incorporation of pixel-based parameters (e.g., precipitation, and temperature) which may achieve better results in the future.

## **ACKNOWLEDGEMENTS**

This study was made possible by a grant from the National Aeronautics and Space Administration Goddard Space Flight Center (NNX08AO90G). ISU would also like to acknowledge the Idaho Delegation for their assistance in obtaining this grant.

## **LITERATURE CITED**

Agee, J.K., C.S. Wright, N. Williamson, M.H. Huff, 2002. Foliar Moisture Content of Pacific Northwest Vegetation and its Relation to Wildland Fire Behavior. *Forest Ecology and Management* 167, 57-66

- Aguado, I., E. Chuvieco, P. Martin, J. Salas, 2003. Assessment of Forest Fire Danger Conditions in Southern Spain from NOAA Images and Meteorological Indices. *International Journal of Remote Sensing* 24:1653-1668
- Boelman, N.T., M. Stieglitz, H.M. Rueth, M. Sommerkorn, K.L. Griffin, G.R. Shaver, J.A. Gamon, 2003. Response of NDVI, Biomass, and Ecosystem Gas Exchange to Long-term Warming and Fertilization in Wet Sedge Tundra. *Oecologia*, 135:414-421
- Bonan, G.B., 1995. Land-atmosphere Interactions for Climate System Models: Coupling Biophysical, Biogeochemical, and Ecosystem Dynamical Processes. *Remote Sensing of Environment* 51:57-73
- Breman, H., C.T. de Wit, 1983. Rangeland Productivity and Exploitation in the Sahel. *Science* 221:1341-1347
- Brewer, C.K., J.C. Winne, R.L. Redmond, D.W. Opitz, M.V. Magrich, 2005. Classifying and mapping wildfire severity: a comparison of methods. *Photogrammetric Engineering & Remote Sensing* 71:1311-1320
- Ceccato, P., S. Flasse, S. Tarantola, S. Jacquemoud, J.M. Gregoire, 2001. Detecting Vegetation Leaf Water Content using Reflectance in the Optical Domain. *Remote Sensing of Environment* 77:22-33
- Chander, G., B. Markham, 2003. Revised Landsat-5 TM Radiometric Calibration Procedures and Post-calibration Dynamic Ranges. *IEEE Transactions on Geoscience and Remote Sensing* 41:2674-2677
- Chavez, P.S. Jr., 1996. Image-based Atmospheric Corrections-revisited and Improved. *Photogrammetric Engineering and Remote Sensing* 62:1025-1036
- Chen, F., J.M. Tang, N. Zheng, 2008. Estimating the Impact of Urbanization on LAI/fPAR in the Baltimore-Washington Corridor Area. *Canadian Journal of Remote Sensing* 34:326-337
- Chen, J.M., 1996. Canopy Architecture and Remote Sensing of the Fraction of Photosynthetically Active Radiation Absorbed by Boreal Conifer Forests. *IEEE Transactions on Geoscience and Remote Sensing* 34:1353-1368
- Chen, J.M., J. Cihlar, 1996. Retrieving Leaf Area Index of Boreal Conifer Forests using Landsat TM Images. *Canadian Journal of Remote Sensing* 55: 153-162
- Chuvieco, E., D. Cocero, D. Riano, P. Martin, J. Martínez-Vega, J. Riva, F. Pérez, 2004. Combining NDVI and Surface Temperature for the Estimation of Live Fuel Moisture Content in Forest Fire Danger Rating. *Remote Sensing of Environment* 92:322-331
- Chuvieco, E., R.G. Congalton, 1989. Applications of Remote Sensing and Geographic Information Systems to Forest Fire Hazard Mapping. *Remote Sensing of Environment* 29:147-159

- Chuvieco, E., D. Riaño, I. Aguado, D. Cocero, 2002. Estimation of Fuel Moisture Content from Multitemporal Analysis of Landsat Thematic Mapper Reflectance Data: Applications in Fire Danger Assessment. *International Journal of Remote Sensing*. 23:2145-2162
- Collins, B.M., P.N. Omi, P.L. Chapman, 2006. Regional Relationships between Climate and Wildfire-burned Area in the Interior West, USA. *Canadian Journal of Forest Research*. 36:699-709
- Crutzen, P.J., L.E. Heidt, J.P. Krasnec, W.H. Pollock, W. Seiler, 1979. Biomass Burning as a Source of Atmospheric Gases CO, H<sub>2</sub>, N<sub>2</sub>O, NO, CH<sub>3</sub>Cl and COS. *Nature*. 282:253-256
- Danson, F.M., P. Bowyer, 2004. Estimating Live Fuel Moisture Content from Remotely Sensed Reflectance. *Remote Sensing of Environment*. 92:309-321
- Daughtry, C.S.T., K.P. Gallo, M.E. Bauer, 1983. Spectral Estimates of Solar Radiation Intercepted by Corn Canopies. *Agronomy Journal*. 75:527-531
- Dennison, P.E., M.A. Moritz, R.S. Taylor, 2008. Evaluating Predictive Models of Critical Live Fuel Moisture in the Santa Monica Mountains, California. *International Journal of Wildland Fire*. 17:18-27
- EPA, 2008. Inventory of U.S. Greenhouse Gas Emissions and Sinks, 1990-2006. (United States Environmental Protection Agency: Washington, DC)
- Epting, J., D. Verbyla, B. Sorbel, 2005. Evaluation of Remotely Sensed Indices for Assessing Burn Severity in Interior Alaska using Landsat TM and ETM+. *Remote Sensing of Environment*. 96:328-339
- Escuin, S., R. Navarro, P. Fernández, 2008. Fire Severity Assessment by using NBR (Normalized Burn Ratio) and NDVI (Normalized Difference Vegetation Index) Derived from LANDSAT TM/ETM Images. *International Journal of Remote Sensing*. 29:1053-1073
- Fernandez, A., P. Illera, J.L. Casanova, 1997. Automatic Mapping of Surfaces Affected by Forest Fires in Spain using AVHRR NDVI Composite Image Data. *Remote Sensing of Environment*. 60:153-162
- Fisher, F.M., J.C. Zak, G.L. Cunningham, W.G. Whitford, 1988. Water and Nitrogen Effect on Growth and Allocation Patterns of Creosote Bush in the Northern Chihuahuan Desert. *Journal of Range Management*. 41:387-391
- Fisher, R., W.E. Bobanuba, A. Rawambaku, G.J. Hill, J. Russell-Smith, 2005. Remote Sensing of Fire Regimes in Semi-arid Nusa Tenggara Timur, Eastern Indonesia: Current Patterns, Future Prospects. *International Journal of Wildland Fire*. 15:307-317
- Franklin, S.E., R.J. Hall, L. Smith, G.R. Gerylo, 2003. Discrimination of Conifer Height, Age and Crown Closure Classes using Landsat-5 TM imagery in the Canadian Northwest. *International Journal of Remote Sensing*. 24:1823-1834

- Fraser, R.H., Z. Li, 2002. Estimating Fire-related Parameters in Boreal Forest using SPOT VEGETATION. *Remote Sensing of Environment*. 82:95-110
- Giglio, L., J. Desloîtres, C.O. Justice, Y.J. Kaufman, 2003. An Enhanced Contextual Fire Detection Algorithm for MODIS. *Remote Sensing of Environment*. 87:273-282
- Gnieting, P., J. Gregory, K.T. Weber, 2005. Datum Transforms Involving WGS84.  
URL = [http://giscenter.isu.edu/research/techpg/nasa\\_tlcc/template.htm](http://giscenter.isu.edu/research/techpg/nasa_tlcc/template.htm) visited February 2007
- Goetz, S.J., 1997. Multi-sensor Analysis of NDVI, Surface Temperature and Biophysical Variables at a Mixed Grassland Site. *International Journal of Remote Sensing*. 18: 71-94
- Greenberg, J.P., P.R. Zimmerman, L. Heidt, W. Pollock, 1984. Hydrocarbon and Carbon Monoxide Emissions from Biomass Burning in Brazil. *Journal of Geophysical Research*. 89:1350-1354
- Hassan, Q.K., C.P-A. Bourque, F. Meng, 2006. Estimation of Daytime Net Ecosystem CO<sub>2</sub> Exchange over Balsam Fir Forests in Eastern Canada: Combining Averaged Tower-based Flux Measurements with Remotely Sensed MODIS Data. *Canadian Journal of Remote Sensing*. 32:405-416
- Hély, C., P.R. Dowty, S. Alleaume, K.K. Caylor, S. Korontzi, R.J. Swap, H.H. Shugart, C.O. Justice, 2003. Regional Fuel Load for Two Climatically Contrasting Years in Southern Africa. *Journal of Geophysical Research (Atmospheres)* 108, doi:10.1029/2002JD002341
- Hill, M.J., G.E. Donald, 2003. Estimating Spatio-temporal Patterns of Agricultural Productivity in Fragmented Landscapes using AVHRR NDVI Time Series. *Remote Sensing of Environment*. 84:367-384
- Hilty, J.H., D.J. Eldridge, R. Rosentreter, M.C. Wicklow-Howard, M. Pellant, 2004. Recovery of Biological Soil Crusts following Wildfire in Idaho. *Journal of Range Management*. 57:89-96
- Holden, Z.A., A.M.S. Smith, P. Morgan, M.G. Rollins, P.E. Gessler, 2005. Evaluation of Novel Thermally Enhanced Spectral Indices for Mapping Fire Perimeters and Comparisons with Fire Atlas Data. *International Journal of Remote Sensing*. 26:4801-4808
- Houghton, R.A., 1992. Biomass Burning from the Perspective of the Global Carbon Cycle. Pages 321-325 in J. S. Levine (Ed.) Global biomass burning, Cambridge, Massachusetts: MIT Press
- Huete, A., K. Didan, T. Miura, E.P. Rodriguez, X. Gao, L.G. Ferreira, 2002. Overview of the Radiometric and Biophysical Performance of the MODIS Vegetation Indices. *Remote Sensing of Environment* 82: 195-213
- Huntsinger, L., P. Hopkinson, 1996. Viewpoint: Sustaining Rangeland Landscapes: A Social and Ecological Process. *Journal of Range Management* 49:167-173

- Illera P., A. Fernandez, J.A. Delgado, 1996. Temporal Evolution of the NDVI as an Indicator of Forest Fire Danger. *International Journal of Remote Sensing* 17:1093-1105
- Keane R.E., R. Burgan, J. van Wagtenok, 2001. Mapping Wildland Fuels for Fire Management Across Multiple Scales: Integrating Remote Sensing, GIS, and Biophysical Modeling. *International Journal of Wildland Fire* 10:301-319
- Kennedy P.J., A.S. Belward, J.M. Gregoire, 1994. An Improved Approach to Fire Monitoring in West Africa using AVHRR Data. *International Journal of Remote Sensing*. 15:2235-2255
- Kercher S.M., C.B. Frieswyk, J.B. Zedler, 2003. Effects of Sampling Teams and Estimation Methods on the Assessment of Plant Cover. *Journal of Vegetation Science*. 14:899-906
- Key, C.H. and N. C. Benson, 1999. The Normalized Burn Ratio (NBR): A Landsat TM Radiometric Index of Burn Severity. URL = <http://www.nrmc.usgs.gov/research/ndbr.htm> visited April 2007
- Knyazikhin Y., J.V. Martonchik, R.B. Myneni, D.J. Diner, S.W. Running, 1998. Synergistic Algorithm for Estimating Vegetation Canopy Leaf Area Index and Fraction of Absorbed Photosynthetically Active Radiation from MODIS and MISR Data. *Journal of Geophysical Research* 103:32257-32274
- Leblon B., M. Alexander, J. Chen, S. White, 2001. Monitoring Fire Danger of Northern Boreal Forests with NOAA-AVHRR NDVI Images. *International Journal of Remote Sensing* 22:2839-2846
- Le Hou rou H.N., C.H. Hoste, 1977. Rangeland Production and Annual Rainfall Relations in the Mediterranean Basin and in the African Sahelo-Sudanian Zone. *Journal of Range Management*. 30:181-189
- Lentile, L.B., Z.A. Holden, A.M.S. Smith, M.J. Falkowski, A.T. Hudak, P. Morgan, S.A. Lewis, P.E. Gessler, and N.C. Benson, 2006. Remote Sensing Techniques to Assess Active Fire Characteristics and Post-Fire Effects. *Intl. Journal of Wildland Fire*. 15(3):319-345
- Li R.R., Y.J. Kaufman, W.M. Hao, J.M. Salmon, B.C. Gao, 2004. A Technique for Detecting Burn Scars using MODIS Data. *IEEE Transactions on Geoscience and Remote Sensing*. 42:1300-1308
- Los S.O., G.J. Collatz, P.J. Sellers, C.M. Malmstr m, N.H. Pollack, R.S. Defries, L. Bounoua, M.T. Parris, C.J. Tucker, D.A. Dazlich, 2000. A Global 9-year Biophysical Land-surface Data Set from NOAA AVHRR data. *Journal of Hydrometeorology*. 1:183-199
- Lyon J.G., D. Yuan, R.S. Lunetta, C.D. Elvidge, 1998. A Change Detection Experiment using Vegetation Indices. *Photogrammetric engineering and remote sensing*. 64:143-150
- Maki M., M. Ishihara, M. Tamura, 2004. Estimation of Leaf Water Status to Monitor the Risk of Forest fires by using Remotely Sensed Data. *Remote Sensing of Environment* 90: 441-450

- Mbow C., G. Kalifa, B. Goze, 2004. Spectral Indices and Fire Behavior Simulation for Fire Risk Assessment in Savanna Ecosystems. *Remote Sensing of Environment*. 91:1-13
- Means J.E., S.A. Acker, D.J. Harding, J.B. Blair, M.A. Lefsky, W.B. Cohen, M.E. Harmon, W.A. McKee, 1999. Use of Large-footprint Scanning Airborne Lidar to Estimate Forest Stand Characteristics in the Western Cascades of Oregon. *Remote Sensing of Environment*. 67:298-308
- Miller J.D., S.R. Yool, 2002. Mapping Forest Post-fire Canopy Consumption in Several Overstory Types using Multi-temporal Landsat TM and ETM Data. *Remote Sensing of Environment*. 82:481-496
- Morisette J.T., L. Giglio, I. Csiszar, C.O. Justice, 2005. Validation of the MODIS Active Fire Product over Southern Africa with ASTER Data. *International Journal of Remote Sensing*. 26:4239 - 4264
- Mutch R.W., 1970. Wildland Fires and Ecosystems-a Hypothesis. *Ecology*. 51:1046-1051
- Myneni R.B., Y. Knyazikhin, Y. Zhang, Y. Tian, Y. Wang, A. Lotsch, J.L. Privette, J.T. Morisette, S.W. Running, R. Nemani, J. Glassy, P. Votava, 1999. MODIS Leaf Area Index (LAI) and Fraction of Photosynthetically Active Radiation Absorbed by Vegetation (FPAR) Product (MOD15) Algorithm Theoretical Basis Document. URL = [http://modis.gsfc.nasa.gov/data/atbd/land\\_atbd.php](http://modis.gsfc.nasa.gov/data/atbd/land_atbd.php)
- Myneni R.B., D.L. Williams, 1994. On the Relationship between FAPAR and NDVI. *Remote Sensing of Environment*. 49:200-211
- Nagler P.L., C.S.T. Daughtry, S.N. Goward, 2000. Plant Litter and Soil Reflectance. *Remote Sensing of Environment*. 71:207-215
- Nelson R., W. Krabill, J. Tonelli, 1988. Estimating Forest Biomass and Volume using Airborne Laser Data. *Remote Sensing of Environment*. 24:247-267
- Paltridge G.W., J. Barber, 1988. Monitoring Grassland Dryness and Fire Potential in Australia with NOAA AVHRR Data. *Remote Sensing of Environment*. 25:381-394
- Paruelo J.M., H.E. Epstein, W.K. Lauenroth, I.C. Burke, 1997. ANPP Estimates from NDVI for the Central Grassland Region of the United States. *Ecology*. 78: 953-958
- Pierson F.B., D.H. Carlson, K.E. Spaeth, 2002. Impacts of Wildfire on Soil Hydrological Properties of Steep Sagebrush-steppe Rangeland. *International Journal of Wildland Fire*. 11:145-151
- Pozo D., F.J. Olmo, L. Alados-arboledas, 1997. Fire Detection and Growth Monitoring using a Multitemporal Technique on AVHRR Mid-infrared and Thermal Channels. *Remote Sensing of Environment* 60:111-120

- Riano D., E. Chuvieco, J. Salas, A. Palacios-Orueta, A. Bastarrika, 2002. Generation of Fuel Type Maps from Landsat TM Images and Ancillary Data in Mediterranean Ecosystems. *Canadian Journal of Forest Resources* 32:1301-1315
- Ridd M.K., J. Liu, 1998. Comparison of Four Algorithms for Change Detection in an Urban Environment. *Remote Sensing of Environment* 63:95-100
- Sandberg D.V., R.D. Ottmar, G.H. Cushon, 2001. Characterizing Fuels in the 21st Century. *International Journal of Wildland Fire*. 10: 381-387
- Sellers P.J., J.A. Berry, G.J. Collatz, C.B. Field, F.G. Hal, 1992. Canopy Reflectance, Photosynthesis, and Transpiration. III. A Reanalysis using Improved Leaf Models and a New Canopy Integration Scheme. *Remote Sensing of Environment*. 42:187-216
- Sellers P.J., S.O. Los, C.J. Tucker, C.O. Justice, D.A. Dazlich, G.J. Collatz, D.A. Randall, 1996. A Revised Land Surface Parameterization (SiB2) for Atmospheric GCMs. Part II: The Generation of Global Fields of Terrestrial Biophysical Parameters from Satellite Data. *Journal of Climate*. 9:706-737
- Serr K., T. Windholz, K.T. Weber, 2006. Comparing GPS Receivers: A Field Study. *Journal of the Urban and Regional Information Systems Association* 18:19-23
- Siegert F., A.A. Hoffmann, 2000. The 1998 Forest Fires in East Kalimantan (Indonesia) - A Quantitative Evaluation using High Resolution, Multitemporal ERS-2 SAR Images and NOAA-AVHRR Hotspot Data. *Remote Sensing of Environment* 72:64-77
- Singh A., 1989. Digital Change Detection Techniques using Remotely-sensed Data. *International Journal of Remote Sensing*. 10: 989-1003
- Smith A.M.S., M.J. Wooster, N.A. Drake, F.M. Dipotso, M.J. Falkowski, A.T. Hudak, 2005. Testing the Potential of Multi-spectral Remote Sensing for Retrospectively Estimating Fire Severity in African Savanna Environments. *Remote Sensing of Environment*. 97: 92-115
- Song C.H., C.E. Woodcock, K.C. Seto, M.P. Lenney, S.A. Macomber, 2001. Classification and Change Detection using Landsat TM Data: When and how to Correct Atmospheric Effects? *Remote Sensing of Environment*. 75: 230-244
- Stenberg, P., M. Rautiainen, T. Manninen, P. Voipio, H. Smolander, 2004. Reduced Simple Ratio better than NDVI for Estimating LAI in Finnish Pine and Spruce Stands. *Silva Fennica*. 38(1): 3-14
- Steven M.D., T.J. Malthus, F. Baret, H. Xu, M.J. Chopping, 2003. Intercalibration of Vegetation Indices from Different Sensor Systems. *Remote Sensing of Environment*. 88: 412-422
- Tarnavsky E., S. Garrigues, M.E. Brown, 2008. Multiscale Geostatistical Analysis of AVHRR, SPOT-VGT, and MODIS Global NDVI Products. *Remote Sensing of Environment*. 112: 535-549

Taylor C.A., 2003. Rangeland Monitoring and Fire: Wildfires and Prescribed Burning, Nutrient Cycling, and Plant Succession. *Arid Land Research and Management*. 17: 429-438

Thomas C.M., S.D. Davis, 1989. Recovery Patterns of Three Chaparral Shrub Species after Wildfire. *Oecologia*. 80: 1432-1939

Tucker, C.J., 1979. Red and Photographic Infrared Linear Combinations for Monitoring Vegetation. *Remote Sensing of Environment*. 8: 127-150

Van Wagtenonk J.W., R.R. Root, 2003. The use of Multi-temporal Landsat Normalized Difference Vegetation Index (NDVI) Data for Mapping Fuel Models in Yosemite National Park, USA. *International Journal of Remote Sensing*. 24: 1639-1651

Verbesselt J., P. Jönsson, S. Lhermitte, J. Aardt, P. Coppin, 2006. Evaluating Satellite and Climate Data-Derived Indices as Fire Risk Indicators in Savanna Ecosystems. *IEEE Transactions on Geoscience and Remote Sensing*. 44: 1622-1632

Weber K.T., S.S. Seefeldt, C. Moffet, J. Norton, 2008a. Comparing Fire Severity Models from Post-fire and Pre/post-fire Differenced Imagery. *GIScience and Remote Sensing*. 45: 392-405

Weber K.T., S.S. Seefeldt, J.M. Norton, C.F. Finley, 2008b. Fire Severity Modeling of Sagebrush Steppe Rangelands in Southeastern Idaho. *GIScience and Remote Sensing*. 45:1-15

Went F.W., 1953. The Effect of Temperature on Plant Growth. *Annual Review of Plant Physiology*. 4: 347-362

West N.E., T.C. Yorks, 2002. Vegetation Responses following Wildfire on Grazed and Ungrazed Sagebrush Semi-desert. *Journal of Range Management*. 55: 171-181

Westerling A.L., T.J. Brown , A. Gershunov, D.R. Cayan, M.D. Dettinger, 2003. Climate and Wildfire in the Western United States. *Bulletin of the American Meteorological Society*. 84: 595-604. DOI: 10.1175/BAMS-84-5-595

Wiedinmyer C., J.C. Neff, 2007. Estimates of CO<sub>2</sub> from Fires in the United States: Implications for Carbon Management. *Carbon Balance and Management*. 2, DOI:10.1186/1750-0680-2-10

Wooster M.J., B. Zhukov, D. Oertel, 2003. Fire Radiative Energy for Quantitative Study of Biomass Burning: Derivation from the BIRD Experimental Satellite and Comparison to MODIS Fire Products. *Remote Sensing of Environment*. 86: 83-107

Yanskey G.R., E.H. Markee Jr., A.P. Richter, 1966. Climatography of the National Reactor Testing Station. USAEC Report IDO-12048. United States Department of Commerce, Environmental Science Services Administration, Air Resources Field Research Office, Idaho Falls, Idaho

**Recommended citation style:**

Chen, F., K.T. Weber, J. Anderson, B. Gokhale, 2011. Assessing the Susceptibility of Semiarid Rangelands to Wildfires using Terra MODIS and Landsat Thematic Mapper Data. Pages 47-68 in K. T. Weber and K. Davis (Eds.), Final Report: Assessing Post-Fire Recovery of Sagebrush-Steppe Rangelands in Southeastern Idaho (NNX08AO90G). 252 pp.

## **Comparison of MODIS fPAR Products with Landsat-5 TM Derived fPAR over Semiarid Rangelands of Idaho**

Fang Chen GIS Training and Research Center, Idaho State University, 921 S. 8<sup>th</sup> Ave, Stop 8104, Pocatello Idaho 83209-8104, chenfang@isu.edu

Keith T. Weber, GIS Director, Idaho State University. GIS Training and Research Center, 921 S. 8th Ave., Stop 8104, Pocatello, ID 83209-8104. webekeit@isu.edu

Jamey Anderson GIS Training and Research Center, Idaho State University, 921 S. 8<sup>th</sup> Ave, Stop 8104, Pocatello Idaho 83209-8104

Bhushan Gokhale GIS Training and Research Center, Idaho State University, 921 S. 8<sup>th</sup> Ave, Stop 8104, Pocatello Idaho 83209-8104

### **ABSTRACT**

While validation of the MODIS fPAR product is well behind that of the LAI product, it is recently receiving more attention. In this study, MODIS fPAR and Landsat-5 TM derived fPAR (TM fPAR) were calculated and quantitatively compared using imagery from 2005 to 2008 for the semiarid rangelands of Idaho, USA. fPAR change maps were calculated between active growth and late-summer senescence periods. Accuracy of the MODIS fPAR and TM fPAR were determined indirectly by incorporating field-based measurements of above-ground forage biomass and percent ground cover from a variety of sites ( $n = 442$ ).

*KEYWORDS: Rangelands, fraction of photosynthetically active radiation absorbed by vegetation (fPAR), Moderate Resolution Imaging Spectroradiometer (MODIS), remote sensing, Idaho*

## INTRODUCTION

Live vegetation responds to radiation, heat, and water balance interactions between the land surface and the atmosphere (Bonan, 1995; Sellers et al., 1997). Currently, most interaction simulation models, including carbon budget models, climate cycle models, and ecosystem productivity models require quantitative vegetation information as a modeling input (Dickinson et al., 1998; Running et al., 1999; Feng et al., 2007). In each case, the fraction of photosynthetically active radiation absorbed by vegetation (fPAR) is a key biophysical parameter (Asner et al., 1998; Running et al., 2004). Many techniques have been developed to measure fPAR and most can be categorized as either a field-based or satellite-based methodology. For example, field-based measurements from flux towers have been widely used to derive fPAR in various ecological environments (Baret et al., 2006; Morisette et al., 2006). Although field-based methods are straightforward and accurate for small scale studies they are also difficult to apply for spatial pattern studies at regional scales.

When it is important to have global or regional measurements of fPAR (e.g., for effective application of interaction simulation models over large areas and long time periods), satellite remote sensing has the advantage of acquiring land surface imagery at broad-spatial scales and frequent temporal periodicity. In addition, satellite based methods provide a unique way to extend the estimations of fPAR into additional productivity metrics such as gross primary production (GPP), net primary production (NPP), and net ecosystem exchange (NEE) (Zhao et al., 2005; Turner et al., 2009).

Moderate Resolution Imaging Spectroradiometer (MODIS) is a key instrument aboard the Terra and Aqua satellites. The MODIS Land Discipline Team (MODLAND) has developed leaf area index (LAI) and fPAR products that provide global 1 km spatial resolution LAI/fPAR images at 8 day intervals (Knyazikhin et al., 1998; Cohen et al., 2003; Morisette et al., 2006). Since the launch of the Terra satellite in December 1999, MODIS LAI/fPAR products have been widely used in many global ecosystem interaction studies including forest (Shabanov et al., 2003; Chen et al., 2008), cropland (Chen et al., 2006; Yang et al., 2007), and grassland ecosystems (Fensholt et al., 2004; Hill et al., 2006).

Experience from previous generations of satellite imaging systems suggests that an independent assessment of product quality is a critical step to the success of MODIS product usage (Justice et al., 2002; Morisette et al., 2002; Turner et al., 2003). For this purpose, the MODIS Science Team has developed several validation projects. "BigFoot" is one such project which provides validation of MODLAND science products (<http://www.fsl.orst.edu/larse/bigfoot/index.html>), including land cover, LAI, fPAR, and NPP (Morisette et al., 2003; Turner et al., 2006). The "Bigfoot" project includes nine carbon flux tower sites (seven in the USA, one in Canada, and one in Brazil) that cover eight major biomes from desert to tundra, and tropical rainforest. fPAR surface images are derived by linking *in situ* measurements to data from Landsat-7 ETM+ and various independent ecosystem process models. Based on validation data from "BigFoot", the quality of MODIS fPAR products and their source error have been assessed, concluding that while it is not possible for a single MODIS pixel accurately estimate fPAR, multiple pixel estimations within and across sites can be accurately estimated (Gower et al., 1999; Milne and Cohen, 1999). The Validation of Land European Remote sensing Instruments (VALERI) project is another project to evaluate the absolute accuracy of the biophysical products (e.g., LAI, fPAR) derived from satellite observations (Garrigues et al., 2007; Baret et al., 2009). More than twenty countries (e.g., Argentina, Australia, China, England, Finland, France, Germany, Spain) collaborate in VALERI project

and MODIS fPAR product is inter-compared with other different sensors and algorithms (Gobron et al., 2006; Weiss et al., 2007). In general, these MODIS validation projects participate in existing long-term ecological research programs (Franklin et al., 1990), scientific data networks such as AERONET (Holben et al., 1998) and FLUXNET (Heinsch et al., 2006), and international validation activities (Swap et al., 2000).

The validation of MODLAND science products is also accomplished by comparison with field measurements or cross-sensor comparison with other satellite sensors. The advantage of field-based validation is that abundant land surface information, such as the exchange of carbon dioxide, water vapor, and energy, across a spectrum of temporal and spatial scales can be used to support the validation. Cross-sensor comparison is another important part of MODLAND science product validation. CYCLOPES LAI/fPAR products (Weiss et al., 2007) and Sea-viewing Wide Field-of-view Sensor (SeaWiFS) fPAR data (Gobron et al., 2006) have been used for the purpose of understanding the difference between MODLAND science products and analogous biophysical parameters derived from other sensors (Garrigues et al., 2008).

Validation of the MODIS LAI/fPAR products have mostly focused on LAI (Tian et al., 2002; Cohen et al., 2003; Shabanov et al., 2003), yet it is important to extend validation to the fPAR product across all biomes. Semiarid rangeland ecosystems (an anthropogenic biome comprising a number of ecological biomes such as semiarid deserts, dry steppes, grasslands and savannas) cover approximately 40% of the earth's terrestrial surface and play an important role in global ecosystem productivity (Bremen and de Wit, 1983; Huntsinger and Hopkinson, 1996). Validation of the MODIS fPAR product in semiarid rangeland ecosystems is important part of the overall product validation.

In September 2006, MODLAND released a new version of MODIS Land Data Products (Collection 5) providing greater data quality than available from Collection 4. Although there are MODIS fPAR validation studies in other semiarid rangelands, (Fensholt et al., 2004; Weiss et al. 2007), previous validation studies were specific to the earlier MODIS fPAR Collection 4 product. To date there have been no papers published for studies of fPAR Collection 5 product validation in the semiarid rangelands of North America.

In this study, fPAR was derived using Landsat 5 TM data following the SR-fPAR retrieval algorithm proposed by Sellers et al. (1992). A cross-sensor comparison was made using MODIS fPAR Collection 5 products and Landsat 5 TM-derived fPAR products. The accuracy of these fPAR products was indirectly determined by incorporating field-based measurements of aboveground forage biomass and percent ground cover from a variety of sites in the semiarid sagebrush-steppe rangelands of Idaho.

## **MATERIALS AND METHODS**

### *Study area*

The study area, known as the Big Desert, lies in southeast Idaho, USA, approximately 71 km northwest of Pocatello. The center of the study area is located at 113° 4' 18.68" W and 43° 14' 27.88" N (Figure 1). This area is managed by the Bureau of Land Management (BLM) and exhibits a large variety of native as well as invasive plant species. The Big Desert is a semiarid sagebrush-steppe ecosystem with a high proportion of bare ground ( $\bar{x}$  bare ground > 17%), and is classified as a Wyoming big sagebrush/blue

bunch wheatgrass habitat type. Annual precipitation is 23 cm with 40% of the precipitation falling from April through June (Yanskey et al., 1966). The area is bordered by geologically young lava formations to the south and west and irrigated agricultural lands to the north and east. Sheep grazing is the primary anthropogenic disturbance to the study area with semi-extensive continuous/seasonal grazing systems used on allotments ranging in size from 1100 to over 125,000 ha. The set stocking rate is low across the study area (>19 ha/animal unit [AU]) with actual utilization approximately 40% of the set stocking rate. Wildfire is a common disturbance and nearly 40% of the study area has burned in the past 10 years.

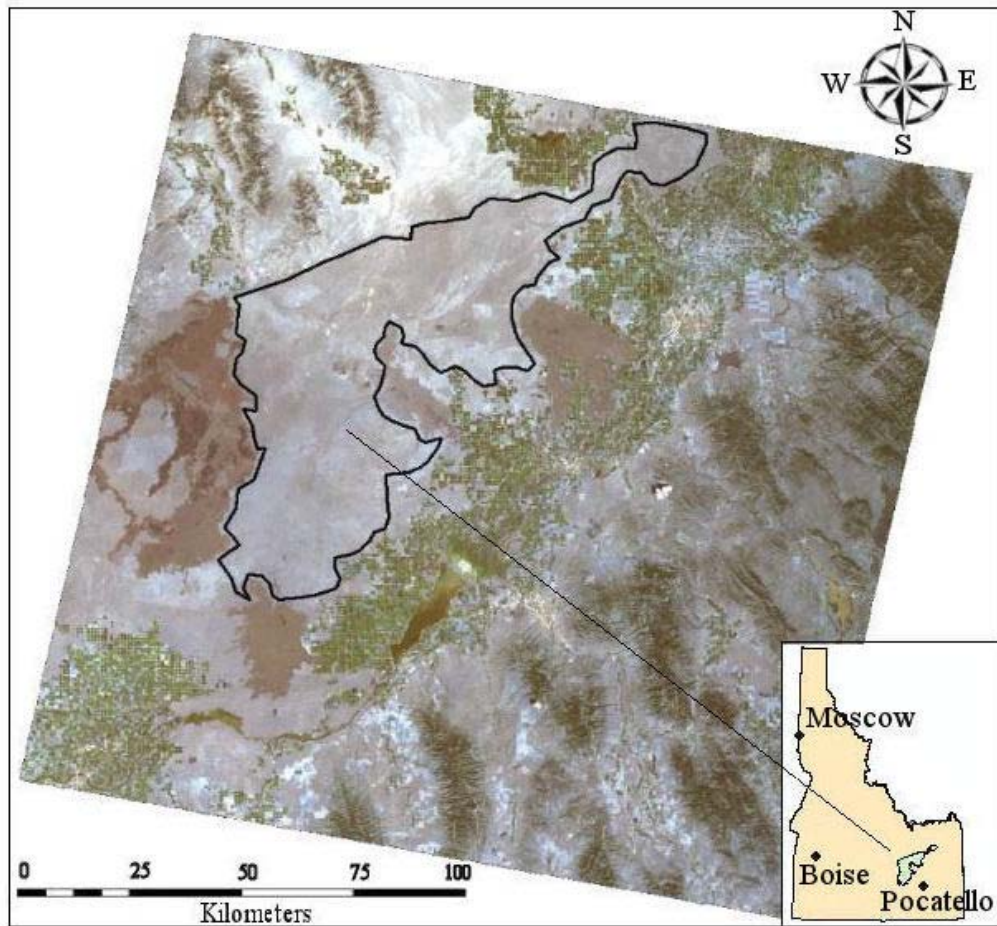


**Figure 1. Location and general characteristics of the Big Desert in southeastern, Idaho, USA. The true color composite of Landsat-5 TM: band3=red, band2=green, band1=blue.**

#### *Sample design and field measurements*

A total of 442 sample points were randomly generated across the Big Desert study area between 2005 and 2008 (Table 1). Each point met the following criteria; 1) >70 meters from an edge (road, trail, or fence line) and 2) < 750 meters from a road. The location of each sample point was recorded using a Trimble Geo XT (2005) or Geo XH (2006-2008) GPS receiver using latitude-longitude (WGS 84) (Serr et al., 2006). Points were occupied until a minimum of 60 positions were acquired for averaging and the Wide Area Augmentation System (WAAS) was used whenever available to improve baseline accuracies. All sample point locations were post-processed differentially corrected (horizontal positional accuracy = +/- 0.70 m (2005) and +/-0.20 m (2006-2008) after post-processing with a 95% CI) using continuously

operation reference stations (CORS) each located <80 km from the study area. All sample points were projected into Idaho Transverse Mercator NAD 83, using ESRI's ArcGIS for datum transformation and projection (Gneiting, et al., 2007).

**Table 1. Dates and numbers of field sample plots used for validation.**

Year	Sampling dates	Number of sample plots
2005	01-June to 15-July	88
2006	05-June to 10-July	175
2007	29-May to 13-June	97
2008	10-June to 11-July	82

Ground cover estimations were made within 10x10m square plots centered over each sample point with the edges of the plots aligned in the cardinal directions. Estimates of percent cover were made for bare ground, litter and duff, grass, shrub, and dominant weed. Cover was classified into one of nine general cover classes (None, 1-5%, 6-15%, 16-25%, 26-35%, 36-50%, 51-75%, 76-95%, and >95%). Available above-ground forage biomass was measured using a plastic coated cable hoop 2.36 meters in circumference. The hoop was randomly tossed into each of four quadrants (NW, NE, SE, and SW) centered over the sample point. All herbaceous species within the hoop that were considered forage for cattle, sheep, and wild ungulates were clipped and weighed (+/-1g) using a Pesola scale tared to the weight of an ordinary paper bag. The measurements were then used to estimate forage amount expressed in kilograms per hectare.

#### *Landsat-5 TM imagery*

Based upon four years of field survey data (2005-2008), it was determined that grasses, shrubs, and dominant weeds tended to be green and most actively growing, resulting in high fPAR values, during spring and early summer (i.e., June) time periods. Later in the summer, high temperatures hasten the desiccation of plants and in contrast to the active growing period, fPAR values are reduced and substantially different at this time. Therefore, we selected Landsat-5 TM and MODIS imagery from these two time periods (henceforth referred to as the active growth and late-summer senescence periods) to optimally detect fPAR changes and thereby better understand seasonal productivity within semiarid rangelands.

Four Landsat-5 TM scenes, path/row 039/030, were collected on 13-August-2005, 13-June-2006, 03-August-2007, and 18-June-2008. Two scenes were acquired during the active growth period of early June 2006 and 2008, while the other two scenes were acquired during the late-summer period when grasses senesced in August 2005 and 2007. Digital Number (DN) values were transformed into radiance using gain and offset coefficients from the metadata of the imagery. The images were then atmospherically corrected based on the dark object subtraction (DOS) method (Chavez, 1996; Song et al., 2001). All imagery was projected into Idaho Transverse Mercator (IDTM), NAD 83 and georectified to < 0.3 pixel root mean square error (RMSE) (Weber, 2006).

#### *Landsat-5 TM fPAR calculation*

Recently, two primary approaches have been used to retrieve fPAR from remotely sensed data. The most common approach has been to establish an empirical relationship between NDVI and fPAR through

fitting ground-based measures of fPAR to corresponding remotely sensed data (Myneni and Williams 1994; Chen, 1996). The limitation of relationship-based approaches is that the resulting formulas are influenced by vegetation type and soil background. Another important fPAR retrieval approach is based on bidirectional reflectance distribution function (BRDF) models (Tian, et al., 2000, 2002; Hu et al., 2007). The model-based approach may be more accurate from a theoretical basis, however it requires lengthy calculation time and is difficult to obtain sufficient model input parameters.

In this study, with limitations on field fPAR measurement data and model input parameters, TM fPAR estimations were developed by applying the SR-fPAR algorithm. To specifically assess the ability of the SR-fPAR retrieval approach for fPAR estimation in semiarid rangelands ecosystems, field-based measurements of aboveground forage biomass and percent ground cover were used to better indirectly assess TM fPAR. Recently, empirical relationship based empirical algorithms are highly site- specific and always emphasizes on forest ecosystem, however SR-fPAR algorithm described by Sellers et al. (1992) is a straightforward fPAR retrieval approach and is considered applicable within a variety of biome types (e.g., broadleaf evergreen trees, needle leaf deciduous trees, and grassland) (Paruelo et al., 1997; Los et al., 2000; Hassan et al., 2006).

Assuming a nearly linear relationship between fPAR and simple ratio (SR) (Equation 1), fPAR can be calculated when two known points are determined. The value of the 98<sup>th</sup> percentile from a normalized difference vegetation index (NDVI) distribution was assumed to represent vegetation at full cover and maximum photosynthetic activity with fPAR values close to unity (0.950). The 5<sup>th</sup> percentile value is assumed to represent no vegetation photosynthetic activity with an fPAR of 0.001. The relation between fPAR and SR is then given by

$$SR = \frac{1+NDVI}{1-NDVI} \quad (1)$$

$$fPAR = fPAR_{min} + (SR - SR_{i,min}) \frac{(fPAR_{max} - fPAR_{min})}{SR_{i,max} - SR_{i,min}} \quad (2)$$

where the maximum ( $fPAR_{max} = 0.950$ ) and minimum ( $fPAR_{min} = 0.001$ ) values of fPAR are independent of vegetation type.  $SR_{i,max}$  and  $SR_{i,min}$  correspond respectively to the 98<sup>th</sup> and 5<sup>th</sup> percentile of the NDVI data population for type  $i$  (sagebrush-steppe) vegetation (Sellers et al., 1996).

#### *MODIS fPAR product*

The theoretical basis of the MODIS fPAR algorithm is the three dimensional radiative transfer theory (Myneni et al., 1999). The inversion of the 3D Radiative transfer is accomplished with Look-Up Table approach (Knyazikhin et al., 1998). A back up method based on the relationship between NDVI and fPAR, used together with a biome classification map, is applied when the primary algorithm fails. In this study, four the Collection 5 MODIS fPAR (MOD15A2) scenes were selected on the basis of temporal coincidence with existing Landsat-5 TM imagery. All MODIS fPAR imagery (1 km spatial resolution) used in this study represent a time interval of eight days. All imagery was projected into ITDM, NAD 83, using ESRI's ArcGIS 9.3 for datum transformation and projection. Using quality control (QC) layers, MODIS fPAR data were screened to reject fPAR data of insufficient quality. Only pixels with the best possible quality (i.e., values on all bit fields are equal to zero) under the QC definition table were retained

(Table 2). The QC filter includes pixels with good quality and removes pixels which were not produced due to cloud or other reasons.

**Table 2. MODIS fPAR general quality control definitions for collection 5 data.**

Bit No.	Parameter Name	Bit Comb.	Description of Bitfield(s)
0	MODLAND_QC_bits	0	Good quality (main algorithm with or without saturation)
1	Sensor	1	Other Quality (back-up algorithm or fill values)
		0	Terra
2	DeadDetector	1	Aqua
		0	Detectors apparently fine for up to 50% of channels 1,2
3-4	CloudState (inherited from Aggregate_QC bits {0,1} cloud state)	1	Dead detectors caused >50% adjacent detector retrieval
		00	0 Significant clouds NOT present (clear)
		01	1 Significant clouds WERE present
		10	2 Mixed cloud present on pixel
5-7	SCF_QC (five level confidence score)	11	3 Cloud state not defined, assumed clear
		000	0, Main (RT) method used, best result possible (no saturation)
		001	1, Main (RT) method used with saturation. Good,very usable
		010	2, Main (RT) method failed due to bad geometry, empirical algorithm used
		011	3, Main (RT) method failed due to problems other than geometry, empirical algorithm used
		100	4, Pixel not produced at all, value couldn't be retrieved (possible reasons: bad LIB data, unusable MODAGAGG data)

*fPAR comparison*

MODIS fPAR and TM fPAR imagery were first compared to determine general similarity. To enable quantitative assessment of MODIS fPAR distributions, all TM fPAR layers were averaged resampled to 1 km spatial resolution in ESRI's ArcGIS 9.3. A total of 350 independent randomly distributed test points were generated using Hawth's analysis tools for ArcGIS. Of these, 302 test points were finally available for analysis after removing all points falling within the “no-retrieve” areas of the imagery. Pixel values were extracted using the ArcGIS "Sample" tool, and correlation coefficients were calculated to evaluate the relative agreement between MODIS fPAR and TM fPAR values.

TM fPAR change layers were calculated using TM fPAR values for 13-August-2005 subtracted from TM fPAR values for 13-June-2006. Similarly, TM fPAR values for 03-August-2007 were subtracted from TM fPAR values for 18-June-2008. The resulting change layers were assumed to represent vegetation growth that occurred following the end of the previous growing season and prior to periods of active livestock grazing in the study area. MODIS fPAR change layers were calculated in the same way. Finally, fPAR

distribution layers and change layers were compared with field-based measurements of aboveground forage biomass and percent ground cover to further indirectly validate these data.

#### *fPAR indirect-validation*

There were no flux tower sites in or surrounding the Big Desert study area and no ground-measured fPAR data were available for the study area. Because actual fPAR values must be considered unknown, direct validation from field measured fPAR was unavailable in this study. For this reason, we consider the seasonal characteristics of fPAR change over semiarid rangelands. Grasses, shrubs, and dominant weeds tended to be green during active growth periods (June). In contrast, most shrubs maintained greenness throughout much of the year while grasses and weeds became senescent, resulting in substantial fPAR reduction (e.g., fPAR value of grass is close to 0) in late summer (August). fPAR difference between late-summer senescence periods (e.g., primarily resulting from shrubs) and the next active growth periods (e.g., resulting from grasses, weeds, and shrubs) describes the amount of grasses and weeds available during the active growth period. Therefore, fPAR change values can be indirectly validated through a careful assessment of the spatial variability of grasses and weeds.

Based upon the reported data, the authors observed that 1) in areas where the percent cover of shrubs and above-ground forage biomass were similar, the area with the higher percent cover of grasses and weeds during the active growth period consistently resulted in higher fPAR change; 2) when the percent cover of shrub and grass functional groups were similar, the area with more above-ground forage biomass during the active growth period lead to higher fPAR change. As a result, the relationship between percent ground cover and fPAR change, and the relationship between above-ground forage biomass and fPAR change was established and fPAR values indirectly validated by comparing changes in fPAR with changes in above-ground forage biomass and percent ground-cover.

## **RESULTS**

MODIS fPAR values and TM fPAR values were relatively similar (Figure 2). The results of quantitative comparisons among aggregated TM fPAR and MODIS fPAR products (1 km spatial resolution in both cases) across the study region from 2005 to 2008 indicate MODIS fPAR values were relatively close to TM fPAR values and a weak relationship between MODIS fPAR and TM fPAR was also noted ( $R^2 \leq 0.51$ ) (Figure 3). In general, MODIS fPAR depicts the same overall trend and offers the advantage of acquiring reliable fPAR data at broad-scales and frequent periodicity.

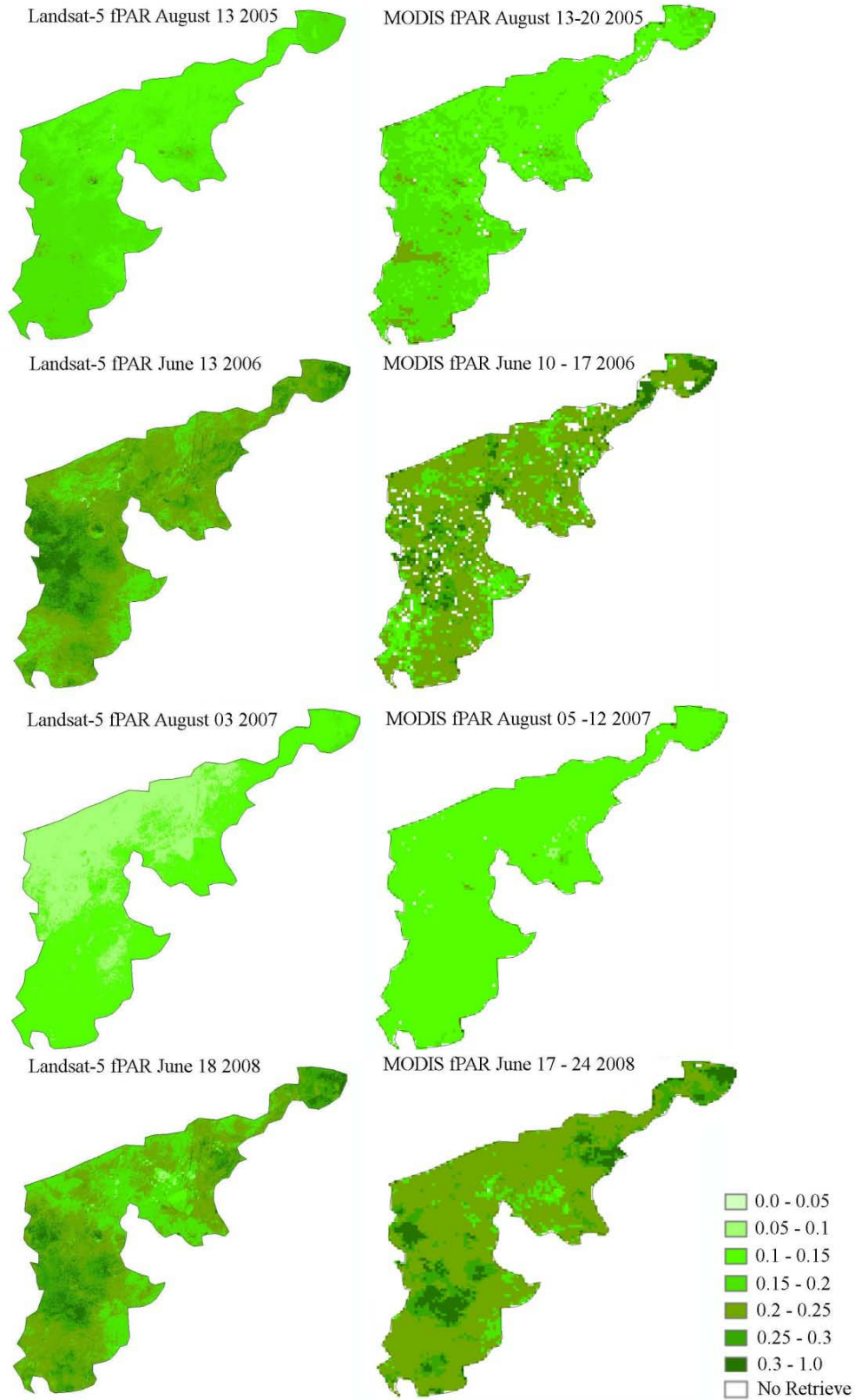


Figure 2. Landsat-5 TM fPAR (30 meters per pixel [mpp]) and eight-day composite MODIS fPAR (1000 mpp) layers.

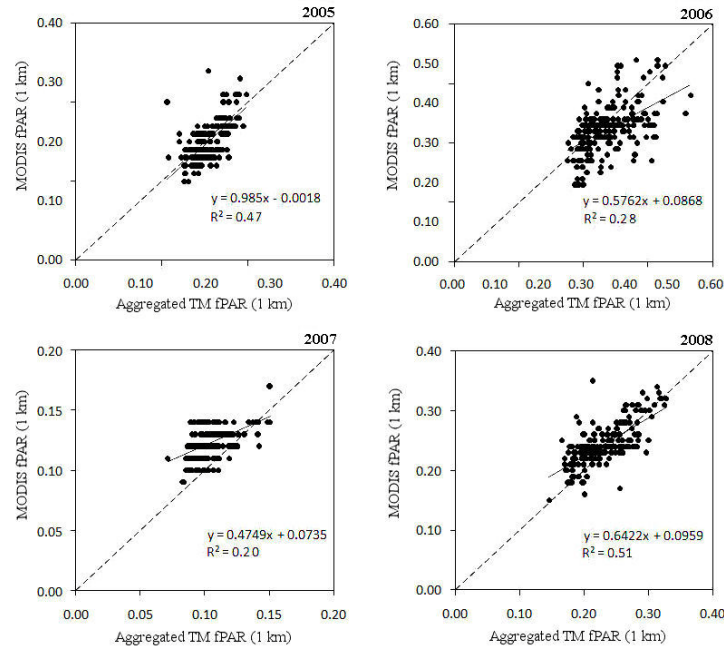


Figure 3. The comparison of aggregated Landsat-5 TM fPAR to the MODIS fPAR product at 1 km resolution.

TM fPAR change layers were nearly identical to MODIS fPAR change layers (Figure 4). Using fPAR change results, areas of major negative change ( $-1 < \text{fPAR change} < -0.05$ ), minor change ( $-0.05 < \text{fPAR change} < 0.05$ ) and major positive change ( $0.05 < \text{fPAR change} < 1$ ) were delineated. A major positive change (MPC) area was defined as an area where fPAR values increased. Similarly, a major negative change (MNC) area was an area where fPAR values substantially decreased, while minor change (MINC) areas were areas where fPAR values changed only slightly.

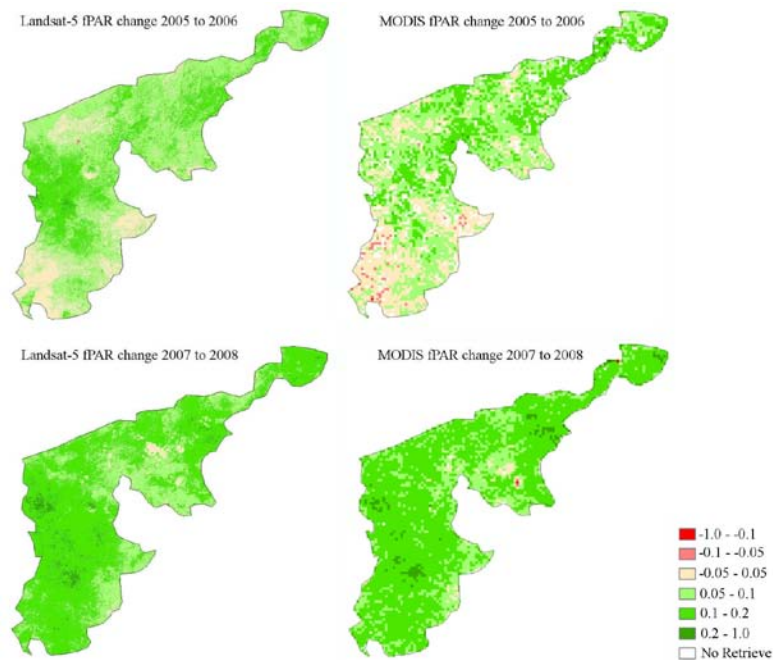


Figure 4. The fPAR change maps of Landsat-5 TM and MODIS.

Field-based measurements of above-ground forage biomass and percent ground-cover in MPC, MNC, and MINC areas are summarized in Table 3 and Table 4. In 2006, average percent shrubcover in MPC areas was similar to that in MINC areas, while higher percent grass cover was present in MPC areas than MINC areas over the same time period. Mean and maximum forage biomass was greater in MPC areas ( $\bar{x}$  = 496 Kg/Ha; maximum = 1668 Kg/Ha) than in MINC areas ( $\bar{x}$  = 328 Kg/Ha; maximum = 1065 Kg/Ha) in 2006, while mean forage biomass reduced in both MPC areas (-115 Kg/Ha) and MINC areas (-223 Kg/Ha) between 2005 and 2006. The reduction of forage biomass in MINC areas was greater than the reduction of forage biomass in MPC areas, hence a major negative change was detected in the MINC areas.

**Table 3. Percent ground cover for fPAR change analysis.**

	Average ground percent cover (%)					Number of sample plots
	Shrub	Grass	Litter	Bare ground	Weed	
MINC areas 2005	5-13	5-13	2-7	49-71	1-6	21
MPC areas 2005	5-13	5-14	2-7	47-69	2-7	67
MINC areas 2006	15-23	6-16	27-37	17-27	6-15	36
MPC areas 2006	14-23	16-25	17-26	16-25	5-14	139
MPC areas 2007	4-9	14-22	6-16	33-46	2-7	97
MPC areas 2008	2-7	14-23	16-26	27-36	5-12	82
Changes in MINC areas 2005-2006	10	1-3	25-30	-(32-44)	5-10	N/A
Changes in MPC areas 2005-2006	9-10	11	15-19	-(31-44)	3-7	N/A
Changes in MPC areas 2007-2008	-(3-5)	0-1	10	-(6-10)	3-5	N/A

*Note: no MINC areas were delineated in 2007 or 2008 and no sample plots was available within MNC area. SD stands for standard deviation.*

**Table 4. Aboveground forage biomass for fPAR change analysis.**

	Forage biomass (Kg/Ha)				Number of sample plots
	Mean	Max.	Min.	SD	
MINC areas 2005	551	2524	34	562	21
MPC areas 2005	612	3138	34	297	67
MINC areas 2006	328	1065	62	249	36
MPC areas 2006	496	1668	51	346	139
MPC areas 2007	356	1302	11	309	97
MPC areas 2008	249	975	11	208	82
Changes in MINC areas 2005-2006	-223	-1459	28	N/A	N/A
Changes in MPC areas 2005-2006	-115	-1470	17	N/A	N/A
Changes in MPC areas 2007-2008	-107	-345	0	N/A	N/A

*Note: no MINC areas were delineated in 2007 or 2008 and no sample plots was available within MNC area. SD stands for standard deviation.*

Analysis of field-based measurements of ground cover and forage biomass between 2005 and 2006 suggest MPC areas should exhibit greater fPAR change trends relative to MINC areas. Furthermore, comparing the change of mean forage biomass in all MPC areas from 2005 to 2006 (-115 Kg/Ha) to the change of mean forage biomass in all MPC areas from 2007 to 2008 (-107 Kg/Ha) revealed very similar change patterns. The information describing field-based above-ground forage biomass and percent ground-cover follow the same distribution and trend as indicated by both the MODIS and TM fPAR change maps. These results support the hypothesis that the seasonal characteristics of fPAR change over semiarid rangelands can be used as an indicator for the relative abundance of grasses and herbaceous weeds.

## DISCUSSION

Many MODIS fPAR validation studies noted that MODIS seems to overestimate fPAR in many regions. Fensholt et al. (2004) demonstrated that in comparison to field measured fPAR the overall level of MODIS fPAR is overestimated by approximately 0.06 - 0.15 in the semiarid grasslands of West Africa and Senegal. Weiss et al. (2007) compared MODIS fPAR and CYCLOPES fPAR products and also concluded that MODIS estimates higher fPAR values than CYCLOPES in grasslands. Similar to

grassland, Steinberg et al. (2006) indicated the MODIS fPAR algorithm overestimates fPAR when compared to Landsat-7 ETM derived fPAR in the boreal forests of Alaska (i.e., MODIS approximately overestimated fPAR by up to 0.2). However, in this study the difference between MODIS fPAR values and TM fPAR values contradicted previous findings ( $\bar{x}$  difference < 0.05). The reduction in MODIS fPAR values may be attributed to the improvement in the Collection 5 MODIS fPAR retrieval algorithm (e.g., all previous MODIS fPAR validation studies used Collection 4 product but this study used Collection 5 product) (Steinberg and Goetz, 2009).

Field sampling was conducted between June and early July throughout this study (2006-2008). This corresponds with the period of peak biomass production in the study area. Remote sensing imagery was acquired during this same time period to similarly capture the active growth period and allow comparison with known field conditions. Imagery for the years 2005 and 2007 were chosen to capture late-summer senescence and thereby better assess changes in fPAR over the growing season. In semiarid rangelands ecosystems, plant growth rates dramatically decrease following the active growth period in early June. However, plant growth does continue and in some years exhibits a spike of activity if sufficient autumn precipitation is present. Therefore, vegetation change derived from field measurement data provided an estimate of growth for the entire summer and following spring, whereas the fPAR change layers developed in this study did not include vegetation changes that occurred between June and early August. Following this approach, the resultant change layers describe the amount of green biomass available (e.g., actively growing grasses) as the difference between the estimated total above-ground biomass during the active growth period (i.e., actively growing grasses, accumulated litter, and residual plant matter) and the estimated total above-ground biomass at the end of the previous growing season.

In this study, fPAR change values help describe the spatial variability of grasses and weeds based on the seasonal characteristics of fPAR change over semiarid rangelands. For example, a positive fPAR change indicates more grasses and weeds would be found during the growing period (i.e., increased spatial distribution). Similarly, a negative fPAR change indicates fewer patches of grasses and weeds would be found in an area during the growing period. fPAR images were selected to represent the active growth and late-summer senescence periods, therefore fPAR change layers do not reflect an entire year of vegetation change (e.g., from June 2005 to June 2006). Hence, a positive fPAR change between 2005 and 2006 does not necessarily mean there was an increase in grass and weed biomass production in June 2006 than June 2005 but that the spatial distribution of grasses and herbaceous weeds was increased across the area. In addition, while the summary of field sample data and fPAR change levels describe the spatial variability of grasses and weeds, differences between years should not be used to quantify inter-annual variability of grasses and weeds. For example, changes in above-ground forage biomass in MPC and MINC areas for the periods 2005-2006 and 2007-2008 (Table 4) showed a reduction in both cases. However, compared to MINC areas, MPC areas showed less of a reduction in above-ground forage biomass. This example supports the use of fPAR change as an indicator of changes in the spatial variability of grasses and weeds and furthermore, demonstrates that more grasses were produced in MPC areas relative to the MINC areas.

Because each MODIS pixel can contain many different types of ground features (e.g., shrubs, grasses, and weeds) the field measurements used in this study represent only a portion of a MODIS pixel's information. It would be inappropriate to directly link a specific MODIS fPAR value to above-ground forage biomass values for an individual sample plot. In addition, since different years' statistics were based on a different

number of sample plots, which consist of different percentages of shrubs, grasses, litter, weeds, and bare ground, we cannot obtain field measured above-ground forage biomass change and percent cover change at a given sample plot across time. For these reasons, the study area was categorized into areas of different fPAR change levels which were indirectly validated using above-ground forage biomass statistics to represent the spatial variability of grasses and weeds. In future field surveys, we plan to measure above-ground biomass for additional functional groups (e.g., forbs) at the same sample plot each year and use composited above-ground biomass values to provide a better link with MODIS fPAR data.

Measurement of field fPAR is an arduous task and an insufficient number of field sites (e.g., flux tower) make field fPAR data unavailable to many studies. Ideally, field measured fPAR data would have been available for this study. However, in lieu of these data, we used an accumulation of 10 years of field data (above-ground biomass and percent cover) for this study. In addition, TM fPAR estimations were developed using the SR-fPAR retrieval algorithm to provide a cross-sensor comparison of fPAR.

The seasonal characteristics of fPAR change over semiarid rangelands (e.g., herbaceous plants have a late-summer senescence period and fPAR values of herbaceous plants in this period declined) were considered in this study, and these fPAR change trends exhibited a positive relationship with changes in above-ground forage biomass and percent cover of grasses and weeds. These results were used to indirectly assess the MODIS fPAR product and the SR-fPAR retrieval algorithm used to produce a Landsat 5 TM fPAR product. The methodology presented herein was specifically designed for use within the semiarid sagebrush-steppe rangelands of southeastern Idaho, and should not be directly applied to other ecosystems. This is because there may be little difference in fPAR between the active growth and late-summer senescence periods in more humid rangelands or woodland ecosystems where precipitation is more uniformly distributed throughout the year and distinct growing seasons/dry seasons are not present. However, similar studies should be undertaken to further validate the MODIS fPAR product.

## **CONCLUSION**

This study focused on the comparison and assessment of the MODIS fPAR product for semiarid rangelands using cross-sensor comparisons with TM fPAR values as well as field-based observations and measurements. Landsat-5 TM and MODIS fPAR data were compared between active growth periods (June) and late-summer senescence periods (August) using measurements of above-ground forage biomass and percent ground-cover from 2005, 2006, 2007, and 2008. Observed fPAR changes appear to be a function of changes in the composition and percent cover of grasses and weeds within the study area as grasses and weeds are more ephemeral and dynamic in nature relative to shrubs. In contrast to previous MODIS fPAR validation studies, which noted that MODIS overestimated fPAR in many regions, this study validated Collection 5 MODIS fPAR products and found the difference between MODIS fPAR and TM fPAR values were very small small ( $\bar{x}$  difference < 0.05). This may be the result of improvements in the Collection 5 MODIS fPAR retrieval algorithm.

Rangeland ecosystems are very important in the assessment of global ecosystem productivity, and abundant field-based measurements are crucial to the validation of satellite-based fPAR products. Future work will aim to collect additional field data to improve MODIS and TM fPAR applications for semiarid rangelands.

## **ACKNOWLEDGEMENTS**

This study was made possible by a grant from the National Aeronautics and Space Administration Goddard Space Flight Center (NNX08AO90G). ISU would also like to acknowledge the Idaho Delegation for their assistance in obtaining this grant.

## **LITERATURE CITED**

Asner, G.P., C.A. Wessman, and S. Archer, 1998. Scale Dependence of Absorption of Photosynthetically Active Radiation in Terrestrial Ecosystems. *Ecological Applications*, 8(4):1003-1021

Baret, F., T.J. Morisette, R.A. Fernandes, J.L. Champeaux, R.B. Myneni, J. Chen, S. Plummer, M. Weiss, C. Bacour, S. Garrigues, and J.E. Nickeson, 2006. Evaluation of the Representativeness of Networks of Sites for the Global Validation and Intercomparison of Land Biophysical Products: Proposition of the CEOS-BELMANIP. *IEEE Transactions on Geoscience and Remote Sensing*, 44(7):1794-1803

Baret, F., M. Weiss, D. Allard, S. Garrigues, M. Leroy, H. Jeanjean, R. Fernandes, R.B. Myneni, J.T. Morisette, J. Privette, H. Bohbot, R. Bosseno, G. Dedieu, C. Di Bella, M. Espana, V. Gond, X.F. Gu, D. Guyon, C. Lelong, P. Maisongrande, E. Mougin, T. Nilson, F. Veroustraete, and R. Vintilla. VALERI: A Network of Sites and a Methodology for the Validation of Medium Spatial Resolution Land Satellite Product, *Remote Sensing of Environment*. (in review)

Bonan, G.B., 1995. Land-atmospheric Interactions for Climate System Models: Coupling Biophysical. Biogeochemical and Ecosystem Dynamical Processes, *Remote Sensing of Environment*, 51(1):57-73

Breman, H., and C.T. de Wit, 1983. Rangeland Productivity and Exploitation in the Sahel. *Science*, 221(4618):1341-1347

Chavez, P.S. Jr., 1996. Image-based Atmospheric Corrections-revisited and Improved, *Photogrammetric Engineering and Remote Sensing*, 62(9):1025-1036

Chen, F., J.M. Tang, and Z. Niu, 2008. Estimating the Impact of Urbanization on LAI/fPAR in the Baltimore-Washington Corridor Area. *Canadian Journal of Remote Sensing*, 34(S2):326-337

Chen, J.M., 1996. Canopy Architecture and Remote Sensing of the Fraction of Photosynthetically Active Radiation Absorbed by Boreal Conifer Forests. *IEEE Transactions on Geoscience and Remote Sensing*, 34(6):1353-1368

Chen, J.M., F. Deng, and M.Z. Chen, 2006. Locally Adjusted Cubic-spline Capping for Reconstructing Seasonal Trajectories of a Satellite-derived Surface Parameter. *IEEE Transactions on Geoscience and Remote Sensing*, 44(8):2230-2238

- Cohen, W.B., T.K. Maier-sperger, Z. Yang, S.T. Gower, D.P. Turner, W.D. Ritts, M. Berterretche, and S.W. Running, 2003. Comparisons of Land Cover and LAI Estimates Derived from ETM+ and MODIS for Four Sites in North America: A Quality Assessment of 2000/2001 Provisional MODIS Products. *Remote Sensing of Environment*, 88(3):233-255
- Dickinson, R.E., M. Shaikh, L. Graumlich, and R. Bryant, 1998. Interactive Canopies for a Climate Model. *Journal of Climate*, 11(11):2823-2836
- Feng, X., G. Liu, J.M. Chen, M. Chen, J. Liu, W.M. Ju, R. Sun, and W. Zhou, 2007. Net Primary Productivity of Terrestrial Ecosystems in China Using a Process Model Driven by Remote Sensing. *Journal of Environmental Management*, 85(3):563-573
- Fensholt, R., I. Sandholt, and M.S. Rasmussen, 2004. Evaluation of MODIS LAI, fAPAR and the Relation Between fAPAR and NDVI in a Semiarid Environment Using In-situ Measurements. *Remote Sensing of Environment*, 91(3-4):490-507
- Franklin, J.F., C.S. Bledsoe, and J.T. Callahan, 1990. Contributions of the Long-term Ecological Research-Program - an Expanded Network of Scientists, Sites, and Programs Can Provide Crucial Comparative Analysis. *Bioscience*, 40(7):509-523
- Garrigues, S., D. Allard, and F. Baret, 2007. Using First- and Second Order Variograms for Characterizing Landscape Spatial Structures from Remote Sensing Imagery, *IEEE Transactions on Geoscience and Remote Sensing*, 45(6):1823-1834
- Garrigues, S., R. Lacaze, F. Baret, J.T. Morisette, M. Weiss, J. Nickeson, R. Fernandes, S. Plummer, N.V. Shabanov, R. Myneni, and W. Yang, 2008. Validation and Intercomparison of Global Leaf Area Index Products Derived from Remote Sensing Data, *Journal of Geophysical Research*, 113(G2):G02028, doi:10.1029/2007JG000635
- Gnieting, P., J. Gregory, and K.T. Weber, 2007. Datum Transforms Involving WGS84, URL = [http://giscenter.isu.edu/research/techpg/nasa\\_tlcc/template.htm](http://giscenter.isu.edu/research/techpg/nasa_tlcc/template.htm)
- Gobron, N., B. Pinty, O. Aussedat, J.M. Chen, W.B. Cohen, R. Fensholt, V. Gond, K.F. Huemmrich, T. Lavergne, F. Me´lin, J.L. Privette, I. Sandholt, M. Taberner, D.P. Turner, M.M. Verstraete, and J. Widlowski, 2006. Evaluation of Fraction of Absorbed Photosynthetically Active Radiation Products for Different Canopy Radiation Transfer Regimes: Methodology and Results Using Joint Research Center Products Derived from SeaWiFS Against Around-based Estimations, *Journal of Geophysical Research*, 111(D13):D13110, doi:10.1029/2005JD006511
- Gower, S.T., C.J. Kucharik, and J.M. Norman, 1999. Direct and Indirect Estimation of Leaf Area Index, fAPAR, and Net Primary Production of Terrestrial Ecosystems. *Remote Sensing of Environment*, 70(1):29-51

- Hassan, Q.K., C. Bourque, and F. Meng, 2006. Estimation of Daytime Net Ecosystem CO<sub>2</sub> Exchange over Balsam Fir Forests in Eastern Canada: Combining Averaged Tower-based Flux Measurements with Remotely Sensed MODIS Data. *Canadian Journal of Remote Sensing*, 32(6):405-416
- Heinsch, F.A., M.S. Zhao, S.W. Running, J.S. Kimball, R.R. Nemani, K.J. Davis, P.V. Bolstad, B.D. Cook, A.R. Desai, D.M. Ricciuto, B.E. Law, W.C. Oechel, H. Kwon, H.Y. Luo, S.C. Wofsy, A.L. Dunn, J.W. Munger, D.D. Baldocchi, L.K. Xu, D.Y. Hollinger, A.D. Richardson, P.C. Stoy, M.B.S. Siqueira, R.K. Monson, S.P. Burns, and L.B. Flanagan, 2006. Evaluation of Remote Sensing Based Terrestrial Productivity from MODIS Using Regional Tower Eddy Flux Network Observations, *IEEE Transactions on Geoscience and Remote Sensing*, 44(7):1908-1925
- Hill, M.J., U. Senarath, A. Lee, M. Zeppel, J.M. Nightingale, R.J. Williams, and T.R. McVicar, 2006. Assessment of the MODIS LAI Product for Australian Ecosystems, *Remote Sensing of Environment*, 101(4):495-518
- Holben, B.N., T.F. Eck, I. Slutsker, D. Tanre, J.P. Buis, A. Setzer, E. Vermote, J.A. Reagan, Y. Kaufman, T. Nakajima, F. Lavenu, I. Jankowiak, and A. Smirnov, 1998. AERONET - a Federated Instrument Network and Data Archive for Aerosol Characterization, *Remote Sensing of Environment*, 66(1):1-16
- Hu, J., Y. Su, B. Tan, D. Huang, W. Yang, M. Schull, M.A. Bull, J.V. Martonchik, D.J. Diner, Y. Knyazikhin, and R.B. Myneni, 2007. Analysis of the MISR LAI/FPAR Product for Spatial and Temporal Coverage, Accuracy and Consistency. *Remote Sensing of Environment*, 107(1-2):334-347
- Huntsinger, L., and P. Hopkinson, 1996. Viewpoint: Sustaining Rangeland Landscapes: a Social and Ecological Process, *Journal of Range Management*, 49(2):167-173
- Justice, C.O., J.R.G. Townshend, E.F. Vermote, E. Masuoka, R.E. Wolfe, N. Saleous, D.P. Roy, and J.Y. Morisette, 2002. An Overview of MODIS Land Data Processing and Product Status, *Remote Sensing of Environment*, 83(1-2):3-15
- Knyazikhin, Y., J.V. Martonchik, R.B. Myneni, D.J. Diner, and S.W. Running, 1998. Synergistic Algorithm for Estimating Vegetation Canopy Leaf Area Index and Fraction of Absorbed Photosynthetically Active Radiation from MODIS and MISR Data, *Journal of Geophysical Research*, 103(D24):32257-32276
- Los, S.O., G.J. Collatz, P.J. Sellers, C.M. Malmström, N.H. Pollack, R.S. Defries, L. Bounoua, M.T. Parris, C.J. Tucker, and D.A. Dazlich, 2000. A Global 9-year Biophysical Land-surface Data Set from NOAA AVHRR Data, *Journal of Hydrometeorology*, 1(2):183-199
- Milne, B.T., and W.B. Cohen, 1999. Multiscale Assessment of Binary and Continuous Landcover Variables for MODIS Validation, Mapping, and Modeling Applications. *Remote Sensing of Environment*, 70(1):82-98

Morisette, J.T., F. Baret, J.L. Privette, R.B. Myneni, J.E. Nickeson, S. Garrigues, N.V. Shabanov, M. Weiss, R.A. Fernandes, S.G. Leblanc, M. Kalacska, G.A. Sanchez-Azofeifa, M. Chubey, B. Rivard, P. Stenberg, M. Rautiainen, P. Voipio, T. Manninen, A.N. Pilant, T.E. Lewis, J.S. Iiams, R. Colombo, M. Meroni, L. Busetto, W.B. Cohen, D.P. Turner, E.D. Warner, G.W. Petersen, G. Seufert, and R. Cook, 2006. Validation of Global Moderate-resolution LAI Products: a Framework Proposed within the CEOS Land Product Validation Subgroup, *IEEE Transactions on Geoscience and Remote Sensing*, 44(7):1804-1817

Morisette, J.T., J. Nickeson, P. Davis, Y. Wang, Y. Tian, C. Woodcock, N. Shabanov, M. Hansen, D.L. Schaub, A.R. Huete, W.B. Cohen, D.R. Oetter, and R.E. Kennedy, 2003. High Spatial Resolution Satellite Observations for Validation of MODIS Land Products: IKONOS Observations Acquired under the NASA Scientific Data Purchase, *Remote Sensing of Environment*, 88(1-2):100-110

Morisette, J.T., J.L. Privette, and C.O. Justice, 2002. A Framework for the Validation of MODIS Land Products, *Remote Sensing of Environment*, 83(1):77-96

Myneni, R.B., Y. Knyazikhin, Y. Zhang, Y. Tian, Y. Wang, A. Lotsch, J.L. Privette, J.T. Morisette, S.W. Running, R. Nemani, J. Glassy, and P. Votava, 1999. MODIS Leaf Area Index (LAI) and Fraction of Photosynthetically Active Radiation Absorbed by Vegetation (FPAR) Product (MOD15) Algorithm Theoretical Basis Document, URL = [http://modis.gsfc.nasa.gov/data/atbd/land\\_atbd.php](http://modis.gsfc.nasa.gov/data/atbd/land_atbd.php)

Myneni, R.B., and D.L. Williams, 1994. On the Relationship between FAPAR and NDVI, *Remote Sensing of Environment*, 49(3):200-211

Paruelo, J.M., H.E. Epstein, W.K. Lauenroth, and I.C. Burke, 1997. ANPP Estimates from NDVI for the Central Grassland Region of the United States, *Ecology*, 78(3):953-958

Running, S.W., D.D. Baldocchi, D.P. Turner, S.T. Gower, P.S. Bakwin, and K.A. Hibbard, 1999. A Global Terrestrial Monitoring Network Integrating Tower Fluxes, Flask Sampling, Ecosystem Modeling and EOS Satellite Data, *Remote Sensing of Environment*, 70(1):108-127

Running, S.W., R.R. Nemani, F.A. Heinsch, M. Zhao, M. Reeves, and H. Hashimoto, 2004. A Continuous Satellite-derived Measure of Global Terrestrial Primary Production, *BioScience*, 54(6):547-560

Sellers, P.J., J.A. Berry, G.J. Collatz, C.B. Field, and F.G. Hal, 1992. Canopy Reflectance, Photosynthesis, and Transpiration. III. A Reanalysis Using Improved Leaf Models and a New Canopy Integration Scheme, *Remote Sensing of Environment*, 42(3):187-216

Sellers, P.J., S.O. Los, C.J. Tucker, C.O. Justice, D.A. Dazlich, G.J. Collatz, and D.A. Randall, 1996. A Revised Land Surface Parameterization (SiB2) for Atmospheric GCMs. Part II: The Generation of Global Fields of Terrestrial Biophysical Parameters from Satellite Data, *Journal of Climate*, 9(4):706-737

- Sellers, P.J., D.A. Randall, A.K. Betts, F.G. Hall, J.A. Berry, G.J. Collatz, A.S. Denning, H.A. Mooney, C.A. Nobre, N. Sato, C.B. Field, and A. Henderson-sellers, 1997. Modeling the Exchanges of Energy, Water and Carbon between Continents and the Atmosphere, *Science*, 275(5299):502-509
- Serr, K, T. Windholz, and K.T. Weber, 2006. Comparing GPS Receivers: A Field Study. *Journal of the Urban and Regional Information Systems Association*, 18(2):19-23
- Shabanov, N.V., Y. Wang, W. Buermann, J. Dong, S. Hoffman, G.R. Smith, Y. Tian, Y. Knyazikhin, and R.B. Myneni, 2003. Effect of Foliage Spatial Heterogeneity in the MODIS LAI and FPAR Algorithm over Broadleaf Forests, *Remote Sensing of Environment*, 85(4):410-423
- Song, C.H., C.E. Woodcock, K.C. Seto, M.P. Lenney, and S.A. Macomber, 2001. Classification and Change Detection Using Landsat TM Data: When and How to Correct Atmospheric Effects? *Remote Sensing of Environment*, 75(2):230-244
- Steinberg, D.C., and S.J. Goetz, 2009. Assessment and Extension of the MODIS FPAR Products in Temperate Forests of the Eastern United States, *International Journal of Remote Sensing*, 30(1):169-187
- Steinberg, D.C., S.J. Goetz, and E.J. Hyer, 2006. Validation of MODIS  $F_{PAR}$  Products in Boreal Forests of Alaska, *IEEE Transactions on Geoscience and Remote Sensing*, 44(7):1818-1828
- Swap, B., T. Suttles, H. Annegarn, Y. Scorgie, J. Closs, J. Privette, and B. Cook, 2000. Report on SAFARI 2000 Outreach Activities, Intensive Field Campaign Planning Meeting, and Data Management Workshop, *Earth Observer*, 12(3):21-25
- Tian, Y.H., C.E. Woodcock, Y.J. Wang, J.L. Privette, N.V. Shabanov, L.M. Zhou, Y. Zhang, W. Buermann, J.R. Dong, B. Veikkanen, T. Häme, K. Andersson, M. Ozdogan, Y. Knyazikhin, and R.B. Myneni, 2002. Multiscale Analysis and Validation of the MODIS LAI Product II. Sampling Strategy, *Remote Sensing of Environment*, 83(3):431-441
- Tian, Y., Y. Wang, Y. Zhang, Y. Knyazikhin, J. Bogaert, and R.B. Myneni, 2002. Radiative Transfer Based Scaling of LAI Retrievals from Reflectance Data of Different Resolutions, *Remote Sensing of Environment*, 84(1):143-159
- Turner, D.P., W.D. Ritts, W.B. Cohen, S.T. Gower, M. Zhao, S.W. Running, S.C. Wofsy, S.D. Urbanski, L. Allison, and J.W. Munger, 2003. Scaling Gross Primary Production (GPP) over Boreal and Deciduous Forest Landscapes in Support of MODIS GPP Product Validation, *Remote Sensing of Environment*, 88(3):256-270.
- Turner, D.P., W.D. Ritts, S. Wharton, C. Thomas, R. Monson, T.A. Black, and M. Falk, 2009. Assessing FPAR Source and Parameter Optimization Scheme in Application of a Diagnostic Carbon Flux Model, *Remote Sensing of Environment*, 113(5):1529-1539

Turner, D.P., W.D. Ritts, M. Zhao, S.A. Kurc, A.L. Dunn, S.C. Wofsy, E.E. Small, and S.W. Running, 2006. Assessing Interannual Variation in MODIS-based Estimates of Gross Primary Production, *IEEE Transactions in Geosciences and Remote Sensing*, 44(7):1899-1907

Weber, K.T., 2006. Challenges of Integrating Geospatial Technologies into Rangeland Research and Management, *Rangeland Ecology & Management*, 59(1):38-43

Weiss, M., F. Baret, S. Garrigues, and R. Lacaze, 2007. LAI and fAPAR CYCLOPES Global Products Derived from VEGETATION. Part 2: Validation and Comparison with MODIS Collection 4 Products, *Remote Sensing of Environment*, 110(3):317-331

Yang, P., R. Shibasaki, W.B. Wu, Q.B. Zhou, Z.X. Chen, Y. Zha, Y. Shi, and H.J. Tang, 2007. Evaluation of MODIS Land Cover and LAI Products in Cropland of North China Plain Using *In-situ* Measurements and Landsat TM Images, *IEEE Transactions on Geoscience and Remote Sensing*, 45(10):3087-3097

Yanskey, G.R., E.H. Markee Jr, and A.P. Richter, 1966. Climatology of the National Reactor Testing Station, USAEC Report IDO-12048. United States Department of Commerce, Environmental Science Services Administration, Air Resources Field Research Office, Idaho Falls, Idaho

Zhao, M.S., F.A. Heinsch, R.R. Nemani, and S.W. Running, 2005. Improvements of the MODIS Terrestrial Gross and Net Primary Production Global Data Set, *Remote Sensing of Environment*, 95(2):164-176

**Recommended citation style:**

Chen, F., K.T. Weber, J. Anderson, B. Gokhale, 2011. Comparison of MODIS fPAR Products with Landsat-5 TM Derived fPAR over Semiarid Rangelands of Idaho. Pages 69-88 in K. T. Weber and K. Davis (Eds.), Final Report: Assessing Post-Fire Recovery of Sagebrush-Steppe Rangelands in Southeastern Idaho (NNX08AO90G). 252 pp.

## **Herbaceous Biomass Estimation from SPOT-5 Imagery in Semiarid Rangelands of Idaho**

Fang Chen, GIS Training and Research Center, Idaho State University, 921 S. 8<sup>th</sup> Ave, Stop 8104, Pocatello Idaho 83209-8104, chenfang@isu.edu

Keith T. Weber, GIS Director, Idaho State University. GIS Training and Research Center, 921 S. 8th Ave., Stop 8104, Pocatello, ID 83209-8104. webekeit@isu.edu

Bhushan Gokhale, GIS Training and Research Center, Idaho State University, 921 S. 8<sup>th</sup> Ave, Stop 8104, Pocatello Idaho 83209-8104

### **ABSTRACT**

Eight vegetation indices (VI) commonly used for above-ground biomass (AGB) estimation were derived from Satellite Pour l'Observation de la Terre 5 (SPOT 5) imagery and used to predict herbaceous AGB at a semiarid rangeland study site in southeast Idaho. The relationship between herbaceous AGB and vegetation water content was also evaluated and as a result, a suite of water sensitive vegetation indices (WSVI) were developed. Correlation coefficients between herbaceous AGB, VI's, and WSVI's were calculated, demonstrating that WSVI's were correlated ( $r^2 \geq 0.51$ ) with vegetation water content and performed better than standard VI's in herbaceous AGB estimates within the semiarid rangelands of Idaho.

*KEYWORDS: Rangelands, biomass, water content, vegetation indices, remote sensing, Idaho*

## INTRODUCTION

Rangelands cover approximately 40% of the earth’s terrestrial surface and are important areas for livestock production and wildlife habitat (Breman and de Wit 1983; Huntsinger and Hopkins 1996). To effectively manage rangelands it is important to assess ecosystem productivity and biomass production (Running et al. 2004). Biomass estimates represent the quantity of matter in a given area and are expressed either as the weight of organisms per unit area or as the volume of organisms per unit volume. Previous total above-ground biomass (AGB) research has demonstrated that vegetation indices (VI) are sensitive to the biophysical and biochemical variations in vegetation and as a result, are the most common parameters used to estimate AGB (Davidson and Csillag 2001; Kawamura et al. 2005; Numata et al. 2008). A remote sensing derived VI is a quantitative optical measure of canopy greenness (Tucker 1979; Weiser et al. 1986). Various VI's such as the normalized difference vegetation index (NDVI), normalized difference water index (NDWI) and soil adjusted vegetation index (SAVI) have been correlated with AGB, and applied to predict AGB within a variety of biomes (Davidson and Csillag 2001; Kogan et al. 2004; Mirik et al. 2005; Wessels et al. 2006; Numata et al. 2008; Cho and Skidmore 2009) (Table 1). Recently, ground-based and satellite-based spectral measurement methods have been developed to better quantify AGB. For instance, many ground-based methods use portable field spectroradiometers or digital cameras (e.g., ASD spectrometers, ASD Inc, Boulder, CO,USA; Dycam Agricultural Digital Camera (ADC), Dycam Inc, Chatworth, CA, USA) to collect canopy radiance and predict AGB through an empirical relationship between spectral values and biomass samples (Boelman et al. 2003; Flynn et al. 2008; Mašková et al. 2008). These methods are straightforward and accurate for small-scale studies (e.g., approximately 1-10 ha), however, they are also labor intensive and difficult to apply over broad spatial scales or long-term temporal scales.

**Table 1. Vegetation indices correlation with total above ground biomass (AGB) reported in different studies**

<i>Study area</i>	<i>Sensor</i>	<i>Index</i>	<i>R<sup>2</sup></i>	<i>Sources</i>
Kentucky, USA	Greenseeker RT500	NDVI	0.68	Flynn et al., 2008
Southern Africa	Landsat7 -ETM+	Green/Blue	0.85	Samimi and Kraus, 2004
Inner Mongolia, China	MODIS	NDVI	0.75	Kawamura et al., 2005
Italy	HyMap	NDVI	0.32-0.58	Cho and Skidmore, 2009
		NDWI	0.49-0.55	
Czech Republic	ADC	NDVI	0.83 (managed) 0.52 (unmanaged)	Mašková et al., 2008
Namibia	AVHRR	NDVI	0.76	Sannier et al., 2002
Northern Alaska	UniSpec-DC	NDVI	0.84	Boelman et al., 2003
Italy		NDVI	0.32	Schino et al., 2003
Brazilian Amazon	Analytical Spectral Device	NDVI	0.03	Numata et al., 2008
		NDWI	0.13	

The increasing availability of satellite-based remote sensing data extends the assessment of AGB into a broader spatiotemporal scale. For example, remotely sensed data acquired from various sensors have been used to assess AGB including NOAA's AVHRR (Box et al. 1989; Sannier et al. 2002; Kogan et al. 2004; Wessels et al. 2006), MODIS (Kawamura et al. 2005; Xu et al. 2008), Landsat-5 TM and Landsat-7 ETM+ (Friedl et al. 1994; Schino et al. 2003; Samimi and Kraus 2004), SPOT VEGETATION (Verbesselt et al. 2006), and hyperspectral sensors such as PROBE-1, Hyperion, and the HyMap system (Mutanga and Skidmore 2004; Mirik et al. 2005; Numata et al. 2008; Cho and Skidmore 2009). Although many studies have investigated the ability to assess AGB from VI's, many problems have been found. One problem is that an empirical relationship derived by a VI for the accurate prediction of AGB at one site or time period may not apply to other sites or even the same site at another time (Foody et al. 2003). This problem is primarily due to variations in the natural environment (e.g., variable precipitation, soil-water content, and temperature conditions), viewing season (e.g., phenology during the growing season), and the sensor used in the study (e.g., differences in spatial resolution and other sensor characteristics) (Davidson and Csillag 2001; Schino et al. 2003; Flynn et al. 2008). In addition, since VI's have differing abilities to provide accurate estimates of AGB, it is difficult to determine an optimal VI for a specific study. For example, the same VI (e.g., NDVI) may have different prediction accuracies within various regions; yet different types of VI's (e.g., NDVI vs NDWI) may perform quite differently within the same region (Table 1). These problems limit the transferability of predictive relationships and the effectiveness of VI's to estimate AGB.

Approximately 48 percent of Idaho is considered rangeland, and many of these areas are categorized as a semiarid sagebrush-steppe ecosystem (<http://www.idrange.org>). AGB estimation in the semiarid rangelands of the Intermountain West plays an important role in rangeland ecosystem assessment. In the semiarid rangelands of Idaho, high temperatures hasten the desiccation of plants and many grass species senesce during the summer. The relationship between herbaceous AGB and VI's is most accurately estimated when the proportion of green or growing material is high (Hill 2004; Numata et al. 2008) relative to the proportion of bare ground and/or litter. While important, determining an optimal VI for the accurate estimation of seasonal herbaceous AGB in semiarid rangelands may be difficult.

Most VI's used for AGB estimation are based on radiance or reflectance from a red band (RED) around 0.66  $\mu\text{m}$  and a near infrared band (NIR) around 0.86  $\mu\text{m}$  (Huete et al. 2002; Chuvieco et al. 2004). The RED band characteristically shows a strong chlorophyll absorption region for vegetation and strong reflectance for soils, while the NIR band is located in the high reflectance plateau of vegetation canopies. Since absorption by liquid water near 0.86  $\mu\text{m}$  is negligible, NIR reflectance is affected primarily by internal leaf structure and cellulose content (Gao 1996). In contrast, the short-wave infrared band (SWIR) (around 1.24 $\mu\text{m}$ ) is located in the high reflectance plateau of vegetation reflectance with weak liquid absorption (canopy scattering enhances the water absorption) (Jacquemoud et al. 1996; Jackson et al. 2004). The SWIR band reflects changes in both the vegetation water content and the spongy mesophyll structure of vegetation. The combination of the NIR band with the SWIR band can remove variation induced by internal leaf structure and leaf dry matter content (Gao 1996; Ceccato et al. 2001). This combination of these bands (NIR and SWIR) is also sensitive to changes in liquid water content within the vegetation canopy (Serrano et al. 2000; Zarco-Tejada et al. 2003).

In this study, a suite of water sensitive vegetation indices (WSVI) were developed incorporating the NIR and SWIR portions of the electromagnetic spectrum, to help characterize plant water content and better estimate herbaceous AGB in semiarid rangeland ecosystems. The study was designed to investigate the applicability of various VI's for the assessment of herbaceous AGB in the semiarid rangelands of Idaho, USA. To accomplish this, eight VI's including difference vegetation index (DVI, Richardson and Everitt 1992), ratio vegetation index (RVI, Jordan 1969), normalized difference vegetation index (NDVI, Rouse et al. 1973), re-normalized difference vegetation index (RDVI, Roujean and Breon 1995), soil adjusted vegetation index (SAVI, Huete 1988), the second modified soil adjusted vegetation index (MSAVI2, Qi et al. 1994), infrared percentage vegetation index (IPVI, Crippen 1990), and modified simple ratio (MSR, Chen 1996), were derived from Satellite Pour l'Observation de la Terre 5 (SPOT 5) imagery. In addition, the relationship between herbaceous AGB and total water content was determined. Finally, correlation estimates between herbaceous AGB, VI's, and WSVI's were calculated, and the performance of herbaceous AGB predictions from both VI's and WSVI's were evaluated using field-based measurements of herbaceous AGB.

## MATERIALS AND METHODS

### Study Area

The study area, known as the Big Desert, lies in southeast Idaho, USA, approximately 71 km northwest of Pocatello. The center of the study area was located at 113° 4' 18.68" W and 43° 14' 27.88" N (Figure 1). This area is managed by the US Bureau of Land Management (BLM) and exhibits a large variety of native as well as invasive plant species. The area is a semiarid sagebrush-steppe ecosystem with a high proportion of bare ground ( $\bar{x}$  bare ground > 17%, Studley et al. 2009). The area is sagebrush-steppe, consisting primarily of native and non-native grasses, forbs, and many shrub species including sagebrush (*Artemisia tridentata*) and rabbit brush (*Chrysothamnus nauseosus*). Annual precipitation is 23 cm with 40% of the precipitation falling from April through June. The area is bordered by geologically young lava formations to the south and west and irrigated agricultural lands to the north and east. Sheep grazing is the primary anthropogenic disturbance to the study area with semi-extensive continuous/seasonal grazing systems used on allotments ranging in size from 1100 to over 125,000 ha. Wildfire is a common disturbance and nearly 40% of the study area has burned in the past 10 years.

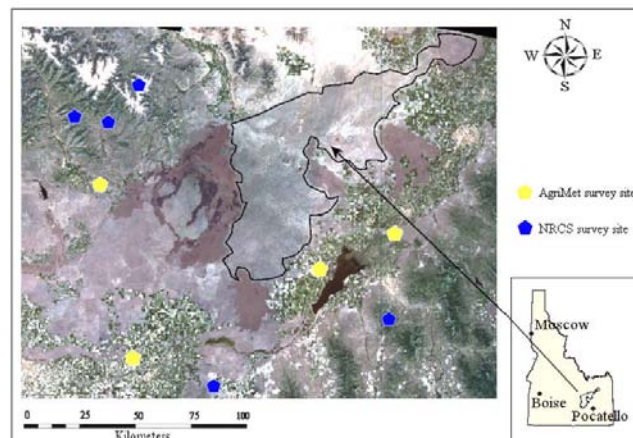


**Figure 1. Location and general characteristics of the Big Desert in southeastern, Idaho. Note: no weather station survey site was available within the Big Desert study area however, nine sites were located which bound the study area. Though some sites are in the mountains, the weather there has identical change trends compared to the snake river plain.**

### *Field Data Collection*

This study presents results using total herbaceous AGB measurements only and does not include any measurements of shrub biomass production. Twenty-nine sample locations were selected for the collection of herbaceous AGB, which has been defined as all grasses, forbs, and standing litter for the purposes of this study. Site selection criteria included the site being a homogeneous area at least 20 m x 20 m in size (cf., spatial resolution of SPOT satellite imagery = 10 m x 10 m in size, thus helping to assure the sample pixel was also homogeneous) with still larger areas being preferred. The domination plants in each site are herbaceous vegetations, with the plot center  $\geq 70$  meters from any “edges” including roads, fences, or power lines, and plot perimeters  $\geq 100$  meters from all other plots. Preference was given to sites with perimeters located  $>250$  meters apart. The location of each sample plot center was recorded using a Trimble Geo XH GPS receiver using latitude-longitude (WGS 84). All GPS data were post-process differentially corrected ( $\pm 0.10$  m after post processing with a 95% CI using reference stations located  $<80$  km from the study area) to ensure the sample location was registered with the correct and representative pixel within the satellite imagery (Weber 2006; Weber et al. 2008).

Available herbaceous AGB was measured using a plastic coated cable hoop 2.36 meters in circumference. The hoop was randomly tossed into each of four quadrants (NW, NE, SE, and SW) centered over the sample point. All herbaceous vegetation within the hoop were clipped as close to the ground as allowed by the clipper (approximately 5mm of the ground surface) and weighed immediately ( $\pm 1$ g) using a Pesola scale tared to the weight of an ordinary paper bag. The samples were taken to the laboratory, and dried in 75 °C ovens for 48 hours. After drying, the samples were re-weighed to determine vegetation water content. Biomass was estimated following Sheley (1999) and expressed in kilograms per hectare.

### *Vegetation Indices Derived from SPOT 5 Imagery*

Satellite Pour l'Observation de la Terre 5 (SPOT 5) multispectral imagery (10 m x 10 m pixels) was acquired for the Big Desert study area on June 27, 2009. The imagery was georectified against 2004 National Agriculture Imagery Program (NAIP) natural color aerial imagery (1 m x 1 m pixels).

Atmospheric correction was performed with Idrisi Taiga (v16.03) using the ATMOSC module (Clark Labs, Worcester, MA). All imagery was corrected for atmospheric effects using the Cos(t) model (Chavez 1996) and input parameters reported in the metadata supplied by SPOT Image Corporation. The imagery was then projected into Idaho Transverse Mercator (NAD 83). The eight VI's used in this study were derived from the SPOT 5 imagery.

### *Water Sensitive Vegetation Indices*

Using the same SPOT5 imagery, eight WSVI's were developed by directly substituting the SWIR band for the RED band within the eight VI's described above (Table 2). The "Sample" tool within ESRI's ArcGIS 10 was then used to extract VI and WSVI values at each sample site ( $n = 29$ ). The resulting data were exported to SPSS (V17.0) for further analysis. Correlations between VI/WSVI values and measured herbaceous AGB were used to determine the applicability and efficacy of each.

**Table 2. Water sensitive vegetation indices (WSVI) used to estimate herbaceous total above ground biomass (AGB) (note the substitution of the SWIR band for the RED band [cf. table 2])**

<i>Index</i>	<i>Formula</i>
DWI	$NIR - SWIR$
RWI	$NIR/SWIR$
NDWI	$\frac{NIR - SWIR}{NIR + SWIR}$
RDWI	$\frac{NIR - SWIR}{\sqrt{NIR + SWIR}}$
SAWI	$\frac{(NIR - SWIR)(1 + L)}{NIR + SWIR + L}$ , where $L = 0.5$
MSAWI2	$\frac{2NIR + 1 - \sqrt{(2NIR + 1)^2 - 8(NIR - SWIR)}}{2}$
IPWI	$\frac{NIR}{NIR + SWIR}$
MWSR	$\frac{\frac{NIR}{SWIR} - 1}{\sqrt{\frac{NIR}{SWIR} + 1}}$

## RESULTS AND DISCUSSION

Field-based herbaceous AGB estimates ranged from 518 kg/ha to 8075 kg/ha ( $\bar{x} = 2982$  kg/ha) based on vegetation samples collected at 29 field locations. Using linear regression analysis between each VI and herbaceous AGB measurements, the relationship between these variables was described (Table 3). Based upon these results, it was noted that the relationships varied greatly and the strength of all correlations were relatively weak ( $0.28 \leq r^2 \leq 0.40$ ). This was likely attributable to the mixture of photosynthetic and non-photosynthetic plant material found in the field and correspondingly, in the herbaceous AGB samples used in this study. As a result, the VI's provided poor estimates of herbaceous AGB. Furthermore, the prediction of herbaceous AGB was least well explained using NDVI ( $r^2 = 0.28$ ,  $p = 0.003$ ) and as a result, NDVI was not considered a reliable predictor of herbaceous AGB in this study area, though it remains one of most widely used VI's for AGB prediction and many other vegetation studies.

**Table 3. Correlation between herbaceous total above ground biomass (AGB) and the VI's and WSVI's used in this study ( $r^2$  = coefficient of determination)**

Standard VI's using Red and NIR bands				Water sensitive VI's using NIR and SWIR bands			
Index	$r^2$	F-value	p	Index	$r^2$	F-value	p
DVI	0.40	17.9	<0.001	DWI	0.53	30.1	<0.001
RVI	0.35	14.3	0.001	RWI	0.54	31.2	<0.001
NDVI	0.28	10.6	0.003	NDWI	0.52	29.0	<0.001
RDVI	0.35	14.3	0.001	RDWI	0.52	29.8	<0.001
SAVI	0.37	15.8	<0.001	SAWI	0.53	29.8	<0.001
MSAVI2	0.39	17.0	<0.001	MSAWI2	0.53	30.3	<0.001
IPVI	0.28	10.6	0.003	IPWI	0.52	29.0	<0.001
MSR	0.32	12.6	0.001	MWSR	0.53	30.3	<0.001

Based on field survey data, the relationship between herbaceous AGB and vegetation water content (Figure 2) revealed a significant correlation ( $r^2 = 0.94$ ,  $P < 0.001$ ). Related studies have shown that grass biophysical parameters such as leaf area index are related to liquid water content (Hunt and Rock 1989; Roberts et al. 1997, 2004). Numata et al. (2008) indicated water absorption spectra between 1100 and 1250 nm had a significant correlation with canopy water content and suggested the use of water absorption features (i.e., water absorption depth and water absorption area) may improve the accuracy of biomass estimation. Therefore, the hypothesis that an index that closely correlates to water content may also exhibit strong correlation with herbaceous AGB was tested.

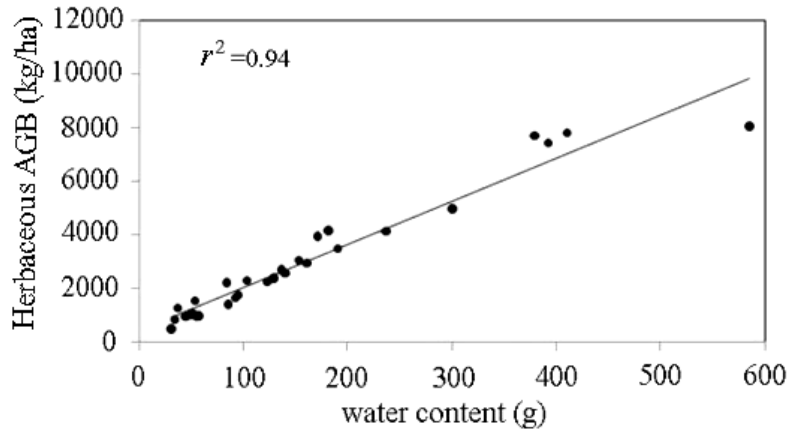


**Figure 2. Relationship between herbaceous total above ground biomass (AGB) and vegetation water content.**

In order to validate this hypothesis, the eight VI's used in this study along with eight WSVI's were correlated against vegetation water content (Table 4). The observed correlation between the VI's and vegetation water content were relatively weak ( $0.30 \leq r^2 \leq 0.40$ ), while the WSVI's were more highly correlated ( $r^2 \geq 0.51$ ) with vegetation water content. These results suggest the combination of NIR and SWIR bands are more sensitive to changes in liquid water content within vegetation, and that WSVI's exhibit a better response to water content of herbaceous vegetation in semiarid rangeland ecosystems.

**Table 4. Coefficients of determination ( $r^2$ ) calculated for the relationships between vegetation water content and vegetation indices**

Standard VI's using Red and NIR bands				Water sensitive VI's using NIR and SWIR bands			
<i>Index</i>	$r^2$	<i>F-value</i>	<i>p</i>	<i>Index</i>	$r^2$	<i>F-value</i>	<i>p</i>
DVI	0.40	17.9	<0.001	DWI	0.52	29.4	<0.001
RVI	0.35	14.8	0.001	RWI	0.52	29.7	<0.001
NDVI	0.30	11.6	0.002	NDWI	0.52	28.5	<0.001
RDVI	0.36	15.0	0.001	RDWI	0.52	29.1	<0.001
SAVI	0.38	16.2	<0.001	SAWI	0.52	29.2	<0.001
MSAVI2	0.39	17.2	<0.001	MSAWI2	0.52	29.5	<0.001
IPVI	0.30	11.6	0.002	IPWI	0.51	28.5	<0.001
MSR	0.33	13.4	0.001	MWSR	0.52	29.2	<0.001

Linear relationships were determined between eight WSVI's and herbaceous AGB (Table 3). In comparison to the more traditional VI's ( $r^2 \leq 0.40$ ), the WSVI's exhibited much stronger relationships with herbaceous AGB ( $r^2 \geq 0.52$ ). In addition, it is noted that the NDWI (based on the same simple band ratio structure as NDVI [NDVI=(NIR-R)/(NIR+R)]), better explained the variation in herbaceous AGB relative to NDVI (i.e., coefficient of determination increased from 0.28 to 0.52). This result is similar to previous research reporting that NDWI performed better in drought conditions than NDVI (Verbesselt et al. 2006a; Gu et al. 2007). These results further suggest that herbaceous AGB is highly correlated with vegetation water content and that WSVI's can more accurately predict herbaceous AGB for semiarid rangeland sites.

This study was designed for herbaceous AGB estimation in semiarid rangeland of Idaho. The relationships revealed by the study are still condition-specific and should not be directly extrapolated to other regions, however, the specific approach developed in this study can be used across other rangeland areas.

*Assessment of Error and Bias*

It is difficult to collect a large numbers of field-measured AGB data, and we used a relatively small sample size ( $n=29$ ) in this study. Because the limitation on sample size may influence the strength of each index, the robustness of the correlation between WSVI's and AGB were tested using the jackknife method (Table 5) (Efron and Gong 1983; Buermann et al. 2008). Small RMSE values were computed and the mean r-square values calculated by the jackknife method were similar to the r-square values given in Table 3. We conclude that the observed correlation between WSVI's and AGB were not highly influenced by a few individual samples and the regression and correlation results presented herein are robust.

**Table 5. The robustness of the correlation between WSVI's and AGB were tested by the jackknife method**

<i>Index</i>	<i>Mean <math>r^2</math></i>	<i>RMSE</i>
DWI	0.52	0.032
RWI	0.54	0.026
NDWI	0.51	0.038
RDWI	0.52	0.031
SAWI	0.51	0.036
MSAWI2	0.51	0.038
IPWI	0.52	0.019
MWSR	0.53	0.037

Previous studies have demonstrated varied results with VI's and each reveal different strengths of correlations with AGB under specific conditions dependent upon the phenology of plants within a given growing season (Reeves et al. 2001). Cho and Skidmore (2009) indicate VI's are highly correlated ( $r^2 \geq 0.50$ ) with AGB when the vegetation was in the early stages of senescence. In semiarid rangeland ecosystems, high summer temperatures hasten the desiccation of plants, and many plants begin senescence in mid-late June. In this study, all herbaceous AGB data were collected between July 1 and July 9, 2009. Based on monthly precipitation data provided by the United States Department of Agriculture (USDA) Natural Resources Conservation Service (NRCS) (<http://www.id.nrcs.usda.gov/snow/data/historic.html>) and the United States Bureau of Reclamation (USBR) AgriMet Program (<http://www.usbr.gov/pn/agrimet/>), it is noted that mean monthly precipitation between April and July 2009 (260 mm) was greater than the monthly precipitation during the same time period in either 2007 (140 mm) or 2008 (92 mm), and that precipitation in June substantially increased in 2009 (48 mm [2007], 21mm [2008], 141 mm [2009]). (Figure 1) (Table 6; Table 7). These statistics, along with cooler than average temperatures, suggest that senescence may have been delayed in 2009, with the experimental time period of this study falling within the early stages of senescence. Numata et al. (2008) achieved very poor correlation between NDWI/NDVI and herbaceous AGB (Table 1) because their field sampling occurred much later in the season (beginning of August) and during a time of the year when most herbaceous plant materials were already senesced.

**Table 6. Natural Resources Conservation Service (NRCS) and AgriMet survey site list along with monthly precipitation (mm) and monthly mean temperature (°C)**

Site name	Lat	Long	Year	Precipitation					Mean temperature		
				April	May	June	July	Total	May	June	July
Garfield R.S.	43°36'	-113°55'	2007	43	8	25	28	104	9	13	19
			2008	23	43	13	23	102	16	19	20
			2009	30	71	203	20	324	8	10	16
Swede Peak	43°37'	-113°58'	2007	56	15	30	38	139	8	13	19
			2008	25	28	3	0	56	7	12	18
			2009	28	43	201	23	295	7	9	15
Smiley Mountain	43°43'	-113°50'	2007	89	33	89	15	226	6	10	17
			2008	30	94	48	13	185	3	8	15
			2009	89	91	180	43	403	5	7	13
Howell Canyon	42°19'	-113°36'	2007	150	30	117	25	322	8	12	18
			2008	56	76	58	15	205	5	10	17
			2009	124	66	170	3	363	7	9	16
Wildhorse Divide	42°45'	-112°28'	2007	86	25	74	13	198	10	13	18
			2008	36	66	33	0	135	7	12	17
			2009	107	58	163	36	364	9	11	16
Fort Hall	43°04'	-112°25'	2007	30	5	39	5	79	13	17	23
			2008	3	37	9	4	53	11	16	20
			2009	31	29	97	15	172	12	15	20
Rupert	42°35'	-113°52'	2007	19	9	20	8	56	14	17	23
			2008	3	17	12	7	39	12	17	21
			2009	26	18	53	6	103	13	15	21
Picabo	43°18'	-114°09'	2007	23	3	10	3	39	13	18	24
			2008	7	22	7	0	36	11	16	21
			2009	20	41	98	8	167	12	14	20
Aberdeen	42°57'	-112°49'	2007	36	3	30	14	83	14	18	23
			2008	4	23	6	1	34	12	16	21
			2009	23	22	102	17	164	13	15	20

**Table 7. Analysis of precipitation (mm) and temperature (°C) on 2007, 2008 and 2009**

Year	Average precipitation				Average temperature			Total precipitation	Standard deviation
	April	May	June	July	May	June	July		
2007	59	15	48	17	11	15	20	140	56 <sup>1</sup>
2008	20	45	21	7	9	14	19	92	
2009	53	49	141	19	10	12	17	260	69 <sup>2</sup>

<sup>1</sup>Standard deviation of precipitation for 2007 and 2008.

<sup>2</sup>Standard deviation of precipitation for 2008 and 2009.

NDVI physically responds to chlorophyll absorption and is not directly related to the quantity of water in the vegetation (Ceccato et al. 2002). Cheng et al. (2008) indicate that NDVI shows correlation with water content was probably due to the correlation to green leaf density. Because of the sparse vegetation and dry plant matter (litter) found in semiarid regions, NDVI was not a reliable indicator of water content or herbaceous AGB in this study. However, some AGB estimates have shown strong NDVI correlations to biomass ( $r^2 \geq 0.50$ ), but this may be because these study areas were more homogeneous and/or contained a higher proportion of green grass cover (Mašková et al. 2008). The accuracy of herbaceous AGB predictions based upon remotely sensed data is strongly influenced by the presence and abundance of grass species as well as the presence and abundance of bare ground and other spectral distraction features. A more homogeneous surface always provides higher correlations between remotely sensed measures and herbaceous AGB estimates compared to more heterogeneous surfaces (Numata et al. 2008). In addition, as opposed to the traditional VI, the WSVI's have the advantage of leveraging liquid water absorption regions to more accurately predict water content even in areas without contiguous spectral coverage (Serrano et al. 2000). This is possibly one reason why the WSVI's performed better in the semiarid rangelands of Idaho.

## **CONCLUSION**

This study focused on the estimation of herbaceous AGB in the semiarid rangelands of Idaho. Based on a survey of herbaceous AGB, a significant correlation ( $p < 0.001$ ) between herbaceous AGB and vegetation water content was found. In addition, a suite of WSVI's were developed that describe water content and herbaceous AGB in semiarid rangeland ecosystems. Correlation estimates between herbaceous AGB, VI's, and WSVI's were calculated, and the performance of herbaceous AGB predictions for both the VI's and WSVI's were evaluated using field-based measurements of herbaceous AGB. Results demonstrate the WSVI's were correlated ( $r^2 \geq 0.51$ ) with vegetation water content and performed better in herbaceous AGB estimation for the semiarid rangelands of Idaho relative to VI's. Furthermore, it was noticed that not only did vegetation water content influence the accuracy of herbaceous AGB estimates, but based on findings reported in other studies, phenological stage and plant community structure also influence the accuracy of herbaceous AGB estimates derived from remotely sensed data. Numerous factors influence the successful use of remote sensing data for the estimation of herbaceous AGB and water content, described using WSVI's, explained approximately 50% of the variance in herbaceous AGB measurements collected as part of this study. Other factors that likely play a role include sun angle, shadow, georegistration, and the varying affect of soils. Future work will seek to assess a more comprehensive characterization of the influence of these factors on herbaceous AGB estimations in semiarid rangelands.

## **ACKNOWLEDGMENTS**

This study was made possible by a grant from the National Aeronautics and Space Administration Goddard Space Flight Center (NNX08AO90G). Idaho State University would also like to acknowledge the Idaho Delegation for their assistance in obtaining this grant.

## **LITERATURE CITED**

Boelman, N.T., M. Stieglitz, H.M. Rueth, M. Sommerkorn, K.L. Griffin, G.R. Shaver, and J.A. Gamon, 2003. Response of NDVI, Biomass, and Ecosystem Gas Exchange to Long-term Warming and Fertilization in Wet Sedge Tundra, *Oecologia*, 135(3): 414-421

- Box, E.O., B.N. Holben, and V. Kalb, 1989. Accuracy of the AVHRR Vegetation Index as a Predictor of Biomass, Primary Productivity and Net CO<sub>2</sub> Flux, *Plant Ecology*, 80(2): 71-89
- Breman, H., and C.T. de Wit, 1983. Rangeland Productivity and Exploitation in the Sahel, *Science*, 221(4618): 1341-1347
- Buermann, W., S. Saatchi, T.B. Smith, B.R. Zutta, J.A. Chaves, B. Milá, and C.H. Graham, 2008. Predicting Species Distributions Across the Amazonian and Andean Regions Using Remote Sensing Data, *Journal of Biogeography*, 35(7): 1160-1176
- Ceccato, P., S. Flasse, S. Tarantola, S. Jacquemond, and J.M. Gregoire, 2001. Detecting Vegetation Leaf Water Content Using Reflectance in the Optical Domain, *Remote Sensing of Environment*, 77(1): 22-33
- Ceccato, P., S. Flasse, and J.M. Gregoire, 2002. Designing a Spectral Index to Estimate Vegetation Water Content from Remote Sensing Data: Part 2. Validation and Applications, *Remote Sensing of Environment*, 82(2-3): 198-207
- Chavez, P.S., 1996. Image-based Atmospheric Corrections: Revisited and Improved, *Photogrammetric Engineering and Remote Sensing*, 62(9): 1025-1036
- Chen, J.M., 1996. Evaluation of Vegetation Indices and a Modified Simple Ratio for Boreal Applications, *Canadian Journal of Remote Sensing*, 22(3): 229-242
- Cheng, Y.B., S.L. Ustin, D. Riaño, and V.C. Vanderbilt, 2008. Water Content Estimation from Hyperspectral Images and MODIS Indexes in Southeastern Arizona, *Remote Sensing of Environment*, 112(2): 363-374
- Cho, M.A., and A.K. Skidmore, 2009. Hyperspectral Predictors for Monitoring Biomass Production in Mediterranean Mountain Grasslands: Majella National Park, Italy, *International Journal of Remote Sensing*, 30(2): 499-515
- Chuvieco, E., D. Cocero, D. Riaño, P. Martin, J. Martínez-Vega, J.D.L. Riva, and F. Pérez, 2004. Combining NDVI and Surface Temperature for the Estimation of Live Fuels Moisture Content in Forest Fire Danger Rating, *Remote Sensing of Environment*, 92(3): 322-331
- Crippen, R.E., 1990. Calculating the Vegetation Index Faster, *Remote Sensing of Environment*, 34(1): 71-73
- Davidson, A., and F. Csillag, 2001. The Influence of Vegetation Index and Spatial Resolution on a Two-date Remote Sensing Derived Relation to C4 Species Coverage, *Remote Sensing of Environment*, 75(1): 138-151

- Efron, B., and G. Gong, 1983. A Leisurely Look at the Bootstrap, the Jackknife, and Cross-validation, *American Statistician*, 37(1): 36-48
- Flynn, E.S., C.T. Dougherty, and O. Wendroth, 2008. Assessment of Pasture Biomass with the Normalized Difference Vegetation Index from Active Ground-based Sensors, *Agronomy Journal*, 100(1): 114-121
- Foody, G.M., D.S. Boyd, and M.E.J. Cutler, 2003. Predictive Relations of Tropical Forest Biomass from Landsat TM Data and Their Transferability between Regions, *Remote Sensing of Environment*, 85(4): 463-474
- Friedl, M.A., J. Michaelsen, F.W. Davis, H. Walker, and D.S. Schimel, 1994. Estimating Grassland Biomass and Leaf Area Index Using Ground and Satellite Data, *International Journal of Remote Sensing*, 15(7): 1401-1420
- Gao, B.C, 1996. NDWI : A Normalized Difference Water Index for Remote Sensing of Vegetation Liquid Water from Space, *Remote sensing of environment*, 58(3): 257-266
- Gu, Y., J.E. Brown, J.P. Verdin, and B. Wardlow, 2007. A Five-year Analysis of MODIS NDVI and NDWI for Grassland Drought Assessment over the Central Great Plains of the United States, *Geophysical Research Letter*, 34(L06407), doi:10.1029/2006GL029127
- Hill, M.J., 2004. Grazing Agriculture: Managed Pasture, Grassland, and Rangeland, Pages 449-530 in S. L. Ustin (Ed.) Manual of Remote Sensing volume 4: Remote sensing for natural resource management and environmental monitoring. Hoboken, NJ, United States: John Wiley & Sons.
- Huete, A.R., 1988. A Soil-adjusted Vegetation Index (SAVI), *Remote sensing of environment*, 25(3): 295-309
- Huete, A.R., K. Didan, T. Miura, E.P. Rodriguez, X. Gao, and L.G. Ferreira, 2002. Overview of the Radiometric and Biophysical Performance of the MODIS Vegetation Indices, *Remote Sensing of Environment*, 83(1-2): 195-213
- Hunt, E.R. and B.N. Rock, 1989. Detection of Changes in Leaf Water Content Using Near- and Middle-Infrared Reflectances, *Remote Sensing of Environment*, 30(1): 43-54
- Huntsinger, L. and P. Hopkinson, 1996. Viewpoint: Sustaining Rangeland Landscapes: A Social and Ecological Process, *Journal of Range Management*, 49(2): 167-173
- Jackson, T.J., D. Chen, M. Cosh, F. Li, M. Anderson, C. Walthall, P. Doriaswamy, and E.R. Hunt, 2004. Vegetation Water Content Mapping Using Landsat Data Derived Normalized Difference Water Index for Corn and Soybeans, *Remote Sensing of Environment*, 92(4): 475-482

- Jacquemoud, S., S.L. Ustin, J. Verdebout, G. Schmuck, G. Andreoli, and B. Hosgood, 1996. Estimating Leaf Biochemistry Using the PROSPECT Leaf Optical Properties Model, *Remote Sensing of Environment*, 56(3): 194-202
- Jordan, C.F., 1969. Derivation of Leaf Area Index from Quality of Light on the Forest Floor, *Ecology*, 50(4): 663-666
- Kawamura, K., T. Akiyama, H. Yokota, M. Tsutsumi, T. Yasuda, O. Watanabe, and S. Wang, 2005. Comparing MODIS Vegetation Indices with AVHRR NDVI for Monitoring the Forage Quantity and Quality in Inner Mongolia Grassland, China, *Grassland Science*, 51(1): 33-40
- Kogan, F., R. Stark, A. Gitelson, L. Jargalsaikhan, and S. Tsooj, 2004. Derivation of Pasture Biomass in Mongolia from AVHRR-based Vegetation Health Indices, *International Journal of Remote Sensing*, 25(14): 2889-2896
- Masková, Z., F. Zemek, and J. Kvet, 2008. Normalized Difference Vegetation Index (NDVI) in the Management of Mountain Meadows, *Boreal Environmental Research*, 13(5): 417-432
- Mirik, M., J. Norland, R. Crabtree, and M. Biondini, 2005. Hyperspectral One-meter-resolution Remote Sensing in Yellowstone National Park, Wyoming: II. Biomass, *Rangeland Ecology and Management*, 58(5): 459-465
- Mutanga, O., and A.K. Skidmore, 2004. Hyperspectral Band Depth Analysis for a Better Estimation of Grass Biomass (*Cenchrus ciliaris*) Measured under Controlled Laboratory Conditions, *International Journal of Applied Earth Observation and Geoinformation*, 5(2): 87-96
- Numata, I., D.A. Roberts, O.A. Chadwick, J.P. Schimel, L.S. Galvão, and J.V. Soares, 2008. Evaluation of Hyperspectral Data for Pasture Estimate in the Brazilian Amazon Using Field and Imaging Spectrometers, *Remote Sensing of Environment*, 112(4): 1569-1583
- Qi, J., A. Chehbouni, A.R. Huete, Y.H. Kerr, and S. Sorooshian, 1994. A Modified Soil Adjusted Vegetation Index. *Remote Sensing of Environment*, 48(2): 119-126
- Reeves, M.C., J.C. Winslow, and S.W. Running, 2001. Mapping Weekly Rangeland Vegetation Productivity Using MODIS Algorithms, *Rangeland Ecology & Management*, 54: A90-A105
- Richardson, A.J., and J.H. Everitt, 1992. Using Spectral Vegetation Indices to Estimate Rangeland Productivity. *Geocarto International*, 7(1): 63-69
- Roberts, D.A., R.O. Green, and J.B. Adams, 1997. Temporal and Spatial Patterns in Vegetation and Atmospheric Properties from AVIRIS. *Remote Sensing of Environment*, 62(3): 223-240

- Roberts, D.A., S.L. Ustin, S. Ogunjemiyo, J. Greenberg, S.Z. Dobrowski, J.Q. Chen, and T.M. Hinckley, 2004. Spectral and Structural Measures of Northwest Forest Vegetation at Leaf to Landscape Scales, *Ecosystems*, 7(5): 545-562
- Roujean, J.L., and F.M. Breon, 1995. Estimating PAR Absorbed by Vegetation from Bidirectional Reflectance Measurements, *Remote Sensing of Environment*, 51(3): 375-384
- Rouse, J.W., R.H. Haas, J.A. Schell, and D.W. Deering, 1973. Monitoring Vegetation Systems in the Great Plains with ERTS, in the 3rd Earth Resources Technology Satellite Symposium, 10-14 December 1973, Washington, D.C., USA, 309-317
- Running, S.W., R.R. Nemani, F.A. Heinsch, M. Zhao, M.C. Reeves, and H. Hashimoto, 2004. A Continuous Satellite-derived Measure of Global Terrestrial Primary Production, *BioScience*, 54(6): 547-560
- Samimi, C., and T. Kraus, 2004. Biomass Estimation Using Landsat-TM and -ETM+. Towards a Regional Model for Southern Africa? *GeoJournal*, 59(3): 177-187
- Sannier, C.A.D., J.C. Taylor, and W. Du Plessis, 2002. Real-time Monitoring of Vegetation Biomass with NOAA-AVHRR in Etosha National Park, Namibia, for Fire Risk Assessment, *International Journal of Remote Sensing*, 23(1): 71-89
- Schino, G., F. Borfecchia, L. Cecco, C. Dibari, M. Iannetta, S. Martini, and F. Pedrotti, 2003. Satellite Estimate of Grass Biomass in a Mountainous Range in Central Italy, *Agroforestry Systems*, 59(2): 157-162
- Serrano, L., S.L. Ustin, D.A. Roberts, J.A. Gamon, and J. Peñuelas, 2000. Deriving Water Content of Chaparral Vegetation from AVIRIS Data, *Remote Sensing of Environment*, 74(3): 570-581
- Sheley, R. 1999. AUM Analyzer Software, Montana State University, Bozeman, Mont. URL = <http://www.montana.edu>, visited 31-March-2010
- Studley, H. and K.T. Weber, 2009. Range Vegetation Assessment in the Big Desert, Upper Snake River Plain, Idaho, URL = [http://giscenter.isu.edu/research/Techpg/nasa\\_postfire/To\\_PDF/2009\\_Big\\_Desert\\_FieldReport.pdf](http://giscenter.isu.edu/research/Techpg/nasa_postfire/To_PDF/2009_Big_Desert_FieldReport.pdf) visited 31-March-2010
- Tucker, C.J., 1979. Red and Photographic Infrared Linear Combinations for Monitoring Vegetation, *Remote Sensing of Environment*, 8(2): 127-150
- Verbesselt, J., P. Jonsson, S. Lhermitte, J. van Aardt, and P. Coppin, 2006a. Evaluating Satellite and Climate Data-derived Indices as Fire Risk Indicators in Savanna Ecosystems, *IEEE Transactions on Geoscience and Remote Sensing*, 44(6): 1622-1632

Verbesselt, J., B. Somers, J. van Aardt, I. Jonckheere, and P. Coppin, 2006. Monitoring Herbaceous Biomass and Water Content with SPOT VEGETATION Time-series to Improve Fire Risk Assessment in Savanna Ecosystems, *Remote Sensing of Environment*, 101(3): 399-414

Weber, K.T., 2006. Challenges of Integrating Geospatial Technologies into Rangeland Research and Management, *Rangeland Ecology and Management*, 59(1): 38-43

Weber, K.T., J. Theau, and K. Serr, 2008. Effect of Co-registration Error on Patchy Target Detection Using High-resolution Imagery, *Remote Sensing of the Environment*, 112(3): 845-850

Weiser, R.L., G. Asrar, G.P. Miller, and E.T. Kanemasu, 1986. Assessing Grassland Biophysical Characteristics from Spectral Measurements, *Remote Sensing of the Environment*, 20(2): 141-152

Wessels, K.J., S.D. Prince, N. Zambatis, S. MacFadyen, P.E. Frost, and D. Van Zyl, 2006. Relationship between Herbaceous Biomass and 1-km<sup>2</sup> Advanced Very High Resolution Radiometer (AVHRR) NDVI in Kruger National Park, South Africa, *International Journal of Remote Sensing*, 27(5): 951-973

Xu, B., X.C. Yang, W.G. Tao, Z.H. Qin, H.Q. Liu, J.M. Miao, and Y.Y. Bi, 2008. MODIS-based Remote Sensing Monitoring of Grass Production in China, *International Journal of Remote Sensing*, 29(17): 5313-5327

Zarco-Tejada, P.J., C.A. Rueda, and S.L. Ustin, 2003. Water Content Estimation in Vegetation with MODIS Reflectance Data and Model Inversion Methods, *Remote Sensing of Environment* 85(1): 109-124

**Recommended citation style:**

Chen, F., K.T. Weber, B. Gokhale, 2011. Herbaceous Biomass Estimation from SPOT-5 Imagery in Semiarid Rangelands of Idaho. Pages 89-104 in K. T. Weber and K. Davis (Eds.), Final Report: Assessing Post-Fire Recovery of Sagebrush-Steppe Rangelands in Southeastern Idaho (NNX08AO90G). 252 pp.

## **NDVI Changes Over a Calendar Year in the Rangelands of Southeast Idaho**

Linda Tedrow, ISU GIS Training and Research Center, Idaho State University, 921 S. 8th Ave., Stop 8104, Pocatello, Idaho 83209-8104

Keith T. Weber, GISP, GIS Director, ISU GIS Training and Research Center, Idaho State University, 921 S. 8th Ave., Stop 8104, Pocatello, Idaho 83209-8104 (webekeit@isu.edu)

### **ABSTRACT**

Annual vegetation trends for the 2007 calendar year were analyzed across rangelands of southeast Idaho using MODIS 16-day composite NDVI. These data characterize rangeland phenology by providing maximum NDVI throughout each compositing period. Results illustrate NDVI values in semiarid rangelands of Idaho exhibit a bimodal curve and suggest maximum productivity occurs early in spring followed by a secondary period of heightened productivity in autumn. While these periods of photosynthetic activity are not analogous with above ground biomass or standing crop, these observations represent important considerations for improved understanding of rangeland dynamics and plant phenology, relative to ecosystem productivity.

*KEYWORDS: Rangeland, remote sensing, NDVI, MODIS, digital change detection, vegetation index*

## INTRODUCTION

NASA's Earth Observing System (EOS) is a coordinated series of polar-orbiting low inclination satellites designed to support long-term global observations. Measurements collected by the Moderate Resolution Imaging Spectroradiometer (MODIS) instruments of EOS are used to calculate Normalized Difference Vegetation Indices (NDVI) which are the basis of this study exploring the phenological cycle of semiarid sagebrush-steppe vegetation communities in southeast Idaho.

The Terra satellite, also known as EOS-AM-1, has a morning equator crossing time (Hobish, 2009) and is considered the flagship of the EOS platforms. Terra provides global data on the state of the atmosphere, land and oceans (Netting, 2008) and includes five state-of-the-art instruments: an Advanced Space borne Thermal Emission and Reflection Radiometer (ASTER), a Multi-angle Imaging Spectro-Radiometer (MISR), a Clouds and the Earth's Radiant Energy System (CERES) monitor, a Measurements of Pollution in the Troposphere (MOPIT) sensor, and MODIS. On February 24, 2000, Terra began collecting a planned 15-year global data set. The Terra satellite orbits the earth at an altitude of 705 km and is sun-synchronous, so that it crosses any given latitude directly overhead at the same time each day.

The MODIS instrument employs a whiskbroom imaging-radiometer that consists of a cross-track scan mirror and collecting optics, and a set of linear detector arrays with spectral interference filters located in four focal planes (Jensen 2005). These instruments provide daylight reflection and day/night emission spectral imaging for any point on the Earth at least every two days, under continuous operation (Graham, 2008). The MODIS sensor is a 36-band spectroradiometer that measures visible and infrared radiation from 0.4 to 14.5  $\mu\text{m}$ , and was selected for diagnostic significance in Earth science. The individual spectral bands have spatial resolutions of 250 m, 500 m, or 1000 m at nadir. The measurements made by the MODIS sensor yield data used to develop products ranging from vegetation indices and productivity estimates, land surface cover, ocean chlorophyll fluorescence, as well as cloud and aerosol properties, fire occurrence, terrestrial snow cover, and sea ice cover (Running *et al.*, 1994).

There are 62 different MODIS products with full descriptions available on the Internet (EOS Data Products Handbook, Volume 1 [King, *et. al*, 2004]). The MODIS product used in this study was MOD13Q1 (250m vegetation indices with 16-day temporal granularity). The MOD13Q1 product is a composite of data from the Terra satellite and includes Normalized Difference Vegetation Index (NDVI) imagery as well as Enhanced Vegetation Index (EVI) imagery. Atmospherically corrected bi-directional surface reflectance with masking for water, clouds, heavy aerosols, and cloud shadows form the basis for these products. The vegetation index products represent a 16-day composite at 250-meter spatial resolution in a Sinusoidal projection. This particular composite allows the algorithm to include only values that are acquired during cloud free days and/or days when the data is considered more reliable due to the absence of water, clouds, and heavy aerosols in the atmosphere.

### *The Normalized Difference Vegetation Index (NDVI)*

NDVI is an environmental model based on deductive logic and empirical data and is the result of the relationship between the amount of near-infrared ( $\rho_{\text{nir}}$ ) and red ( $\rho_{\text{red}}$ ) spectral reflectance of land cover (Skidmore, 2002). Both near-infrared ( $\rho_{\text{nir}}$ ) and red ( $\rho_{\text{red}}$ ) spectral reflectance are measured at the sensor and are therefore considered empirically derived field measurements. However, because reflected energy travels through a large amount of atmosphere before it is measured by the sensor, numerous attenuation

factors affect the signal measured at the sensor. While atmospheric correction algorithms can be used to eliminate these factors, none are perfect as several input variables required to complete the calculations are estimates or constants (e.g., optical thickness) while other factors are variable across a scene (i.e., viewing angle changes slightly from scene center to its edges). Nonetheless, NDVI is a valuable product that has been used to monitor seasonal and inter-annual changes in vegetation growth and activity (Jensen, 2005).

Bands 1 and 2 of the MODIS sensor collect measurements of surface reflectance in the visible red (620 – 670 nm) and near infrared (841-876 nm) regions of the electromagnetic spectrum (EMS). These bands are then used in a simple band ratio to estimate NDVI (Equation 1)

$$NDVI = (\rho_{nir} - \rho_{red}) / (\rho_{nir} + \rho_{red}) \quad (1)$$

The chlorophyll of green leaves absorb most of the visible light within the red portion of the EMS for use in active photosynthesis, while the cell structure of leaves reflects light in the near-infrared portion of the EMS (Figure 1). A plant that is actively photosynthesizing will absorb most of the visible light available, resulting in  $\rho_{red}$  being very small and NDVI values being very close to one (1). In contrast, senescent vegetation will absorb much less visible light resulting in smaller NDVI values (close to zero). Water typically has an NDVI value less than 0, bare soils between 0 and 0.1 and vegetation >0.1 (Table 1).

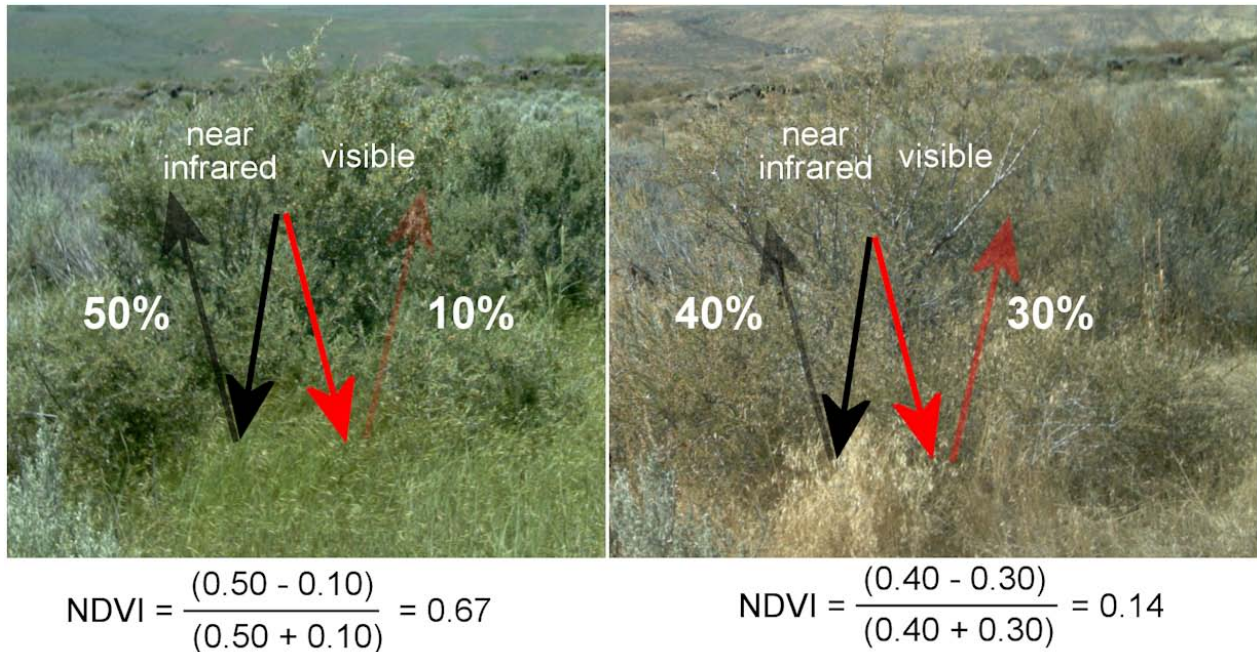


**Figure 1. Photograph illustrating how the ratio of reflectance can change within a growing season. Photo on the left was taken in late-May while the photo on the right was taken in September (illustration by Keith T. Weber, modeled after Weier and Herring, 2008).**

**Table 1. Typical NDVI values for various cover types (from Holben [1986])**

COVER TYPE	RED	NIR	NDVI
Dense vegetation	0.100	0.500	0.700
Dry Bare soil	0.269	0.283	0.025
Clouds	0.227	0.228	0.002
Snow and ice	0.375	0.342	-0.046
Water	0.022	0.013	-0.257

The NDVI equation (Equation 1) results in a dimensionless value (index) that indicates the abundance and relative level of photosynthetic activity of green vegetation. Environmental conditions such as soil color, atmospheric conditions, litter abundance, etc., effect reflectance values in both the red and near-infrared regions of the EMS and thereby effect NDVI. The theory behind ratioing the components in the NDVI equation was that these noise factors (atmospheric conditions, etc.) would be compensated for; however, some still affect vegetation index values (e.g., litter) making these data difficult to apply directly. However, the calibrated hyperspectral sensor system of MODIS and the algorithms used to generate its various products further reduce the effects of the environmental factors and thereby increase the reliability of MODIS products. The MODIS product used in this study (MOD13Q1) includes the two vegetation indices (NDVI and EVI) as well as the source data (red and near-infrared reflectance) used to compute the respective indices (Table 2). In addition MOD13Q1 includes a layer indicating a reliability rating for each pixel throughout the 16-day compositing period (Table 3).

**Table 1. Science Data Sets for MODIS Terra Vegetation Indices 16-Day L3 Global 250m SIN Grid V005 (MOD13Q1)**

Science Data Sets	UNITS	BIT TYPE	FILL	VALID RANGE	MULTIPLY BY SCALE FACTOR
<b>(HDF Layers) (12)</b>					
250m 16 days NDVI	NDVI	16-bit signed integer	-3000	-2000, 10000	0.0001
250m 16 days EVI	EVI	16-bit signed integer	-3000	-2000, 10000	0.0001
250m 16 days VI Quality detailed QA	Bits	16-bit unsigned integer	65535	0, 65534	NA
250m 16 days red reflectance (Band1)	Reflectance	16-bit signed integer	-1000	0, 10000	0.0001
250m 16 days NIR reflectance (Band2)	Reflectance	16-bit signed integer	-1000	0, 10000	0.0001
250m 16 days blue reflectance (Band3)	Reflectance	16-bit signed integer	-1000	0, 10000	0.0001
250m 16 days MIR	Reflectance	16-bit signed integer	-1000	0, 10000	0.0001

reflectance (Band7)		integer			
250m 16 days view	Degree	16-bit signed	-	-9000, 9000	0.01
zenith angle		integer	10000		
250m 16 days sun	Degree	16-bit signed	-	-9000, 9000	0.01
zenith angle		integer	10000		
250m 16 days rel.	Degree	16-bit signed	-4000	-3600, 3600	0.1
azimuth angle		integer			
250m 16 days	Julian day of	16-bit signed	-1	1, 366	NA
composite	the year	integer			
day of the year					
250m 16 days	Rank	8-bit signed	-1	0, 3	NA
pixel reliability		integer			
summary QA					

**Table 2. MOD13Q1 pixel reliability codes and descriptions**

Rank Key	Summary QA	Description
-1	Fill/No Data	Not Processed
0	Good Data	Use with confidence
1	Marginal Data	Useful, but look at other QA information
2	Snow/Ice	Target covered with snow/ice
3	Cloudy	Target no visible, covered with cloud

This study used MOD13Q1 imagery data collected throughout 2007 to investigate the intra-annual NDVI curve for the Big Desert study area in southeast Idaho. The investigation sought to determine the type of trendline exhibited over semiarid sagebrush-steppe rangelands to better understand seasonal changes in vegetation and the phenological cycle of the shrubs, grasses, and forbs found in the region.

**METHODS**

*Study Area*

The Big Desert study area is approximately 71 km northwest of Pocatello with the center of the study area located at approximately 113° 4' 18.68" W and 43° 14' 27.88" N. The Big Desert study area extends over nearly 120,000 hectares (Figure 2) and exhibits a topography that is flat to gently rolling hills with frequent lava outcrops. Dominant shrubs include Wyoming big sagebrush (*Artemisia tridentate wyomingensis*), three-tip sagebrush (*A. tripartite*), and Green Rabbitbrush (*Chrysothammus viscidiflorus*). The understory is mainly bluebunch wheatgrass (*Agropyron spicatum*) with Sandberg bluegrass (*Poa sandbergii*) and bottlebrush squirreltail (*Sitanion hystrix*). Cheatgrass (*Bromus tectorum*) is the most common non-native invasive species. In addition, some portions of the Big Desert study area have been seeded with crested wheatgrass (*Agropyron cristatum*) (Wakkinen *et al.*, 1992) (Sander and Weber, 2005) as a result of wildfires. Livestock (primarily sheep) graze much of the study area and in August 2006, the Crystal Fire burned nearly 90,000 ha (Osmond *et al.*, 2006) of the Big Desert.

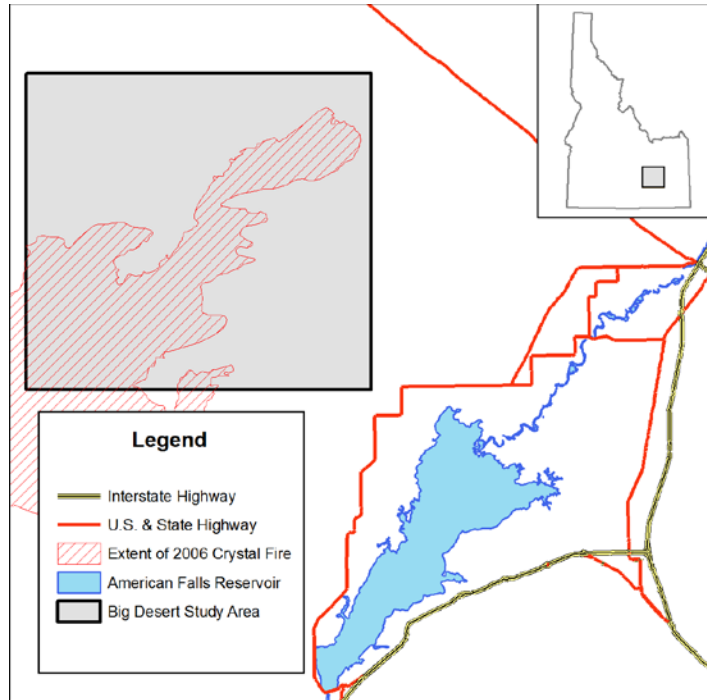


Figure 2. Location of the Big Desert study area in southeast Idaho.

*Sample Design*

The sample points ( $n = 119$ ) used to extract NDVI values from the MODIS NDVI product were a subset of field sample locations used in previous studies between 2006 and 2008 (Tedrow *et al.*, 2008; Anderson *et al.*, 2007; Underwood *et al.*, 2006). In each of these previous studies, vegetation data were collected at approximately 100 randomly located sample points. Many of these sampling points were linked to a set of four photographs taken at the sample site looking north, south, east, and west. The subset of sample points used in this study were outside the perimeter of the 2006 Crystal Fire and were a minimum of 350 meters from all other sample points to avoid the possibility of two sample points being located in the same 250-m pixel and to reduce any spatial autocorrelation effects. In cases where two points were located within the same pixel, the sample point containing more current and complete field data was selected for use in this study. The final set of samples ( $n = 119$ ) included 69 with field photographs taken at the time of data collection (Figure 3).

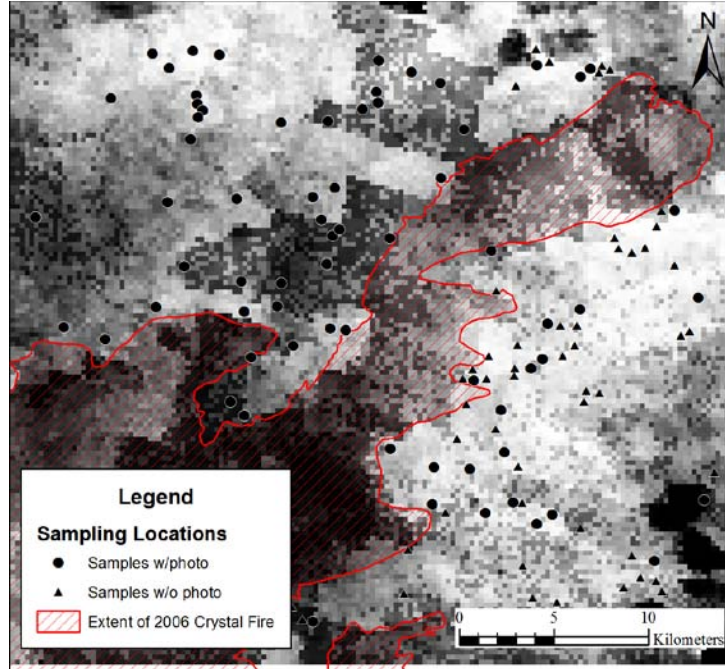


Figure 3. Locations within the Big Desert study area used to extract NDVI values from MODIS imagery (cf. Figure 2).

*Image Data*

The MOD13Q1 data for the 2007 calendar year included 23 data files obtained via the Internet (<ftp://e4ftl01u.ecs.nasa.gov/MOLA/MYD13Q1.005>). The file naming system employed at this site followed convention that provided much useful information and facilitated the discovery and selection of imagery (e.g., file names [MOD13Q1.A2007145.h09v04.005.2007181101531.hdf] can be interpreted using Table 4).

**Table 4 File naming Convention used for MODIS files obtained from NASA**

<b>Name Part</b>	<b>Description</b>
MOD13Q1	Product Short Name – MODIS Sensor from Terra Satellite
A2007145	Julian Date of Acquisition (A-YYYYDDD)
H09v04	Tile Identifier (horizontal XX vertical YY) from the Sinusoidal Tiling System (Figure 4). The longitudinal minimum is -140.0151 and the longitudinal maximum is -104.4217. The latitudinal minimum is 40.00 and the latitudinal maximum is 50.00.
005	Collection Version
2007181101531	Julian date of Production (YYYYDDDHHMMSS) Y = 2007, D = 181, H = 10, M = 15, S = 31
Hdf	Data format

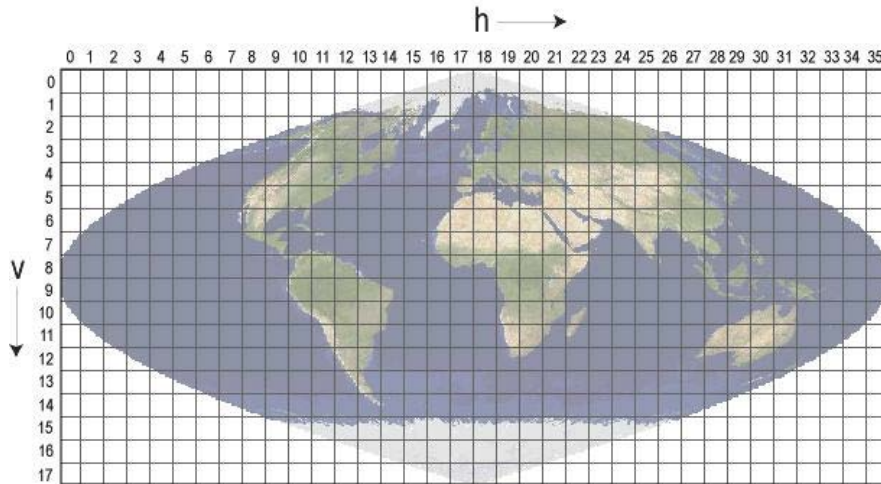


Figure 4. MODIS Sinusoidal Tiling System (from [http://modis-land.gsfc.nasa.gov/MODLAND\\_grid.htm](http://modis-land.gsfc.nasa.gov/MODLAND_grid.htm)).

### GIS Processing

The first of the 12 layers in each HDF dataset contained NDVI imagery. These data were projected into Idaho Transverse Mercator (NAD83) and then clipped to the Big Desert study area using ESRI ArcGIS. The ESRI Spatial Analyst Tool (Sample) was used to create a spreadsheet of the NDVI values extracted at each of the 119 sample points throughout the 2007 calendar year. These data were then summarized, graphed, and analyzed to illustrate and interpret the minimum, maximum, and mean NDVI for each 16-day compositing period across the 2007 calendar year.

## RESULTS AND DISCUSSION

The annual NDVI curve for the semiarid sagebrush-steppe vegetation communities of Big Desert study area (Figure 5) shows an initial increase in vegetation productivity in early March with maximum NDVI values achieved in early June.

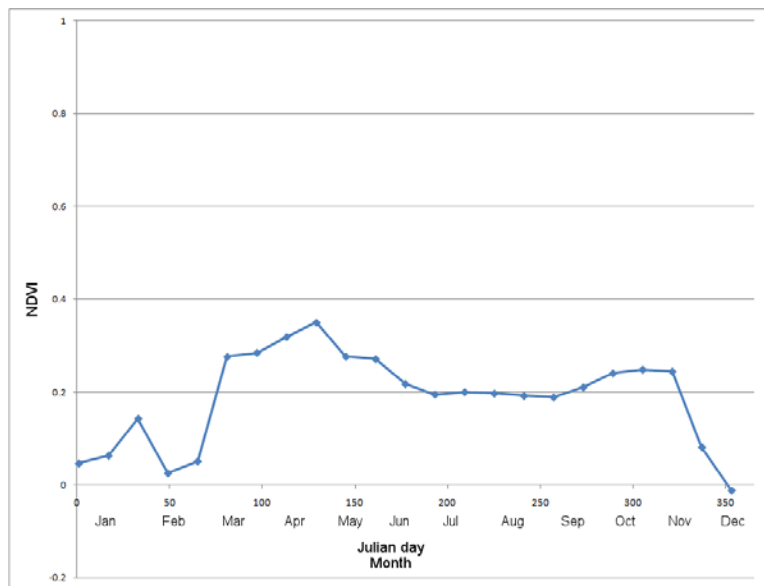
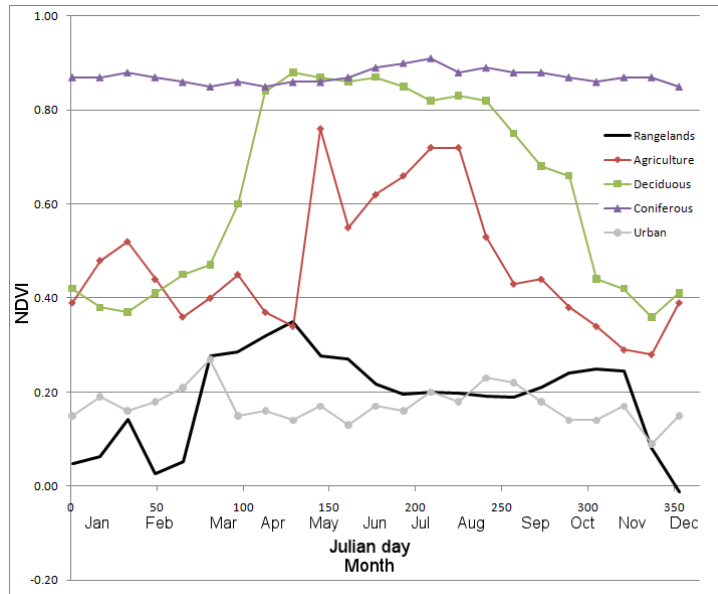


Figure 5. Extracted mean NDVI values for the Big Desert study area throughout the 2007 calendar year.

To visualize difference between vegetation dynamics in semiarid ecosystems relative to other ecosystems, data for the Big Desert were plotted with data for the Albermarle Pamlico Estuarine System (APES), a drainage area in North Carolina and Virginia (Figure 6). The APES plot is also based on similar MODIS 250 m NDVI composites (Knight *et al.*, 2006).



**Figure 6. Intra-annual NDVI curves comparing the Big Desert study area (a semiarid sagebrush-steppe rangeland ecosystem) with other land cover types.**

The intra-annual NDVI trends illustrated in figure 6 show curves with characteristics distinctive of each land cover type. Coniferous forests show little variation in NDVI values throughout the calendar year which is the result of the "evergreen" nature of these forests. Urban areas exhibit NDVI values between 0.1 and 0.3 with a peak in March. Deciduous and agricultural land cover types exhibit intra-annual NDVI variation resembling a bell-shaped curve. NDVI values for these land cover types exhibit early spring green-up which remain green and retain relatively high NDVI values even late in the calendar year.

Semiarid rangeland vegetation exhibits a unique intra-annual NDVI curve that is consistently lower than that seen in more mesic vegetation communities. In addition, the NDVI curve for the rangeland vegetation described in this study exhibited a singular bimodal distribution (cf. mean NDVI curve, figure 5). This trend accurately captures the vegetation dynamics of rangelands which may be responding to periods of high ambient temperature, low soil moisture, and low humidity levels, resulting in periods of non-optimal photosynthesis due to a potentially negative evapotranspiration balance (Potter 1993; Ivits *et al.*, 2009).

Another of the EOS satellites is AQUA. Like Terra, AQUA also contains a MODIS sensor and collects data similar to Terra. However, AQUA has an afternoon equatorial overpass time with an alias of EOS-PM. Among the MODIS/Aqua vegetation index products is a similar 250-meter 16-day composite. Together, these two products, MOD13Q1 and MYD13Q1 (TERRA and AQUA, respectively) have a

phased production cycle. The Terra 16-day period starts on Julian Day 1 while the Aqua 16-day period starts 8 days later on day 9. The use of both products would result in doubling the number of composite observations ( $n = 46$ ) and may provide a more detailed insight into intra-annual vegetation dynamics and the phenological cycles of semiarid rangelands.

## **CONCLUSIONS**

Many rangeland studies in semiarid ecosystems have used satellite imagery acquired during the months of June and July (Weber and McMahan, 2003; Anderson, J. *et al.*, 2007; Tedrow, L. *et al.* 2008; Underwood, J. *et al.* 2006) as this time period is widely considered representative of peak biomass production. However, intra-annual NDVI values and the annual NDVI curve presented in this paper indicate that imagery acquired in earlier months (April and May) or still later in the growing season (September) may result in a more accurate estimation of productivity in semiarid ecosystems. Peak biomass production, however, is not necessarily the same as peak photosynthetic activity and the relationship between these two metrics requires further study and understanding. This is especially important to sound land management and land stewardship to better ensure the sustainability of semiarid rangeland ecosystems.

## **ACKNOWLEDGEMENTS**

This study was made possible by a grant from the National Aeronautics and Space Administration Goddard Space Flight Center (NNX08AO90G). Idaho State University would also like to acknowledge the Idaho Delegation for their assistance in obtaining this grant.

## **LITERATURE CITED**

- Anderson, J., J. Tibbits, and K. T. Weber, 2007. Range Vegetation Assessment in the Upper Snake River Plain, Idaho 2007. Pages 17-26 in K. T. Weber (Ed.), Final Report: Impact of Temporal Landcover Changes in Southeastern Idaho Rangelands (NNG05GB05G). 354 pp. URL = [http://giscenter.isu.edu/research/techpg/nasa\\_tlcc/PDF/Ch3.pdf](http://giscenter.isu.edu/research/techpg/nasa_tlcc/PDF/Ch3.pdf) visited 01 July 2009
- Graham, S., 2008. MODIS Science. URL = [http://aqua.nasa.gov/about/instrument\\_modis\\_science.php](http://aqua.nasa.gov/about/instrument_modis_science.php) visited 1 July 2009
- Hobish, M. K., 2009. EOS Platforms/Sensors and Mission Profiles. Section 16, Earth Systems Science. URL = [http://www.fas.org/irp/imint/docs/rst/Sect16/Sect16\\_7.html](http://www.fas.org/irp/imint/docs/rst/Sect16/Sect16_7.html) visited 1 July 2009
- Holben, B.N., 1986. Characteristics of Maximum-value Composite Images from Temporal AVHRR Data, *IJRS*, 7(11): 1417-1434
- Ivits, E., G. Buchanan, M. Cherlet, and W. Mehl, 2009. Phenological Trends Derived from Spot VEGETATION Time Series to Indicate European Biodiversity Decline: Case Study of Farmland Birds. *Transactions of the 2009 International Society for Photogrammetry and Remote Sensing*, Stresa, Italy
- Jensen, J. R., 2005. *Introductory Digital Image Processing*, 3rd Ed., Upper Saddle River, NJ: Prentice Hall, 526 pp.

King, M. D., J. Closs, S. Spangler, R. Greenstone, S. Wharton, and M. Myers, 2004. EOS Data Products Handbook, Volume 1. URL = [http://eosps0.gsfc.nasa.gov/ftp\\_docs/data\\_products\\_1.pdf](http://eosps0.gsfc.nasa.gov/ftp_docs/data_products_1.pdf) visited 1 July 2009

Knight, J.F., R. L. Lunetta, J. Ediriwickrema, and S. Khorram, 2006. Regional Scale Land-Cover Characterization using MODIS-NDVI 250 m Multi-Temporal Imagery: A Phenology Based Approach. *GIScience and Remote Sensing*, 43(1): 1-23

Netting, R., 2008. TERRA, NASA Science Missions. URL = <http://nasascience.nasa.gov/missions/terra> visited 1 July 2009

Osmond, S., K. Pipkin, R. Belger, and C. Ourada, 2006. Eastern Idaho Interagency Fire Center 2006 Annual Report, URL = [http://www.idahofireinfo.blm.gov/east/eiifc\\_internal/main/archive/2006/2006\\_annual\\_report.pdf](http://www.idahofireinfo.blm.gov/east/eiifc_internal/main/archive/2006/2006_annual_report.pdf) visited 16 Nov 2009

Potter, C. S., J. T. Randerson, C. B. Field, P. A. Matson, P. M Vitousek, H. A. Mooney, and S. A. Klooster, 1993. Terrestrial Ecosystem Production: A Process Model Based on Global Satellite and Surface Data. *Global Biogeochemical Cycles*. 7(4): 811-841

Running, S.W., C.O. Justice, V. Salomonson, D. Hall, J. Barker, Y. J. Kaufmann, A. H. Strahler, A. R. Huete, J. P. Muller, V. Vanderbilt, Z. M. Wan, P. Teillet, D. Carneggie, 1994. Terrestrial Remote Sensing Science and Algorithms Planned for EOS/MODIS, *International Journal of Remote Sensing*. 15(17): 3587 – 3620

Sander L. and K. T. Weber, 2005. Range Vegetation Assessment in the Big Desert, Upper Snake River Plain, Idaho, GIS Training and Research Center. Pages 85-90 in K. T. Weber (Ed.), Final Report: Detection, Prediction, Impact, and Management of Invasive Plants using GIS. 196pp. URL = [http://giscenter.isu.edu/Research/techpg/nasa\\_weeds/to\\_pdf/fieldreport\\_2003-2004.pdf](http://giscenter.isu.edu/Research/techpg/nasa_weeds/to_pdf/fieldreport_2003-2004.pdf) visited 1 July 2009.

Skidmore, A.K., 2002. Taxonomy of Environmental Models in the Spatial Sciences. In A. Skidmore (Ed.) Environmental Modeling with GIS and Remote Sensing. Taylor & Francis, England. 268pp.

Tedrow, L., K. Davis, and K.T. Weber, 2008. Range Vegetation Assessment in the Big Desert Upper Snake River Plain, Idaho 2008, Pages 41-50 in K. T. Weber and K. Davis (Eds.) Final Report: Comparing Effects of Management Practices on Rangeland Health with Geospatial Technologies (NNX06AE47G). 176pp.

Underwood, J., J. Tibbits, and K. T. Weber, 2006. 2006 Range Vegetation Assessment in the Upper Snake River Plain, Idaho. Pages 11-18 in K. T. Weber and K. Davis (Eds.) Final Report: Forecasting Rangeland Condition with GIS in Southeastern Idaho. 193 pp. URL = [http://giscenter.isu.edu/research/techpg/nasa\\_oneal/to\\_pdf/2006\\_field\\_report.pdf](http://giscenter.isu.edu/research/techpg/nasa_oneal/to_pdf/2006_field_report.pdf) visited 1 July 2009

Wakkinen, W.L., K. P. Reese, J. W. Connelly, 1992. Sage Grouse Nest Locations in Relation to Leks, *JSTOR The Journal of Wildlife Management*, 56(2): 381-383

Weber K. T. and B. J. McMahan, 2003. Field Collection of Fuel Load and Vegetation Characteristics Wildfire Risk Assessment Modeling: 2002 Field Sampling Report. Pages 12-17 in K. T. Weber (Ed.) Final Report: Wildfire Effects on Rangeland Ecosystems and Livestock Grazing in Idaho. 209pp. URL = [http://giscenter.isu.edu/Research/techpg/nasa\\_wildfire/Final\\_Report/Documents/Chapter2.pdf](http://giscenter.isu.edu/Research/techpg/nasa_wildfire/Final_Report/Documents/Chapter2.pdf) visited 16 Nov 2009

Weier, J., and D. Herring. 2008. Measuring Vegetation (NDVI & EVI). URL = <http://earthobservatory.nasa.gov/Features/MeasuringVegetation/printall.php> visited 5 May 2009.

**Recommended citation style:**

Tedrow, L. and K. T. Weber, 2011. NDVI Changes Over a Calendar Year in the Rangelands of Southeast Idaho. Pages 105-116 in K. T. Weber and K. Davis (Eds.), Final Report: Assessing Post-Fire Recovery of Sagebrush-Steppe Rangelands in Southeastern Idaho (NNX08AO90G). 252 pp.

## **Diurnal NDVI Fluctuations in Semiarid Rangelands**

Keith T. Weber, GISP, GIS Director, Idaho State University, GIS Training and Research Center, 921 S. 8th Ave., Stop 8104, Pocatello, Idaho 83209-8104

Fang Chen, Idaho State University, GIS Training and Research Center, 921 S. 8th Ave., Stop 8104, Pocatello, Idaho 83209-8104

### **ABSTRACT**

This study explored the diurnal cycle of photosynthetic activity of C3 plants growing in semiarid ecosystems using NDVI as an indicator metric. A field-based sensors was calibrated and deployed to record NDVI at 30-minute intervals throughout the 2009 and 2010 spring growing seasons. The diurnal pattern of NDVI consistently followed a trough-shaped trend of low NDVI values (low photosynthetic rate) during the periods of solar noon with significantly higher NDVI values (50% higher;  $P < 0.001$ ) during the early morning and evening hours. Physiologically, the C3 plants typical of semiarid rangelands exhibit a survival strategy that minimizes evapotranspiration losses by reducing their photosynthetic rate during times when high ambient temperatures and high irradiance have created a sub-optimal environment. These results, viewed from the context of global climate change modeling, may have resounding effects as higher than previously estimated carbon assimilation levels resulting from increased photosynthetic activity would affect carbon sequestration estimates and proliferate necessary changes across global models. Additional data collection and analysis is being conducted to validate and further explore this topic.

*KEYWORDS: NDVI, vegetation indices, primary productivity, photosynthesis*

## INTRODUCTION

The normalized difference vegetation index (NDVI) is arguably the most widely used simple band ratio (SBR) ever developed (Rouse et al., 1973; Tucker 1979). It, along with a host of other SBR's, uses various ratio's of reflectance from the red (approximately 650nm) and near-infrared (NIR) (approximately 850nm) portions of the electromagnetic spectrum to estimate above-ground vegetation productivity and photosynthetic activity. NDVI has been applied to nearly every biome around the world including numerous forest (Hall-Beyer 2003; Knight et al., 2006), grassland (Yang et al., 1998; Hall-Beyer 2003), desert (Richard and Pocard 1998; Dall'Olmo and Karnieli 2002) and agricultural areas (Doraiswamy et al., 2003; Knight et al., 2006). Some studies have used NDVI as the basis for comparison among ecosystem types including Huete et al. (1997) who reported limitations of NDVI and biome-specific differences in NDVI response.

Other studies have used NDVI as the basis for interannual comparisons of phenological trends (Reed et al., 1994; Ivits et al., 2009) and the investigation of global climate change effects on primary productivity in grasslands (Yang et al., 1998). Similarly, intra-annual NDVI curves have been used to understand photosynthetic activity within a growing season (Tedrow and Weber 2011) and make comparisons between ecosystems (Knight et al., 2006).

Satellite remote sensing platforms such as the Moderate Resolution Imaging Spectroradiometer (MODIS) give scientists the ability to sample the earth's surface at broad scales and frequent temporal periodicity and thereby construct relatively accurate models of phenological change. However, no individual airborne or space-borne sensor routinely acquires repeated estimates of NDVI for the same area within a single day. To do this, requires an *in situ* spectroradiometer and data logger. This study was designed to explore and characterize diurnal NDVI fluctuations within semiarid rangeland ecosystems relative to the effect these cycles may have on comparative studies and global ecosystem productivity models. In addition, the physiological mechanism responsible for observed diurnal fluctuations are described.

## MATERIALS AND METHODS

### *Study area*

Spectral data were collected at the O'Neal Ecological Reserve, an area of semiarid sagebrush-steppe rangelands in southeastern Idaho approximately 30 km southeast of Pocatello, Idaho (42° 42' 25"N 112° 13' 0" W). The O'Neal Ecological Reserve receives < 0.38 m of precipitation annually (primarily in the winter) and is relatively flat with an elevation ranging from 1420 m - 1439 m ( $\bar{x}$  = 1431 m). The dominant plant species include big sagebrush (*Artemisia tridentata* Nutt.) and various native and non-native grasses and forbs, including Indian ricegrass (*Achnatherum hymenoides* (Roem. & Schult.) Barkworth) and needle-and-thread (*Hesperostipa comata* (Trin. & Rupr.) Barkworth). Each of these plant species follow a C3 carbon fixation pathway. While variations in ground cover and bare ground exposure are typical of sagebrush-steppe ecosystems, at the landscape scale the O'Neal Ecological reserve can be considered quite similar to other regions of sagebrush-steppe found across the Intermountain west.

## NDVI DATA COLLECTION

NDVI uses the reflectance of light from the red and near-infrared portions of the electromagnetic spectrum. Specifically, it is the quotient of the difference in reflectance values between the NIR and red bands over the sum of these same reflectance values. The bandwidths and band-centers of each specific

sensor used to calculate NDVI varies, but in general the wavelength of red band-centers is 650 nm while the wavelength of NIR band-centers is 850 nm. Measures of NDVI are collected by numerous satellite sensors at temporal scales ranging from one (MODIS) to 16 (Landsat 5 TM) days or more.

To obtain repeated diurnal measures of NDVI one option was the use of a handheld spectroradiometer. This posed numerous logistical difficulties however, as 1) this option was manpower intensive and 2) a potential bias would have been introduced if the same area was not sampled in the same way during each visit. To avoid these problems and improve the sampling interval, two QuadPod instruments were used (Garrity et al. 2010).

Each QuadPod instrument measures upwelling radiation (radiance) and downwelling radiation (irradiance). The red band was sampled at 676 nm while the NIR band was sampled at 800 nm. While slightly different than the band-center wavelengths used by satellite-based sensors, these specific wavelengths characterize the regions of peak chlorophyll absorption by the red band and peak reflectance in the NIR band and fall well within the red and NIR bandwidths of all common multispectral sensors (Rahman et al. 2001; Huete et al. 2002; Sims et al. 2006). Prior to deployment at the O'Neal study area, each QuadPod was calibrated using a white reference panel (Gamon et al. 2006). Calibration was conducted continuously and throughout periods of varying atmospheric and cloud cover conditions from 1-August-2008 through 5-August-2008 with observations collected every five minutes ( $n = 1440$  observations). Only those observations collected during daylight periods (0500hrs-2100hrs) were used to calculate the cross-instrument calibration factor (CICF; equation 1) ( $n = 225$ ).

$$\text{CICF} = \frac{\text{irradiance}_{\text{sky}}}{\text{radiance}_{\text{white panel}}} \quad (1)$$

Reflectance (R) was determined for both the red and NIR bands by dividing radiance by irradiance and multiplying that result by the CICF (Garrity et al., 2010) (equation 2).

$$R = \left( \frac{\text{radiance}_{\text{target}}}{\text{irradiance}_{\text{sky}}} \right) \times \text{CICF} \quad (2)$$

NDVI was calculated following standard methodology (equation 3) (Rouse et al., 1973; Tucker 1979).

$$\text{NDVI} = \frac{R_{(800 \text{ nm})} - R_{(676 \text{ nm})}}{R_{(800 \text{ nm})} + R_{(676 \text{ nm})}} \quad (3)$$

Using a 60° field of view (FOV) the QuadPod instrument was mounted upon a rigid platform with the radiance sensor positioned to image an area approximately 2.4 m x 2.4 m. The spatial resolution of the deployed QuadPod was arranged to mimic the resolution of the multispectral sensor onboard the Quickbird satellite (2.4 m x 2.4 m). During field deployment, each platform was oriented with the radiance sensor facing a southerly direction (165°) to minimize platform shadows falling within the instrument's FOV and maximize collection of early morning data (Figure 1).

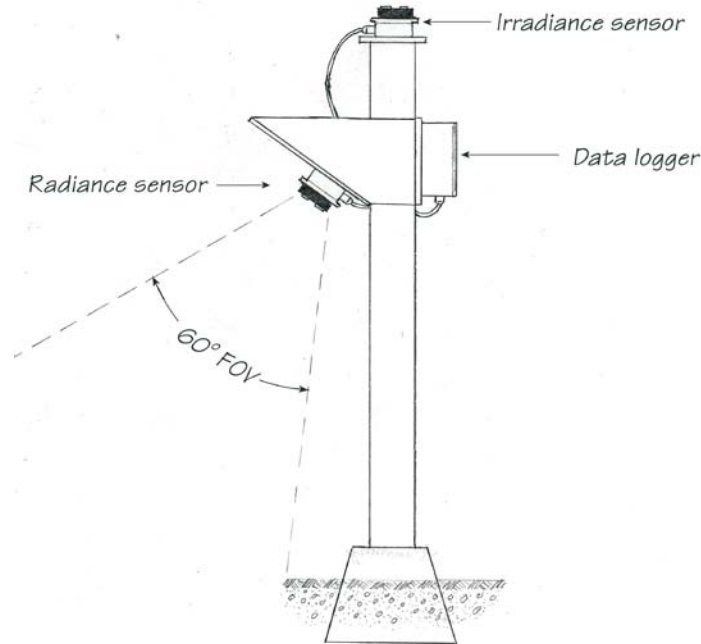


**Figure 1. A drawing of the QuadPod instrument mounted upon a platform as deployed in the field.**

Two QuadPod instruments were deployed on 14-April-2009 at independent locations (approximately 90 m apart) within the O'Neal Ecological Reserve and collected data throughout the remainder of April and May (a period of highly active early growth) using a sampling interval of 30 minutes. The data loggers were then retrieved and downloaded to a computer workstation. The QuadPod instruments were similarly deployed on 14-March-2010 and data loggers retrieved and downloaded later in the growing season. Reflectance for both the red and NIR bands were calculated following equation 2.

Since data collections were made throughout the day this resulted in measurements being taken across differing solar incidence angles ( $\theta$ ). This factor plays an important part in the apparent reflectance calculation (Eq. 4). The effect of varying  $\theta$  can be corrected using a bi-directional reflectance distribution function (BRDF) (Vermote et al. 1997; Collet et al 1998; Furby and Campbell 2001) and in this study, BRDF corrections for varying  $\theta$  were made following Danaher et al. (2002). NDVI was then determined following equation 3 and resulting data visually analyzed for diurnal trends.

$$L_0(\lambda) = L_{\text{sun}}(\lambda) T(\lambda) R(\lambda) \cos(\theta) + L_{\text{path}}(\lambda)$$

- $L_0(\lambda)$  = observed radiance at sensor
- $L_{\text{sun}}(\lambda)$  = Solar irradiance above atmosphere
- $T(\lambda)$  = total atmospheric transmittance
- $R(\lambda)$  = surface reflectance
- $\theta$  = incidence angle
- $L_{\text{path}}(\lambda)$  = path scattered radiance

(4)

#### *Cross-reference with satellite imagery*

To aid in the interpretation of calculations made using the QuadPod instrument, four MODIS Terra (surface reflectance daily L2G [MOD09GQ] 250 m pixels) and four Landsat 5 TM (30 m pixels) scenes were acquired throughout the data collection period (April 18, 2009; May 20, 2009; April 21, 2010 and

May 23, 2010) during cloud-free or nearly cloud-free days. The MODIS Terra imagery effectively represents an overpass acquisition of 1030 hrs (mountain local time) while Landsat TM imagery represents a solar noon acquisition ( $\bar{x}$  acquisition time = 1158 hrs mountain local time). These data were corrected for atmospheric effects with Idrisi Taiga (v16.03) using the ATMOSC module (Clark Labs, Worcester, MA). All atmospheric correction calculations followed the Cos(t) model (Chavez, 1996) using input parameters reported in the metadata supplied with the imagery. NDVI values were calculated for each scene and mean NDVI determined using 300 point locations randomly generated over the study area and adjacent sagebrush-steppe rangelands.

#### *Analysis and statistical comparisons*

Following retrieval of the data loggers from the field and download to a PC, all tabular data were imported into Microsoft Excel and NDVI values calculated for each 30-minute interval following equations 2-4 above. These data were then graphed for visual interpretation. To facilitate cross-reference with both MODIS and Landsat 5 TM imagery, daily NDVI values at 1030 hrs and 1200 hrs were selected and saved as new tables. In addition the daily maximum NDVI was selected and saved as a new table.

These data allowed for the comparison of NDVI values throughout each day and for a relative comparison between the *in situ* QuadPod instruments and both MODIS and Landsat NDVI values. Analysis of variance (ANOVA) was used to statistically compare maximum QuadPod NDVI values with NDVI values observed at 1030 hrs and 1200 hrs.

## **RESULTS AND DISCUSSION**

Throughout the 2009 and 2010 spring sampling periods NDVI was measured at 30 minute intervals from 15-April through 27-May, 2009 and 1-April through 21-April, 2010. In both years, battery life was less than expected and a full spring season collection (1-April through 31-May) was not achieved. Nonetheless, a total of 46 days were sampled providing a relatively rich dataset for analysis ( $n = 2,208$  NDVI observations).

The diurnal trend of NDVI exhibited a consistent trough-shaped pattern with NDVI values highest during the early morning and evening hours (approximately 0730hrs; Figure 2). The lowest NDVI values during photosensitive daylight hours were found within one-hour of solar noon (approximately 1230 hrs during the growing season). This paradoxical situation was consistent across both years of observation and further explored to better understand the biophysical mechanism underlying this pattern.

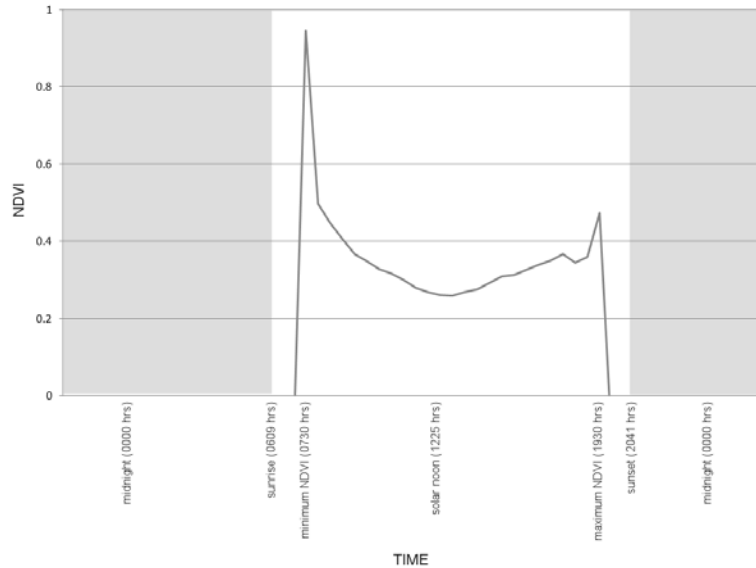


**Figure 2. Example of daily NDVI pattern (May 13, 2009) typical of that observed throughout this study.**

The mean difference between daily maximum NDVI ( $\bar{x} = 0.42$ ; SE = 0.04) and the NDVI-values recorded at 1230hrs ( $\bar{x} = 0.17$ ; SE = 0.02) (i.e., solar noon) was 0.25 (SE = 0.03) (Fig. 3). ANOVA comparing these values indicated significant differences ( $P < 0.001$ ). Overall, maximum NDVI and solar noon NDVI-values followed similar curves throughout the data collection period with solar noon NDVI values up to 50% lower than maximum NDVI. The NDVI-values observed at solar noon approximate Landsat 5 TM observations suggesting NDVI for semiarid rangelands may underestimate the productivity of these ecosystems.

The mean difference between daily maximum NDVI and the NDVI-values recorded at 1030hrs ( $\bar{x} = 0.19$ ; SE = 0.02) was 0.23 (SE = 0.03) (Fig. 3), with ANOVA results indicating a significant difference exists between these values ( $P < 0.001$ ). The NDVI-values observed at 1030hrs approximate MODIS Terra observations and, like Landsat TM, may underestimate the productivity of semiarid ecosystems. While NDVI-values observed at 1030hrs were slightly higher than those values observed at 1230hrs, they were not significantly different ( $P = 0.44$ ). This trend was also observed between actual MODIS Terra ( $\bar{x} = 0.41$ ; SE = 0.04) and Landsat 5 TM ( $\bar{x} = 0.27$ ; SE = 0.06) NDVI-values, with no significant difference found ( $P = 0.11$ ;  $n = 4$ ). A similar trend was observed by Busetto et al. (2008) in a study comparing MODIS and Landsat NDVI imagery.

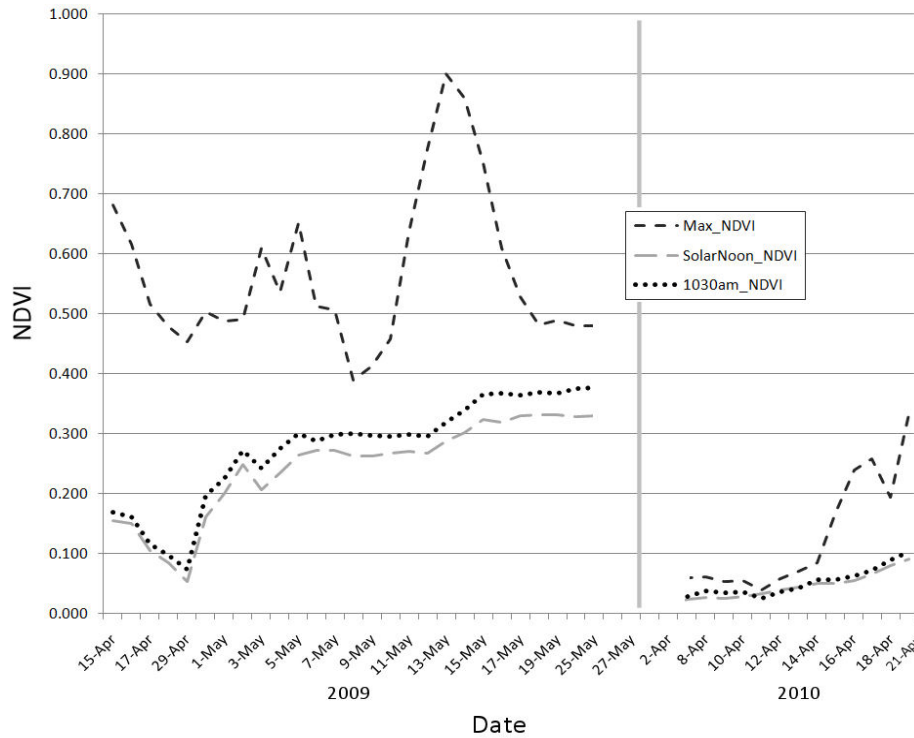


**Figure 3. Daily NDVI values at 1030hrs and 1230hrs (solar noon) relative to maximum NDVI (note: lines have been smoothed using a 3-point running average).**

The overall trend of NDVI was similar in both the spring of 2009 and 2010; NDVI was slightly higher at 1030hrs compared to 1230hrs and neither characterized the maximum NDVI. Between years, one should note a depressed NDVI curve early in the 2010 growing season (cf. 15-April Fig. 3) which is principally attributable to slightly cooler minimum temperatures experienced in 2010, effectively delaying the growing season (Fig. 4). In addition, spring 2010 was a slightly drier year (Fig. 5).

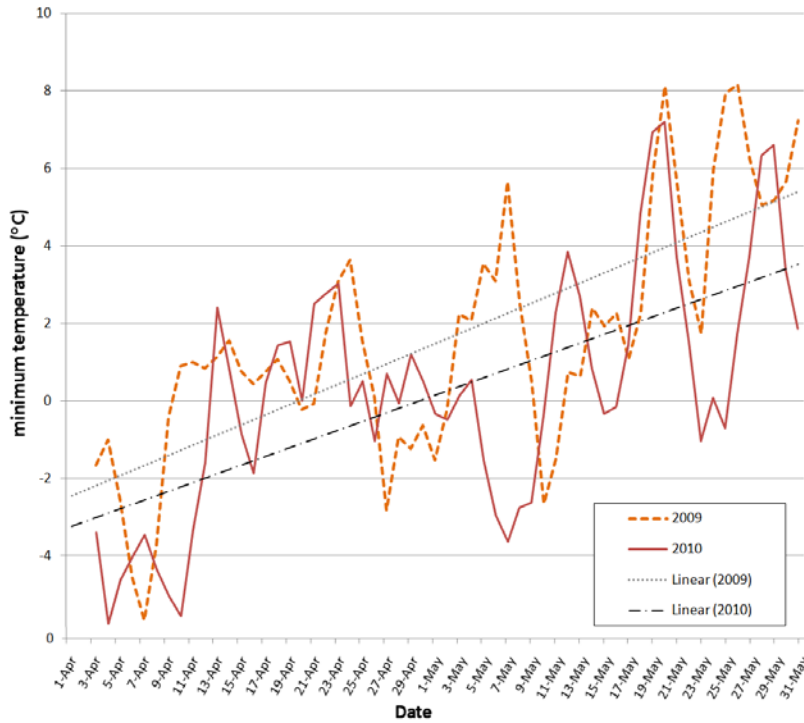


Figure 4. Minimum daily temperature throughout the spring growing seasons 2009-2010. Linear trendlines have been added to illustrate the overall cooler temperatures observed in 2010.

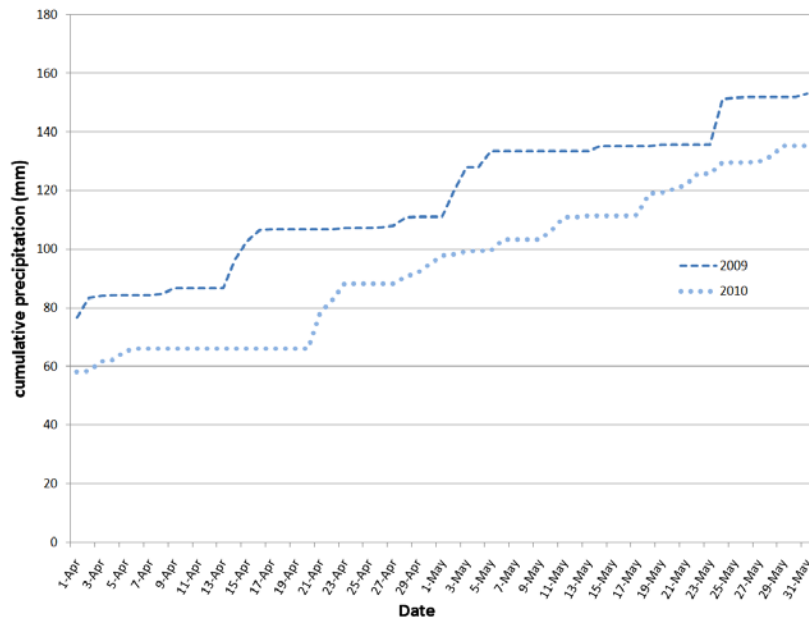


Figure 5. Cumulative precipitation throughout the spring growing seasons 2009-2010. A delayed green-up was observed in 2010 which is attributed to both cooler temperatures (cf. figure 4) and a reduction in precipitation.

Within the plant, the result of photosynthesis is the production of sugars. This process is affected by several interrelated factors, namely light irradiance, CO<sub>2</sub> concentration, and ambient temperature. Frederick Frost Blackman in his 1905 law of limiting factors, proposed that photosynthesis is limited by

the pace of the slowest of these three factors. In this study, irradiance and temperature are of particular interest as their interaction may help explain our observations. As irradiance increases (and temperature is constant) the rate of photosynthetic activity similarly increases but ultimately reaches a plateau at high irradiance levels (cf. Blackman). When temperature increases concomitant with increasing irradiance however, the environment quickly becomes sub-optimal for the plant and light use efficiency drops rapidly (Schulze and Chapin 1987; Amthor 1989; Ryan 1991; Potter et al., 1992). These factors, combined within an arid or semiarid environment, may cause plants to close their stomata to conserve water and temporarily reduce their rate of photosynthesis (Larcher 2003). Initially, a reduced photosynthetic rate appears detrimental, however when viewed from a longer-term, ultimate perspective, this strategy allows the plant to survive in a relatively harsh environment, punctuated by diurnal periods of stress. Similar findings were reported by Hanan et al. (2005) relative to diurnal CO<sub>2</sub> flux in plants.

NDVI provides a metric related to the photosynthetic activity of plants (Tucker 1979; Chander and Groeneveld 2009). High NDVI values indicate plants are actively photosynthesizing while low NDVI values suggest the opposite. NDVI, and numerous other vegetation indices using the red and NIR bands, has also been used as an indicator of primary productivity. A problem arises however, in that a majority of satellite sensors use an oblique, sun-synchronous orbit and acquire imagery within an hour or two of solar noon (Barrett and Curtis 1992). This configuration is used to maximize illumination of the earth's surface and best ensure strong reflective signals are received at the sensor. Within semiarid rangelands however, this configuration may fail to capture peak daily photosynthetic activity during the growing season.

The implications of these results are many and additional data collection needs to be conducted to further explore this topic. Of primary importance is the understanding that productivity estimates based upon remotely sensed imagery (e.g., NDVI and MSAVI) appear to underestimate the productivity of semiarid rangelands, especially when NDVI values are based on satellite data acquired at or near solar noon. Acquiring satellite imagery at earlier times of the day is also problematic however as resulting imagery will be fraught with shadow and increased BRDF effects (Danaher 2002). Correcting for these effects may also be problematic as maximum NDVI is highly variable and its trendline does not exhibit the same slope as observed for solar noon NDVI. Hanan et al. (2005) reported scaling adjustments may be appropriate for light-saturated (mid-day) photosynthesis estimation but may result in an underestimate of early morning and late afternoon (light-limited conditions) CO<sub>2</sub> flux. These results, viewed from within the context of global climate change modeling, can have resounding effects as higher carbon assimilation levels resulting from a net increase in photosynthetic activity would affect carbon sequestration estimates within semiarid ecosystems worldwide when these estimates are derived from NDVI or similar indices.

## **CONCLUSIONS**

Semiarid rangelands represent diverse ecosystems that are the home of numerous plant species well adapted to these harsh environments. One adaptation observed in this study is an apparent plant survival strategy where photosynthetic rate is reduced or halted in response to sub-optimal conditions that may exist during mid-day (light saturated conditions) as a result of high ambient temperatures, high irradiance, and potential net evapotranspiration losses. This study used two QuadPod instruments to measure NDVI at 30-minute intervals throughout the spring growing season. The diurnal pattern of NDVI followed a consistent trend of low NDVI values (low photosynthetic rate) during solar noon with significantly higher

NDVI values (50% higher;  $P < 0.001$ ) during the early morning and evening hours. These results, viewed from the context of global climate change modeling, may have resounding effects as higher carbon assimilation levels resulting from a true net increase in photosynthetic activity and net ecosystem exchange would affect carbon sequestration estimates and proliferate necessary changes across numerous global models.

## **ACKNOWLEDGEMENTS**

This study was made possible by a grant from the National Aeronautics and Space Administration Goddard Space Flight Center (NNX08AO90G). Idaho State University would also like to acknowledge the Idaho Delegation for their assistance in obtaining this grant. The QuadPod instruments used in this study were developed by Steve Garrity and Lee Vierling from the University of Idaho.

## **LITERATURE CITED**

- Amthor, J.S., 1989. Respiration and Crop Productivity. Springer-Verlag, New York
- Barrett, E.C. and L.F Curtis, 1992. Introduction to Environmental Remote Sensing. Chapman and Hall, London England, 3:426 pp.
- Busetto, L., M. Meroni, and R. Colombo, 2008. Combining Medium and Coarse Spatial Resolution Satellite Data to Improve the Estimation of Sub-pixel NDVI Time Series. Remote Sensing of Environment. 112:118-131
- Chander, G. and D.P. Groeneveld, 2009. Intra-annual NDVI Validation of the Landsat 5 TM Radiometric Calibration. 30(6):1621-1628
- Chavez, P.S. Jr., 1996. Image-based Atmospheric Corrections-revisited and Improved. Photogrammetric Engineering and Remote Sensing. 62:1025-1036
- Collett, L., B. Goulevitch, and T.J. Danaher, 1998. SLATS radiometric correction : A semi automated multi stage process for the standardisation of temporal and spatial radiometric differences. Proceedings of the 9th Australasian Remote Sensing and Photogrammetry Conference, Sydney, Australia.
- Dall'Olmo G. and A. Karnieli, 2002. Monitoring Phenological Cycles Of Desert Ecosystems Using NDVI and LST Data Derived From NOAA-AVHRR Imagery. Int. J. Remote Sensing, 23(19): 4055–4071
- Danaher, T.J., 2002. An Empirical BRDF Correction for Landsat TM and ETM+ imagery. Proceedings of the 11th Australasian Remote Sensing and Photogrammetry Conference, Brisbane, Australia. URL = [http://www.derm.qld.gov.au/slats/pdf/arspc11\\_danaher.pdf](http://www.derm.qld.gov.au/slats/pdf/arspc11_danaher.pdf)
- Doraiswamy, P.C., S. Moulin, P.W. Cook, and A. Stern, 2003. Crop Yield Assessment from Remote Sensing. Photogrammetric Engineering & Remote Sensing 69(6):665-674
- Furby S.L. and N.A. Campbell, 2001. Calibrating Images from Different Dates to like-value Digital Counts. Remote Sensing of Environment, 77:1-11

- Gamon J.A., Y.F. Cheng, H. Claudio, L. MacKinney, D.A. Sims, 2006. A Mobile Tram System for Systematic Sampling of Ecosystem Optical Properties. *Remote Sensing of Environment*, 103(3):246-254
- Garrity, S.R., L.A. Vierling, and K. Bickford, 2010. A Simple Filtered Photodiode Instrument for Continuous Measurement of Narrowband NDVI and PRI over Vegetated Canopies. *Agricultural and Forest Meteorology*. doi:10.1016/j.agrformet.2010.01.004
- Hall-Beyer, M. 2003. Comparisons of Single-Year and Multiyear NDVI Time Series Principal Components in Cold Temperate Biomes. *IEEE Transactions on Geoscience and Remote Sensing*. 42(11): 2568-2574.
- Hanan, N.P., J.A. Berry, S.B. Verma, E.A. Walter-Shea, A.E. Suyker, G.G. Burba, and A.S. Denning, 2005. Testing a Model of CO<sub>2</sub>, Water and Energy Exchange in Great Plains Tallgrass Prairie and Wheat Ecosystems. *Agricultural and Forest Meteorology* 131:162-179
- Huete, A. R., H. Q. Liu, K. Batchily, and W. van Leeuwen, 1997. A Comparison of Vegetation Indices over a Global Set of TM Image for EOS-MODIS. *Remote Sens. Environ.* 59:440-451
- Huete, A., K. Didan, T. Miura, E.P. Rodriguez, X. Gao, and L.G. Ferreira, 2002. Overview of the Radiometric and Biospherical Performance of the MODIS Vegetation Indices. *Remote Sensing of Environment*. 83:195-213
- Ivits, E., G. Buchanan, M. Cherlet, and W. Mehl, 2009. Phenological Trends Derived from SPOT VEGETATION Time Series to Indicate European Biodiversity Decline: Case Study of Farmland Birds. *Proceedings of International Symposium for Remote Sensing of Environment, Stresa Italy (ref 347)*
- Knight, J.F., R.L. Lunetta, J. Ediriwickrema, and S. Khorram, 2006. Regional Scale Land-Cover Characterization using MODIS-NDVI 250 m Multi-Temporal Imagery: A Phenology Based Approach. *GIScience and Remote Sensing*, 43(1): 1-23
- Larcher W., 2003. *Physiological Plant Ecology*. Springer-Verlag Heidelberg, Germany. 4:513 pp.
- Potter, C.S., J.T. Randerson, C.B. Field, P.A. Matson, P.M. Vitousek, H.A. Mooney, and S.A. Klooster, 1993. Terrestrial Ecosystem Production: A Process Model Based on Global Satellite and Surface Data. *Global Biogeochemical Cycles* 7(4):811-841
- Rahman, A.F., J.A. Gamon, D.A. Fuentes, D.A. Roberts, and D. Prentiss, 2001. Modeling Spatially Distributed Ecosystem Flux of Boreal Forest using Hyperspectral Indices from AVIRIS Imagery. *Journal of Geophysical Research*. 106:33579-33591
- Reed, B.C., J.F. Brown, D. VanderZee, T.R. Loveland, J.W. Merchant, D.O. Ohlen, 1994. Measuring Phenological Variability from Satellite Imagery, *Journal of Vegetation Science* 5:703-714

- Richard, Y. and I. Pocard, 1998. A Statistical Study Of NDVI Sensitivity To Seasonal and Interannual Rainfall Variations in Southern Africa. *Int. J. Remote Sensing*, 19(15):2907-2920
- Rouse, J.W., R.H. Haas, J.A. Schell, and D.W. Deering, 1973. Monitoring Vegetation Systems in the Great Plains with ERTS-1, 3rd Earth Resources Technology Satellite Symposium, 309-317
- Ryan, M.G., 1991. Effects of Climate Change on Plant Respiration. *Ecol. Appl.* 1: 157-167
- Schulze, E.D. and F.S. Chapin III, 1987. Plant Specialization to Environments of Different Resource Quality. Pages 120-148 in E. D. Schulze and H. Zwolfer (Eds.) Potentials and Limitations in Ecosystem Analysis. Springer-Verlag, New York
- Sims, D.A., H. Luo, S. Hastings, W.C. Oechel, A.F. Rahman, and J.A. Gamon, 2006. Parallel Adjustments in Vegetation Greenness and Ecosystem CO<sub>2</sub> Exchange in Response to Drought in a Southern California Chaparral Ecosystem. *Remote Sensing of Environment*. 103:289-303
- Tedrow, L. and K.T. Weber, 2011. NDVI Changes over a Calendar Year in the Rangelands of Southeast Idaho. Pages 105-116 in K. T. Weber and K. Davis (Eds.), Final Report: Assessing Post-Fire Recovery of Sagebrush-Steppe Rangelands in Southeastern Idaho (NNX08AO90G). 252 pp.
- Tucker, C.J., 1979. Red and Photographic Infrared Linear Combinations for Monitoring Vegetation. *Remote Sensing of Environment*, 8:127-150
- Vermote, E., D. Tanré, J.L. Deuzé, M. Herman, and J.J. Morcrette, 1997. Second Simulation of the Satellite Signal in the Solar Spectrum (6S), 6S User Guide Version 2, July 1997
- Yang, L., B.K. Wylie, L.L. Tieszen, and B.C. Reed, 1998. An Analysis of Relationships among Climate Forcing and Time-Integrated NDVI of Grasslands over the US Northern and Central Great Plains. *Remote Sensing of Environment* 65(1): 25-37

**Recommended citation style:**

Weber, K.T., F. Chen, 2011. Diurnal NDVI Fluctuations in Semiarid Rangelands. Pages 117-128 in K. T. Weber and K. Davis (Eds.), Final Report: Assessing Post-Fire Recovery of Sagebrush-Steppe Rangelands in Southeastern Idaho. 252 pp.

## **Detection Thresholds for Rare, Spectrally Unique Targets within Semiarid Rangelands**

Keith T. Weber, GISP, GIS Director, GIS Training and Research Center, Idaho State University, 921 S. 8th Ave., Stop 8104, Pocatello Idaho 83209-8104 (webekeit@isu.edu)

Fang Chen, GIS Training and Research Center, Idaho State University, 921 S. 8th Ave., Stop 8104, Pocatello Idaho 83209-8104 (chenfang@isu.edu)

### **ABSTRACT**

Many factors influence classification accuracy and this study assessed detection thresholds for various sub-pixel targets using Quickbird multispectral imagery. Six iterations of maximum-likelihood classification were used to determine classification accuracy for 100 spectrally unique targets randomly placed over a semiarid rangeland site. Error matrices were calculated using independent validation sites and producer's, user's, and overall accuracy, Kappa Index of Agreement, and transformed divergence were analyzed to compare the performance of each classification and determine detection thresholds. Results indicate a strong relationship between target size and classification accuracy ( $R^2 = 0.94$ ) as well as an increasingly prominent role played by training site selection as target size decreased. Strong spectral separability and good classification accuracies were achieved for targets >25% cover. Sub-pixel targets <25% in size were not detectable. This study highlights the effect of target size upon classification accuracy and has direct implications for invasive plant research and rare target detection.

*KEYWORDS: sub-pixel classification, Quickbird, cover threshold, accuracy assessment*

## INTRODUCTION

Much has been written about the effects of various input parameters and processing decisions on classification accuracy. Researchers have investigated and described the 1) selection of appropriate classification algorithms (Foody and Arora, 1997), 2) effects of orthorectification (Cheng et al., 2003; Robertson, 2003; Toutin and Chenier, 2004; Wijnant and Steenberghen, 2004; Parcharidis *et al.*, 2005), 3) effect of mis-registration between image layers (Townshend *et al.*, 1992; Dai and Khorram, 1998; Stow, 1999; Roy, 2000; Verbyla and Boles, 2000; Wang and Ellis, 2005), 4) influence of spectral resolution (Mehner *et al.*, 2004), 5) effects of co-registration between training sites and imagery (Weber, 2006; Weber *et al.*, 2008), 6) influence of atmospheric anomalies and correction processes (Lillesand and Kiefer, 2000), and 7) effects of training site purity relative to minimum ground cover threshold (Mundt *et al.*, 2006). The result of these and other efforts has allowed geospatial scientists to construct a fairly complete error budget and, thereby, better understand and interpret image classification results. The latter topic is the focus of this paper with emphasis upon the detection threshold of sub-pixel targets.

In semiarid environments, the ability to detect sub-pixel targets is critical because landscape features such as sagebrush, shrubs, invasive weeds, and bare soil are frequently encountered in relatively small patches (i.e., 1-4 m<sup>2</sup>). Past research investigating detection limitations in remote sensing have frequently focused upon invasive plants and have reported detection thresholds from 10% cover (Parker-Williams and Hunt, 2002) to 40% cover (Glenn *et al.*, 2005; Weber *et al.*, 2006) for leafy spurge (*Euphorbia esula* L.), 30% cover for hoary cress (*Cardaria draba*) (Mundt *et al.*, 2006), and 20% cover for Rush skeletonweed (*Chondrilla juncea*) (Mundt *et al.*, 2006). In all cases, detection thresholds in these studies were determined using hyperspectral imagery with high spatial resolutions (e.g. 5 m).

The purpose of this research was to experimentally address the following questions related to the reliable detection (i.e.  $\geq 75\%$  overall accuracy; Goodchild *et al.*, 1994) of spectrally unique, patchy, and rare targets within semiarid rangeland ecosystems: 1) what is the detection threshold (100%, 50%, 25%, 5%, and 1% of a pixel) that can be achieved using high spatial resolution multispectral imagery? and 2) what is the impact of target size and site selection on sub-pixel target detection and classification accuracy? To address the former objective various measures of classification accuracy and spectral separability were used including transformed divergence, error matrices, and the Kappa Index of Agreement (KIA). The latter objective (2) was addressed by exploring the variability of the above measures following six iterations of each classification trial and by examining the relationship between KIA and target size using linear regression analysis.

## METHODS

### *Study Area*

The experiment was performed in sagebrush-steppe rangelands of southeast Idaho approximately 30 km south of Pocatello, Idaho, at the O'Neal Ecological Reserve. This 50 ha site contains sagebrush-steppe upland areas located on lava benches. The Reserve receives <38 cm of precipitation annually (primarily in the winter) and is relatively flat, with a mean elevation of approximately 1,400 m (1,401-1,430 m). The dominant plant species is big sagebrush (*Artemisia tridentata*) with various native and non-native grasses, including Indian rice grass (*Oryzopsis hymenoides*) and needle-and-thread (*Stipa comata*) present throughout the Reserve.

*Field Data*

Throughout the study area, 20 target locations were randomly generated for each of five target sizes ( $n=100$ ) (Table 1). Bright blue tarps were placed at each of these locations using the following set of criteria established for final placement in the field: 1) no part of the tarp was placed beneath vegetation, 2) tall vegetation ( $>1$  m) that could cast a shadow on a portion of the tarp during image acquisition was not located near the tarps ( $\pm 2$  m), and 3) tarps were installed flat and horizontal to avoid deformation and changes in their apparent size within the imagery (Fig. 1). All blue tarps were secured into the ground using four to eight, 25 cm spikes approximately one month prior to the acquisition of remotely sensed imagery. The location of the tarps was recorded by occupying each site until 120 positions were acquired with a Trimble GeoXH GPS receiver. The averaged positions were post-process differentially corrected using data from five base stations each within 80 km of the Reserve. Resulting horizontal positional accuracy was  $\pm 0.3$  m (95% confidence interval [CI]). An equal number of non-target points ( $n=20$ ) typical of the semiarid rangelands found at the Reserve (i.e., sites dominated by big sagebrush) were randomly located throughout the study area and used as non-target training sites for all analyses and classifications. This was done to eliminate variability and bias due to disproportionate sample sizes. None of these points fell within 10 meters of a target site.

**Table 1. Percent target size and actual target size of the five classes used in this study (note: Quickbird multispectral imagery has a spatial resolution of 2.40 x 2.40 m).**

Target class (%)	Actual size (m)
100	2.40 x 2.40
50	1.70 x 1.70
25	1.20 x 1.20
5	0.55 x 0.55
1	0.24 x 0.24

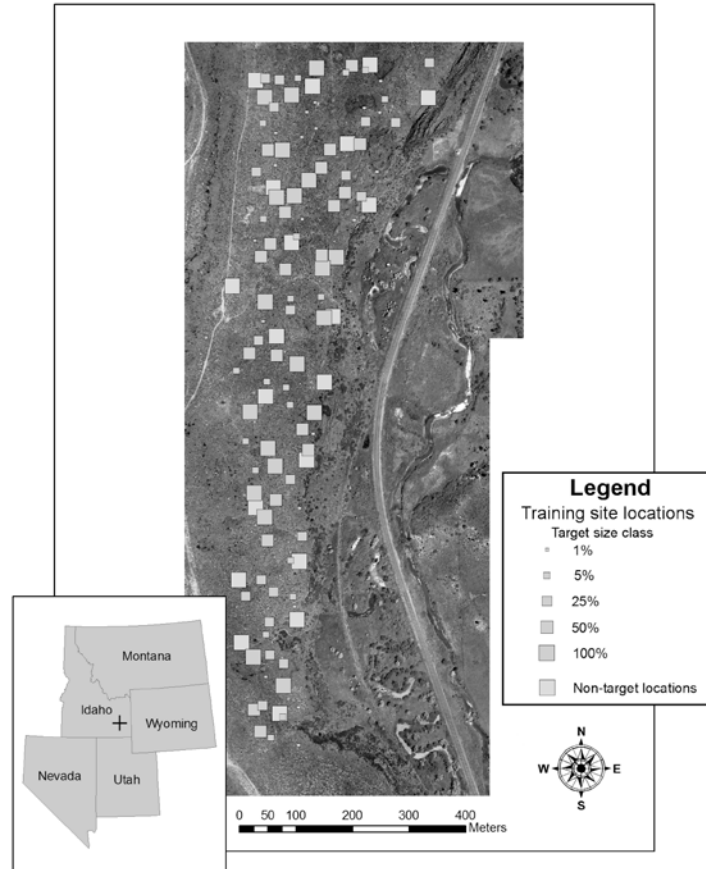


**Figure 1. Map of study area with location of tarps (target sites) and location of non-target sites (note: the size of the training sites is not drawn to scale).**

To better understand the results of subsequent classification, the spectral properties of the blue tarps targets were compared to the spectral properties of the common rangeland elements found at non-target sites using an Analytical Spectral Device (ASD) FieldSpecPro hand-held field spectroradiometer. Measurements were made during a sunny day (without clouds) at +/- 1 hour of solar noon prior to image acquisition. For each target, between 15 and 25 spectral recordings were taken. Spectral comparison included blue tarps, bare soil, basalt, low sagebrush (*Artemisia arbuscula*), and big sagebrush (*Artemisia tridentata*).

### *Imagery*

Standard Quickbird imagery (July 6, 2009) was delivered by DigitalGlobe Corporation and projected into Idaho Transverse Mercator (NAD83) using nearest neighbor resampling to match the reference system of all other GIS data used in this study. The imagery was corrected for atmospheric effects using Chavez' Cos(t) model in Idrisi Taiga's ATMOSC module (Chavez, 1996). To improve georegistration of the imagery and co-registration between the imagery and ground truth locations (Weber *et al.*, 2008) within the relatively small, flat study area, five permanent ground control platforms were used. Each platform was 2.4 m x 2.4 m in size and stood 1.2 m above the ground. During satellite image acquisition periods, highly reflective silver tarps were tightly secured to the platforms. The location of the platform's corners were recorded and processed in the same fashion as noted above. All five ground control platforms were

used to georectify the Quickbird imagery using first order, affine transformation and nearest neighbor resampling (RMSE=0.678).

### *Analysis*

To determine how small a target can be detected using high spatial resolution Quickbird multispectral imagery a series of supervised presence/absence classifications were performed. To accomplish this, a geodatabase feature class containing 100 points representing the location of the blue tarp sites was created. This blue tarp feature class was randomly resampled without replacement to select 50% of the points in each target size class ( $n=5$  target size classes). This process was repeated six times (Table 1) to achieve a better estimation of classification accuracy (Weber and Langille, 2007). A single resampling event was used to randomly select 50% of the non-target training sites ( $n=10$ ). The remaining non-target sites were used as independent validation sites.

Bootstrap resampling was used in this study (Good 2006) and for each target class 10 points were randomly selected while the remaining 10 points were reserved for validation. Ten non-target points were randomly selected and these same points were used in every classification trial while the remaining 10 non-target points were used in all validations. To eliminate between-trial variability in the non-target class iterative resampling of non-target sites was not performed.

The result of each resampling iteration produced two datasets for use in the classification process. The first dataset contained 20 training sites (10 blue tarp training site points per size class and 10 non-target training site points) and the second contained 20 validation sites (10 blue tarp points per size class and 10 non-target points). Each individual dataset was saved as a shapefile ( $n=30$ ; 6 iterations of 5 size classes) and used to extract spectral signatures from Quickbird imagery (bands 1-4) at the locations of the training sites using Idrisi's MAKESIG module. Spectral signature extraction is a required step for maximum likelihood classification and the resulting signature files statistically describe the spectral characteristics (minimum, maximum, mean, variance, and covariance) of those pixels identified as a target (i.e., the pixel contains a blue tarp) or non-target site (i.e., the pixel was a typical sagebrush-steppe rangeland site).

Spectral signatures were evaluated using the SEPSIG module of Idrisi which calculated a transformed divergence score (Richards and Jia, 2006). This score was used to indicate the separability of target and non-target sites for each spectral signature file ( $n=30$ ). Using a constant value of 2000, spectral endmembers with separability values exceeding 1600 were considered good candidates for successful differentiation during the classification process. Regardless of the separability score, all maximum likelihood trials were completed ( $n=30$ ).

A series of maximum likelihood classifications (Richards and Jia, 2006) were performed using Idrisi (MAXLIKE) and validated using the ERRMAT module, which calculates both a standard error matrix (Congalton and Green, 2009) and KIA (Cohen, 1960; Titus *et al.*, 1984; Foody, 1992; Monserud and Leemans, 1992). A cumulative error matrix (CEM) was developed by calculating the sum of each individual error matrix within each target size class. To determine the statistical difference among classification results, the CEM for a given target class was compared with the CEM of all other target size classes using variance of KIA by calculating a pairwise Z-statistic following Congalton and Green (2009) (Equation 1).

$$Z_{\text{pairwise}} = \frac{|K_1 - K_2|}{\sqrt{\text{var}(K_1) + \text{var}(K_2)}} \quad (1)$$

Where  $K_1$  and  $K_2$  are the KIA's for error matrices 1 and 2 and  $\text{var}(K_1)$  and  $\text{var}(K_2)$  are estimates of variance for matrices 1 and 2. The  $Z_{\text{pairwise}}$  critical value at the 95% confidence interval is 1.96.

## RESULTS AND DISCUSSION

### Detection threshold

Transformed divergence separability scores of the spectral signature files for the 100% and 50% target classes ( $n=6$  signature files/target class) exceeded the threshold value of 1600 ( $\bar{x} = 1998.8$  and  $1991.4$  for the 100% and 50% classes, respectively), indicating the spectral signatures of those targets were statistically differentiable from the signatures of non-target sites. This result compares well with results from spectroradiometer analysis indicating the blue tarps were spectrally unique and separable from the adjacent matrix of features (Fig. 2). Four of six (67%) signature files for the 25% target class had transformed divergence scores in excess of 1600 ( $\bar{x} = 1657.8$ ), suggesting that under most instances targets with 25% cover were differentiable from non-target sites. Since the same non-target sites were used in all cases throughout this study, no effect can be inferred related to sub-sampling non-target sites. Rather, the observed difference in separability must be due to the specific combination of target training sites selected and the ground conditions within the remainder of the pixel not covered by the blue-tarp target. Only one of six signature files for both the 5% and 1% target cover classes had transformed divergence scores exceeding 1600 ( $\bar{x} = 1172.0$  and  $1242.3$  for the 5% and 1% classes, respectively) suggesting that a reliable classification at these cover levels was highly unlikely.

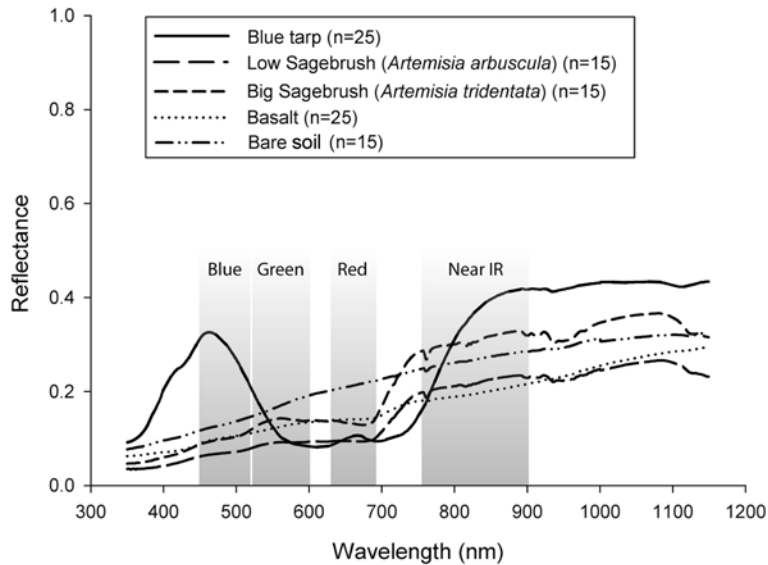


**Figure 2. A comparison of spectral signatures from common rangeland targets and the artificial blue tarps used in this study. Signatures were acquired with a spectroradiometer and the mean signatures of  $n$  (15-25) spectra are shown. Quickbird image bands are shown in grey for reference.**

Following six iterations of maximum likelihood classifications, mean producer's accuracy for the 100% blue tarp target class was 75%, mean user's accuracy was 92%, and mean overall accuracy was 84% (Table 2). While all measures of accuracy were reduced for the 50% target class ( $\bar{x}$  overall accuracy =

70%) and even further reduced for the 25% target class ( $\bar{x}$  overall accuracy = 69%), the user's accuracy exceeded 80% in all cases ( $n=6$  classifications/target class). In contrast, the 5% and 1% target classes performed poorly with mean overall accuracies of 60% and 55%, respectively. In addition, both producer's and user's accuracies for the 5% and 1% target classes were  $\leq 65\%$  in all cases corroborating well with the results of separability testing reported above.

**Table 2. Resulting measures of accuracy and standard error (SE) for each blue tarp target class following six iterations of maximum likelihood classification**

Target class (%)	Accuracy (%)		
	Producer's	User	Overall
100	0.75 (SE = 0.05)	0.92 (SE = 0.03)	0.84 (SE = 0.02)
50	0.50 (SE = 0.08)	0.83 (SE = 0.08)	0.70 (SE = 0.05)
25	0.45 (SE = 0.03)	0.87 (SE = 0.05)	0.69 (SE = 0.02)
5	0.45 (SE = 0.11)	0.64 (SE = 0.09)	0.60 (SE = 0.04)
1	0.22 (SE = 0.08)	0.65 (SE = 0.15)	0.55 (SE = 0.07)

*Target Size and Site Selection*

Resulting mean KIA statistics reported a similar trend (Fig. 3) of decreasing agreement with decreasing target size ( $R^2 = 0.94$ ) but also indicated that only the 100% target class resulted in substantial agreement (0.68) between known/modeled blue tarp target locations (Landis and Koch, 1977). Following Landis and Koch (1977) a fair level of agreement was found for the 50% and 25% target classes (0.40 and 0.38, respectively) while the mean KIA for the 5% and 1% target classes (0.20 and 0.10, respectively) were considered slight and similar to that expected from a chance (random) classification.

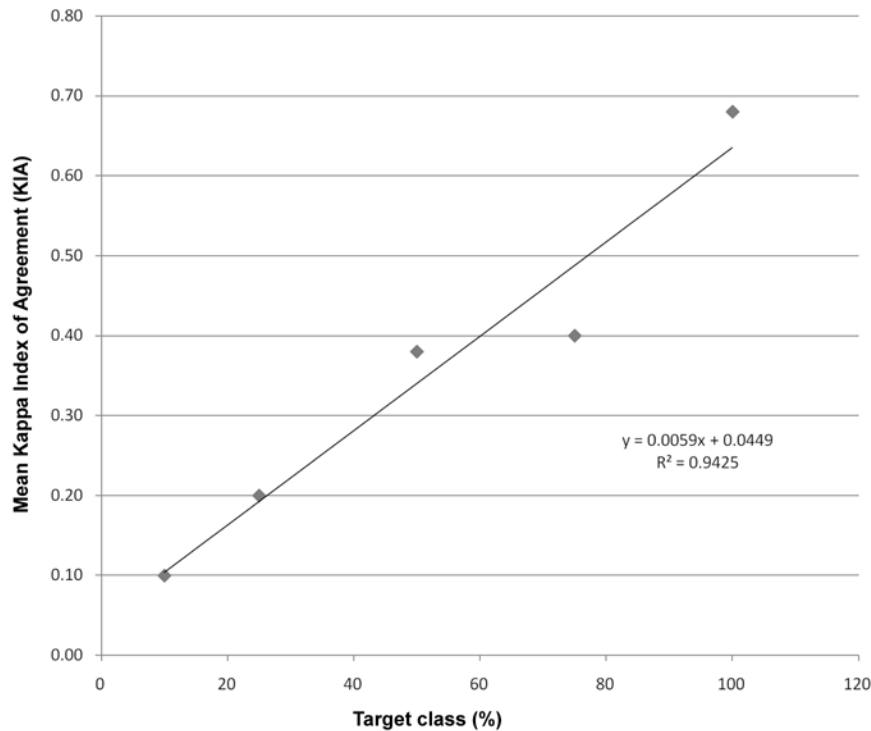


**Figure 3. Mean KIA followed a strong negative trend with target class size. The line of best fit resulted in a coefficient of determination of 0.94**

A pairwise Z-statistic was calculated to compare resulting error matrices between target classes (Table 3). These results indicate the 100% target class performed significantly better than all other target classes ( $z > 1.96$ ). This may be attributable to the fact that the 100% target class had the potential to occupy full pixels homogeneously while all other target classes represented sub-pixel, heterogeneous classes. While the size of the blue tarps used for the 100% target class were equal to that of a Quickbird pixel, it is unlikely that each tarp was positioned to perfectly fit the extent of a pixel as acquired by the sensor. Consequently, it is more likely that individual training sites contained  $<100\%$  cover by a blue tarp. This same problem is encountered regularly in all field studies and the results reported here are considered applicable and valid. Indeed, target detection thresholds should be stated in terms of the size of the *in situ* target with full understanding that many training sites will be subdivided during image acquisition by the sensor.

**Table 3. Pairwise z-statistic results comparing variance of Kappa from cumulative error matrices of each target class. Comparisons with z-scores  $> 1.96$  represented significantly different classification results.**

		Target Class (%)				
		100	50	25	5	1
Target Class (%)	100	--	2.84	3.16	4.56	7.46
	50		--	0.20	1.81	3.54
	25			--	1.67	3.47
	5				--	1.08
	1					--

The pairwise comparison between the 50% and 25% sub-pixel target classes showed no difference ( $z = 0.20$ ) indicating these classifications performed similarly. The comparison between the 50% and 5% target classes had a z-score of 1.81 while the z-score comparing error matrices for the 25% and 5% target classes also showed no difference ( $z = 1.63$ ). While the resulting classification accuracies reported in this study demonstrate the reliable detection of the 50% and even 25% target classes, the results of pairwise comparisons indicate that none of these classifications performed statistically different relative to one another.

Nearly all pairwise comparisons with the 1% target class were statistically significant (different) save for the comparison with the 5% target class ( $z = 1.08$ ). In these cases, the overwhelming majority of each training site pixel was occupied by non-target features and classification results were similar to that expected by a chance (random) classification. It is not surprising then, that pairwise comparisons with the 1% target class showed statistical differences ( $z > 1.96$ ) as effectively no trace of the blue tarp's spectra may have been present and classification results followed a random distribution. The 5% target class performed similar to the 1% target class for many of the same reasons, resulting in pairwise comparisons that showed no difference. These results serve to emphasize the observation suggested by the results of separability testing; targets covering  $< 25\%$  of a pixel were unlikely to achieve reliable classification results under the conditions of this study.

Goodchild et al. (1994) suggested 75% overall accuracy be used as a benchmark of classification reliability and hence, detection. Under these guidelines, only the 100% target class achieved a reliable classification. However, the 50% and 25% target classes achieved a mean user's accuracy of  $>80\%$ , albeit

with producer's accuracies of only 50% and 45%, respectively ( $\bar{x}$  KIA = 0.40 and 0.38, respectively). These results suggest that while the 50% and 25% target classes were spectrally differentiable, other classification methods (e.g., linear spectral unmixing or classification and regression tree) may be required to achieve accurate classification results with multispectral sensors. A detailed study of the resulting error matrices indicates there was confusion between target and non-target classes. This may be reduced however, by including simple band ratio layers (e.g., NDVI, MSAVI2), data reduction layers (e.g., principal components analysis image layers), or by excluding individual image bands where the greatest spectral similarity existed (e.g., the green and red bands in this study [Fig. 2]).

This study was performed using Quickbird satellite imagery (2.4 mpp) as this sensor's spatial and spectral characteristics best facilitated the need to accurately locate rare and spectrally unique, sub-pixel targets. In semiarid environments, this ability is critical because landscape features such as sagebrush, shrubs, patches of invasive weeds, and patches of bare soil are frequently encountered at the same spatial order (i.e., 1-4m). We believe these results may be applicable to other multispectral sensors regardless of the instrument's spatial resolution with 25% cover suggested as the detection threshold of these systems. However more research is required before such statements can be unequivocally made. To substantially improve the ability to detect small targets (i.e., < 0.25) the use of hyperspectral imagery may be required (Parker-Williams and Hunt, 2002; Glenn *et al.*, 2005) and/or techniques other than maximum likelihood to improve sub-pixel detection.

#### *Assessment of Error and Bias*

All efforts were made to design and execute an experiment that would rigorously and empirically test the detection capabilities of multispectral imagery relative to rare and spectrally unique targets in semiarid ecosystems. The results reported here may vary somewhat if repeated in other ecosystems but the ability to significantly reduce sub-pixel detection with multispectral sensors is not anticipated. In many ways, the results observed in this study may represent a best-case scenario as all targets were spectrally unique and both physically homogeneous (i.e., laid flat upon the earth with no neighboring shadow), and spectrally homogeneous (i.e.,  $\bar{x}$  standard deviation = 0.0001 for target spectra).

One potential error in this study relates to the exact placement of each target relative to the location and "edge" of each pixel acquired by the Quickbird sensor. It is possible, and indeed likely, that some of the targets were captured across pixels instead of within a single pixel as was assumed throughout the image analysis process. In these cases, target size was effectively reduced and the training site corrupted. For example, if a 50% blue tarp target site was captured across two pixels, the training site (located in the center of the target) might represent a 25% target spectrally as only a portion of reflectance from that tarp affected the training site pixel. This problem was most likely to have occurred with the larger target classes ( $\geq 50\%$ ) and was less probable with smaller target classes (5% and 1%). This unavoidable error is not attributable to the experimental nature of this study but is common to all remote sensing studies and especially problematic with any study focusing upon patchy and rare target detection (e.g., the early detection of invasive weed infestations).

The number of samples used in this study presents another concern. To emulate the presence of rare targets, 100 blue tarps were prepared for this experiment, with 20 created for each target class. Of these 20, 10 were randomly selected to be used for training sites while the remaining 10 were used for

independent validation in each trial, thus the sample size for each classification trial was 10. However, this bootstrap resampling technique was repeated six times to better capture the variability within the training site samples (Weber and Langille 2007). While this remains a potential bias of this study, it should be understood that the spectral variance of the blue tarp targets was very low ( $\bar{x}$  std. dev. = 0.0001;  $\bar{x}$  reflectance 0.07, 0.10, 0.06, and 0.26 for the blue, green, red, and NIR bands respectively) and the majority of variance was explained within the existing sample size. In addition, if the sample size were insufficient for this particular experiment, one would expect to see accuracy and KIA values that varied greatly between trials. This was not observed however, and indeed the standard error for all measures of classification accuracy were small for target classes  $\geq 25\%$  (Table 2).

## **CONCLUSIONS**

This study sought to experimentally determine the detection capabilities of multispectral imagery and was not designed to develop and test new algorithms for sub-pixel classification. For this reason, the authors used a common classification technique (maximum likelihood) and only basic (atmospherically corrected) image bands (i.e., blue, green, red, and near infra-red). To address the objectives of this study, six iterations of maximum-likelihood classification were used to determine classification accuracy for 100 spectrally unique targets randomly placed over a semiarid rangeland site. Error matrices were calculated using independent validation sites and producer's accuracy, user's accuracy, overall accuracy, KIA, and transformed divergence were analyzed to compare the performance of each classification and determine detection thresholds. The results of this study suggest training site selection (both initial site selection in the field and the selection of sites during resampling operations in the laboratory) has significant effect on classification accuracy. This effect became more pronounced as target size decreased, as the standard deviation of overall accuracy increased from 0.06 (100% target class) to 0.16 (1% target class).

This study demonstrated 1) the applicability of transformed divergence separability scores as an indicator of potential classification success, 2) an empirical relationship ( $R^2 = 0.94$ ) between target size and classification accuracy, and 3) the limitation of multispectral imagery for sub-pixel target detection. Regarding the latter, it appears the detection threshold of spectrally unique targets is approximately 25% cover within semiarid rangelands. This has direct implication for invasive plant research and rare target detection as targets such as leafy spurge or purple loosestrife may be undetectable until an infestation covers 25% or more of a pixel. If the results and relationships demonstrated in this study transfer directly to other multispectral sensors and furthermore, if Landsat imagery (30 x 30 m pixels) were used, then weed infestations would need to be 225 m<sup>2</sup> in area before the infestation would be detectable. This is problematic as land managers rely upon early detection for effective control and eradication of weeds.

While the classification results reported in this study for both the 50% and 25% target classes were not ideal (overall accuracy was  $< 75\%$ ), the user's accuracy was satisfactory ( $> 80\%$ ). To substantially improve the ability to detect proportionally small targets ( $< 0.25$  pixel) the use of hyperspectral imagery may be required and/or techniques other than maximum likelihood (e.g., linear spectral unmixing or classification and regression trees) to improve sub-pixel detection.

## **ACKNOWLEDGEMENTS**

This study was made possible by a grant from the National Aeronautics and Space Administration Goddard Space Flight Center (NNX08AO90G). Idaho State University would also like to acknowledge the Idaho Delegation for their assistance in obtaining this grant.

## **LITERATURE CITED**

- Chavez, P. S., 1996. Image-based Atmospheric Corrections: Revisited and Improved, *Photogrammetric Engineering and Remote Sensing*, 62 (9): 1025-1036
- Cheng, P., T. Toutin, Y. Zhang, and M. Wood, 2003. Quickbird - Geometric Correction, Path and Block Processing and Data Fusion, *Earth Observation Magazine (EOM)*, May 2003, 24-30
- Cohen, J., 1960. A Coefficient of Agreement for Nominal Scales, *Educational and Psychological Measurement*, 20 (1): 37-46
- Congalton, R. G., and K. Green, 2009. *Assessing the Accuracy of Remotely Sensed Data: Principles and Practices*, CRC Press, Inc., Boca Raton, Florida, 183pp
- Dai, X., and S. Khorram, 1998. The Effects of Image Misregistration on the Accuracy of Remotely Sensed Change Detection. *IEEE Transactions on Geoscience and Remote Sensing*, 36: 1566-1577
- Foody, G. M., 1992. On the Compensation for Chance Agreement in Image Classification Accuracy Assessment, *Photogrammetric Engineering and Remote Sensing*, 58 (10): 1459-1460
- Foody, G. M., and M. K. Arora, 1997. An Evaluation of some Factors Affecting the Accuracy of Classification by an Artificial Neural Network, *International Journal of Remote Sensing*, 18 (4): 799-810
- Glenn, N. F., J. T. Mundt, K. T. Weber, T. S. Prather, L. W. Lass, and J. Pettingill, 2005. Hyperspectral Data Processing for Repeat Detection of Small Infestations of Leafy Spurge, *Remote Sensing of Environment*, 95 (3): 399-412
- Good, P. I. 2005. *Resampling Methods: A Practical Guide to Data Analysis*. Birkhauser. 3:218 pp
- Goodchild, M. F., G. S. Biging, R. G. Congalton, P. G. Langley, N. R. Chrisman, and F. W. Davis, 1994. *Final Report of the Accuracy Assessment Task Force*. California Assembly Bill AB1580, Santa Barbara: University of California, National Center for Geographic Information and Analysis (NCGIA)
- Landis, J. R., and G. G. Koch, 1977. The Measurements of Observer Agreement for Categorical Data, *Biometrics*, 33 (1): 159-174
- Lillesand, T. M., and R. W. Kiefer, 2000. *Remote Sensing and Image Interpretation*. John Wiley and Sons, New York 4

- Mehner, H., M. Cutler, D. Fairbairn, and G. Thompson, 2004. Remote Sensing of Upland Vegetation: the Potential of High Spatial Resolution Satellite Sensors, *Global Ecology and Biogeography*, 13 (4): 359-369
- Monserud, R., and R. Leemans, 1992. Comparing Global Vegetation Maps with the Kappa Statistic, *Ecological Modeling*, 62 (4): 275-293
- Mundt, J. T., N. F. Glenn, K. T. Weber, and J. Pettingill, 2006. Determining Target Detection Limits and Accuracy Delineation using an Incremental Technique, *Remote Sensing of Environment*, 105 (1): 34-40
- Parcharidis, I., M. Fouvelis, E. Papageorgiou, M. Segou, and V. Sakkas, 2005. Orthorectification and Assessment of Quickbird Imagery using D-GPS Measurements over Paros Urban Area. *Proceedings of International Society for Photogrammetry and Remote Sensing 2005 Joint Conference*, Tucson, Arizona, USA
- Parker-Williams, A., and E. R. Hunt, 2002. Estimation of Leafy Spurge Cover from Hyperspectral Imagery using Mixture Tuned Matched Filtering, *Remote Sensing of Environment*, 82 (2): 446-456
- Richards, J. A., and X. Jia, 2006. *Remote Sensing Digital Image Analysis*. Springer-Verlag, Berlin, 4:439pp
- Robertson, B. C., 2003. Rigorous Modeling and Correction of Quickbird Imagery, *Proceedings of IEEE International Geoscience and Remote Sensing Symposium (IGARSS '03)*. Toulouse, France, pp.797-802
- Roy, D. P., 2000. The Impacts of Misregistration upon Composited Wide Field of View Satellite Data and Implications for Change Detection, *IEEE Transactions on Geoscience and Remote Sensing*, 38 (4): 2017-2032
- Stow, D. A., 1999. Reducing the Effects of Misregistration on Pixel-level Change Detection, *International Journal of Remote Sensing*, 20 (12): 2477-2483
- Titus, K., J. A. Mosher, and B. K. Williams, 1984. Chance-corrected Classification for use in Discriminant Analysis: Ecological Applications, *The American Midland Naturalist*, 111 (1): 1-7
- Toutin, T., and R. Chenier, 2004. GCP Requirement for High-resolution Satellite Mapping, *Proceedings of International Society for Photogrammetry and Remote Sensing 2004 Congress*, Istanbul, Turkey
- Townshend, J. R. G., C. O. Justice, C. Gurney, and J. McManus, 1992. The Impact of Misregistration on Change Detection, *IEEE Transactions on Geoscience and Remote Sensing*, 30 (5): 1054-1060
- Verbyla, D. L., and S. H. Boles, 2000. Bias in Land Cover Change Estimates Due to Misregistration, *International Journal of Remote Sensing*, 21 (18): 3553-3560
- Wang, H., and E. C. Ellis, 2005. Image Misregistration Error in Change Measurements, *Photogrammetric Engineering and Remote Sensing*, 71 (9): 1037-1044

Weber, K. T., 2006. Challenges of Integrating Geospatial Technologies into Rangeland Research and Management, *Rangeland Ecology and Management*, 59 (1): 38-43

Weber, K.T., and J. Langille, 2007. Improving Classification Accuracy Assessments with Statistical Bootstrap Resampling Techniques, *GIS Science and Remote Sensing*, 44 (3): 237-250

Weber, K. T., N. F. Glenn, J. T. Mundt, and B. Gokhale, 2006. A Comparison between Multi-spectral and Hyperspectral Platforms for early Detection of Leafy Spurge in Southeastern Idaho, In K. T. Weber (Ed.), Final Report: Detection, Prediction, Impact, and Management of Invasive Plants Using GIS 185-196  
URL = [http://giscenter.isu.edu/research/techpg/nasa\\_weeds/pdf/multi\\_vs\\_hyper.pdf](http://giscenter.isu.edu/research/techpg/nasa_weeds/pdf/multi_vs_hyper.pdf), visited 20-Jun-2007

Weber, K. T., J. Theau, and K. Serr., 2008. Effect of Co-registration Error on Patchy Target Detection using High-resolution Imagery, *Remote Sensing of the Environment*, 112 (3): 845-850

Wijnant, J., and T. Steenberghen, 2004. Per-parcel Classification of Urban Ikonos Imagery, *Proceedings of 7<sup>th</sup> AGILE Conference on Geographic Information Science*. Heraklion, Greece, 447-455

**Recommended citation style:**

Weber, K.T. and F. Chen, 2011. Detection Thresholds for Rare, Spectrally Unique Targets within Semiarid Rangelands. Pages 129-142 in K. T. Weber and K. Davis (Eds.), Final Report: Assessing Post-Fire Recovery of Sagebrush-Steppe Rangelands in Southeastern Idaho. 252 pp.

[THIS PAGE LEFT BLANK INTENTIONALLY]

## **Comparison of Atmospheric Correction Algorithms for Multispectral Satellite Imagery**

Keith T. Weber, GISP. GIS Director Idaho State University, GIS Training and Research Center,  
921 S. 8th Ave., stop 8104. Pocatello, ID 83209-8104

### **ABSTRACT**

Correcting satellite imagery for atmospheric effects is a common procedure today. Indeed there are many techniques and software applications that offer atmospheric correction processes. This study compared several techniques (apparent reflectance, dark-object subtraction, Cos(t), and the full cost model) in both Idrisi and ENVI software to determine the level of similarity between resulting imagery and the interoperability of these data. In nearly all cases comparison of resulting imagery revealed no differences ( $r = 1.0$ ). However, other results suggest that for a given project, all imagery should be corrected using the same technique within the same software application. Furthermore, use of full cost models should probably be avoided unless optical thickness and spectral diffuse sky irradiance parameters can be accurately computed and consistently applied. As an alternative, both Cos(t) and dark-object subtraction algorithms offer viable correction techniques that are well documented and appear to be robust and reliable.

*KEYWORDS: atmospheric correction, full-cost model, Cos(t), Dark object subtraction, apparent reflectance, Lake Superior*

## **INTRODUCTION**

The effect (e.g., attenuation and scattering) the atmosphere has on ground response signals has been an active area of research since Chandrasekhar's radiative transfer theory was published in 1960. Since that time, numerous algorithms have been developed to correct satellite imagery for known atmospheric effects (Dave 1980; Forster 1984). Most, if not all approaches have been similar and apply the same parameters. These parameters include 1) the date and time of image acquisition, 2) ambient weather conditions (temperature, humidity, atmospheric pressure), 3) solar zenith angle ( $\theta_0$ ) and derived  $\mu_0$  as the  $\cos(\theta_0)$ , 4) normal optical thickness (derived from ozone optical thickness for affected bands and aerosol optical thickness of each band), 5) satellite viewing angle, 6) atmospheric transmittance, 7) spectral solar irradiance, 8) path radiance, and 9) global irradiance. Many of these parameters represent known values (1 and 3), values considered waveband-dependent constants (4) or values derived from previous steps in the atmospheric correction process (4, 6-9). Other parameters, such as ambient weather conditions (2) and satellite viewing angle (5), are applied generalized values even though variability exists across the extent of the imagery being corrected. Potential errors associated with this approach are well recognized and areas of active research today. For instance the satellite viewing angle and solar zenith angle are used to calculate the solar incidence angle (SIA). However, without the use of an adequately resolved digital elevation model, SIA is at best an estimate. The associated error can be partially corrected for using the bi-directional reflectance distribution factor (BDRF) (Schott 1997) although this is not commonly done as it is computationally expensive. In addition, it should be realized that BDRF corrections represents a generalized estimate as the characteristics of the earth's surface (surface roughness, vegetation, soil moisture and albedo, etc.) play a significant role in determining the amount of light reflected by that surface. In essence, while the application of atmospheric correction processes are critical to geographic information science, it is equally important to recognize that imagery corrected for atmospheric effects will always retain residual errors.

Today, numerous techniques exist within various software applications that perform atmospheric correction. In some cases, analysts are even presented a choice among several techniques within the same software. Frequently, one technique will be chosen and applied repeatedly over the course of a career because the analyst understands that technique or feels comfortable with the procedure. Others working alongside the analyst may apply a different technique. Ultimately, imagery that has been atmospherically corrected using different techniques, may be involved in an analysis (e.g., temporal land cover change) with little consideration given to the affect the atmospheric correction techniques will propagate through the subsequent analysis. For this reason, a study was undertaken to compare various atmospheric correction techniques and determine the potential error mixed techniques might have on image analysis.

## **METHODS**

Landsat 5 TM imagery was acquired for path 39, row 30 representing a region of semiarid rangelands in southeast Idaho (scene acquisition date: July 20, 2008). Bands 3 (red) and 4 (near infrared) were corrected for atmospheric effects using each of the following algorithms, 1) Cost(t) (Chavez 1996) using Idrisi Taiga, 2) Dark object subtraction (DOS) (Chavez 1988; Cracknell and Hayes 1991) using Idrisi Taiga, and DOS using ENVI IDL, Apparent reflectance (AR) in Idrisi Taiga, and the Idrisi Full-Cost Model (FCM) (Forster 1984). Within each of these algorithms input parameters were modified as appropriate. For instance, Lmin Lmax was used and compared with results where gain and bias were used instead. In addition, Dn haze settings were either read from an apparent black body (American Falls Reservoir

[Figure 1]) or set at zero (0) (Lillesand et al. 2008). In total, 13 variations in atmospheric correction were performed for each band.

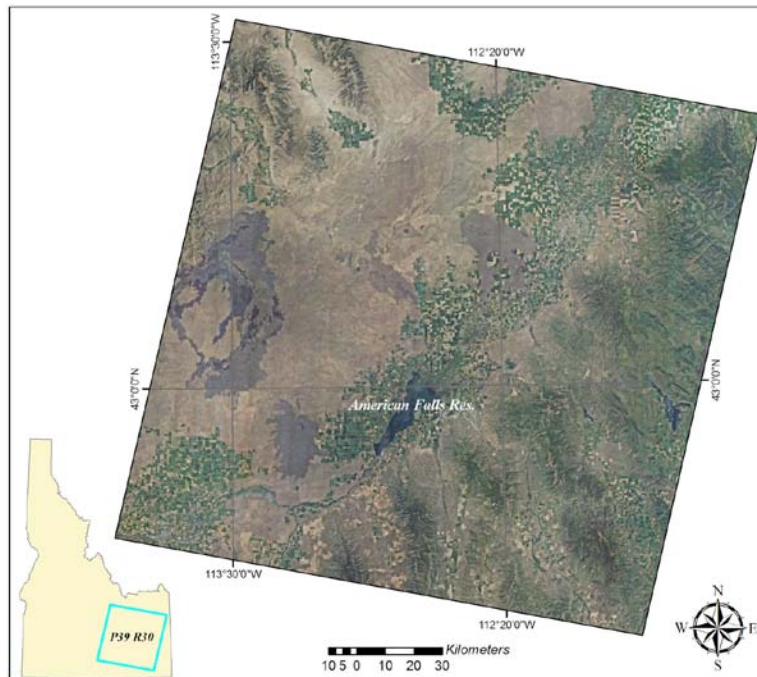


**Figure 1. Extent of Landsat imagery (path 39 row 30) used in this study and the American Falls Reservoir (an apparent black body) which was used to derive Dn haze values.**

The atmospherically corrected imagery was windowed to exclude all background pixels and thereby facilitate a robust statistical comparison of techniques that would not be skewed by agreement among background pixels (pixel values = 0). The resultant imagery was statistically compared using regression analysis within Idrisi Taiga (REGRESS) and a t-test of  $r$ . These tests allowed eight fundamental questions to be answered relative to this set of Landsat 5 TM imagery; specifically, is there a difference in atmospherically corrected imagery 1) using gain/offset versus Lmin/Max, 2) using different Dn haze settings within the Cos(t) algorithm, 3) using different Dn haze settings with the DOS algorithm, 4) between AR and Cos(t) when Dn haze equaled zero, 5) between AR and DOS when Dn haze equaled zero, 6) between Cos(t) and DOS, 7) between Cos(t) and a FCM, and 8) between DOS performed within Idrisi versus an ENVI IDL algorithm.

## RESULTS AND DISCUSSION

In nearly all cases, atmospherically corrected imagery was identical, or nearly so, regardless of the type of atmospheric correction technique applied within Idrisi Taiga. More specifically, the Y-intercept equaled zero, the slope of the line equaled 1.0000,  $r$  equaled 1.0000, the coefficient of determination equaled 100%, and the t-test of  $r$  was not significant ( $P < 0.0001$ ).

The exceptions to these observations were as follows: 1) while not statistically significant ( $P < 0.0001$ ;  $r = 1.0$ ), the comparison between AR and Cos(t) corrected imagery when Dn haze equaled zero revealed a resulting slope of 0.864, 2) similar comparisons between Cos(t) and DOS corrected imagery resulted in a slope of 0.864 ( $r = 1.0$ ). Of greater interest were differences observed between DOS correction methods

performed in Idrisi and ENVI (Figure 2). These comparisons were dissimilar enough ( $r = 0.67$ ) to prudently suggest that imagery corrected with different software applications not be used in the same image analysis project.

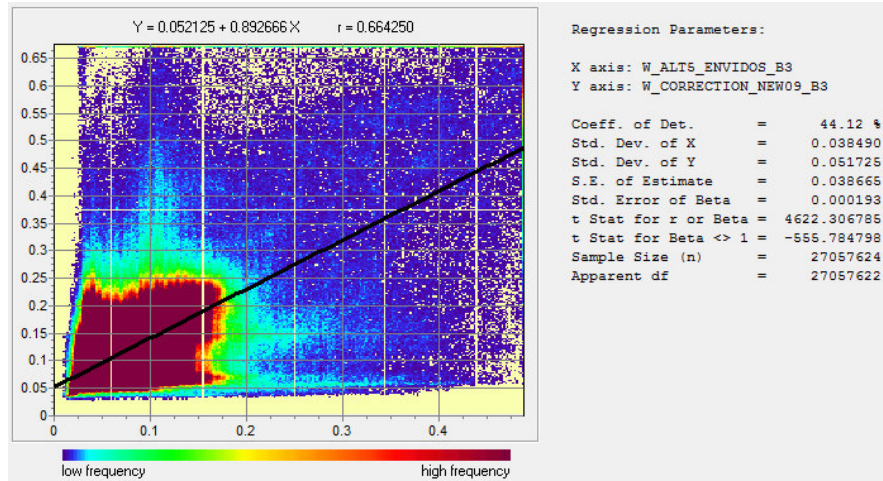


**Figure 2. Comparison of DOS-corrected imagery calculated in ENVI (X-axis) and Idrisi (Y-axis) demonstrating an incompatible difference.**

Similar results were observed by comparing Cos(t) and FCM corrected imagery (Figure 3;  $r = 0.66$ ). These results suggest that while all other algorithms exhibited near perfect agreement, the FCM within Idrisi Taiga responded differently. This is of interest as the response appears to be attributable to a change in only two input parameters, optical thickness and spectral diffuse sky irradiance. In this study, optical thickness values for the FCM were set at 0.05 and 0.01 (red and near-infrared bands, respectively) following Forster (1984). Spectral diffuse sky irradiance followed the BRITE code (Bird 1984). Optical thickness is itself an estimate primarily influenced by aerosols in the atmosphere (Turner and Spencer 1972) which varies as a function of standard pressure and declines exponentially with altitude. In mountainous regions, optical thickness is typically generalized to facilitate processing.

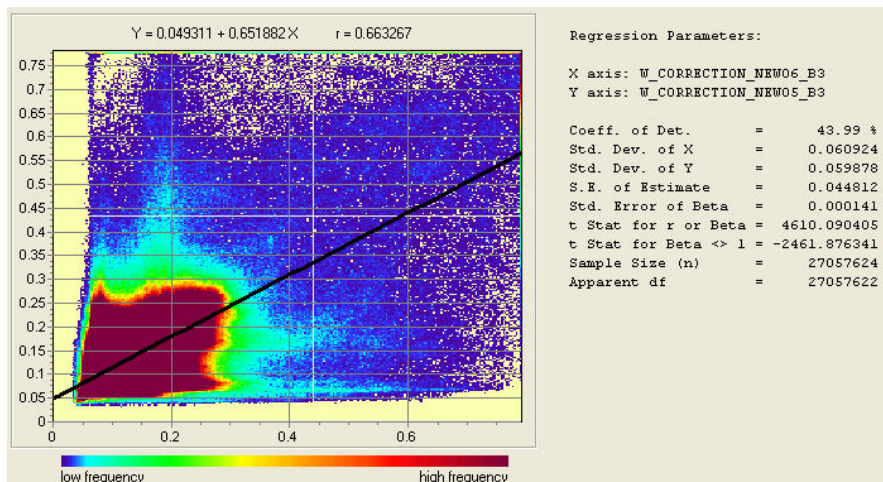


**Figure 3. Comparison of imagery corrected with the FCM (X-axis) and Cos(t) (Y-axis) demonstrating relatively large but yet non-significant differences.**

Spectral diffuse sky irradiance assumes a cloudless atmosphere and is a modeled variable which will vary depending upon solar incidence angle. There are five primary model parameters required to determine spectral diffuse sky irradiance and no less than five alternatives algorithms as well (Bird 1984; Justus and Paris 1984). In light of these complexities and uncertainties it seems use of the FCM is not advisable under most conditions. Rather, to maintain consistency, other well accepted atmospheric correction techniques should be utilized.

It is interesting to note that no difference was observed between atmospherically corrected imagery where Dn haze was equal to zero and where Dn haze values were extracted from an apparent black body (deep water areas within American Falls Reservoir). The extracted values used consistently throughout this study were 15 and 14 for the red and near infrared bands, respectively. Still, even with these differences in Dn haze, no difference in atmospherically corrected imagery was detected (Y-intercept = 0.000, slope = 1.000,  $r = 1.000$ , and  $P < 0.0001$ ).

It was considered that perhaps American Falls Reservoir did not adequately approximate a black body and for this reason, no difference was noted among comparisons. To investigate this, three additional Landsat 5 TM scenes were acquired for the Lake Superior and Keweenaw Peninsula region (path 024 row 027). This area was selected as the lake is very deep and oligotrophic (secchi disk depths range from 10-20 meters [cf. Minnesota Sea Grant]). As a result, the characteristics of Lake Superior should better approximate a black body. Analysis of these images proceeded in the same way as described earlier with no difference in atmospherically corrected results observed between Dn haze settings of zero and when Dn haze settings were read from deep water areas within the imagery (Y-intercept = 0.005, slope = 1.01,  $r = 1.00$ , and  $P < 0.0001$ ).

## **CONCLUSIONS**

Landsat 5 TM imagery was atmospherically corrected using a variety of algorithms within both Idrisi and ENVI software. In nearly all cases comparison of resulting imagery revealed no differences, including corrected imagery where Dn haze was intentionally set to zero in comparison with imagery where Dn haze was derived from an apparent black body. This suggests that Dn haze values have little overall effect within the correction algorithms and may not be necessary. The only notable exceptions to these general observations were comparisons of 1) imagery corrected in Idrisi with imagery corrected in ENVI (Figure 2) and 2) imagery corrected using the FCM technique (Figure 3). It is suggested that within a given analysis project, all imagery be corrected following the same technique and within the same software application. Furthermore, use of the FCM should probably be avoided unless optical thickness and spectral diffuse sky irradiance parameters can be accurately computed and consistently applied. As an alternative, both Cos(t) and DOS algorithms are viable correction techniques that are well documented and appear robust and reliable.

## **ACKNOWLEDGEMENTS**

This study was made possible by a grant from the National Aeronautics and Space Administration Goddard Space Flight Center (NNX08AO90G). Idaho State University would also like to acknowledge the Idaho Delegation for their assistance in obtaining this grant.

**LITERATURE CITED**

Bird, R. E. 1984. A Simple Spectral Model for Direct Normal and Diffuse Horizontal Irradiance. *Solar Energy* 32:461-471

Chandrasekhar, S. 1960. *Radiative Transfer*. Dover Press, New York. 393 pp.

Chavez, P. S. 1996. Image-Based Atmospheric Corrections- Revisited and Improved. *PE&RS* 62(9):1025-1036

Chavez, P. S. 1988. An Improved Dark-Object Subtraction Technique for Atmospheric Scattering Correction of Multispectral Data. *Remote Sensing of Environ.* 24:5459-479

Cracknell, A. P. and L. W. B. Hayes. 1991. *Introduction to Remote Sensing*, Taylor and Francis, London. 352 pp.

Dave, J. V. 1980. Effect of Atmospheric Conditions on Remote Sensing of a Surface Non-homogeneity. *PE&RS*, 46: 1173

Forster, B. C. 1984. Derivation of Atmospheric Correction Procedures for Landsat MSS with Particular Reference to Urban Data. *Int. J. Remote Sensing*, 5(5):799-817

Lillesand, T. M., R. W. Kiefer, and J. W. Chipman. 2008. *Remote Sensing and Image Interpretation*. J.W. Wiley and Sons, 6:756 pp.

Schott 1997. *Remote Sensing: The Image Chain Approach*. Oxford, NY

**Recommended citation style:**

Weber, K.T., 2011. Comparison of Atmospheric Correction Algorithms for Multispectral Satellite Imagery. Pages 143-148 in K. T. Weber and K. Davis (Eds.), Final Report: Assessing Post-Fire Recovery of Sagebrush-Steppe Rangelands in Southeastern Idaho. 252 pp.

## **Comparing Two Ground-Cover Measurement Methodologies for Semiarid Rangelands**

Keith T. Weber GISP, GIS Director, GIS Training and Research Center, Idaho State University, 921 S. 8th Ave., Stop 8104, Pocatello, Idaho 83209-8104 webekeit@isu.edu (corresponding author)

Fang Chen, GIS Training and Research Center, Idaho State University, 921 S. 8<sup>th</sup> Ave., Stop 8104, Pocatello, Idaho, 83209-8104

D. Terrance Booth, Rangeland Scientist, High Plains Grassland Research Station, USDA Agricultural Research Service, 8408 Hildreth Road, Cheyenne, Wyoming 82009  
Terry.Booth@ars.usda.gov

Mansoor Raza, GIS Training and Research Center, Idaho State University, 921 S. 8th Ave., Stop 8104, Pocatello, Idaho 83209-8104

Kindra Serr, Systems Administrator, GIS Training and Research Center, Idaho State University, 921 S. 8<sup>th</sup> Ave., Stop 8104, Pocatello, Idaho, 83209-8104, serrkind@isu.edu

Bhushan Gokhale, GIS Training and Research Center, Idaho State University, 921 S. 8th Ave., Stop 8104, Pocatello, Idaho 83209-8104

### **ABSTRACT**

The limited field-of-view (FOV) associated with single-resolution very-large scale aerial (VLSA) imagery requires users to balance FOV and resolution needs. This balance varies by the specific questions being asked of the data. Here, we tested a FOV-resolution question by comparing ground-cover measured in the field using point-intercept transects with similar data measured from 50 millimeters per pixel (mmpp) VLSA imagery of the same locations. Particular care was given to spatial control of ground and aerial sample points from which observations were made, yet percent cover estimates were very different between methods. An error budget was used to calculate error of location and error of quantification. Budget results indicated location error (0.435) played a substantial role, compared to quantification error (0.216); however, significant quantification error was present. We conclude that 1) while the georectification accuracy achieved in this project was actually quite good, the level of accuracy required to match ground and aerial sample points represents an unrealistic expectation with currently available positioning technologies, 2) 50-mmpp VLSA imagery is not adequate for accurate ground-cover measurement, and 3) the balance between resolution and FOV needs is best addressed by using multiple cameras to simultaneously acquire nested imagery at two or three VLSA resolutions. We recommend ground-cover be measured from 1-mmpp imagery and that the imagery be nested in lower resolution, larger FOV images simultaneously acquired.

**KEYWORDS:** *aerial imagery, GIS, remote sensing, VLSA*

## **INTRODUCTION**

Ground-cover is the vegetation, litter, rocks and gravel that cover bare soil and thereby reduce the risk of erosion (Branson et al. 1972). Quick and accurate assessments of ground-cover are not only useful to land managers for assessing soil stability (NRC 1994), but are also highly important for the sustainable management of millions of hectares of rangelands worldwide. In the past, the evaluation and monitoring of expansive landscapes has relied heavily on judgment and experience (NRC 1994; Stoddart and Smith 1995). However, conventional field surveys and sampling techniques may be nearly impossible or simply impractical to implement across vast areas like the US Intermountain West. As a result, many people on all sides of management issues are calling for increasingly quantitative and expedient monitoring approaches (Donahue 1999) such as those available through remote sensing. New measures are needed that are cost-effective and provide timely information within acceptable error rates (Floyd and Anderson 1987; Brady et al. 1995; Brakenhielm and Quinghong 1995; Sivanpillai and Booth 2008).

High spatial resolution satellite and aerial remote sensing have been used to conduct many studies across large landscapes. Blumenthal (2007) used high resolution imagery to study and measure infestations of invasive terrestrial weeds. Anderson et al. (1996), Bradley and Mustard (2006), Everitt et al. (1995 and 1996), and Lass et al. (2005) suggested that satellite and aerial imagery can be used to obtain accurate identification of invasive weeds. Sivanpillai and Booth (2008) used various remote sensing techniques to determine percent cover of vegetation over the 9,000 ha Hay Press Creek Pasture near Jeffrey City, Wyoming. Most recently, advancements in digital camera development and lens technologies have improved image sharpness to 1 millimeter per pixel (mmpp) (Booth et al. 2006). This has allowed for the differentiation of plant functional groups and even plant species with aerial photography (Booth et al. 2007; Booth et al. 2010).

One problem with Very-Large Scale Aerial (VLSA) imagery is the trade-off between spatial resolution and aerial extent. For example, achieving a spatial resolution of 1-mmpp commonly limits resulting scenes to 4 x 3 m (12 m<sup>2</sup>). In addition, accurate georectification (+/- 0.5 pixel; Weber 2006) of the imagery is quite difficult due to current limitations of positioning technologies such as the NAVSTAR GPS (+/- 1 cm under survey conditions). For these reasons, an alternative solution was sought that could deliver high spatial resolution imagery (50-mmpp), with relatively large individual scene sizes (0.5 km x 0.5 km), and accurate georectification.

The objectives of this study were to use VLSA imagery (50-mmpp spatial resolution) to: 1) compare individual point observations read in the field with observations read from aerial imagery to better understand the current capabilities and uncertainty associated with the use of VLSA imagery and, 2) compare percent ground-cover measurements derived from field observations with percent ground-cover measurements derived from aerial photography to better understand the management implications of VLSA imagery for range scientists.

## **METHODS**

### *Study Area*

The study was conducted in the sagebrush-steppe rangelands of southeast Idaho, US, approximately 30 km south of Pocatello, Idaho, at the O'Neal Ecological Reserve (Figure 1). This 50-ha site contains sagebrush-steppe upland areas located on lava benches. The Reserve receives < 380 mm of precipitation

annually (primarily in the winter) and is relatively flat, with a mean elevation of approximately 1,400 m (1,401-1,430 m). The dominant plant species is big sagebrush (*Artemisia tridentata* Nutt.) with various native and non-native grasses, including Indian rice grass (*Oryzopsis hymenoides* [R. & S.] Ricker.) and needle-and-thread (*Stipa comata* Trin. & Rupr.) present throughout the Reserve.

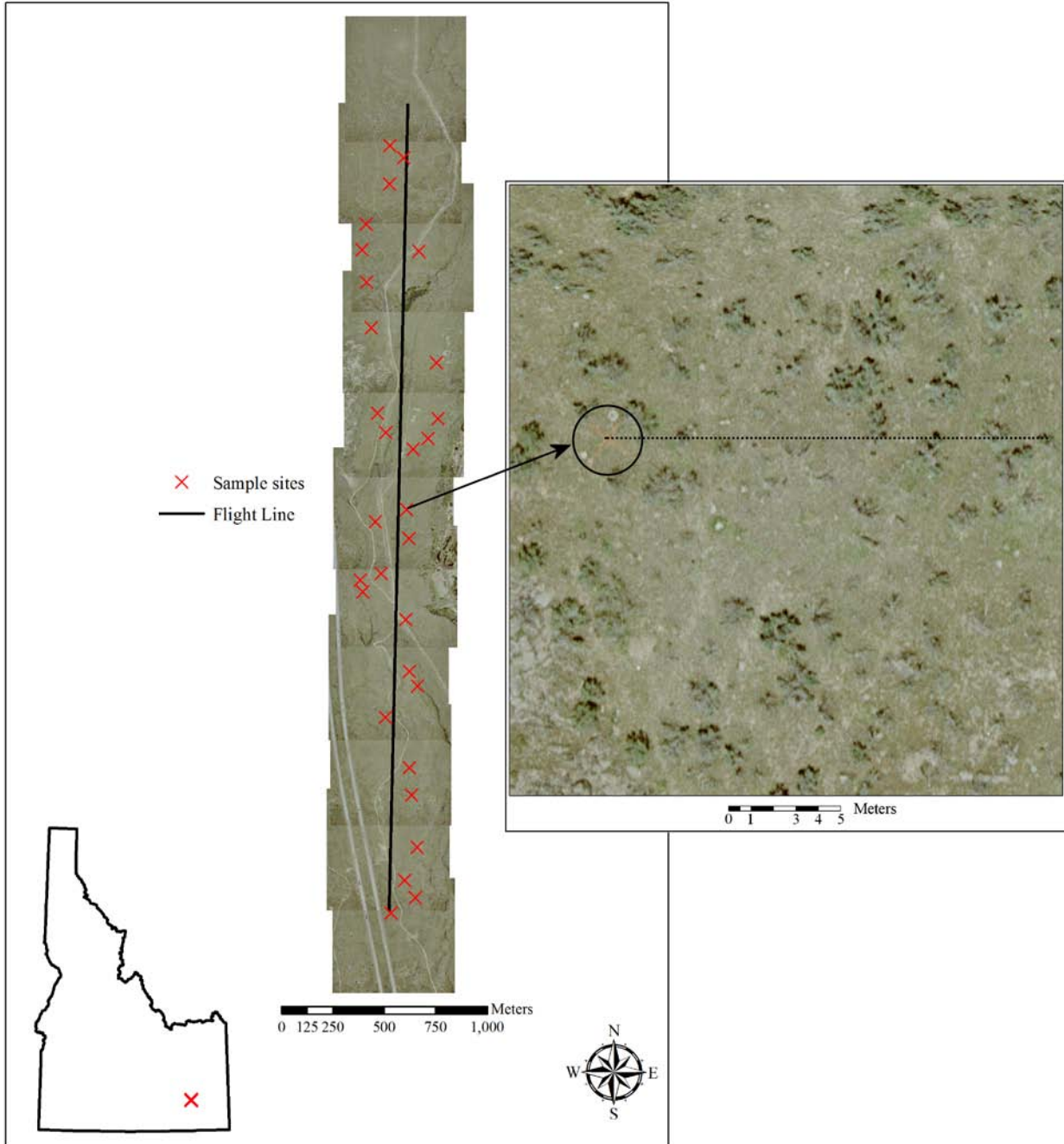


**Figure 1. The flight line and 50-mmpp VLSA imagery collected at the O'Neal Ecological Reserve in 2009. Inset shows an example of the imagery and illustrates the red-X painted on the ground (circled). The black dots extending west to east indicate the location where point observations and corresponding API observations were made.** *Aerial Photography Acquisition*

VLSA natural-color digital photography (50-mmp) was acquired by Valley Air Photo (Boise, Idaho) on May 22nd, 2009. All imagery tiles were collected +/- 2 hours of solar noon (1230 hrs MST) to minimize shadow at a mean above-ground elevation of 450 m (1:3000 flight scale;  $\bar{x}$  flight speed = 240 km/h). Aerial image tiles were collected using a Zeiss RMK Top 15 Pleogon A3 wide-angle lens having a calibrated focal length of 152.812 mm, an angular field of view (FOV) of 28.34 m (diagonal), and continuous aperture of f/4 to f/22 resulting in <3  $\mu$ m of distortion. The imagery was then scanned at 12  $\mu$ m resolution and resampled to 50-mmp. All imagery tiles were delivered in uncompressed TIFF format and georeferenced to Idaho Transverse Mercator (NAD 83).

### *Field Sampling*

Percent cover was determined using point-intercept transects (Gysel and Lyon 1980; ITT 1996). The location of transect starting points ( $n = 30$ ) was randomly generated using Hawth's tools within ArcGIS 9.3.1 and based on the following criteria: all points were 1) >70 meters from an edge (road, trail, or fence line) and 2) <750 meters from a road. All transects were read in an east-west direction from the starting point. Prior to acquisition of the aerial imagery, starting points were navigated to using a Trimble GeoXH GPS receiver (+/-0.20 m @ 95% CI after post processing). A large cross (mean arm length = 2.0 m and mean arm width = 0.1 m) was painted on the ground using red surveyor's spray paint to ensure the starting point would be readily visible in the imagery (Figure 1). The physical marker served two purposes; 1) it was easy for field personnel to revisit each site, and 2) it ensured the same starting point was used for both field observation and VLSA image interpretation.

During the week of aerial imagery acquisition, field personnel revisited each sample location and placed a 20-m flexible tape upon the ground from the starting point (indicated by the painted marker) and in the designated direction (directly east or west) with the aid of a compass. Photographs were taken using a Sony digital camera in each cardinal direction. Ground-cover type was determined by looking straight down at the transect tape and recording the cover feature in the upper most canopy directly indicated at the designated observation point. Observation points began at 10 cm from the starting point (observation point one) and continued every 20 cm thereafter (observation points 2-100). Ground cover at each observation point was classified as either shrub, rock (if the rock was over 7.5 cm in surface diameter), bare ground, invasive weed, grass, forb, litter, standing dead herbaceous material, standing dead woody material (e.g., a dead tree or sagebrush shrub still intact at the ground), or microbial crust. A total of 100 observations were made at each transect and recorded in a GPS-based field form. Percent cover was calculated in the laboratory and results of this sampling effort are henceforth referred to as FIELD observations.

### *Aerial Photography Interpretation (API)*

A personal geodatabase point feature class was created where each point represented the location of an observation along the transect used for field data collection. These features were overlaid on the VLSA imagery (50-mmp) within ArcGIS 9.3.1 to ensure the starting point for each transect feature was correctly aligned with the painted starting point visible in the imagery. Each set of transect points contained 101 points, with one point representing the starting point followed by 100 observation points consistent with FIELD observation protocols. Each point vector feature was effectively equivalent to a 25 cm<sup>2</sup> region in the field, as each point feature was used to extract the value of the pixel at the coincident geographic location. Each pixel, in turn, represents a region (25 cm<sup>2</sup>), within which all ground features are

mixed, or generalized, and displayed as one "color" within the imagery. In theory, the value of the color displayed in the imagery will be most representative of the feature occupying the majority of each pixel given that all feature categories have similar albedo and reflectance. While the location of the vector point features may not have been precisely at the same location as the point observed in the field, following this procedure allowed for the best co-registration possible. Three independent observers trained in GIS, aerial photo interpretation, and/or range science identified the cover type (bare ground, shrub, or grass) found immediately beneath each point feature at each observation point ( $n = 100$ ) along each transect ( $n = 30$ ). These observations were recorded in separate spreadsheets which were then compiled together and contained the observations made by each person in separate columns of the same spreadsheet ( $n = 9000$  observations). Each observer worked independently throughout this process following an initial briefing and did not have access to FIELD observations for these transects.

*Data Analysis: Point-observation scale*

The spreadsheet was reviewed and a new column created containing the consensus (MAJORITY) cover type (bare ground, shrub, or grass) found for each observation point record. In addition, FIELD observation data were imported as a separate column within the spreadsheet and related to the corresponding observation using the unique combination of transect and observation point identifiers. The MAJORITY column was reviewed and if no consensus was reached for an observation point, that row of data was deleted and not used in subsequent processing or analysis (note: copies of these data were made and no original data was permanently deleted during this study). Corresponding FIELD observations were also removed to eliminate incorrect cross-referencing. The cover types (bare ground, shrubs, and grass) were then assigned a numeric value of 1, 2, and 3 respectively, throughout both the MAJORITY and FIELD observation columns.

Since FIELD data were collected for 10 cover types instead of the three used during the aerial photo interpretation, all rows of data that did not contain bare ground, shrub, or grass entries (1, 2, or 3) were deleted. The remaining data ( $n = 2465$  records or 82% of original records) were rearranged in a new text file to conform to ESRI's ASCII raster format. The header of this file indicated the raster layer would contain 30 rows (one for each transect) and 100 columns (one for each observation). For those rows (transects) that did not contain a full complement of 100 columns (observations) due to the data reduction processes described above, the value of zero (0) was used as a no-data indicator to thereby maintain the consistency of the files for analysis. Two ASCII raster files were created, one describing aerial photography interpretation (API) observations and the other describing FIELD observations. These files were imported into Idrisi Taiga and displayed for visual inspection. The ERRMAT module of Idrisi Taiga was used to assess agreement between API and FIELD observations.

*Data Analysis: Transect-scale*

Percent cover measurements for bare ground, shrubs, and grasses were calculated for both FIELD and MAJORITY observations along the transects. Single-factor ANOVA was used to compare percent cover measurements for each cover type and assess the significance of agreement between the two cover measurement methodologies.

*Analysis of Georectification Accuracy*

The georectification accuracy of the VLSA imagery was independently assessed by comparing the X,Y location of 10 readily identifiable features visible in the imagery (utility poles, distinctive trees, etc.) with the X,Y location of the same feature visible in 150-mmpp imagery acquired in 2005 for the same study area. The latter reference imagery (Gregory et al. 2010) was orthorectified using the X,Y, and Z of visible ground control points (GCP's) strategically located throughout the flight path (+/- 2.0 cm). The 2005 aerial imagery was therefore considered a high-quality reference image relative to its horizontal positional accuracy.

**RESULTS AND DISCUSSION**

Ground-cover types at the point-observation scale were very different between FIELD and API observations using the 50-mmpp aerial imagery as user's, producer's, and overall accuracies were < 50% (Table 1). The shrub cover type had the lowest producer's accuracy (9%) and was the cover type least documented using API techniques (compare 9% API observations with 26% field observation rates). Bare ground had the lowest user's accuracy rate (26%) and was most commonly misclassified as the grass cover type. The Kappa Index of agreement (KIA) was 0.008 indicating any agreement between the observations was likely due entirely to chance.

**Table 1. Comparison of field-based land cover point observations with point observations made using aerial photography interpretation (API).**

Land cover type	Accuracy (%)	
	Producer's	User's
Bare ground	48	26
Shrub	9	28
Grass	44	46

Overall accuracy = 35%

Kappa Index of Agreement = 0.008

The results of ANOVA tests comparing percent cover of each cover type at the transect-scale indicated a fairly similar disagreement between observational methodologies (Table 2). All comparisons were statistically different (P < 0.0001) save for the comparison of the grass cover type (P = 0.81).

**Table 2. Results of ANOVA tests comparing FIELD and aerial photography interpretation (API) measurements of percent cover at the transect-scale (n = 30).**

Land cover type	P-value
Bare ground	< 0.001
Shrub	< 0.001
Grass	0.811

The georectification accuracy of the VLSA imagery as provided by the vendor was 3.17 m (SE = 0.49) relative to the reference imagery. The VLSA imagery and location of each transect were corrected to ensure accurate coregistration using the GPS-acquired location of each start point and the location of each cross painted on the ground at each start point that was visible in the VLSA imagery. While the

georectification of the VLSA imagery as delivered by the vendor was not able to achieve an accuracy  $\leq$  50% of a pixel (i.e., 0.025 m), this level of accuracy represents an unrealistic expectation with currently available positioning technologies. From an applications-based perspective the georectification accuracy achieved in this project was actually quite good.

What is more interesting and perhaps more central to the focus of this paper is the high degree of disagreement between FIELD and API observations. In all cases, agreement between these data were very poor and any agreement at all was attributable only to chance. This suggests that while the identification of landscape features common to semiarid sagebrush-steppe ecosystems (bare ground, shrubs, and grasses) can be made using aerial imagery, the spatial resolution of 50-mmpp is not adequate for accurate ground-cover measurement (cf., Booth and Cox 2009). However, error of location (Pontius 2000; Weber et al. 2008) may explain some of the disagreement. For example, if the tape measure used to identify the transect and its subsequent observation points was not tight, or if the tape was blown by the wind during observation, or not perfectly aligned in an east-west direction, or the observers eye was not perfectly positioned at nadir over the observation point, the probability of agreement between discrete observations would decrease as the observation locations would not be the same. In addition, errors or slight deviations in compass trend could also have been a source of variation between FIELD and API observations. In these cases, the error of location would be more pronounced at the extremes of the transect. In other words, if the rate of agreement was better at the first observations relative to the last observations, a measurable error of location would be demonstrated. To test for this type of error, the rate of agreement between first observations (FIELD and API) and last observations (FIELD and API) was determined. The results of this comparison revealed that 17 of 30 (57%;  $R^2 = 0.108$ ) first observations made in the field agreed with the first observations made from VLSA imagery, whereas only 8 of the last observations agreed (27%;  $R^2 = 0.005$ ). An error budget was estimated following Pontius (2000) using the VALIDATE module of Idrisi to calculate error of location and error of quantification. This result indicates error of location (0.435) played a substantial role, compared to quantification error (0.216), in the cumulative error budget associated with this study.

An additional source of potential error relates to parallax within the VLSA imagery especially along those transects furthest from the flight line. To minimize, albeit not eliminate, this error and yet retain a random sampling design, all transect observations were read toward the flight line.

Accurately measuring percent cover from 50-mmpp imagery was also problematic. The sample “point” on the 50-mmpp imagery is actually a small plot on the ground ( $25 \text{ cm}^2$ ), an area large enough to contain all of the ground-cover types to be identified; thus, the 50-mmpp resolution was considered too coarse to measure percent bare ground (Booth and Cox 2009) and illustrates again, the importance of matching resolution with task (Congalton et al. 2002). FIELD data were collected as point observations since small-plot sampling (e.g.  $2.9 \text{ cm}^2$ ) has been previously demonstrated to show only poor relationships with plant cover (Cook and Stubbendieck 1986, reviewing the method of Parker 1951). Cook and Stubbendieck (1986) also review evidence that cover measurements obtained using blunt-point sampling apparatuses result in biased data. These findings imply a 1-mmpp (sharp) digital sample point will provide a more accurate cover measurement than a point 50 times more blunt. Since percent cover is ultimately derived from individual transect observations and, given the heterogeneity exhibited in the vegetation of semiarid ecosystems (Norton 2008), it is understandable that percent cover measurements

did not agree. These results call into question the feasibility of such comparisons as the ability to replicate observations is extremely difficult even though the individual methodologies used may be applicable and sound.

This study compared the agreement between two cover measurement methodologies (i.e., FIELD and API) and did not test the accuracy of either method as this requires a true answer be known. While one may argue or assume that field observations represent the truth, this argument is only correct if the observations were repeatable (i.e., have high precision) and without other bias (e.g., observer bias). Furthermore, a true accuracy test would require API observations be made at the identical point observed in the field. While all attempts were made to eliminate discrepancies between actual observation points, the inherent uncertainty present in these studies suggests the results are best viewed in terms of agreement between methodologies and not a test of accuracy.

### *Management Implications*

Properly comparing methods to characterize ground cover in semiarid rangelands is very difficult. While both field-based and API observations have their place, API observations using VLSA imagery is becoming more common and more reliable. VLSA image interpretation presents several advantages: 1) cover can be measured anywhere within the imagery regardless of difficulty of access or proximity to roads, 2) measurements are repeatable (though observer bias is still present [Booth et al. 2006, Cagney et al. submitted]), and 3) the acquired aerial imagery represents an historical record of the rangelands that may be used for numerous other management applications in addition to cover measurement.

The proper design of any API-based ground cover assessment is critical to its success and a primary consideration relates to the granularity of observations. For instance, complete species differentiation using only aerial imagery, even with a 1-mmpp spatial resolution is not always possible. At present, the 50-mmpp imagery does not provide sufficient clarity to resolve or differentiate shrubs, grasses and bare ground, and cover assessments of plant functional groups, like that used in this study, requires a spatial resolution < 50-mmpp (Booth and Cox 2009; Booth et al. 2010). While 1-mmpp imagery may be more difficult to coregister, there are techniques to accomplish reliable coregistration, such as the nested imagery technique described by Moffett (2009; 2010). This will help reduce error of location (a large part of the total error budget) and could be applied to either 1-mmpp or 50-mmpp imagery in a similar way. However, the part of the error budget is the error of quantification and here only the 1-mmpp imagery will provide an improvement. Additional research is required to refine these spatial resolution guidelines.

The trade-off between spatial resolution and aerial extent is being addressed by using multiple cameras for simultaneously acquiring nested imagery at two or three resolutions, such as 1-, 10-, and 20-mmpp (Booth and Cox 2009, Booth et al. 2010). The utility of this approach is evident by the limited increase in operational cost to obtain multi-resolution data compared to single resolution data (the added cost is largely the cost of examining the additional images) and in the efficiency demonstrated by Booth et al. (2010) where the larger FOV was most valuable for assessing an area infested with a noxious weed, and where identification of the weed was confirmed using nested 1-mmpp imagery.

## **CONCLUSIONS**

We tested agreement between ground cover measurements from point-intercept transects and 50-mmpp VLSA imagery. Both individual observation-point and transect-scale percent cover measurements were compared, with results indicating very poor agreement between methodologies. This does not necessarily indicate that either method was incorrect however. While it may be possible to improve agreement between observations as well as percent cover measurements using a revised study design and collection of higher spatial resolution imagery (< 50-mmpp), it is more important to appreciate that 1) VLSA imagery can be used to measure ground-cover in semiarid rangelands and 2) like all other cover-measurement or estimation methodologies, the use of VLSA imagery and API has limitations (e.g., species cannot be identified at the spatial resolution used in this study) as well as advantages; 1) ground-cover can be measured anywhere within the imagery regardless of difficulty of access or proximity to roads, 2) measurements are repeatable (though observer bias is still present), and 3) the acquired aerial imagery represents an historical record of the rangelands that may be used for numerous other management applications in addition to cover measurement .

## **ACKNOWLEDGEMENTS**

This study was made possible by a grant from the National Aeronautics and Space Administration Goddard Space Flight Center (NNX08AO90G). Idaho State University would like to acknowledge the Idaho Delegation for their assistance in obtaining this grant. In addition, the assistance of Jamey Anderson, Kerynn Davis, and Heather Studley (ISU GIS Training and Research Center) are acknowledged for their assistance with data collection, and Kevin Graville (Valley Air Photo) for sharing his expertise in aerial photogrammetry.

## **LITERATURE CITED**

- Anderson, G. L., J. H. Everitt, D. E. Escobar, N. R. Spencer, and R. J. Andrascik, 1996. Mapping Leafy Spurge (*Euphorbia esula*) Infestations using Aerial Photography and Geographic Information Systems. *Geocarto International* 11:81–89
- Blumenthal, D., D. T. Booth, S. E. Cox., and C. E. Ferrier, 2007. Large-scale Aerial Images Capture Details of Invasive Plant Populations. *Rangeland Ecology and Management*, 60:523-528
- Booth, D.T. and S.E. Cox, 2009. Dual-camera, High-resolution Aerial Assessment of Pipeline Revegetation. *Environmental Monitoring and Assessment* 158:23-33
- Booth, D.T., S.E. Cox, and D. Teel, 2010. Aerial Assessment of Leafy Spurge (*Euphorbia esula* L.) on Idaho's Deep Fire /Burn. *Native Plant Journal* 11:327-339
- Booth, D. T., S. E. Cox, and G. Simonds, 2007. Riparian Monitoring using 2-cm GSD Aerial Photography. *Ecological Indicators* 7:636-648
- Booth, D. T., S. E. Cox, T. W. Meikle., and C. Fitzgerald, 2006. The Accuracy of Ground-Cover Measurements. *Rangeland Ecology and Management*, 59: 179-188

- Bradley, B. A., and J. F. Mustard, 2006. Characterizing the Landscape Dynamics of an Invasive Plant and Risk of Invasion using Remote Sensing. *Ecological Applications* 16:1132–1147
- Brady, W. W., J. E. Mitchell, C. D. Bonham, and J. W. Cook, 1995. Assessing the Power of the Point-line Transect to Monitor Changes in Plant Basal Cover. *Journal of Range Management* 48:187–190
- Branson, F. A., G.F. Gifford, and J. Robert Owen, 1972. *Rangeland Hydrology: Range Science Series No. 1*. Society for Range Management, Denver, CO. 84 pp.
- Brakenhielm, S., and L. Quighong, 1995. Comparison of Field Methods in Vegetation Monitoring. *Water Air and Soil Pollution* 79:75–87
- Cagney, J., S.E. Cox, and D.T. Booth. submitted. Comparison of Point Intercept and Image Analysis for Monitoring Rangeland Transects. *Rangelands Ecology and Management*
- Congalton, R.G., K. Birch, R. Jones, and J. Schriever, 2002. Evaluating Remotely Sensed Techniques for Mapping Riparian Vegetation. *Computers and Electronics in Agriculture*. 37:113-126
- Cook, C.W. and J. Stubbendieck, 1986. *Range Research: Basic Problems and Techniques*. Society for Range Management, Denver, CO 317 pp.
- Donahue, D. L., 1999. *The Western Range Revisited: Removing Livestock from Public Lands to Conserve Native Biodiversity*. University of Oklahoma Press, Norman, OK. 352 pp.
- Everitt, J. H., G. L. Anderson, D. E. Escobar, M. R. Davis, N. R. Spencer, and R. J. Andrascik, 1995. Use of Remote Sensing for Detecting and Mapping Leafy Spurge (*Euphorbia esula*). *Weed Technology* 9:599–609
- Everitt, J. H., D. E. Escobar, M. A. Alaniz, M. R. Davis, and J. V. Richerson, 1996. Using Spatial Information Technologies to Map Chinese Tamarisk (*Tamarisk chinensis*) Infestations. *Weed Science* 44:194–201
- Floyd, D. A., and J. E. Anderson, 1987. A Comparison of Three Methods for Estimating Plant Cover. *Journal of Ecology* 75:221–228
- Gregory, J., S. Panda, and K. T. Weber, 2010. Accurate Mapping of Ground Control Points for Image Rectification and Holistic Planned Grazing Preparation. Pages 49-54 in K. T. Weber and K. Davis (Eds.), Final Report: Forecasting Rangeland Condition with GIS in Southeastern Idaho (NNG06GD82G). 189 pp.
- Gysel, L. W. and L. J. Lyon. 1980. Habitat Analysis and Evaluation. Pages 305-317 in S. D. Schemnitz (Ed.), Wildlife Management Techniques Manual, revised. The Wildlife Society, Washington, DC. 4:686 pp.

Interagency Technical Team (ITT), 1996. Sampling vegetation attributes, Interagency Technical Reference, Report BLM/RS/ST-96/002. Denver, CO, USA: US Dept of the Interior, Bureau of Land Management–National Applied Resources Science Center. 164 p.

Lass, L. W., T. S. Prather, N. F. Glenn, K. T. Weber, J. T. Mundt, And J. Pettingill, 2005. A Review of Remote Sensing of Invasive Weeds and Example of the Early Detection of Spotted Knapweed (*Centaurea maculosa*) and Baby's-breath (*Gypsophila paniculata*) with a hyperspectral sensor. *Weed Science* 53:242–251

Moffet, C. A., 2009. Agreement Between Measurements of Shrub Cover Using Ground-Based Methods and Very Large Scale Aerial Imagery. *Rangeland Ecology and Management*: 62:268-277

Moffet, C. A., J. B. Taylor, and D. T. Booth, 2010. Submitted. Postfire Shrub Cover Dynamics: a 70-year Fire History in Mountain Big Sagebrush Communities. *Rangeland Ecology and Management*

Norton, J., 2008. Comparison of Field Methods. Pages 41-50 in Weber, K. T. (Ed.), Final Report: Impact of Temporal Land cover Changes in Southeastern Idaho Rangelands (NNG05GB05G). 354 pp.

NRC (National Research Council), 1994. *Rangeland Health*. National Academy Press, Washington, DC. 180 pp.

Parker, K.W., 1951. A Method for Measuring Trend in Range Condition on National Forest Ranges. USDA Forest Service, Washington, D.C. 26 pp.

Pontius, R. G., 2000. Quantification Error Versus Location Error in Comparison of Categorical Maps. *Photogrammetric Engineering and Remote Sensing* 66:1011–1016

Sivanpillai, R. D. and D. T. Booth, 2008. Characterizing Rangeland Vegetation using Landsat and 1-mm VLSA Data in Central Wyoming (USA). *Agroforest System* 73:55-64

Stoddart, L. A., and A. D. Smith, 1955. *Range Management*. McGraw-Hill, New York. 433 pp.

Weber, K. T., 2006. Challenges of Integrating Geospatial Technologies into Rangeland Research and Management. *Rangeland Ecology and Management* 59:38-43

Weber, K. T., J. Theau, and K. Serr, 2008. Effect of Coregistration Error on Patchy Target Detection using High-resolution Imagery. *Remote Sensing of Environment* 112:845-850

**Recommended citation style:**

Weber, K.T., F. Chen, D.T. Booth, M. Raza, K. Serr, and B. Gokhale, 2011. Comparing Two Ground-Cover Measurement Methodologies for Semiarid Rangelands. Pages 149-160 in K. T. Weber and K. Davis (Eds.), Final Report: Assessing Post-Fire Recovery of Sagebrush-Steppe Rangelands in Southeastern Idaho. 252 pp.

[THIS PAGE LEFT BLANK INTENTIONALLY]

## **Evaluating Land Degradation Indicators in Semiarid Ecosystems Relative to Wildfire**

Keith T. Weber, GISP, GIS Director, Idaho State University, 921 S. 8th Ave., Stop 8104,  
Pocatello, Idaho 83209-8104 webekeit@isu.edu

Fang Chen, Idaho State University, 921 S. 8th Ave., Stop 8104, Pocatello, Idaho 83209-8104  
chenfang@isu.edu

### **ABSTRACT**

Arid and semiarid rangeland ecosystems cover vast areas of the earth's land surface. Current research has placed heightened importance upon these regions because of their role in the carbon sequestration process and related concerns of rangeland degradation. Various approaches have been used to investigate land degradation with several techniques applying remote sensing technology. Most of these techniques use vegetation indices as a surrogate of primary productivity. This study, applied season-long composite NDVI to begin an assessment of degradation in the semiarid sagebrush-steppe rangelands of southeast Idaho following the 2006 Crystal fire. Further refinements on the cNDVI approach were also used including rain-use efficiency, water-use efficiency, and local net primary productivity scaling. These indicators were calculated annually over a 10-year period and a trend in rangeland condition observed. In nearly all cases, the indicators suggest a slight decline in primary productivity. However, trend lines for most observations were not statistically significant ( $P > 0.05$ ) save for several rain-use efficiency indices ( $P < 0.05$ ). Results from this study highlight the importance of long-term observation periods and demonstrate the significance of the seasonality of precipitation in semiarid rangelands.

*KEYWORDS: NDVI, desertification, Landsat, SOGS, ET, METRIC, carbon sequestration*

## **INTRODUCTION**

### *Background*

Arid and semiarid rangeland ecosystems cover approximately 45% of the earth's land surface (Huntsinger and Hopkins 1996, Branson et al. 1981; Reid et al. 2008) and represent nearly 80% of the areas grazed by livestock across the globe (Asner et al. 2004). These areas are typically dominated by grass and shrub communities and can be highly productive, though nearly always limited by the availability of water. When the hydrologic cycle (the capture, storage, and release of available water) is disturbed, rangelands desertify and as a result, typically exhibit increasing amounts of bare ground. Chronic disturbance shifts lead to a loss of ecosystem functionality and a reduction in biodiversity (Daubenmire 1959, Schlesinger et al. 1990) with associated social and economic underpinnings (Savory 1999, Arnalds and Archer 2000, Griffin et al. 2001).

Ecosystem productivity is a related and important metric to evaluate and monitor, especially when desertification and the potential effects of global climate change are concerned (Tian et al 2000; Weber et al. 2009). Measures of productivity are less direct however, than measures of bare ground as the latter exists along a horizontal plane and—for the most part—can be measured and expressed as a unit of area or percent exposure. Unlike bare ground, the definition of ecosystem productivity tends to be vague and open to interpretation. Further, measures of productivity tend to be more difficult to quantify with numerous methods available including above ground biomass (Chambers and Brown 1983), percent cover (Canfield 1941; Daubenmire and Daubenmire 1968), and canopy coverage (Gysel and Lyon 1980) to name but three. In most ecosystems, productivity measures are confounded by the fact that herbivores consume vegetation (the product of ecosystem productivity) during the same period in which one is trying to measure productivity.

Productivity estimates are typically made across large landscapes to better account for the high degree of variability in semiarid ecosystems and for this reason, satellite remote sensing has been frequently used. Similar to field based measures; remote sensing estimates have varied with no single algorithm being considered universally applicable. Some of the earliest and most common productivity algorithms use simple band ratios (SBR) that express an index of photosynthetically active vegetation. Vegetation indices (VI's) vary also, but typically leverage a ratio of reflectance in the red band to that of the near infra-red band of a given sensor. Perhaps the best known and most widely applied VI is the normalized difference vegetation index (NDVI) (Rouse et al. 1973; Tucker 1979).

### *Composite NDVI*

Arid and semiarid rangeland ecosystems exhibit strong seasonal dynamics and the use of single-date NDVI may result in an incorrect assessment of ecosystem productivity. To avoid such errors, composite NDVI (cNDVI) can be used to better capture seasonal variability and the flush of grasses and forbs throughout an entire growing season. Stoms and Hargrove (2000) followed a similar approach when they calculated a time-integrated NDVI using the mean of nineteen 14-day cNDVI layers. Similarly, Prince et al. (2009) used the sum of 16-day cNDVI layers acquired throughout the growing season to estimate net primary productivity (NPP), while Weber et al. (2009) used a composite of maximum NDVI throughout the growing season to compare two biophysically similar semiarid regions. While the statistic extracted from each composite varied (mean, sum, and maximum respectively), the use of several NDVI layers to characterize a growing season was critical to the success of each study.

### Rain Use Efficiency

The principle factor limiting plant productivity in semiarid rangelands is precipitation or more precisely, soil moisture (Taylor, 1986; Thomas and Squires 1991; Niamir-Fuller and Turner 1999; Booth and Tueller 2003; Hill 2006; Weber and Gokhale 2010). The response in plant biomass to precipitation appears highly correlated and field measurements reported by Studley and Weber (2010) reveal a high coefficient of determination ( $R^2 = 0.93$ ) between June precipitation and average forage availability (kg/ha). Because rangelands exhibit a high degree of inter-annual variability, determining a long-term trend in rangeland condition using cNDVI alone might be misleading. Le Houerou (1984) and Hountondji et al. (2009) argue that since the vegetation in semiarid areas is strongly associated with precipitation, several years of favorable rainfall may lead one to erroneously conclude that rangelands are in good condition or improving from a degraded condition. To avoid this error, Le Houerou (1984) introduced the concept of Rain Use Efficiency (RUE) as the "quotient of annual primary production by annual rainfall". Subsequent applications of RUE have typically used  $\sum$ NDVI to estimate above ground biomass. Hountondji et al. (2009) suggest integrating the sum of rainfall throughout the growing season (RR) to estimate RUE (Eq. 1) and observe the trend in integrated-NDVI (iNDVI) to better assess rangeland condition.

$$iNDVI/RR = \frac{\sum NDVI_{(growing\ season)}}{\sum Rainfall_{(growing\ season)}} \quad \text{Eq. 1}$$

The direct use of total rainfall is not without problems as this approach does not account for run-off, evaporation, and ground water recharge fractions, each of which detract from the amount of water that is available to and used by plants. Modeling RUE in such a way may be further complicated by the seasonality of rainfall, rate of precipitation, soil type and depth, as well as the interaction with ambient temperature, wind, and humidity as the fraction of what available to plants is not constant in either time or space.

### Water Use Efficiency

Water Use Efficiency (WUE) is similar to RUE save that it substitutes total evapotranspired water (i.e.,  $\sum$  of actual evapotranspiration [ET]) for the rainfall divisor. While this approach may be more accurate (Floret et al. 1983; Seiny-Boukar et al. 1992; Aronson et al. 1993) it is also more difficult to calculate correctly. Actual evapotranspiration is a very challenging parameter to measure and requires a weighing lysimeter for direct measurement. In addition, a number of environmental factors affect ET including phenology, soil exposure, and wind, further complicating the extrapolation of lysimeter measurements to entire landscapes. One model used to estimate ET is the Surface Energy Balance Algorithm for Land (SEBAL). SEBAL uses energy balance modeling instead of a catchment water balance approach (which relies on estimates or measures of ground water recharge, stream flow, etc) to estimate ET using satellite data. By indexing radiometric surface temperature from Landsat's thermal band, a near-surface temperature gradient can be determined. These data, along with net solar radiation and soil heat flux are then used to calculate actual evapotranspiration.

Allen et al. (2007) modified the SEBAL algorithm using *in situ* reference ET to internally calibrate surface energy balance estimates and thereby determine a more accurate estimate of actual ET. Using either the SEBAL or Mapping Evapotranspiration at high Resolution with Internalized Calibration

(METRIC) model (Allen et al. 2007), WUE can be calculated and used to visualize trends in rangeland condition over time.

#### *Local Net Primary Productivity Scaling*

Another approach used to assess rangeland degradation which effectively circumvents the potential errors associated with RUE as well as the computational challenges of accurately quantifying actual ET and hence, WUE, is Local Net Primary Productivity Scaling (LNS) introduced by Prince in 2004. LNS determines potential productivity within biophysically homogeneous areas and then compares site potential to the actual productivity observed at intrinsically similar sites. This method also relies upon NDVI as the fundamental source for estimates of productivity but makes no estimate of RUE apart from the inherent assumption that sites in proper functioning condition will exhibit higher primary productivity as a result of higher RUE and WUE. A potential problem with the LNS approach noted by Prince (*pers. comm.*) is if the entire study area is degraded then no reasonable potential can be identified. As a result, few sites will be identified as degraded when scaled against equally degraded counterparts.

The process of monitoring land degradation or identifying sites of desertification are essentially applications of land cover change analysis (Yuan et al. 1998). The most basic approach uses vegetation index differencing (Perry and Lautenschlager 1984) between two or more imagery dates while the more complex approaches described above, effectively build upon this concept. Trend lines are sometimes applied across datasets exhibiting long-term fluctuations in productivity with the slope of these lines interpreted as indicators of desertification trend (Hountondji et al., 2009). The accurate identification of land cover change, and especially desertification, is an active area of remote sensing research and many papers have been published that question the approach or conclusions of other papers (Hein and De Ridder 2006; Veron et al., 2006). A related, and perhaps equally active area of research, focuses not upon the identification of degraded areas but on identifying the drivers or causes of land degradation in semiarid rangelands. From these debates, three main paradigms have emerged: 1) environmental factors (rainfall) are the primary drivers of ecosystem change (Westoby et al. 1989), 2) anthropic factors (livestock grazing) are the primary drivers of ecosystem change (Le Houerou 1989; Hein and de Ridder 2006), and 3) both environmental and anthropic factors drive ecosystem change and exhibit interesting interactions over time (Briske et al, 2003; Vetter 2005; Hein and de Ridder 2006). One area of interaction relates to wildfire, a source of punctuated and geographically distributed change, as fires can be initiated and/or suppressed by humans. In addition, fuel load, a factor having substantial influence on a fire's effect (specifically fire intensity), can be influenced by humans and their livestock grazing animals (Weber et al. 2004).

This study, while acknowledging the importance of understanding the causative agents of change, focused on comparing four approaches commonly used to assess land degradation status and trend, namely cNDVI, RUE, WUE, and LNS. To accomplish this, 24 Landsat 5 TM scenes (2000-2009) were acquired for the Big Desert study area in southeast Idaho, USA. Analysis emphasized the effect of the 2006 Crystal fire, the second largest fire (890 km<sup>2</sup>) documented in southeast Idaho since 1936. This study sought to determine the trend of primary productivity for Big Desert rangelands 1) in areas where no fire had occurred since 2000 and, 2) in areas burned by the 2006 Crystal fire. In addition, this study compared various methodologies used to assess land degradation relative to their agreement, accessibility, and efficacy.

## Materials and Methods

### Study Area

The Big Desert study area lies approximately 71 km northwest of Pocatello Idaho and the center of the study area is approximately 113° 4' 18.68" W and 43° 14' 27.88" N (Figure 1). The Big Desert is managed by the United States Department of the Interior Bureau of Land Management (USDI BLM) and is a semiarid sagebrush-steppe ecosystem with relatively high proportions of bare ground. The vegetation in the study area consists primarily of native and non-native grasses, forbs, and several shrub species including big sagebrush (*Artemisia tridentata*) and rubber rabbitbrush (*Ericameria nauseosa* [Pall. ex Pursh]). The study area is relatively flat with elevation ranging from 1349 to 2297 m above sea level. The mean annual precipitation is 210 mm (1992-2009) with the majority falling as snow during the winter months (48%) and another 33% falling from April through June (cf. Yanskey *et al.* 1966). Sheep grazing is the primary anthropic disturbance with continuous/seasonal grazing systems used on allotments ranging in size from 1,100 to over 125,000 ha. The stocking rate is low (approximately 19 ha/animal unit [AU]) with only 10% of permitted grazing utilized in most seasons. Wildfire is a common disturbance and 58% of the study area has burned since 2000 with the Crystal fire burning 31% of the Big Desert in 2006.

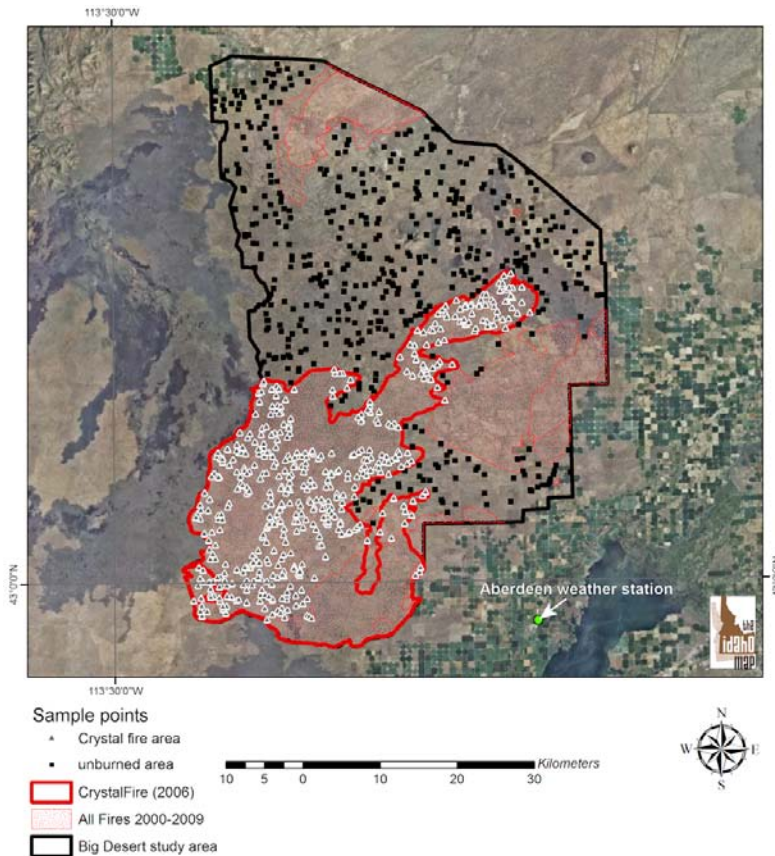


Figure 1. The Big Desert study area in SE Idaho and location of documented wildfires between 2000 and 2009 along with sample sites used in this study ( $n = 600$ ).

The geology of the Big Desert is typified by shallow soils overlying basalt. Fissures are quite common (approximate spacing of the smallest aperture fractures is 2-4 m [Johannesen 2000]) and water that infiltrates the soil surface can move to a fissure and relatively quickly become inaccessible to plants. As a

result, soil water content in the root zone (upper 0.25 m) can drop as low as 5-10% throughout much of the growing season (Kaminsky 1991).

The Big Desert is one of the few remaining large areas (2837 km<sup>2</sup>) of contiguous sagebrush-steppe rangelands in the Intermountain West and for this reason is an important conservation area for sagebrush-obligate species like the Greater Sage Grouse (*Centrocercus urophasianus*). In addition, the Big Desert represents an area of importance for livestock production and recreation as well.

*The Crystal Fire*

The Crystal fire burned approximately 890 km<sup>2</sup> across the Big Desert study area between August 15 and August 31, 2006. This lightning-caused wildfire was the second largest documented in southeast Idaho since 1936 (cf. the DR62 fire of 2007 which burned 1500 km<sup>2</sup>). More than 90% of the fire burned land managed by the USDI BLM with another 3% of the fire burning lands managed by the State of Idaho and National Park Service.

*Primary Productivity Modeling*

Twenty-four Landsat 5 TM scenes (path 039 row 030) were acquired for the Big Desert study area between 2000 and 2009 (Table 1). To capture the phenology and ephemeral productivity periods of the various grasses, forbs, and shrubs in these semiarid rangelands it was advantageous to use numerous scenes collected across each growing season (Weber et al. 2009). Capturing peak photosynthetic activity in this region was accomplished by acquiring one or two scenes in the spring (April or May) and one or two scenes in the early fall (September or October) (Tedrow and Weber 2010). By satisfying these criteria, an increased probability of capturing peak photosynthetic activity throughout the growing season was more likely achieved.

**Table 1. Year and date of Landsat 5 TM imagery used in this study (all scenes were acquired for path 039 row 030).**

Year	Date of image acquisition
2000	May 27
	June 28
	September 16
2001	May 14
	June 15
	September 19
2002	May 17
	July 4
	September 22
2003	May 20
	July 7
	August 24
2004	May 6
	June 7
	September 11
2005	May 25
	September 14
	September 30

2006	April 26 May 12 September 1
2007	May 15 May 31 September 20
2008	May 17 September 6 October 8
2009	April 18 September 9 September 25

All acquired imagery were corrected for atmospheric effects using Chavez' Cos(t) model in Idrisi Taiga's ATMOSC module (Chavez, 1996). The imagery were then tested for georegistration error using National Agricultural Imagery Program (NAIP) aerial orthophotography (1m x 1m pixels) and corrected as needed (RMSE < 0.50 pixel). NDVI was calculated for each scene and used to estimate primary productivity following Prince (1991; 2009). Composite NDVI (cNDVI) layers were created for each year of the study (2000-2009) using the NDVICOMP utility of Idrisi Taiga. cNDVI used maximum NDVI values observed throughout a growing season and in each case, three Landsat scenes were used per year to calculate the respective cNDVI layers. Imagery pairs (e.g., 2004 cNDVI and 2005 cNDVI) were co-registered to eliminate false positive/false negative change detection due to misalignment of features within the imagery. The resulting cNDVI layers were then used as estimates of maximum primary productivity for this study (Pettorelli et al 2005).

#### *Precipitation Modeling and RUE*

Precipitation data were used for the development of RUE models and while winter precipitation can be a very important contributor to spring plant growth in areas with deep soils, spring precipitation is also considered important, especially in areas with shallows soils, such as the Big Desert. In this study, five measures of precipitation (PPT) were used; total precipitation accumulated throughout the 1) hydrologic water year ( $PPT_{\text{hwy}}$  [October 1<sub>(year - 1)</sub> - September 30]), 2) growing season ( $PPT_g$  [April 1 - September 30]), 3) winter ( $PPT_w$  [October 1<sub>(year - 1)</sub> - March 31]), 4) spring ( $PPT_s$  [April 1 - June 30]), and 5) winter and spring seasons ( $PPT_{ws}$  [October 1<sub>(year - 1)</sub> - June 30]). These values were determined using data from the Aberdeen weather station (ABEI) located on the southern edge of the Big Desert study area (<http://www.usbr.gov/pn/agrimet/>). In addition, surface observation gridding system (SOGS) rasters (1000 m x 1000 m pixels) were used which provided spatially continuous models of meteorological conditions and were acquired through the Numerical Terradynamic Simulation Group (NTSG) at the University of Montana. The specific dataset used in this study described daily precipitation from 2004 through 2009.

Data from the Aberdeen weather station assumed a constant value throughout the study area. To integrate these tabular data into a geospatial format, raster layers were created where all pixels were assigned the value corresponding to the PPT measurement. While SOGS data were considered a better predictor of precipitation across large land areas (Weber et al., 2010) these data were not available for all years included in this study. All raster precipitation layers were projected into Idaho Transverse Mercator

(NAD 83), with 30 m x 30 m pixels, using ArcGIS 9.3.1 and nearest neighbor resampling. These parameters matched those for the Landsat 5 TM imagery described above. All precipitation values were expressed in millimeters. Annual RUE was determined using cNDVI and PPT (Eq. 1) from each of the alternative precipitation models.

#### *Evapotranspiration Modeling and WUE*

Actual evapotranspiration (ET) was required to calculate WUE for the Big Desert study area. Data describing actual ET were obtained from the METRIC-ET datasets for 2000, 2002, and 2006. These raster layers estimated the monthly sum of evapotranspired water (mm) across the study area. Total ET for the growing season ( $ET_g$  [April 1 - September 30]) was determined by summing each of the monthly estimates. These data, like all raster data used in this study, was projected into Idaho Transverse Mercator (NAD 83), with 30 m x 30 m pixels, using ArcGIS 9.3.1 and nearest neighbor resampling. All ET values were expressed in millimeters. WUE was determined for years 2000, 2002, and 2006 using cNDVI and  $ET_g$ .

#### *Local Net Primary Productivity Scaling (LNS) Modeling*

Calculating LNS requires two input layers; primary productivity (e.g., cNDVI) and land capability classification (LCC). LCC may be determined using a combination of precipitation, soils, land use, and land cover and is intended to delineate areas with similar intrinsic potential. Prince (2009) described several LCC procedures using k-prototypes clustering techniques (Huang, 1997; Hargrove and Hoffman, 2004) for an LNS study of Zimbabwe. For the Big Desert study area, a similar process was followed by incorporating SOGS precipitation (NTSG, 2010), SSURGO soils (NRCS, 2007), GAP land cover (InsideIdaho, 1999), and southeast Idaho land use/management layers (GIS TReC, 2010). Both land cover and land use layers for the Big Desert study area were constant and had no effect on the stratification of LCC because the entire study area was 1) classified as a basin and Wyoming big sagebrush land cover type (Redmond et al., 1996; Homer et al., 1998) and 2) similarly managed (i.e., livestock grazing allotments) by the USDI BLM Idaho Falls District. Intra-annual precipitation across the study area exhibited little variability (MSE = 0.50 [2004-2009]) and was similarly treated as a constant. As a result of this stratification exercise, LCC was based entirely upon 15 soil associations identified in the SSURGO soils database.

The 15 LCC polygons were rasterized and used as a Boolean mask with each year's cNDVI layer. This procedure produced 15 LNS layers per year, or a total of 120 layers for this study (i.e., 15 layers/yr x 8 years). To specifically examine the effect of the 2006 Crystal fire, an additional Boolean mask was created for the fire area and used as another stratification layer for 2007-2009. The Crystal fire burned parts of seven LCC areas and concomitantly increased the number of total LNS layers. Within each LNS layer, potential productivity was estimated as the cNDVI value at the 90<sup>th</sup> percentile ( $cNDVI_{p90}$ ). The LNS metric of degradation ( $LNS_d$ ) was determined using the following equation (Eq. 2).

$$LNS_d = cNDVI_{p90} - cNDVI_{actual} \quad \text{Eq. 2.}$$

where  $cNDVI_{actual}$  is the cNDVI value of each pixel assessed against the potential within each LCC area.

The standard deviation for each  $LNS_d$  layer was found and used to quantify the area (km<sup>2</sup>) within each LCC where primary productivity was >2 standard deviations below the potential. This *below potential*

*threshold* was conservatively chosen to allow for natural variability within each LCC and to help eliminate type I and type II errors.

### Analysis

To determine the trend in primary productivity and assess rangeland health/land degradation in the Big Desert study area, annual cNDVI, RUE, and WUE was examined at 600 random locations. Half of these locations ( $n = 300$ ) were within the area burned by the 2006 Crystal fire, but outside other areas of disturbance (i.e., earlier fires). The remaining 300 locations were outside the area burned by the Crystal fire, yet within the Big Desert study area (figure 1). All random sample points were generated using Hawth's tools in ESRI's ArcGIS 9.3.1 using the following criteria: sample points were not located within 70 m of a fire perimeter or within 70 m of another sample point. The value of the pixel at each sample point was extracted from each cNDVI, RUE, and WUE layer using the SAMPLE tool in ArcGIS and saved in a MS Excel spreadsheet. Scatter plots were created with year along the X-axis and the value of the productivity estimator (cNDVI, RUE, or WUE) along the Y-axis. A linear trend line was established for each scatter plot and the line's correlation coefficient, slope and Y-intercept recorded. Regression statistics were calculated for each scatter plot and an ANOVA was used to determine the significance of each relationship.

To assess the trend in primary productivity using  $LNS_d$  required a slightly different approach. In this case, the total area ( $km^2$ ) characterized using the *below potential threshold* was summed for each year and graphed as a scatter plot with year along the X-axis and total area below potential given on the Y-axis. A linear trend line was established for the scatter plot and the line's coefficient of determination, slope, and Y-intercept recorded. In total, ten scatter plots were created, one describing cNDVI, seven describing RUE (five using ABEI data to estimate  $PPT_{hwy}$ ,  $PPT_g$ ,  $PPT_w$ ,  $PPT_s$ , and  $PPT_{ws}$  [2000-2009], another using ABEI data for  $PPT_g$  in years 2004-2009 only to directly compare results with the seventh plot where  $PPT_g$  was estimated using SOGS data [2004-2009]), another describing WUE, and finally, one describing  $LNS_d$ .

## RESULTS AND DISCUSSION

Scatter plots and trend lines of cNDVI calculated for each growing season between 2000 and 2009 initially suggest primary productivity throughout the Big Desert study area declined (Figure 2). The rate of decline, as indicated by the slope of the trend lines, was quite slow for both the Crystal fire (-0.002) and unburned parts of the Big Desert study area (-0.004). In both cases however, large residual values existed due to inter-annual variability. Consequently, the coefficient of determination was quite low ( $R^2 = 0.01$  and  $0.04$  for the Crystal fire and unburned areas, respectively). The results of ANOVA tests used to determine the significance of the observed trend indicates the relationships were not statistically significant ( $P = 0.74$  and  $0.58$  for the Crystal fire and unburned areas, respectively). However, the high inter-annual variability in cNDVI did correspond fairly well with variability in precipitation ( $R^2 = 0.34$ ), serving to empirically validate the work of Le Houerou (1984) and Hountondji et al. (2009), and to illustrate the importance of water in these xeric environments (Niamir-Fuller and Turner 1999; Hill 2006).

RUE metrics (2000-2009) were calculated based upon five different measures of precipitation ( $PPT_{hwy}$ ,  $PPT_g$ ,  $PPT_w$ ,  $PPT_s$ , and  $PPT_{ws}$ ) (Figure 3). Results of RUE analysis also suggest primary productivity in the Big Desert declined (Figure 4a-e). However, when plotting data for 2004-2009 only, the results were

contradictory (Figure 4f-g), illustrating the need to observe trend over fairly long time periods (~10 years) to gain meaningful and reliable information (Washington-Allen et al., 2006). This observation is supported by an increased coefficient of determination ( $\bar{x} R^2 = 0.28$  [2000-2009] compared with  $\bar{x} R^2 = 0.05$  [2004-2009]). In contrast to the cNDVI results, several RUE metrics revealed a significant trend ( $P < 0.05$ ) including those metrics calculated using  $PPT_{hwy}$ ,  $PPT_s$ , and  $PPT_{ws}$  (Table 2).

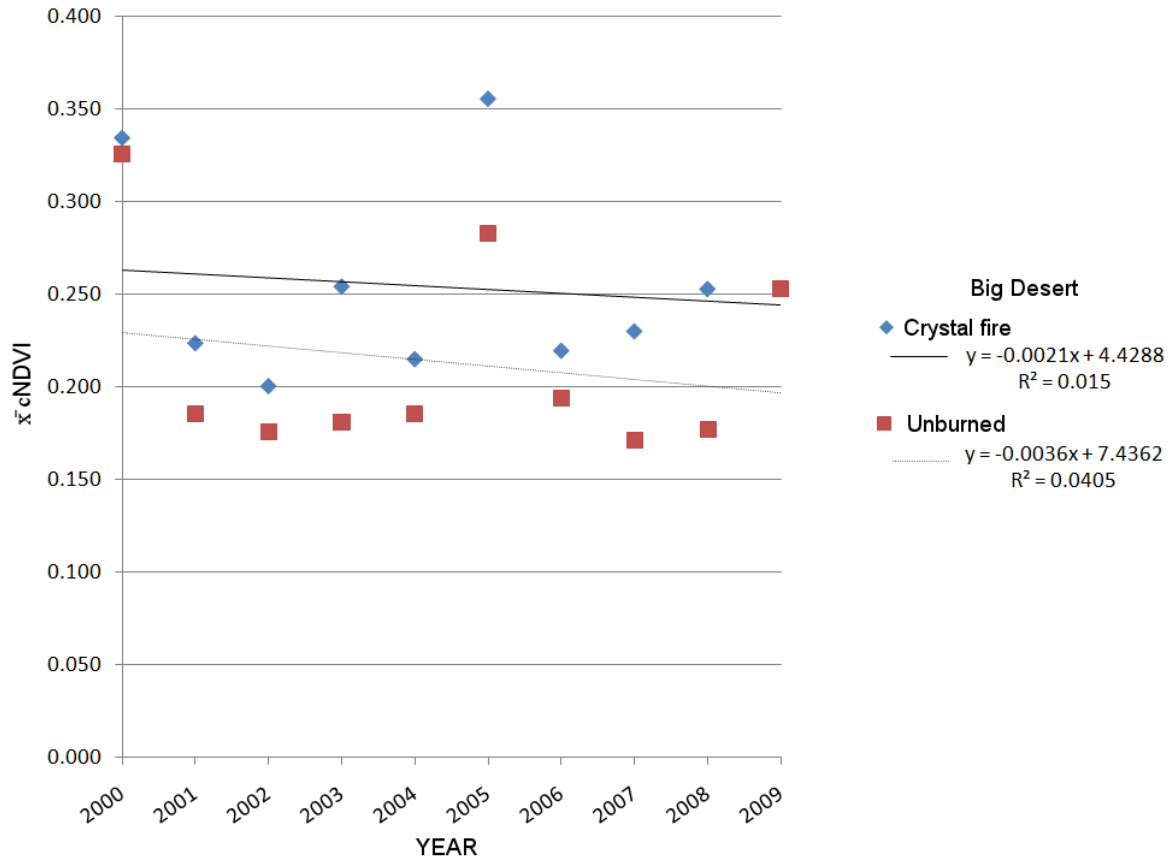


Figure 2. Scatter plot of mean cNDVI values at 600 sample sites in the Big Desert study area ( $n = 300$  in both the Crystal fire and unburned regions of the study area).

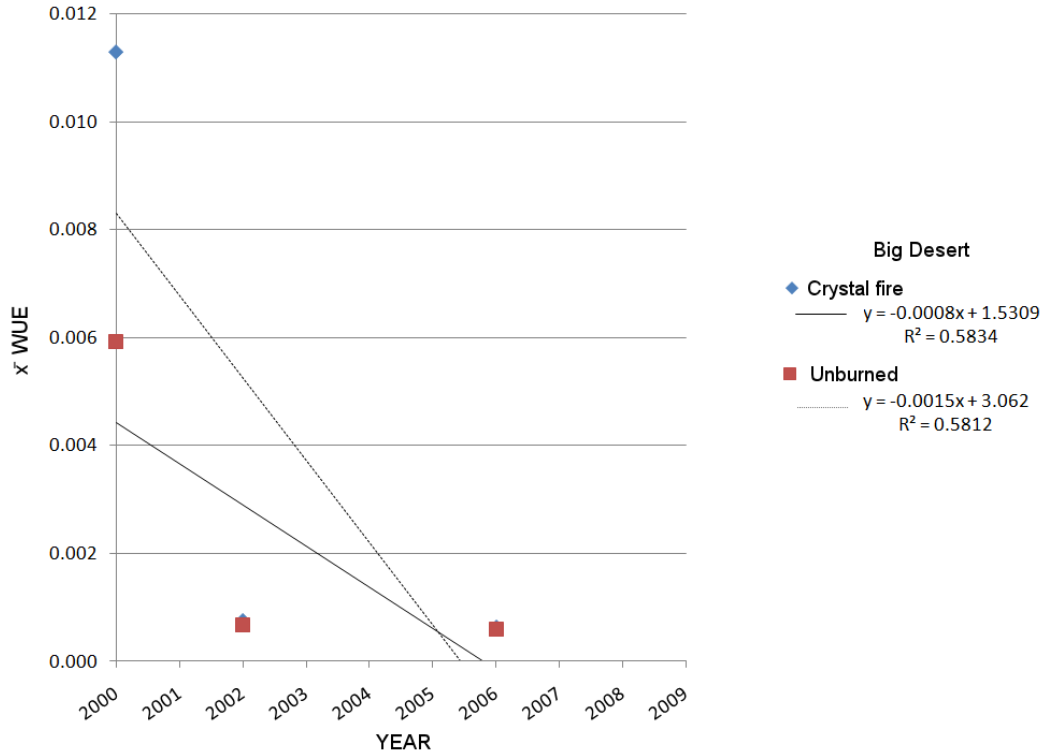
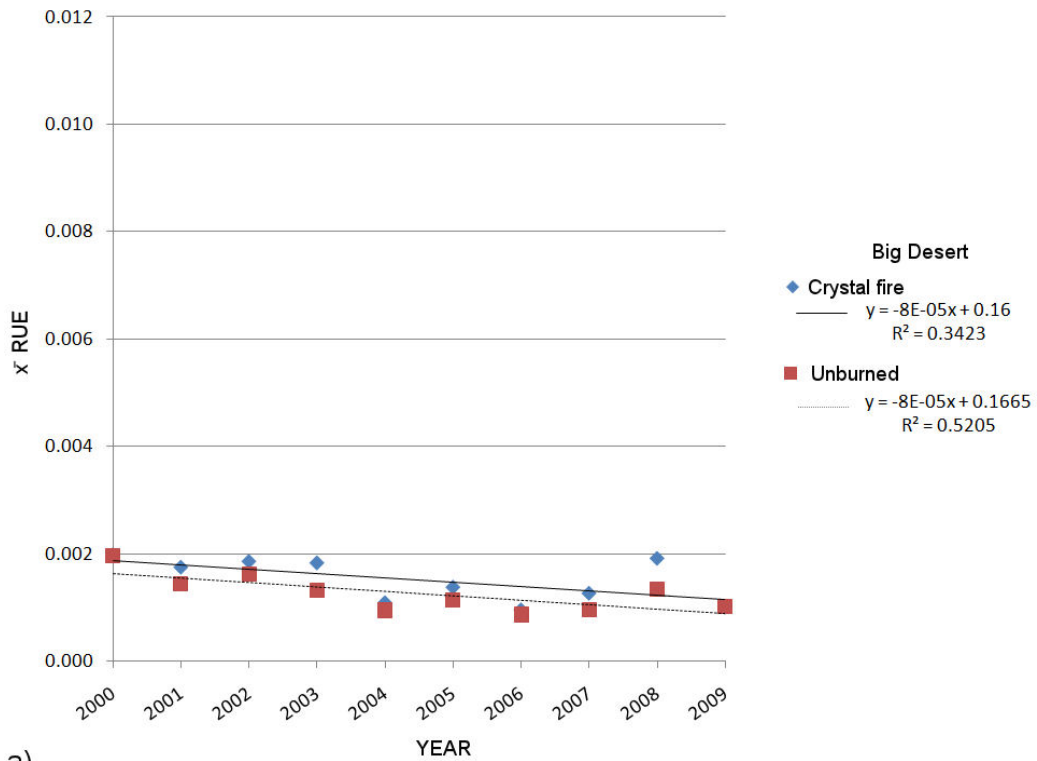
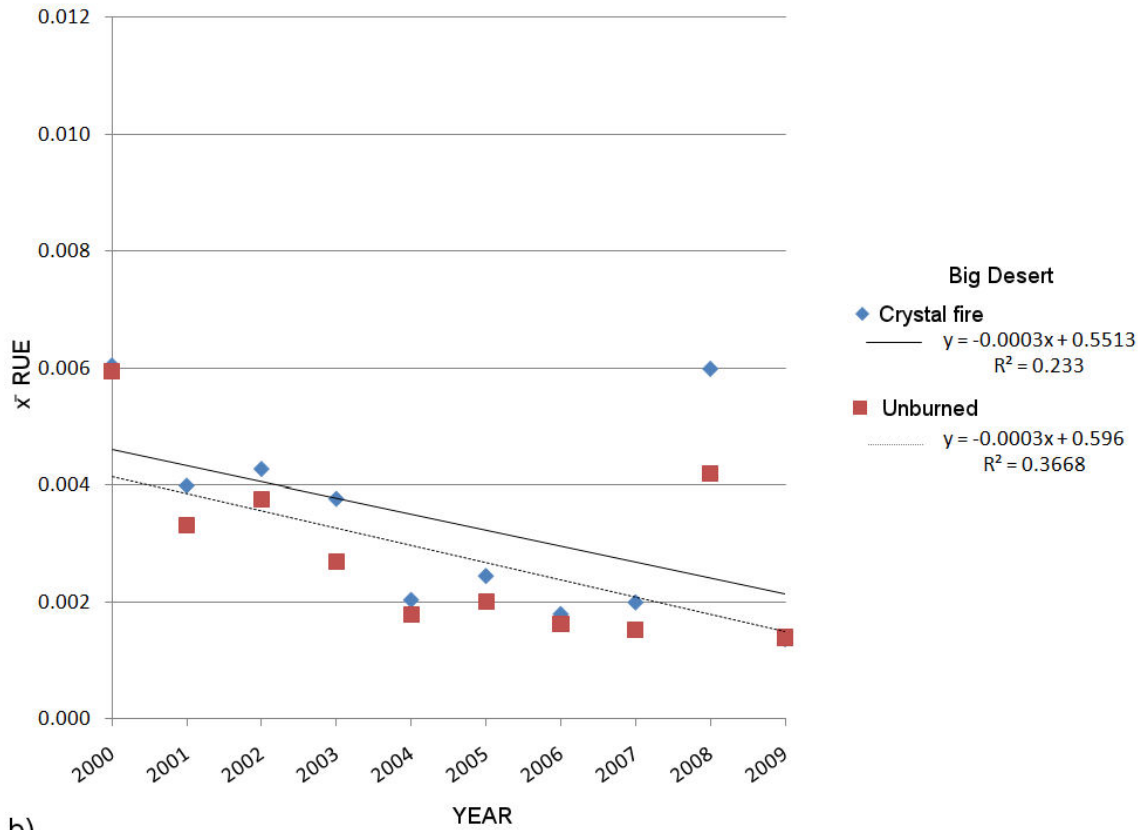


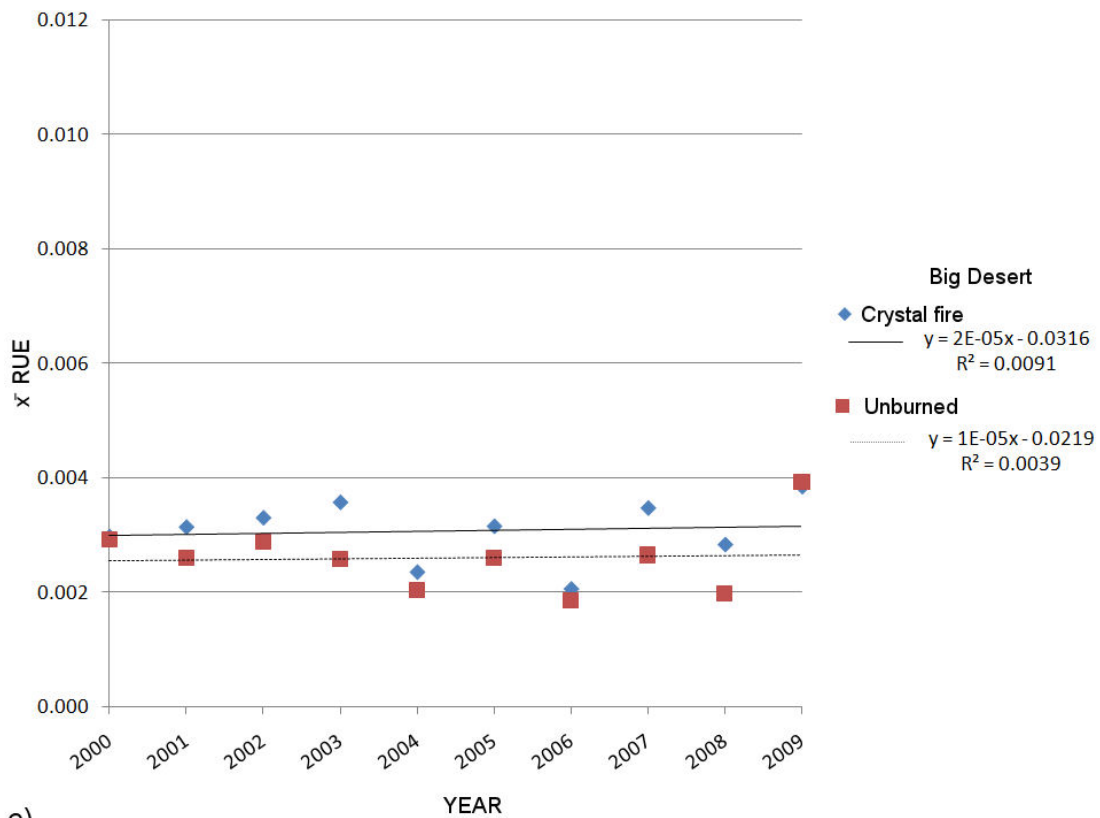
Figure 3. Stack bar chart of precipitation at the Aberdeen weather station (ABEI) for each hydrologic water year (2000-2009) illustrating the portion accumulated during the winter ( $PPT_w$ ), spring ( $PPT_s$ ), and other months of the year ( $PPT_{other}$ ). Mean precipitation is indicated by the dashed horizontal line ( $\bar{x} = 181.5$  mm).



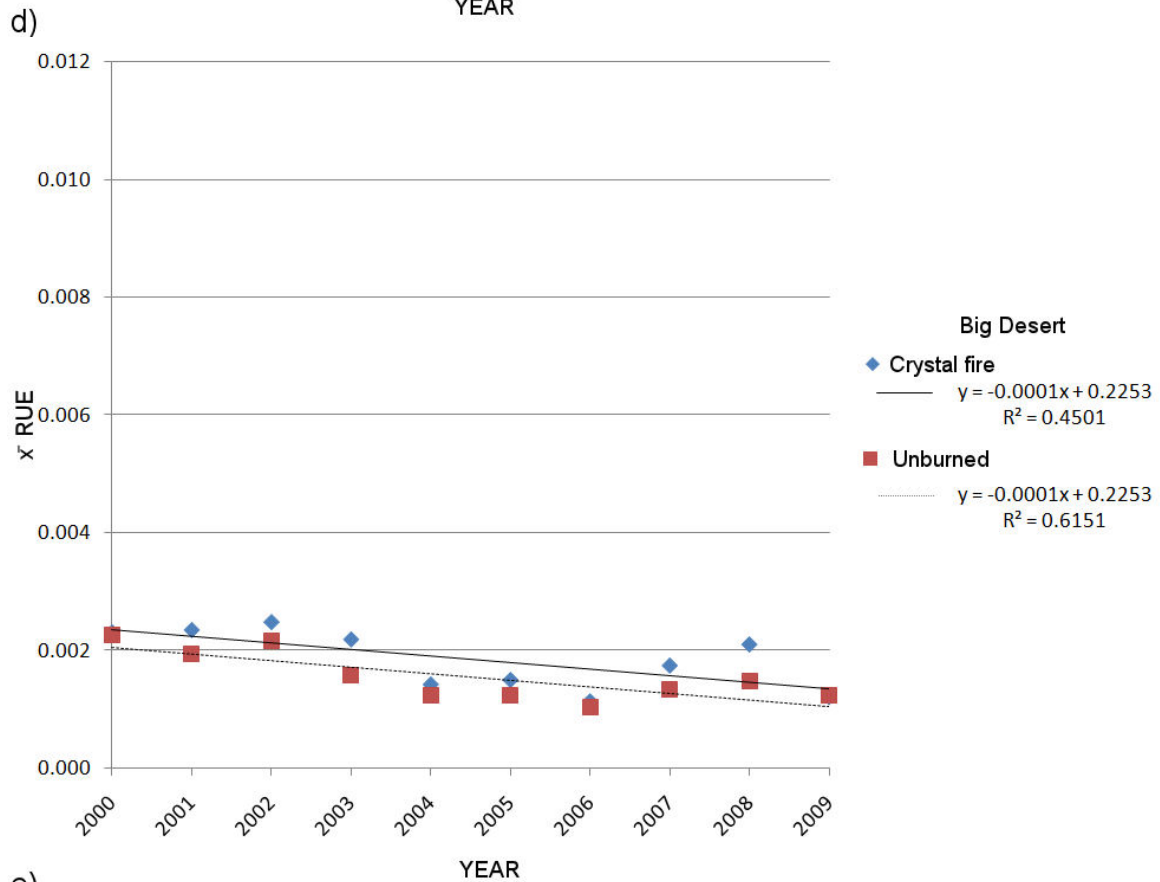
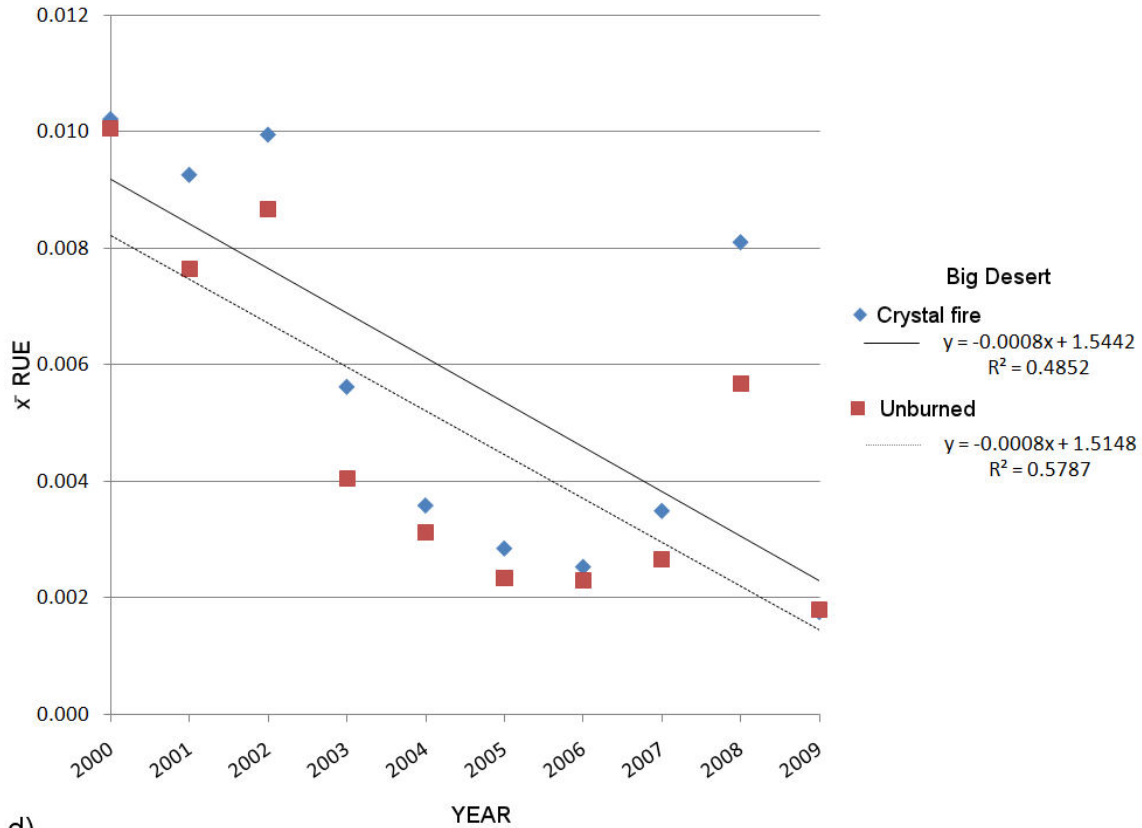
a)



b)



c)



e)

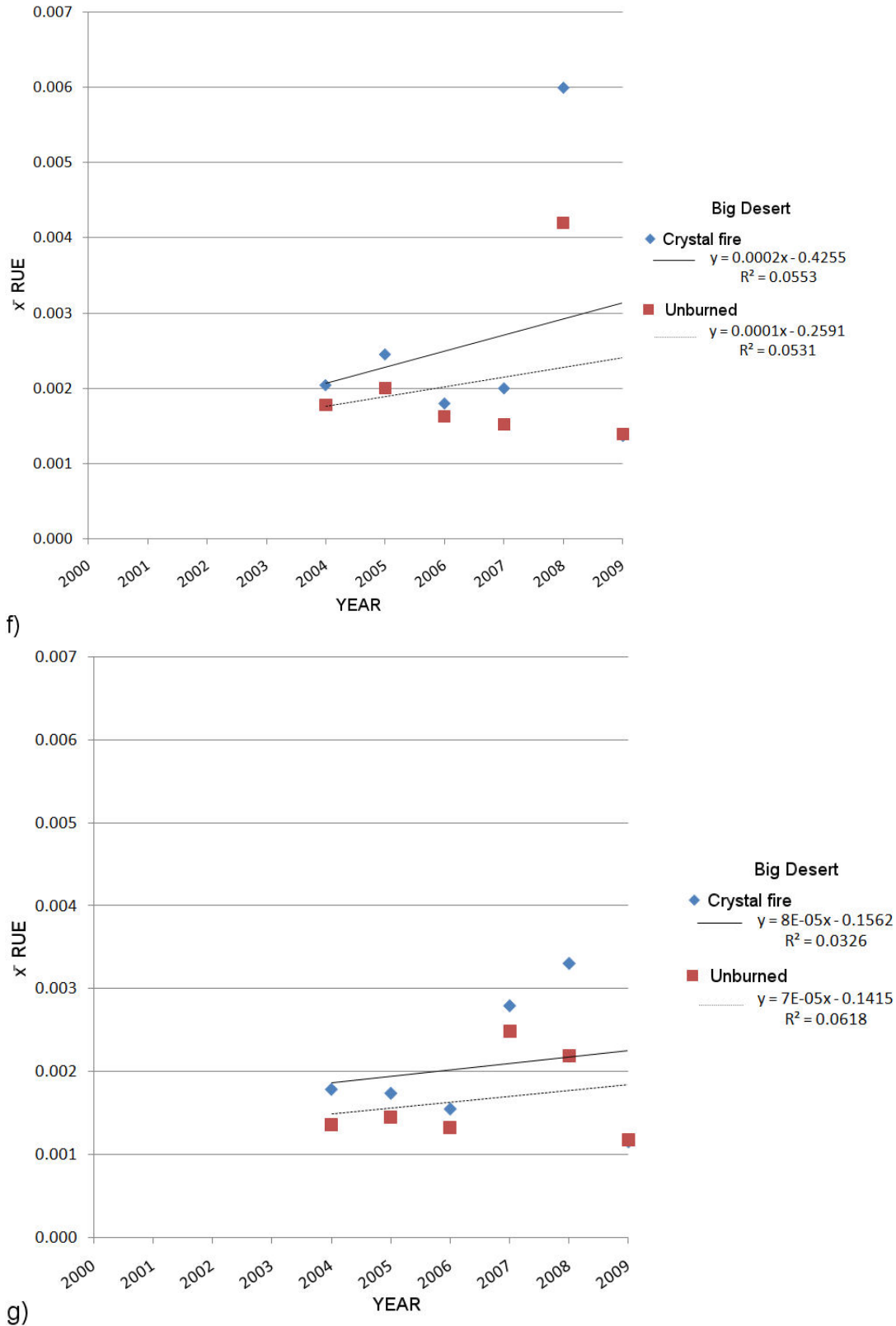


Figure 4. Scatter plot of mean RUE values at 600 sample sites in the Big Desert study area ( $n = 300$  in both the Crystal fire and unburned regions of the study area) for years 2000-2009 using a)  $PPT_{hwys}$ , b)  $PPT_g$ , c)  $PPT_w$ , d)  $PPT_s$ , e)  $PPT_{ws}$ , and years 2004-2009 using f)  $PPT_g$  from ABEI, and g)  $PPT_g$  from SOGS.

**Table 2. Coefficients of determination assessed in this study**

<b>Analysis Area</b>	<b>R2</b>	<b>Adjusted-R2</b>	<b>Slope</b>	<b>P</b>
cNDVI Crystal fire	0.015	-0.108	-0.0021	0.74
cNDVI unburned	0.041	-0.079	-0.0036	0.56
RUE Crystal fire (PPT <sub>hwy</sub> )	0.342	0.260	-0.0000	0.07
RUE unburned (PPT <sub>hwy</sub> )	0.521	0.461	-0.0000	0.02*
RUE Crystal fire (PPT <sub>g</sub> )	0.233	0.137	-0.0003	0.16
RUE unburned (PPT <sub>g</sub> )	0.367	0.288	-0.0003	0.06
RUE Crystal fire (PPT <sub>w</sub> )	0.009	-0.115	0.0000	0.79
RUE unburned (PPT <sub>w</sub> )	0.004	-0.121	0.0000	0.86
RUE Crystal fire (PPT <sub>s</sub> )	0.485	0.421	-0.0008	0.02*
RUE unburned (PPT <sub>s</sub> )	0.579	0.526	-0.0008	0.01*
RUE Crystal fire (PPT <sub>ws</sub> )	0.450	0.381	-0.0001	0.03*
RUE unburned (PPT <sub>ws</sub> )	0.615	0.567	-0.0001	0.01*
RUE Crystal fire (PPT <sub>g</sub> 2004-2009)	0.055	-0.181	0.0002	0.65
RUE unburned (PPT <sub>g</sub> 2004-2009)	0.053	-0.184	0.0001	0.66
RUE Crystal fire (SOGS PPT <sub>g</sub> 2004-2009)	0.033	-0.209	0.0000	0.73
RUE unburned (SOGS PPT <sub>g</sub> 2004-2009)	0.062	-0.173	0.0000	0.63
WUE Crystal fire	0.583	0.162	-0.0008	0.45
WUE unburned	0.581	0.167	-0.0015	0.45
LNS <sub>d</sub> Crystal fire	0.019	-0.104	-1.5416	0.71
LNS <sub>d</sub> unburned	0.170	0.067	8.6102	0.24

\* statistically significant

WUE metrics (2000, 2002, and 2006) similarly describe a marginally declining trend of primary productivity throughout the Big Desert study area (Figure 5). However two problems arose which question the validity of this observation if made independent of the previously reported results; 1) the established trend was based on only three observation points and lacks statistical power of analysis and 2) the ET<sub>g</sub> values used in the calculation may be erroneous as ET<sub>g</sub> exceeded precipitation ( $\bar{x} \Delta (PPT_g - ET_g) = -67.7$  mm). It is recalled that ET<sub>g</sub> is a predictor of actual ET, not potential ET, and for this reason it is assumed the METRIC model, which was originally designed for use under irrigated agricultural conditions, incorrectly estimated ET for the semiarid rangelands of Idaho.

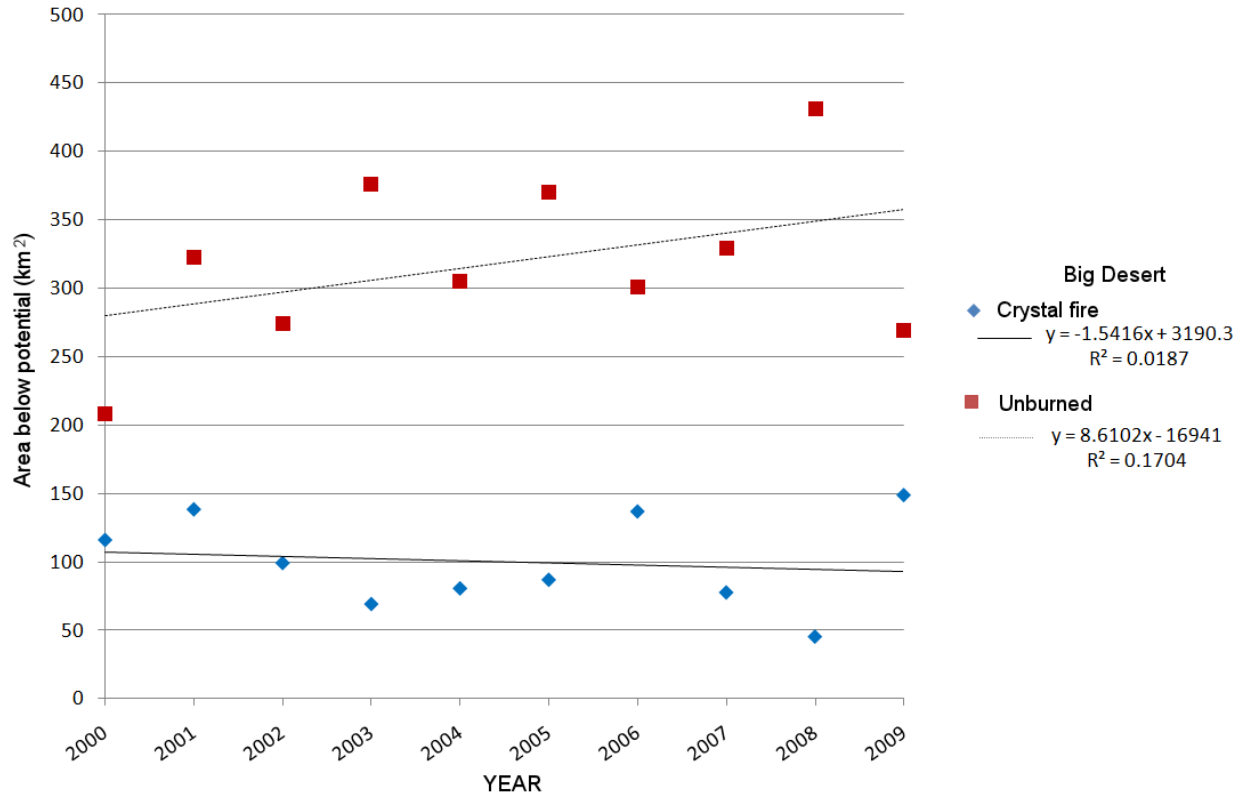


**Figure 5. Scatter plot of mean WUE values at 600 sample sites in the Big Desert study area for 2000, 2002, and 2006 ( $n = 300$  in both the Crystal fire and unburned regions of the study area).**

To explore this potential error, the sum of accumulated precipitation for each Hydrologic Water Year (HWY) was determined using ABEI precipitation data (e.g.,  $HWY_{2000} = \sum \text{precipitation October 1, 1999-September 30, 2000}$ ) and compared to  $ET_g$ . All precipitation accumulated during the HWY was considered to be available to plants during the growing season (i.e., April 1-September 30) with no soil-water carryover from the previous growing season.  $ET_g$  was sampled at the same random locations described previously for this study ( $n = 600$ ) and differences between HWY and  $ET_g$  determined by subtracting  $ET_g$  from HWY (e.g.,  $\Delta_{2000} = HWY_{2000} - ET_{g2000}$ ). While mean precipitation for the HWY was 169 mm, mean  $ET_g$  was 226 mm. The resulting mean difference ( $\bar{x}\Delta$ ) was -67.7 mm or approximately 40% of  $\bar{x}HWY$  precipitation input. This simple calculation is itself not without error as one may argue the observed difference suggests soil-water carryover from previous growing seasons. This is unlikely however as the soils in the Big Desert typically do not hold water for long periods of time due to the fractured geology underlying this region. The high degree of fissuring in the underlying basalt allows water that infiltrates the soil surface to become inaccessible to plants relatively quickly (Kaminsky 1991). Furthermore, a deep aquifer (50-300 m [IDWR 2010]) coupled with a shallow active root zone (approximately 60-75% of cumulative root distribution occurs in the first 100 mm of the soil surface [Snyman 2009]) suggest the  $ET_g$  values used in this study may not be reliable.

$LNS_d$  metrics also suggest primary productivity is declining in areas of the Big Desert outside the Crystal fire as the total area considered *below potential* has increased from 208 km<sup>2</sup> (9% of Big Desert) in 2000 to 269 km<sup>2</sup> (12% of the Big Desert) in 2009 (Figure 6). The relationship however, exhibits much variability

and is weakly correlated at best ( $R^2 = 0.17$ ). The trend line for  $LNS_d$  metrics within the Crystal fire area is similarly weak with a low coefficient of determination ( $R^2 = 0.02$ ). Upon closer examination, the total area *below potential* has increased from 116 km<sup>2</sup> (7%) in 2000 to 149 km<sup>2</sup> (8%) in 2009. However, the data points quantifying the area *below potential* for the two years immediately following the Crystal fire (2007 and 2008) were atypically low relative to all other years. This suggests entire LCC areas was effectively degraded by the Crystal fire and no reasonable potential could be identified (Prince 2009). Subsequently, very few areas were identified as degraded when scaled against equally degraded counterparts. Neither  $LNS_d$  trend line was significant ( $P = 0.71$  and  $0.24$  for the Crystal fire and unburned areas, respectively) (Table 2).

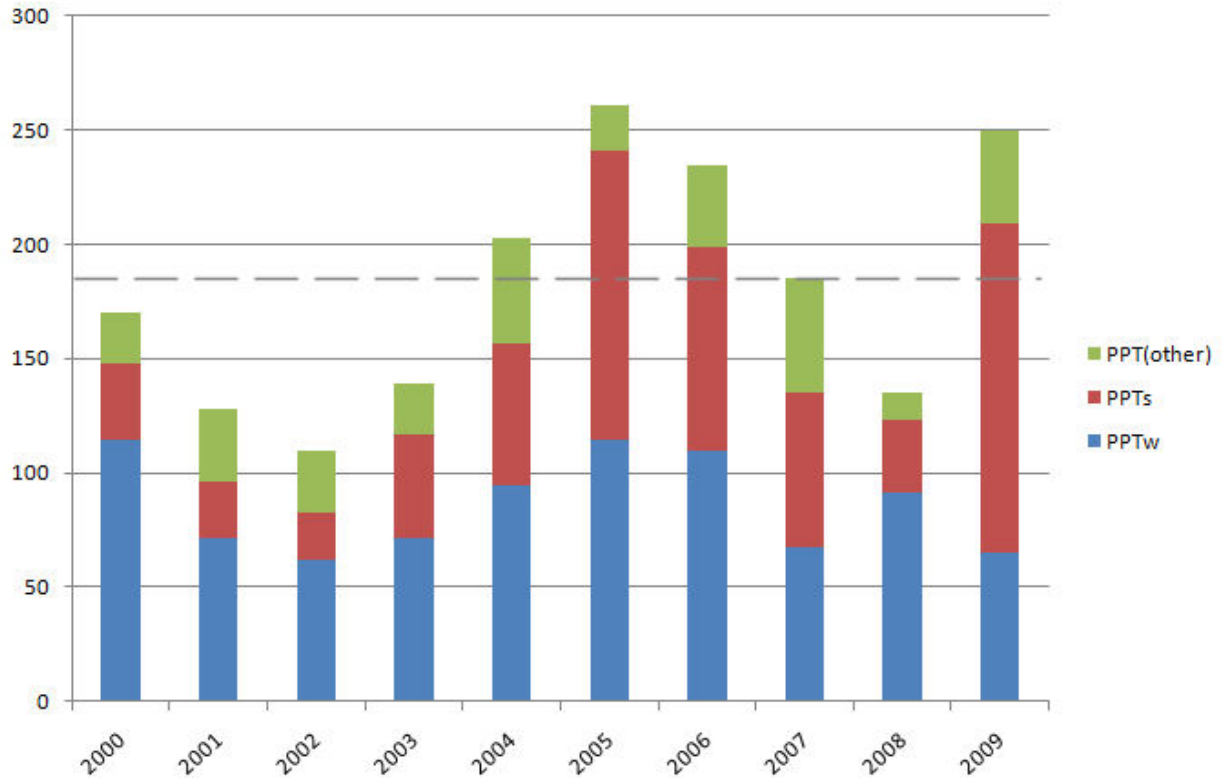


Figure 6. Scatter plot of total area (in km<sup>2</sup>) considered below potential ( $\leq LNS_{potential} - 2SD$ ) using the  $LNS_d$  assessment method.

## CONCLUSIONS

This study compared four assessments of primary productivity status and trend (cNDVI, RUE, WUE, and LNS) in the Big Desert of southeast Idaho, USA, with emphasis on the effects of the 2006 Crystal fire. Within the area burned by the Crystal fire, all indices, save for the  $LNS_d$  metric, suggest primary productivity has been slowly declining since 2000. In areas outside the Crystal fire, all indices and metrics indicated primary productivity in the Big Desert has been similarly declining since 2000 save for short-term RUE evaluations (2004-2009). The consistency among these observations suggest the Big Desert may be degrading or exhibiting a stable state of low primary productivity. The majority of ANOVA tests were not significant ( $P > 0.05$ ) and the only metrics yielding significant results were RUE metrics calculated using  $PPT_{hwy}$  (unburned areas only),  $PPT_s$ , and  $PPT_{ws}$ . These RUE metrics are interesting for several reasons; 1) they suggest the importance of the seasonality of precipitation and specifically, the importance of winter snow fall and early spring rains for the vegetation in the Big Desert, 2) they

illustrate that while a relatively strong relationship exists between precipitation and primary productivity, precipitation alone is not a perfect estimator of productivity. For example, in both 2002 and 2008 (figure 4d,e), productivity exceeded what was expected during years of below average precipitation (figure 3). Lastly, these metrics reveal that the Crystal fire and unburned regions of the Big Desert have very similar levels of primary productivity as evidenced by the nearly identical patterns of RUE values (Figure 4d,e) as well as similar slope and y-intercept values.

Each of these methodologies relied upon cNDVI layers derived from Landsat 5 TM as a surrogate for primary productivity (Prince 2009). While the long history of applications using both NDVI and Landsat enhance the qualitative reliability of this study, using cNDVI alone to assess rangeland condition yielded the weakest coefficients of determination ( $\bar{x} R^2 = 0.10$ ). RUE, WUE, and  $LNS_d$  each produced stronger coefficients of determination and merit additional investigation. RUE is perhaps the simplest to compute of the three derived indices/metrics and when coupled with SOGS precipitation data to better account for spatial variability over long time periods (approximately 10 years), RUE may be one of the best assessment indicators available. In contrast, the difficulty of producing accurate ET models required for WUE estimation nearly negates its use, especially within arid and semiarid ecosystems where it has been well documented that nearly all precipitation (~96%) is returned to the atmosphere through ET processes (Snyman, 1988; Wight and Hanson 1990; Snyman 1998). In this case, WUE could be effectively estimated using RUE.

The  $LNS_d$  metric, while time consuming to produce, offers several advantages for rangeland assessment. First, the nature of the methodology ensures that biophysically similar areas are compared to one another through the delineation of LCC regions. This helps eliminate type I and type II errors by ensuring highly productive areas or areas under varying land treatments are not directly compared to one another. Second, degraded areas are readily identified using the *below potential* threshold for each LCC which in turn supports further investigation in the field. In this study however, only 1% of those areas identified as *below potential* were consistently designated as degraded in all ten years. In contrast, nearly 25% were designated as *below potential* only once throughout the ten year period while >36% of the study area was never identified as degraded.

Arid and semiarid rangelands constitute a significant portion of the earth's terrestrial surface. These regions are increasingly being recognized for the ecosystem services they provide and for the role they play in the global carbon cycle (Follett et al. 2001). For these, and other reasons, the long-term sustainability of rangelands is essential and as a consequence, assessing and monitoring the health/condition of rangelands has become equally important. This paper describes a study investigating four assessment methodologies relying upon primary productivity estimates derived through satellite remote sensing. In nearly all cases, the methodologies concur that the Big Desert study area may be degrading. RUE appears to have provided the most reliable results and in all cases the need to use long-term datasets (10 years or more) was apparent. Additional research is merited to better understand and validate the techniques and results.

## **ACKNOWLEDGEMENTS**

This study was made possible by a grant from the National Aeronautics and Space Administration Goddard Space Flight Center (NNX08AO90G). Idaho State University would also like to acknowledge the Idaho Delegation for their assistance in obtaining this grant. The authors would like to thank Dr. Maosheng Zhao from The University of Montana's NTSG laboratory for his assistance with the SOGS datasets used in this study.

## **LITERATURE CITED**

Allen, R. G., M. Tasumi, and R. Trezza, 2007. Satellite-Based Energy Balance for Mapping Evapotranspiration with Internalized Calibration (METRIC)-Model. *Journal of Irrigation and Drainage Engineering*. 133(4):380-394

Arnalds O. and S. Archer, 2000. *Rangeland Desertification*. Kluwer Academic publishers, Dordrecht, Netherlands. 209 pp.

Aronson, J., C. Floret, E. LeFloch, C. Ovalle, and R. Pontanier, 1993. Restoration and Rehabilitation of Degraded Ecosystems in Arid and Semi-Arid Lands. I. A View from the South. *Restoration Ecology*. March 8-17

Asner, G. P., A. J. Elmore, L. P. Olander, R. E. Martin, and A. T. Harris, 2004. Grazing Systems, Ecosystem Responses, and Global Change. *Annual Review of Environment and Resources* 29:261-299

Bastiaanssen, W. G. M., 1995. Regionalization of Surface Flux Densities and Moisture Indicators in Composite Terrain: A Remote Sensing Approach under Clear Skies in Mediterranean Climates. Ph.D. Dissertation, CIP Data Koninklijke Bibliotheek, Den Haag, The Netherlands

Booth, D.T., Tueller, P.T., 2003. Rangeland Monitoring Using Remote Sensing. *Arid Land Research and Management* 17:455-467

Branson, F.A., G.F. Gifford, K.G. Renard, and R.F. Hadley, 1981. Evaporation and Transpiration. 179–200 in E.H. Reid (Ed.) *Rangeland Hydrology*. Range Sci. Ser. 1. Soc. for Range Management, Denver, CO 2(1)

Briske D. D., S. D. Fuhlendorf, and F. E. Smeins, 2003. Vegetation Dynamics on Rangelands: A Critique of the Current Paradigms. *Journal of Applied Ecology*, 40:601–614

Canfield, R. H., 1941. Application of Line Interception in Sampling Range Vegetation. *Journal of Forestry* 39:388-394

Chambers, J. C. and R. W. Brown, 1983. Methods for Vegetation Sampling and Analysis on Re-vegetated Mine Lands. USDA FS Gen. Tech. Rep. INT-151 57 pp.

Chavez, P. S., 1996. Image-based Atmospheric Corrections: Revisited and Improved, *Photogrammetric Engineering and Remote Sensing*, 62 (9): 1025-1036

- Daubenmire, R. F., 1959. A Canopy-coverage Method of Vegetation Analysis. *Northwest Science* 33:43-64
- Daubenmire, R. F. and J. B. Daubenmire. 1968. Forest Vegetation of Eastern Washington and Northern Idaho. Wash. Agric. Exp. Stn. Tech. Bull. 60pp.
- Floret, C., E. Le Floch, and R. Pontainier, 1983. Phytomasse et Production en Tunisie presaharienne. *Acta Oecologia* 4:133-152
- Follett, R. F., J. M. Kimble, and R. Lal, 2001. The Potential of US Grazing Lands to Sequester Soil Carbon. Pages 401-430 in R.F. Follett, J. M Kimble, and R. Lal (Eds.) The Potential of US Grazing Lands to Sequester Carbon and Mitigate the Greenhouse Effect, Lewis Publishers, Boca Raton, Florida, 442 pp.
- GIS TReC, 2010. Boundaries Geodatabase with the Land Use and Public Lands Feature Class. URL = [http://giscenter-sl.isu.edu/AOC/AOC\\_Municipal/](http://giscenter-sl.isu.edu/AOC/AOC_Municipal/) visited 11-May-2010
- Griffin, D.W., C.A. Kellogg, and E.A. Shinn, 2001. Dust in the Wind: Long Range Transport of Dust in the Atmosphere and Its Implications for Global Public and Ecosystem Health. *Global Change and Human Health* 2(1): 20-33
- Gysel, L. W. and L. J. Lyon, 1980. Habitat Analysis and Evaluation. Pages 305-317 in S. D. Schemnitz (Ed.) Wildlife Management Techniques Manual, 4<sup>th</sup> ed. Revised. The Wildlife Society, Washington, DC
- Hein, L. and N. de Ridder, 2006. Desertification in the Sahel: A Reinterpretation. *Global Change Biology* 12:751-758
- Hill, J. B., 2006. Human Ecology in the Wadi Al-Hasa: Land Use and Abandonment through the Holocene. The University of Arizona, Press, Tucson, Ariz. 194 pp.
- Homer, C.G., 1998. Idaho/Western Wyoming Landcover Cassification. Remote Sensing/GIS Laboratories, Utah State University, Logan, UT
- Hountondji, Y. C., N. Sokpon, J. Nicolas, and P. Ozer, 2009. Ongoing Desertification Processes in the Sahelian Belt of West Africa: An Evidence from the Rain-Use Efficiency. Pages 173-186 in Roder and Hill (Eds.) Recent Advances in Remote Sensing and Geoinformation Processing for Land Degradation Assessment. CRC Press, Taylor and Francis, London UK. 400 pp.
- Huntsinger, L. and P. Hopkinson, 1996. Viewpoint: Sustaining Rangeland Landscapes: A Social and Ecological Process. *Journal of Range Management* 49:167-173
- InsideIdaho, 1999. Land Cover of Idaho: Idaho Cooperative Fish and Wildlife Research Unit, Moscow, ID. URL = [http://data.insideidaho.org/data/icfwru/archive/landcov\\_id\\_icfwru.zip](http://data.insideidaho.org/data/icfwru/archive/landcov_id_icfwru.zip) visited 12-May-2010

- IDWR 2010. Idaho Department of Water Resources: Hydro Online. Ground water levels. URL = <http://www.idwr.idaho.gov/hydro.online/gwl/default.html> visited 4-June-2010
- Johannesen, C.M. 2000. Basalt Surface Morphology on the Eastern Snake River Plain, Idaho: Implications for the Emplacement of High Porosity Materials in the ESRP Aquifer; Idaho State University Master's Thesis, Pocatello, ID 209 pp.
- Kaminsky, J.F. 1991. In Situ Characterization of Unsaturated Hydraulic Properties of Surficial Sediments Adjacent to the Radioactive Waste Management Complex, INEL, Idaho; Idaho State University Master's Thesis, Pocatello, ID 95 pp.
- Le Houerou, H. N. 1984. Rain-use Efficiency: A Unifying Concept in Arid Land Ecology. *Journal of Arid Environments*, 7:213–247
- Le Houerou, H. N. 1989. *The Grazing Land Ecosystems of the African Sahel*. Springer, Berlin
- Niamir-Fuller, M. and M. D. Turner, 1999. A Review of Recent Literature on Pastoralism and Transhumance in Africa. Pages 18-46 in M. Niamir-Fuller (Eds.), Managing Mobility in African Rangelands: The Legitimization of Transhumance. FAO: IT Publications. 314 pp.
- NRCS, 2007. SSURGO Soils Data. USDA Natural Resources Conservation Service. URL = <http://soildatamart.nrcs.usda.gov/> visited 12-May-2010
- NTSG, 2010, NTSG Images: News Archive. Numerical Terradynamic Simulation Group. URL = <http://images.ntsug.umt.edu/index.php> visited 11-May-2010
- Perry, C. R. and L. F. Lautenschlager. 1984. Functional Equivalence of Spectral Vegetation Indices. *Remote Sensing of Environ.* 14:169-182
- Pettorelli, N., Vik, J.O., Mysterud, A., Gaillard, J.M., Tucker, C.J., Stenset, N.C., 2005. Using the Satellite-derived NDVI to Assess Ecological Responses to Environmental Change. *Trends in Ecology and Evolution*, 20:503-510
- Prince, S. D. 1991. A Model of Regional Primary Production for use with Coarse Resolution Satellite Data. *International Journal of Remote Sensing*, 12, 1313–1330
- Prince, S. D. 2004. Mapping Desertification in Southern Africa. Pages 163-184 in G. Gutman, A. Janetos, C. O. Justice, E. F. Moran, J. F. Mustard, R. R. Rindfuss, D. Skole, & B. L. Turner II (Eds.), Land change science: Observing, Monitoring, and Understanding Trajectories of Change on the Earth's Surface. Dordrecht, NL: Kluwer
- Prince, S. D., I. Becker-Reshef, and K. Rishmawi. 2009. Detection and Mapping of Long-term Land Degradation using Local Net Production Scaling: Application to Zimbabwe. *Remote Sensing of Environment* 113:1046-1057

Redmond, R.L., Z. Ma, T.P. Tady, J.. Winne, J. Schumacher, J. Troutwine, and S.W. Holloway. 1996. Mapping Existing Vegetation and Land Cover Across Western Montana and Northern Idaho. Wildlife Spatial Analysis Laboratory, Missoula, MT

Reid, R. S., K. A. Galvin, and R. S. Kruska. 2008. Global Significance of Extensive Grazing Lands and Pastoral Societies: An Introduction. Pages 1-24 in K. A. Galvin, R. S. Reid, R. H. Behnke, Jr, and N. Thompson Hobbs (Eds.) Fragmentation in Semi-Arid and Arid Landscapes: Consequences for Human and Natural Systems. Springer, Dordrecht, The Netherlands. 411 pp.

Rouse, J.W., Jr., R.H. Haas, J.A. Schell, and D.W. Deering, 1973. Monitoring the Vernal Advancement and Retrogradation (green wave effect) of Natural Vegetation. Prog. Rep. RSC 1978-1, Remote Sensing Center, Texas A&M Univ., College Station, 93pp. (NTIS No. E73-106393)

Running, S. W., R. Nemani , J. M. Glassy, and P. E. Thornton, 1999. MODIS Daily Photosynthesis (Psn) and Annual Net Primary Production (NPP) Product (MOD17), Algorithm Theoretical Basis Document, Version 3.0, 29 April 1999, 1-59

Savory, A. 1999. Holistic Management: A New Framework for Decision Making. Island Press, 2:616pp.

Seiny-Boukar, L., C. Floret, and R. Pontanier, 1992. Degradation of Savanna Soils and the Reduction of Water User Efficiency: The Case of Northern Cameroon Vertisols. Canadian Journal of Soil Science. 72:481-488

Schlesinger, W. H., J. F. Reynolds, G. L. Cunningham, L. F. Huenneke, W. M. Jarrell, R. A. Virginia, and W. G. Whitford, 1990. Biological Feedbacks in Global Desertification. Science 247:1043-1048

Sellers, P.J., 1992. Canopy Reflectance, Photosynthesis and Transpiration. Part III: A Re-analysis using Enzyme Kinetics-electron Transport Models of Leaf Physiology. Remote Sens. Environ., 42: 187-216

Snyman, H. A., 1998. Dynamics and Sustainable Utilization of Rangeland Ecosystems in Arid and Semi-arid Climates of Southern Africa. Journal of Arid Environments. 39:645-666

Snyman, H. A., 2009. Root Studies on Grass Species in a Semi-arid South Africa along a Degradation Gradient. Agriculture, Ecosystems, and Environment. 130:100-108

Stoms D. M. and W. W. Hargrove, 2000. Potential NDVI as a Baseline for Monitoring Ecosystem Functioning. Int. J. Remote Sensing 21(2):401-407

Stoms, D. M. and W. W. Hargrove, 2000. Potential NDVI as a Baseline for Monitoring Ecosystem Functioning. Int. Journal of Remote Sensing. 21(2):401-407

Studley, H. and K. T. Weber, 2010. 2009 Range Vegetation Assessment in the Big Desert, Upper Snake River Plain, Idaho. URL = [http://giscenter.isu.edu/research/Techpg/nasa\\_postfire/To\\_PDF/2009\\_Big\\_Desert\\_FieldReport.pdf](http://giscenter.isu.edu/research/Techpg/nasa_postfire/To_PDF/2009_Big_Desert_FieldReport.pdf) visited 31-March-2010

- Taylor, J.E., 1986. Cover Data in Monitoring Rangeland Vegetation. Use of Cover, Soils and Weather Data in Rangeland Monitoring Symposium Proceedings. Society for Range Management, Denver, CO. pp. 15-24
- Tedrow, L. and K. T. Weber, 2010. NDVI Changes over a Calendar Year in the Rangelands of Southeast Idaho. URL = [http://giscenter.isu.edu/research/Techpg/nasa\\_postfire/to\\_PDF/msAnnual\\_NDVICurve.pdf](http://giscenter.isu.edu/research/Techpg/nasa_postfire/to_PDF/msAnnual_NDVICurve.pdf) visited 2-April-2010
- Thomas, D.A. and V. R. Squires, 1991. Available Soil Moisture as a Basis for Land Capability Assessment in Semi-arid Regions. *Plant Ecology* 91:183-189
- Tian, Y. and Y. Zhang, Y. Knyazikhin, R. B. Myneni, J. M. Glassy, G. Dedieu, and S. W. Running, 2000, Prototyping of MODIS LAI and FPAR Algorithm with LASUR and LANDSAT Data, *IEEE Transactions on Geoscience and Remote Sensing*, 38(5):2387-2401
- Tucker, C.J., 1979. Red and Photographic Infrared Linear Combinations for Monitoring Vegetation. *Remote Sensing of Environment*, 8:127-150
- Vetter, S., 2005. Rangelands at Equilibrium and Non-equilibrium: Recent Developments in the Debate. *Journal of Arid Environments*, 62:321-341
- Veron, S. R., J. M. Paruelo, and M. Oesterheld, 2006. Assessing Desertification. *Journal of Arid Environments* 66:751-763
- Walko, R. L. and C. J. Tremback, 2005. Modifications for the Transition from LEAF-2 to LEAF-3. ATMET Technical Note. 1. 13pp.
- Washington-Allen, R. A., N. E. West, R. D. Ramsey, and R. A. Efroymson, 2006. A Protocol for Retrospective Remote Sensing-based Ecological Monitoring of Rangelands. *Rangeland Ecol. and Manage.* 59:19-29
- Weber, K. T., J. B. McMahan, and G. P. Russell, 2004. Effect of Livestock Grazing and Fire History on Fuel Load in Sagebrush-Steppe Rangelands. *Intermountain Journal of Sciences*. 10:1-9
- Weber, K. T., F. Chen, B. Gokhale, C. G. Bueno, and C. L. Alados, 2009. Application of Composite-NDVI in Semiarid Rangelands. Pages 71-84 in K.T. Weber and K. Davis (Eds.), Final Report: Comparing Effects of Management Practices on Rangeland Health with Geospatial Technologies (NNX06AE47G). 168 pp.
- Weber, K. T. and B. S. Gokhale, 2010. Effect of Grazing Treatment on Soil Moisture in Semiarid Rangelands. Pages 165-180 in K. T. Weber and K. Davis (Eds.) Final Report: Forecasting Rangeland Condition with GIS in Southeastern Idaho. 193pp.

Westoby M., B. H. Walker, I. Noy-Meir, 1989. Opportunistic Management for Rangelands not at Equilibrium. *Journal of Range Management*, 42:266–274

Wight, J. R. and C. L. Hanson, 1990. Crop Coefficients for Rangeland. *Journal of Range Management*. 43:482-485

Yuan, D., C. D. Elvidge, and R. S. Lunetta, 1998. Survey of Multispectral Methods for Land Cover Change Analysis. Pages 21-39 in R. S. Lunetta and C. D. Elvidge (Eds.) Remote Sensing Change Classification. Ann Arbor Press, Chelsea Mich. 318 pp.

**Recommended citation style:**

Weber, K.T. and F. Chen 2011. Evaluating Land Degradation Indicators in Semiarid Ecosystems Relative to Wildfire. Pages 161-184 in K. T. Weber and K. Davis (Eds.), Final Report: Assessing Post-Fire Recovery of Sagebrush-Steppe Rangelands in Southeastern Idaho. 252 pp.

## **Comparison of Image Resampling Techniques for Satellite Imagery**

Heather Studley, Idaho State University, GIS Training and Research Center, 921 S. 8th Ave., Stop 8104, Pocatello, ID 83209-8104 USA

Keith T. Weber, GIS Director, Idaho State University, GIS Training and Research Center, 921 S. 8th Ave., Stop 8104, Pocatello, ID 83209-8104 USA. e-mail [webekeit@isu.edu](mailto:webekeit@isu.edu)

### **ABSTRACT**

Image resampling is a process used to interpolate the new cell values of a raster image during a resizing operation. There are many resampling methods available, through a variety of platforms, including GIS and image-editing software. Each resampling method has strengths and weaknesses which should be considered carefully. The purpose of this paper was not to find a “best” method, but rather to explore how different methods implemented by different software vendors (in this case, ArcGIS and Paint Shop Pro) compared. Aggregated Average and Nearest Neighbor are two commonly used resampling methods, but numerous other methods are available (e.g., bicubic, bilinear, cubic convolution, pixel resize, and weighted average). To compare these methods, Landsat imagery was iteratively resampled from 28.5 to 100 meters per pixel (mpp) using each of the available methodologies. Correlation coefficients were determined comparing each resampled image against imagery resampled using 1) aggregated average and 2) nearest neighbor. Resulting correlation coefficients ( $R^2$ ) ranged from 0.98 to 0.34. Correlation between aggregated average and nearest neighbor was relatively low ( $R^2 = 0.41$ ) as was the correlation between two bilinear interpolation results ( $R^2 = 0.393$ ) as implemented by different software programs. It was concluded that resampling methods should be considered carefully and tested before selecting a software program or technique, as different programs can implement the same method very differently.

*KEYWORDS: aggregated average, nearest neighbor, bicubic, bilinear, interpolation, cubic convolution, pixel resize, weighted average*

## **INTRODUCTION**

Image resampling is a process by which new pixel values are interpolated from existing pixel values whenever the raster's structure (number of rows and columns) is modified such as during projection, datum transformation, or cell resizing operations (Wade and Sommer, 2006). Various resampling methods can be employed to resize an image (Corel Corp., 2007) and when an image is enlarged or reduced, changes are necessarily made to the value assigned to each pixel. To reduce an image, entire rows and columns are removed, while the enlargement of an image requires the opposite change by adding rows and columns of pixels. In both cases, the spatial extent (minimum and maximum X and Y coordinates) of the imagery is unchanged and only the raster's structure is modified. The effect of image resampling is a concern for image quality in general, and when dealing with remotely sensed data for scientific interpretation, data integrity (i.e., how closely the interpolated value matches the original value of each pixel) becomes a concern as well. This is because raster images store data within the feature (pixel) itself as for example, each pixel from a satellite image represents a measured surface reflectance value derived from a satellite or airborne sensor.

The enlargement of satellite imagery (i.e., increasing the number of rows and columns) is typically not of concern relative to data integrity issues as the rows and columns of pixels added are simply duplicates of existing pixels. This is particularly true when the enlargement factor is a whole number, but not necessarily true when imagery is enlarged fractionally (e.g., spatial resolution of an image is changed from 15 meters per pixel [mpp] to 10 mpp) as this specific procedure does require interpolation. In contrast, the reduction of an image means fewer rows and columns (and hence fewer pixels) will be used to represent the same geographic features across the same spatial extent. A fairly common resampling task involves the conversion of satellite imagery at a relatively fine spatial resolution (e.g., 10 mpp) to a more coarse resolution (e.g., 30 mpp) to readily accommodate comparison with imagery from another satellite sensor. In this scenario, blocks of pixels (kernels) are involved in an iterative resampling process. The value of each pixel within each kernel is evaluated and a new value calculated for the output pixel in the new "resampled" image layer. To effect this change various forms of interpolation have been developed to minimize data integrity losses as a result of resizing. Hence, the study described in this paper was designed to enable a better understanding of the consequences of resampling satellite imagery during a reduction-type resize operation.

Commonly used resampling methods are:

### ***Aggregated Average***

The arithmetic mean of all pixels within each kernel is used as the value for the new image pixel. Using aggregated average (AA) all pixels are equally weighted but like all metrics using mean, the output pixel will be strongly influenced by outlier or extreme values that belong to the kernel (Przydatek et al., 2003; Wagner 2004; Li et al., 2005).

### ***Bicubic***

Bicubic interpolation is a variation of cubic interpolation (see below) where the process is performed in both X and Y directions (Losinger, 2006). This method is more accurate than nearest neighbor or bilinear interpolation, but slower to run (Goldsmith, 2009). Paint Shop Pro (PSP) graphics software specifically defines its bicubic method as using 16 neighboring pixels in a 4x4 pixel neighborhood (Corel Corp., 2007).

### ***Bilinear Interpolation***

Bilinear interpolation uses the arithmetic mean of the four pixels nearest the focal cell to calculate a new pixel value. This resampling method tends to produce a “smoother” image (Goldsmith, 2009), retains better positional accuracy than nearest neighbor resampling (Verbyla, 2002), but may introduce new values never found in the original image with some blurred edges introduced as well (Goldsmith, 2009). As applied within PSP, the new value is based on the average of four neighboring cells in a 2x2 kernel (Corel Corp., 2007) (Figure 1).

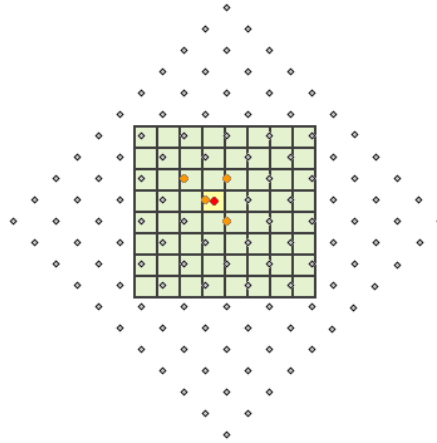


**Figure 1. Bilinear Interpolation:** The centers of the cells of the input raster are marked with gray dots. The green grid represents the output raster. The red dot marks the center of the target cell (in yellow). The orange dots are the four nearest cells from the input raster that will be used to calculate the value for the desired output cell.

*Note: Image courtesy of ESRI.*

### ***Cubic Convolution***

Cubic convolution (CC) resampling uses a weighted average of the 16 pixels nearest to the focal cell (Figure 2) and produces the smoothest (or most continuous) image compared to bilinear interpolation or nearest neighbor resampling (Verbyla, 2002; Huber, 2009). However, CC resampling takes approximately 10 to 12 times longer to process the computation than nearest neighbor (eXtension, 2008; Huber, 2009).

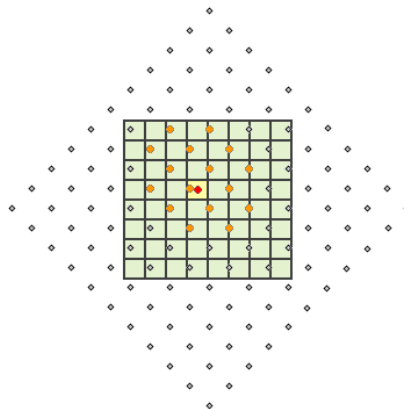


**Figure 2. Cubic Convolution:** Again, the gray dots represent the centers of the input raster cells and the green grid represents the output raster. The target cell is yellow with the red dot showing the center. For cubic convolution the 16 nearest cells (orange dots) are used for input to calculate the new output value.

*Note: Image courtesy of ESRI.*

### ***Nearest Neighbor***

Nearest Neighbor (NN) resampling is very commonly used and it functions by matching a pixel from the original image to its corresponding position in the resized image. If no corresponding pixel is available, the pixel nearest is used instead (Figure 3). NN works well with horizontal or vertical lines (Goldsmith, 2009) but introduces noticeable error along other linear features where pixel realignment is obvious (eXtension, 2008) and for that reason is generally considered the least accurate method. NN remains widely used because of the speed of implementation and simplicity (Dodgson, 1992). As computers become more and more powerful it is easy to dismiss a less computationally intensive process for one with more accurate results, but with remotely sensed images computation time can still a concern, as imagery can be very large (>1 GB). A notable advantage of NN is that no interpolated values are created; making it ideal for the retention of discrete or categorical data sets (ESRI, 2008; ESRI, 2009; Verbyla, 2002).

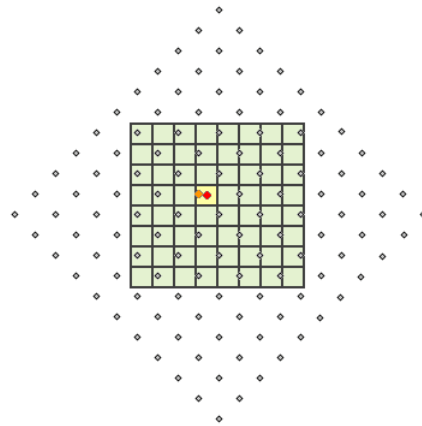


**Figure 3. Nearest Neighbor:** Using the same setup as in Figures 1 and 2, there is only one value (orange dot) used to create the new output value, which is derived from the cell nearest the target.

*Note: Image courtesy of ESRI.*

As well as the common methods, many image-editing programs such as PSP have their own, specialized, resampling methods. As well as modified versions of bicubic and bilinear interpolation, PSP also offers the following resampling methods:

### ***Pixel Resize***

Pixel Resize duplicates (when increasing the size) or removes (if decreasing the size) the value of the pixel nearest the focal cell to achieve the desired height and width of the new image (Corel Corp., 2007). It is best for simple images (Shea, n/d) and is the only resample method that can be used on images using 8 bit (or less) color schemes in Paint Shop Pro (Corel Corp., 2009).

### ***Weighted Average***

This method uses a weighted-average value of neighboring pixels to determine the value of newly created pixels in the new image (Corel Corp., 2007). It is best for reducing images (Chastain et al., 2005; Shea, 2009).

### ***Affects of resampling***

Remotely sensed data, be they from satellite or airborne sensors, are incredibly variable. Spatial resolutions can be very coarse (>100 mpp) to very fine (< 0.1 mpp) and choosing which scale to use for a study can be a difficult process, with limitations including availability of fine resolution imagery, cost constraints, and data processing considerations. With a variety of platforms to choose from, it is fairly common that imagery from one platform may need to be compared to imagery from a different platform (e.g., SPOT 4 [20 mpp] and SPOT 5 [10 mpp]).

In order to compare data from one spatial resolution to another, imagery from the finer resolution are typically resampled to match the spatial resolution of the coarser imagery. This type of resampling can have substantial effects on the integrity of the data being compared (João, 2001). Gotway and Young (2002) provided a brief overview concerning incompatibility of spatial data and looked at some of the methods used to overcome that concern. Bian and Butler (1999) looked at the three most common types of resampling (1-averaging; uses the averaged value of a kernel for the output pixel, 2-central-pixel; uses the most centrally located pixel of a kernel for the output value, and 3- median value; uses the statistical middle value in a kernel dataset as the output) and found that averaging had the most predictable statistical errors. It is noted however, that Goodin and Henebry (2002) found averaging may not accurately preserve the spatial properties desired for research.

Nearest neighbor (NN) and aggregated average (AA) are two commonly used resampling methods applied to remote sensing imagery. NN is useful for its speed and ability to maintain the integrity of categorical data while AA can accurately preserve mean values of images across many levels of aggregation (Bian and Butler, 1999). The purpose of this study was to compare the results of numerous resampling methods to the results of NN and AA resampling, and thereby better understand the affect of resampling and its potential implications on the introduction and propagation of error.

### **Methods**

One Landsat 5 TM scene (path 39 row 30) acquired on June 13, 2006 was used in this study. Prior to applying experimental resampling, the imagery was corrected for atmospheric effects using the Cos(T) method (Chavez, 1996) available in Idrisi Andes. A normalized difference vegetation index (NDVI) was calculated as a simple band ratio of the red and near-infrared bands (bands 3 and 4) following Rouse et al (1974). NDVI was selected for use in this study as it is a very common application for satellite imagery making the reported results more meaningful.

Idrisi Andes, ESRI ArcGIS 9.3, and Corel Paint Shop Pro X2 (PSP) were used to perform resampling (aggregated average, bicubic, bilinear, cubic convolution, nearest neighbor, pixel resize, and weighted average) of the NDVI layer (Table 1). In all cases, Landsat-derived NDVI imagery was resampled from its native 28.5 mpp to 100 mpp. In total, eight resampled layers were produced and using these layers, 100 pixel-values were extracted using the ArcGIS sample tool. The extracted values for bicubic, bilinear interpolation, cubic convolution, pixel resize, and weighted average were then compared to pixel values derived using AA and NN resampling methods. AA and NN values were also compared as were the results of bilinear interpolation using ESRI ArcGIS and PSP. Statistical comparisons were facilitated by calculating a correlation coefficient ( $R^2$ ) between each pair of image values ( $n = 12$ ; Table 2).

**Table 1.** NDVI image layers were systematically resampled using a variety of techniques and software applications.

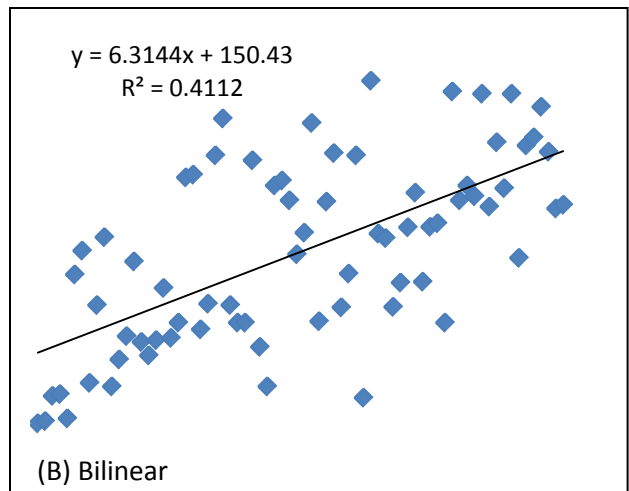
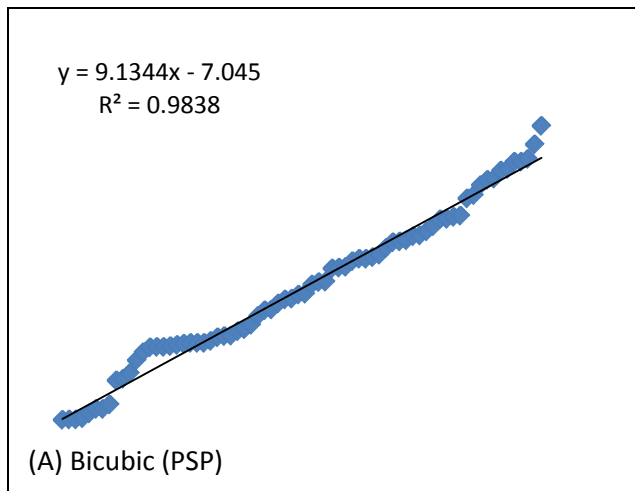
Resampling technique	Idrisi Andes	ESRI ArcGIS	Corel Paint Shop Pro
Aggregated Average (AA)	*		
Bicubic			*
Bilinear interpolation		*	*
Cubic convolution		*	
Nearest Neighbor (NN)		*	
Pixel resize			*
Weighted average			*

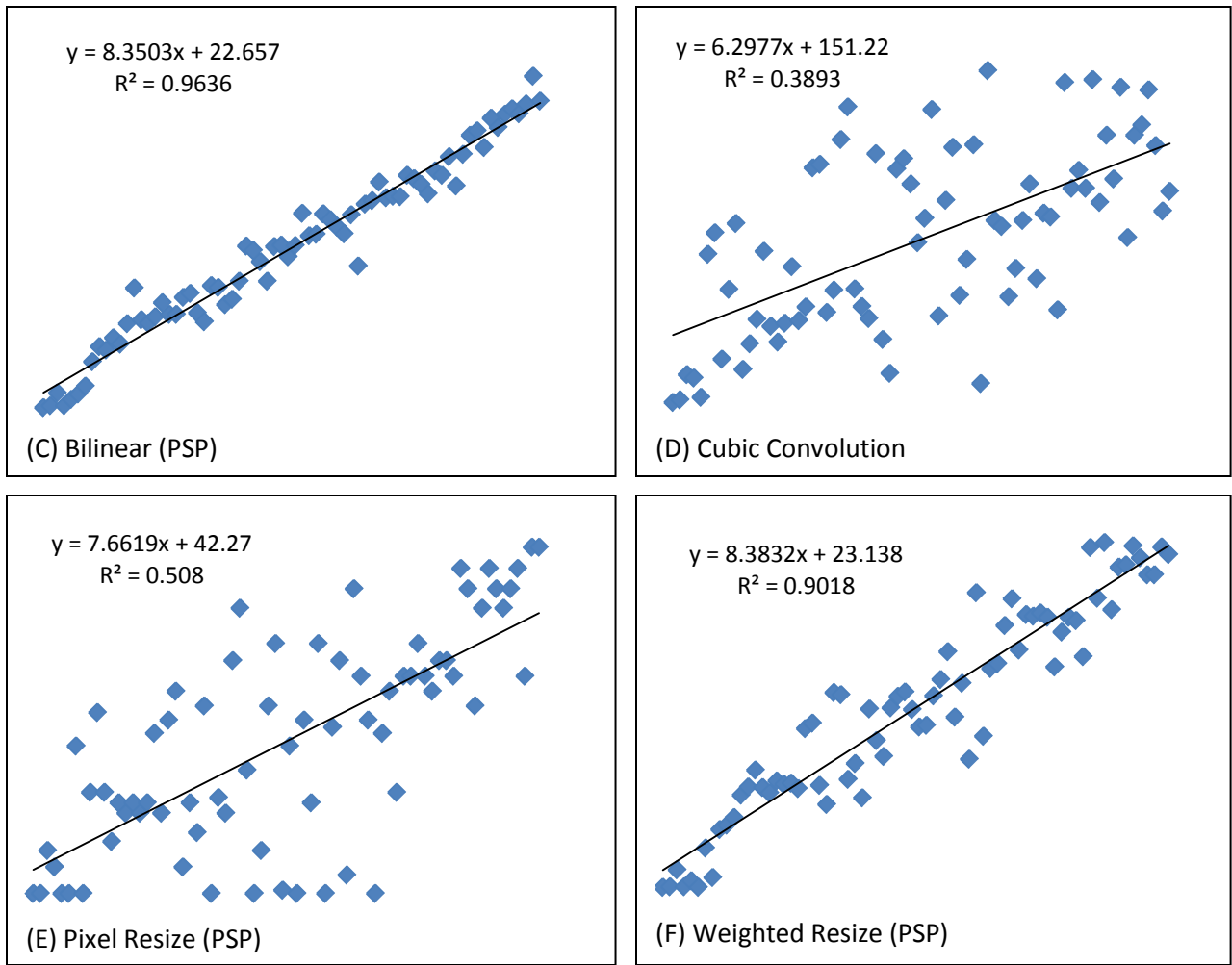
**Table 2.** Pairs of resampled images were statistically compared using linear regression and correlation coefficients ( $R^2$ )

Method	AA	BC	BL	CC	NN	PR	WA
AA		*	*	*	*	*	*
BC	*				*		
BL	*		*		*		
CC	*				*		
NN	*	*	*	*		*	*
PR	*				*		
WA	*				*		

**RESULTS AND DISCUSSION**

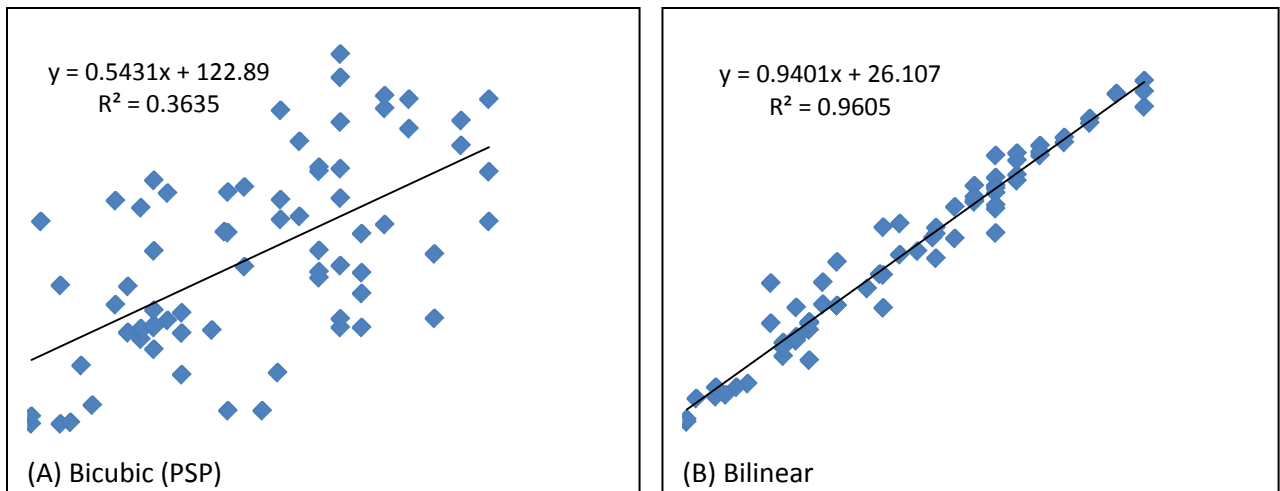
The most similar resampling results ( $R^2 = 0.984$ ) were found between the bicubic and AA methods (Figure 4a). PSP’s calculations for Bilinear interpolation resampling were also very similar to AA values ( $R^2 = 0.964$ ) (Figure 4b). This is not surprising as all three resampling methods calculate output values by averaging values within the input kernel. The only real change from one process to the next is the size of the kernel. The kernel size for AA is unknown, but it is probably close to 16 pixels given how closely it compares to PSP’s bicubic results. Some variation can be expected since it is not uncommon for software companies to have specific, patented algorithms that are slightly different from others. This concept is further illustrated in Figure 7 which compares results from ArcGIS’s bilinear resampling with PSP’s bilinear resampling method. The resulting  $R^2$  value of only 0.393 illustrated that, even though results should be fundamentally identical, each product produced drastically different values.





**Figure 4. Various resampling method results compared to the results of Aggregated Average resampling. Graphs are shown with linear trendlines, slope and intercept, and correlation coefficient ( $R^2$ ) values.**

The resampling method most similar to NN was CC resampling ( $R^2 = 0.963$ ) (Figure 5d), and ArcGIS’s bilinear resampling ( $R^2 = 0.960$ ) (Figure 5b). However, it must be remembered that neither of these options would maintain original categorical data values as NN will and both require more computational power relative to NN. Bilinear interpolation does not require as much computational power as CC, so for very large images it may be a suitable substitution to achieve results similar to NN but in less time than CC.



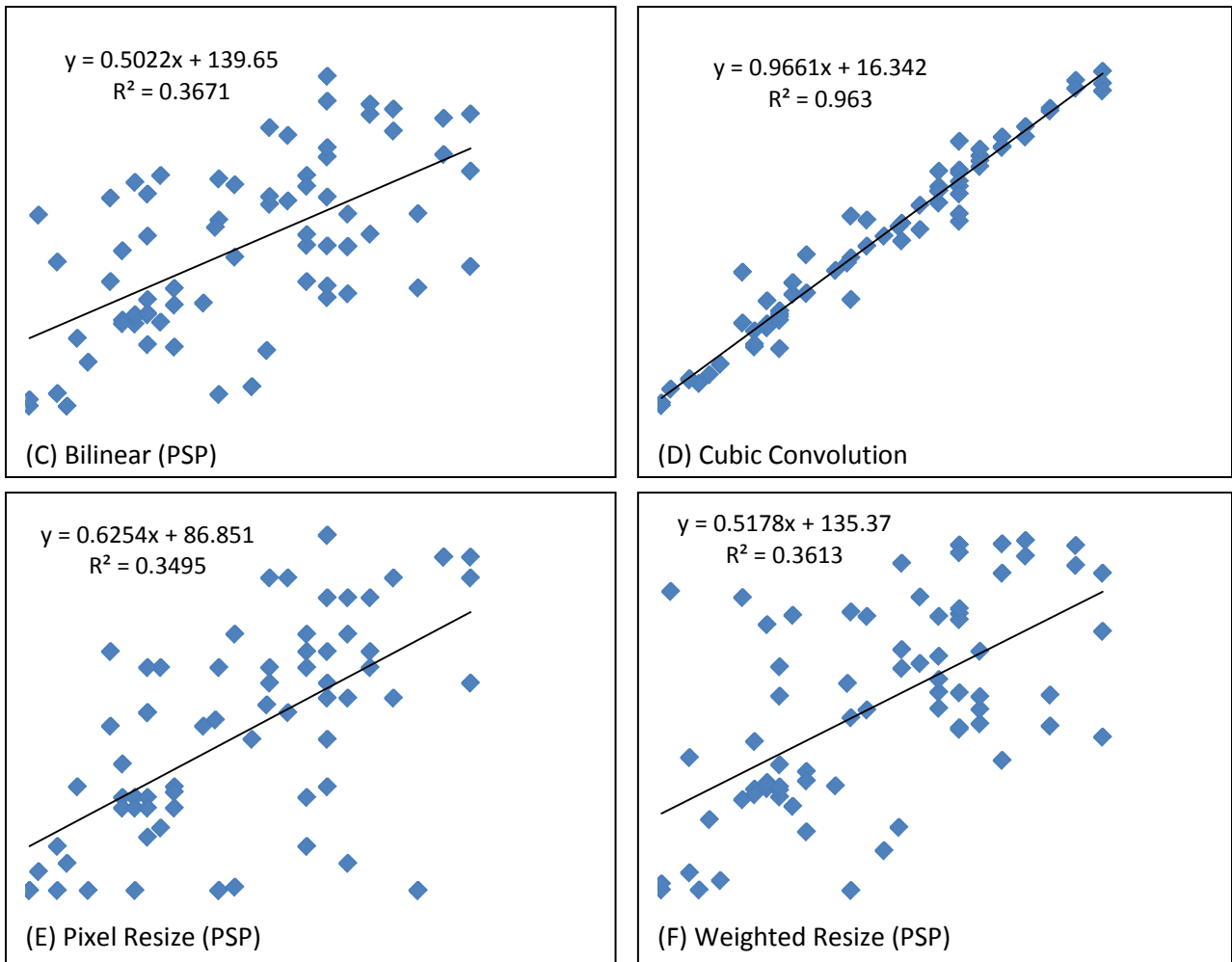


**Figure 5. Various resampling method results compared to the results of Nearest Neighbor resampling. Graphs are shown with linear trendlines, slope and intercept, and correlation coefficient ( $R^2$ ) values.**

Figure 6 shows that NN and AA produce very different results ( $R^2 = 0.409$ ) and imagery resampled using these methods are not directly comparable. This is not surprising however, considering how different the resampling methods are. This finding also explains why the other methods tested either compared better with either AA (PSP’s bicubic, bilinear, and weighted average), NN (ArcGIS’s bilinear and PSP’s CC), or neither (PSP’s Pixel Resize).

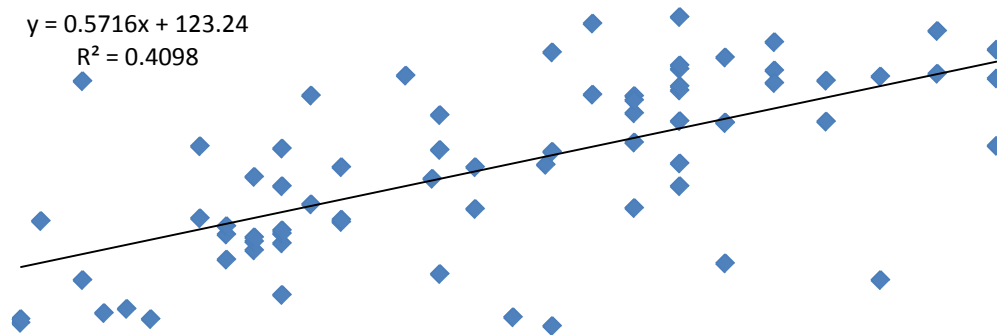


**Figure 6. Comparison of values obtained by resampling with the Nearest Neighbor and Aggregated Average methods.**

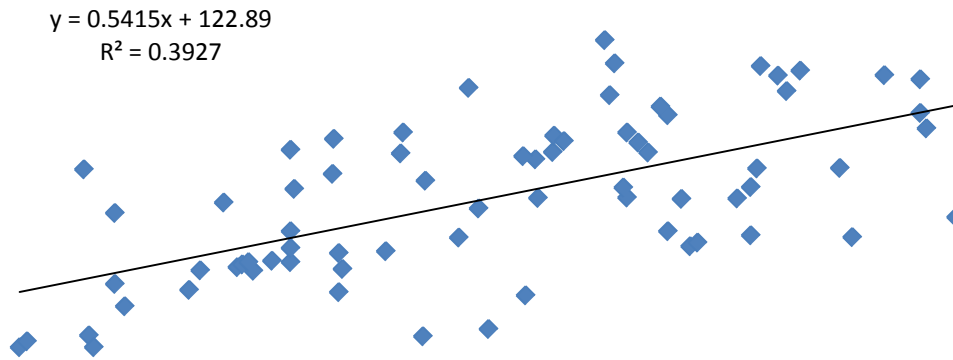


**Figure 7. Comparison of values obtained by using an ArcGIS Bilinear resampling and Corel's PSP Bilinear resampling method.**

### **CONCLUSIONS**

The purpose of this study was not to determine the best method for image resampling but rather to learn how various methods of image resampling compare to NN and AA as these are most commonly used. Atkinson (2001) raised a concern that those using remotely sensed data tended to choose images without properly considering if the pixel size of that image was appropriate for the study being conducted. The same could be said for resampling methods. There are a many options available for resampling images, and all options should be considered and tested before applying a method.

Additional considerations include the degree to which data values need to be maintained (especially when categorical data is resampled), whether the resulting dataset needs to be statistically or spatially accurate, how much processing power is available to perform the resampling, and what software is available to perform the resampling.

It was determined that image-editing software such as Corel's Paint Shop Pro can be used to perform image resampling, with results comparable to those created from remote sending - or GIS-specific software. However, due to proprietary differences in algorithms, care needs to be taken to make sure the results from one resampling software application can be compared to the results from another. For example, it is not recommended that another image-editing software (e.g., Adobe's Photoshop) be used in lieu of PSP without prior testing.

Based upon results presented in this paper, it is important to carefully select the most appropriate resampling technique for a given set of circumstances and seems most prudent to apply the same resampling technique using the same software to all imagery that is part of a given study. Lastly, it is noted that NN is a unique resampling process in that it is the only method that does not interpolate new values into the dataset, and is therefore the only method that should be used for categorical data.

### **ACKNOWLEDGEMENTS**

This study was made possible by a grant from the National Aeronautics and Space Administration Goddard Space Flight Center (NNX08AO90G). ISU would also like to acknowledge the Idaho Delegation for their assistance in obtaining this grant.

## **LITERATURE CITED**

- Atkinson, P., 2001. Geostatistical Regularization in Remote Sensing. 237-260 in N. Tate, & P. Atkinson (Ed.), Modelling Scale in Geographical Information Science. Chinchester: John Wiley & Sons Ltd.
- Bian, L. and R. Butler, 1999. Comparing Effects of Aggregation Methos on Statistical and Spatial Properties of Simulated Spatial Data. *Photogrammetric Engineering & Remote Sensing* , 65 (1), 73-84
- Chavez, P.S., 1996. Image based atmospheric corrections — Revisited and improved, *Photogrammetric Engineering and Remote Sensing*, 62:1025-1036
- Corel Corp., 2007. Resizing Images. Corel Paint Shop Pro Photo X2 Help
- Corel Corp., 2009. Answer Id 757099. URL = <http://corel.custhelp.com> visited June 17, 2009
- Dodgson, N.A., 1992. Image Resampling. University of Cambridge, Computer Laboratory. Cambridge: University of Cambridge Computer Laboratory
- ESRI, 2008. ESRI Support Center. visited May 27, 2009, from FAQ: What's the Difference between Nearest Neighbor, Bilinear Interpolation and Cubic Convolution?
- ESRI, 2009. Spatial Analyst: Cell size and resampling in analysis. ArcGIS Help
- eXtension, 2008. Remote Sensing Resampling Methods. URL = [http://www.extension.org/pages/Remote\\_Sensing\\_Resampling\\_Methods](http://www.extension.org/pages/Remote_Sensing_Resampling_Methods) visited May 11, 2009
- Goldsmith, N. 2009. Resampling Raster Images. URL = <http://www.jiscdigitalmedia.ac.uk/stillimages/advice/resampling-raster-images/> visited May 11, 2009
- Goodin, D.G. and G.M. Henebry, 2002. The Effect of Rescaling on Fine Spatial Resultion NDVI Data: A Test using Multi-resolution Aircraft Sensor Data. *International Journal of Remote Sensing* , 23 (18), 3865-3871
- Gotway, C.A. and L.J. Young, 2002. Combining Incompatible Spatial Data. *Journal of the American Statistical Association* , 97 (458), 632-648
- Huber, W. 2009. Map Algebra: Resampling. URL = [http://www.quantdec.com/SYSEN597/GTKAV/section9/map\\_algebra.htm](http://www.quantdec.com/SYSEN597/GTKAV/section9/map_algebra.htm) visited May 2009
- João, E., 2001. Measuring Scale Effects Caused by Map Generalization and the Importance of Displacement. Pages 161-179 in N. Tate, & P. Atkinson (Ed.), Modelling Scale in Geographical Information Science. Chinchester: John Wiley & Sons Ltd.
- Kay, D.C. and W. Steinmetz, 2005. Paint Shop Pro 9 for Dummies. Hoboken: Wiley, Inc.

- Li, Z., W. Trappe, Y. Zhang, and B. Nath, 2005. Robust Statistical Methods for Securing Wireless Localization in Sensor Networks. IEEE 09/05:91-98
- Losinger, C., 2006. Resizing (updated for v4.0). Smaller Animals Software vBulletin – ImgSource articles. URL = <http://www.smalleranimals.com/vforum/showthread.php?t=1878> visited June 17, 2009
- Przydatek, B., D. Song, and A. Perrig, 2003 SIA: secure information aggregation in sensor networks, in SenSys '03: Proceedings of the 1st International Conference on Embedded Networked Sensor Systems, 255–265
- Rouse, J.W. Jr., R.H. Haas, D.W. Deering, J.A. Schell, and J.C. Harlan, 1974. Monitoring the Vernal Advancement and Retrogradation (Green Wave Effect) of Natural Vegetation, Greenbelt: NASA/GSFC Type III Final Report, 371 pp.
- Shea, S. 2009. Resizing Versus Resampling: Corel Paint Shop Pro Photo Basics – Lesson 4. About.com: Graphics Software. URL = <http://graphicssoft.about.com/od/paintshoppro/ig/lesson4/Resizing-Versus-Resampling.htm> visited June 17, 2009
- Verbyla, D.L., 2002. Practical GIS analysis. London: Taylor & Francis
- Wade, T., and S. Sommer, 2006. A to Z GIS. Redlands: ESRI Press
- Wagner, D., 2004. Resilient aggregation in sensor networks, in SASN '04: Proceedings of the 2nd ACM workshop on Security of ad hoc and sensor networks, 78–87

**Recommended citation style:**

Studley, H. and K. T. Weber, 2011. Comparison of Image Resampling Techniques for Satellite Imagery. Pages 185-196 in K. T. Weber and K. Davis (Eds.), Final Report: Assessing Post-Fire Recovery of Sagebrush-Steppe Rangelands in Southeastern Idaho. 252 pp.

[THIS PAGE LEFT BLANK INTENTIONALLY]

## **Applying Indigenous Pastoralist Experiences to Western Range Management**

Keith T. Weber, GISP, Idaho State University, GIS Training and Research Center, 921 S. 8<sup>th</sup> Ave. Stop 8104, Pocatello, Idaho 83209-8104. [webekeit@isu.edu](mailto:webekeit@isu.edu) (corresponding author)

Shannon Horst, 1 El Nido Amado, SW, Albuquerque, NM 87121

### **ABSTRACT**

Pastoralism is an ancient form of self-provisioning that is still in wide use today throughout the world. While many pastoral regions are the focus of current desertification studies, the long history of sustainability evidenced by these cultures is of great interest. Numerous studies suggesting a general trend of desertification intimate that degradation is a recent phenomenon principally attributable to changes in land tenure, management, and treatment. This paper explores the suggested causes of land degradation and identifies the land management and grazing treatments shared by many pastoral cultures. The singular commonality found in nearly all studies of degradation is the prevalence of partial or total rest. While historical observations suggest that desertification is the result of both climatic and anthropic factors, recent focus has been placed upon the effect of sedenterization. These studies suggest that "management systems" be re-considered and supplanted by more inclusive planning processes focusing upon improving arid and semiarid rangeland ecosystems through the use of livestock as a solution to the problem of land degradation.

*KEYWORDS: Desertification, grazing, ranching, nomadism, transhumance*

## **INTRODUCTION**

This paper is the result of over a decade of research devoted to understanding land cover change in semiarid ecosystems, and the realization some years ago, that people can affect tremendous changes on the landscapes which we all rely for survival. The idea of course is not novel, but nonetheless, it initiated an investigation into the commonalities and differences among the many societies and cultures inhabiting the semiarid regions of the world. Of particular interest, were those commonalities in land use and most specifically, livestock grazing. The results revealed some surprising patterns while at the same time raised additional research questions that today are areas of active research by the author. The fundamental postulate explored in this paper is whether the changing face of pastoral societies, as a result of market integration and sedentization, has consistently lead to land degradation.

To discuss and appreciate the study of desertification or land degradation in arid and semiarid ecosystems, one must begin with an understanding of pastoralism as this has historically been the principal land use known in many of these regions. Pastoralism is an ancient craft which on the surface, may be perceived to demand only minimal skills. The shepherd or herdsman is simply tasked with keeping his stock alive so that he may subsist on the animals' milk, blood, wool, meat, and value in trade. Just beneath this thin veneer however, rests a myriad of complexities involving forage, animal health, reproduction, predation, weather, and the social and cultural fabric within which the pastoralist functions. Over time, pastoral cultures have developed and these complexities have been mastered, with learned animal husbandry skills and the wisdom of experienced pastoralists handed down through generations<sup>1</sup> (Mapinduzi et al. 2003; Stock 2004). As a result, contemporary pastoralism is a dynamic form of subsistence.

### *What is Pastoralism?*

It is not without debate that pastoralism developed after agriculturalism (Khazanov 1994). By 7000 BCE pastoralism was well established (Flannery 1965) and most likely developed as people migrated into areas of low productivity and/or regions of unreliable rainfall (i.e., the arid and semiarid regions of the world). As a result, these people came to rely upon domesticated animals for subsistence instead of agricultural crops (Salzman 2004; Cummins 2009). Over time, three unique forms of pastoral production took hold: 1) sedentary production, 2) transhumance, and 3) nomadism (Yalcin 1986). Sedentary pastoralism involves keeping livestock near farms and villages year-round while transhumance includes the seasonal movement of animals and people from valley bottoms to mountain pastures (Yalcin 1986; Ott 1993; Cummins 2009). Nomadic pastoralism may have developed in response to recurring and wide-spread drought (Salzman 2004) or widespread and erratic rainfall and is typified by livestock being moved in constant search of forage. Nomadism differs from transhumance in that no permanent base (home or village) is developed and likewise, no pre-defined series of movements are used. Of all the forms of pastoralism, nomadism is least systematic.

### *What are Rangelands?*

More than simply a matter of semantics, the sometimes painstaking and critical use of language is very important to communicate the true meaning of a writer's thoughts. Especially within multidisciplinary fields of scholarship, defining key terms up-front can be very useful to avoid confusion later. One

---

<sup>1</sup> This is not to imply that ancient pastoralists developed a utopian society as perfect long-term ecological sustainability of arid and semiarid landscapes have yet to be achieved (Khazanov 1994).

important term used throughout this paper is rangeland, and due to the prominence of this term it is important that the reader understand it in the same way intended by the author.

Much of what is considered rangeland today (Bedell 1998) falls within the arid and semiarid regions of the world. These areas are typically dominated by grasses, forbs, and shrubs and are managed without cultivation, irrigation, herbicides, pesticides, or fertilizers. Indeed, the primary management tools of the traditional pastoralist are livestock (principally sheep, goats, cattle, horses, donkeys, and camels) and fire (Savory 1999). Through the use of these tools, the pastoralist has learned how to manipulate his/her flock (or herd) to graze or avoid certain patches of vegetation with subsequent changes in land cover over time.

While the term rangeland is a more inclusive term than "grasslands" (many savanna ecosystems are also considered rangelands), within the scope of this paper, rangelands are defined by land use (i.e., livestock grazing) and land management (i.e., non-irrigated, etc.) than by any geographic or environmental classification.

Within arid and semiarid rangelands, water is the limiting factor (Niamir-Fuller and Turner 1999; Hill 2006) and precipitation is highly variable both spatially and temporally. In seasons of increased precipitation, forage availability improves dramatically (Niamir-Fuller and Turner 1999; Gregory et al. 2008) whereas in years of drought, grass becomes scarce. Unfortunately, contemporary grazing systems may create ineffective water cycles (cf. rain use efficiency [Le Houerou 1984]) resulting in increasingly frequent and severe pastoral drought events (Savory 1999; Neely et al. 2009). As a result, some pastoral cultures (e.g., the Herero of Namibia and the Samburu of Northern Kenya) have degraded their environments to the point where temporary abandonment was required (Hill 2006), and all have altered their environment to some degree (Wilson 2007). Still, numerous pastoral cultures (e.g., Rashayada Bedouin of the Sudan, Mongolian and Chinese herdsman, and Pyrenean herders) (Figure 1) have subsisted on rangelands for thousands of years despite various complexities, hardships, and challenges. We are not intimating that the landscapes used by all pastoral cultures are pristine as many are the focus of on-going desertification research. There is evidence however, suggesting that pastoral landscapes were in better condition throughout the 1800's and early 1900's (Niamir-Fuller and Turner 1999) and that the observed degradation described in the literature today is a relatively recent phenomenon that has accelerated during the latter parts of the 20th and current centuries (Waller 1985; Gritzner 1988; Smith 1992). Based upon these reports, one wonders what caused this recent decline.

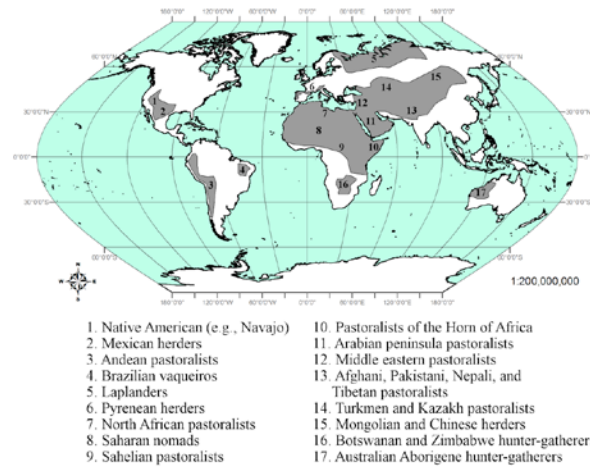


**Figure 1. Map of general distribution of traditional pastoralists worldwide (note: the terms pastoralist, herders, and hunter-gatherers and general region map from Niamir-Fuller 1999).**

### *Is Desertification Real?*

Similar to the term rangelands, a working definition of desertification is necessary to properly construct this paper. Desertification is a term first used by Auberville (1949) which refers to the severe degradation of the arid, semiarid, and sub-humid areas of the world due principally to climatic and anthropic factors (UNCCD 1995; Arnalds 2000). The term implies a nearly irreversible condition (Dougill and Cox 1995; Niamir-Fuller and Turner 1999). Desertification was also used by Savory (1999) to refer to the manifested symptom of biodiversity loss in arid and semiarid environments while more recently, Reynolds (2001) defined desertification as a reduction in the productive potential of the land. A common thread throughout each of the many definitions is the concept of a degraded landscape which is no longer as productive as it once may have been. It is this concept that embraces the term desertification as it is used in this paper.

While most scholars will agree that substantial areas of the earth's surface have desertified (Prince et al. 2009), an active debate has emerged challenging the estimates and inferences made as a result of some earlier studies (Tucker et al. 1991; Hellden 1998; Prince et al. 1998; Veron et al. 2006). Whether all estimates of desertification ever published are wholly accurate or not is a moot point when one considers the belief by many decision-makers and land managers that rangelands are degrading and that some intervention or change of policy must be enacted to prevent further desertification.

### *Variability in Grazing Treatments*

To improve degraded rangelands a common remedy has been the removal of livestock (i.e., de-stocking). Under the most systematic grazing regimes, *rest* is deliberately used as a temporary de-stocking that often serves dual roles as both a pre-determined scheduling process and conservation practice. Under less systematic regimes, the term *recovery* is often applied, inferring an active management decision that allows plants to recuperate before additional grazing is allowed. In contrast to rested pastures, the length of the *recovery* period is not pre-determined (Voisin 1988) but rather, decided upon by the pastoralist based on his/her knowledge, experience, and goals. *Rest* then, as part of a grazing system, may or may not have any relationship to actual leaf and root *recovery* though the recovery period is a more important consideration than the grazing period (Snyman 1998).

The most extreme form of de-stocking is *abandonment*. In western cultures, *abandonment* is equated with failure, while in other pastoral cultures, *abandonment* is viewed as part of the normal management process (Stone 1993; Hill 2006). In essence, all pastoral cultures have applied intervals of no-grazing (rest, recovery, and abandonment) along with periods of active grazing as part of their historic and traditional grazing practices. The only real difference --apart from semantics-- is the duration of the no-grazing period which may be a function of seasonality (Voisin 1988) and the resilience or brittleness of the environment (Savory 1999). Regardless of the term used, all grazing management involves periods of total or near total absence of use throughout a growing season or grazing cycle.

It may seem a logical conclusion, that the period of rest or recovery constitutes an entirely positive influence on the environment. Such a conclusion however, is paradoxical, because just as using too brief a recovery period degrades an environment, so too may a prolonged recovery period. This is because arid and semiarid grass species have co-evolved with herbivores and the prolonged absence of herbivory can lead to excessive standing litter accumulations referred to as moribund grass. Moribund grass breaks down through a gradual physical weathering process, rather than the more rapid biological decay process, and is particularly detrimental to grazing-dependent bunchgrasses (Sheppard et al., 2009) . With sufficient time, this condition can kill individual plants leaving only patches of bare soil (Savory 1999; Figure 2). Savory (1999) draws a clear distinction between the recovery period required by individual plants --to minimize or avoid overgrazing-- and the episodic, yet high levels of disturbance the plants and soil surface requires to maintain the health of its biological communities through the trampling of moribund material to ensure rapid biological decay, increase soil organic matter and soil organic carbon (Follett 2001), and provide soil-covering litter to promote improved rain use efficiency (Snyman 2005). Furthermore, Savory observed that under most western livestock grazing management systems, the grazing period represents a period of near-rest as livestock are distributed in a fashion that typically yields inadequate animal impact/disturbance. To describe this effect, Savory used the term *partial rest*.



**Figure 2. An example of excessive litter accumulation degrading through oxidative rather than biological means.**

### *The Concept of Partial Rest*

Under conditions of *partial rest*, livestock are grazed at low density (i.e., few animals graze a large pasture in an un-bunched manner resulting in low stocking density). When herds remain relatively sedentary over long periods of time (e.g., a month or more) overgrazing of plants occurs. Overgrazing of plants, combined with the adverse effects of partial rest (bare soil, moribund grasses, etc), exacerbates an already declining rain use efficiency through both increased run-off and soil surface evaporation of water (Savory 1999; Huxman et al. 2004). While some plants within a pasture will be grazed repeatedly others may remain un-grazed and over time, moribund grass accumulations form just as they do in over-rested areas. The moribund grasses present a less palatable option to the herbivore, which tend to select the same individual grass plants resulting in further overgrazing. As a result, overgrazing damages or kills grazed plants while un-grazed moribund grasses are weakened, and the rangeland enters a feedback cycle of slow but progressive degradation. Today, numerous studies support these observations and demonstrate that 1) partial and total rest have remarkably similar affects on arid and semiarid grassland environments (Gomez-Ibanez 1975; Cummins 2009; Weber et al. 2009a; Weber et al. 2009b) and 2) few tangible differences can be identified among any of the rotational grazing schemes commonly used today (Jahnke 1982; Sandford 1983; Behnke 1999; Quirk 2002; Coughenour 2008; Homewood 2008) .

### *Causes of Rangeland Degradation*

The cause of rangeland desertification has been attributed repeatedly to a combination of climatic and anthropic factors (UNCCD 1995; Geist and Lambin 2004; Hill 2006; Lambin et al. 2009) with specific emphasis placed on overgrazing and drought (Bedell 1998; Puigdefabregas 1998). Climate theories have focused upon changes that have occurred over the past ten thousand years of the current Holocene and note several periods of increased aridity (drought) and still other periods of increasing humidity. In addition, some changes were localized (Stebbing 1935; Niamir-Fuller and Turner 1999) while others were global in nature. Some changes persisted over long time periods while others were much shorter in duration (Brooks 1949; Khazanov 1994). In essence, changes in the earth's climate since the last Ice age have not been progressive but rather oscillatory. Indeed, it is speculated that the periods of increased aridity have led to the emergence and increased prevalence of nomadic pastoralism and not the inverse, nor a global increase in desertification due to pastoralism (Khazanov 1994). This is because nomadic and transhumant pastoralism are successful adaptations for survival within highly variable semiarid and arid environments (Niamir-Fuller 1999; Khazanov 1994; Salzman 2004; Cummins 2009).

One reason for the success of nomadic and transhumant pastoralism in semiarid and arid ecosystems in contrast to cultivated agriculture, relates to effective rainfall, rain-use efficiency or soil moisture storage capacity. Thurow (2000) has described various hydrologic effects on rangelands and noted that soil structure, soil texture, and organic matter content are key factors governing soil moisture storage capacity. While the particular soil type or soil association does not change with treatment, a soil's structure and organic matter content can be affected. In the absence of large herbivores, organic matter inputs are dramatically reduced and the surface of soils tend to become capped (Khazanov 1994). Both of these factors degrade a soil's ability to retain water (Thurow 2000) and lead to a reduction of plant production. Similar to, and often compounded upon the effects of prolonged rest, these rangeland ecosystems enter a feedback cycle which ultimately leads to desertification (Le Houerou 1984; Thurow 1991).

While literature from the 1980's and early 1990's repeatedly linked livestock to the degradation and desertification of rangelands (Lamprey 1983; Sinclair and Frywell 1985; Wolfson 1990) more recent studies have refuted this by suggesting that prolonged rest leads to even more serious degradation than overgrazing (Seligman and Perevolotsky 1994; Olaizola et al., 1999; Cummins 2009). Thus, it seems that neither climatic or anthropic factors are solely to blame for the degradation of the earth's rangelands. It stands to reason then, that some interactive or combinatory explanation should be sought. Indeed Hill (2006) arrived at a similar conclusion when he examined the arid rangelands of the Transjordan plateau. His conclusion was that climate change was a major factor explaining the disappearance of surface water and changes in vegetation due to increased aridity (Bar-Matthews et al. 1999; Hill 2006). This, however may also be attributed to reduced soil moisture storage capacity, increased surface runoff, and increased soil surface evaporation because too *few* animals were present on the rangelands for too *long* a period of time (Savory 1999). A second major factor cited by Hill was human ignorance regarding the consequences of mismanagement (McGovern et al. 1988) (i.e., land use decisions and practices). The third causal factor was the role of politics (i.e., land management or land tenure [Lundsgaard 1974]) and his hypothesis that environmental sustainability is inversely related to the levels of hierarchy and dissociation present in the governing/managing body (Hill 2006).

What is most interesting among these studies is the clear admission of the substantial role played by humans (albeit not a solitary role) in shaping and altering the environment and the inseparability of humans and nature (Goldman and Schurman 2000). It seems reasonable then, to consider what humans may be able to do to improve the environment instead of focusing solely upon what we have done to degrade it.

Land use, and specifically pastoral land use is highly variable both temporally and spatially across the rangelands of the world (Niamir-Fuller 1999). To enable modern scientific inquiry, some means of classifying and quantifying land use is required (Funtowicz and Ravetz 2003). The most fundamental grazing classification considers a rangeland either intensive or extensive relative to the degree of management effort involved (Bedell 1998). Quantifying land use requires other measurements such as stocking density or stocking rate, which describe the number of animals grazing an area relative to the size of the area (density) or the amount of time allocated to an area (rate).

While a plethora of terms are applied to specific styles of grazing (rest-rotation, deferred-rotation, high intensity-low frequency, short-duration, continuous, etc.[Holechek et al. 2001]) these differ only in the proportion of time spent grazing relative to the proportion of time allowed for recovery of the plants. In western societies, extensive or semi-extensive management has become the norm, and graziers typically apply a single grazing system for their herd/herds which is repeated on an annual basis. One problem with this approach is that it places the focus of livestock management upon the herd and in essence, the "herd" *is* the management unit. In contrast, the "season" is the management unit for transhumant pastoralists and as a result, the latter is less systematic and more responsive to current conditions. In neither case, however, is "time" (the period over which plants are exposed to a grazing animal and rangelands experience disturbance through the impact of the herd) the focal management unit even though numerous studies have stressed its importance to ensuring long-term sustainability (Voisin 1988; Snyman 1998; Savory 1999). Voisin, for instance, points out that promoters of the rotational method "overlooked the necessity for the periods of occupation being sufficiently short" and instead emphasized "dividing the

pasture into a greater or smaller number of paddocks...and then shifting the herd from one paddock to the next".

Range scientists have recommended and tested a great many "grazing systems" varying from continuous grazing through an abundance of rotational grazing practices which seem to have been designed without taking into account the full complexity of cultural/social issues, wildlife, alternative uses, market forces, etc. To effectively address complexity requires a planning process that embraces complexity, rather than a pre-determined management system designed for simplicity (Savory 1999).

Niamir-Fuller and Turner (1999) note the importance of mobility within highly variable environments (i.e., arid and semiarid areas) and while they opt to focus upon *mobility* itself, the reason why mobility is so important is intimately tied to Voisin's emphasis upon *time*. Behnke (1999) echoes these same concerns and the importance of highly mobile herds in his study of the Etanga pastoralists of Namibia. In both cases, mobile pastoralism (e.g., transhumant and nomadic pastoralism) is considered an ideal adaptation within arid and semiarid rangelands especially in contrast to the alternative, sedenterization (Salzman 2004). Sedenterization is the process by which once highly mobile pastoral cultures are converted to less mobile ones concentrated near major trade routes, villages, and other communities. As a result, the pastoralist no longer needs to rely upon himself and his livestock for subsistence, but upon his ability to purchase goods and services using money gained through the sale of his livestock. In such emerging market economies lessons in business acumen are quickly learned and the adage of "location, location, location" is proven true again.

The consequence of such change is the pastoralist's herd may spend nearly the entire year within a relatively small area and in response to market demands --instead of personal needs or the carrying capacity of the land-- the herder may increase his number of livestock adding further stress to the brittle environment.

In a study of nomadic cultures, Khazanov (1994) described a global trend in which nomadism is being replaced by market-oriented ranching (cf., sedenterization). In these cases, the result is the prolonged occupation of livestock within a given area and the subsequent impoverishment and desertification of the landscape. Keohane (2008) reports a similar transition of Bedouin tribes where livestock were traditionally moved every three to five days to one of increased sedenterization around settlements. Again, the result was an observed decline in rangeland condition.

If sedenterization leads to the overgrazing of plants, a loss of biodiversity, and ultimately desertification, it seems reasonable to expect the opposite treatment (nomadism) to yield opposing results upon the landscape. However it does not (Savory 1999) and what has been observed is that both nomadism and more sedentary grazing practices can lead to desertification, albeit at different rates of degradation. Pastoralism, given adequate land area and freedom to move, simply leads to more gradual desertification than sedentary practices.

Hence, mobility alone is not the key and simply describing nomads as mobile does not adequately capture the essence of the grazing practices followed by the nomadic pastoralist. To look at it another way, would a grazer who moves his livestock to fresh pasture twice each year be considered a nomadic pastoralist?

What if he moved his herd or flock 12 times per year, or 150 times per year covering hundreds of kilometers in the process? Only in the latter example would one consider the hypothetical grazer a nomadic pastoralist. In terms of land management, the effective difference between the former examples of punctuated sedenterism and nomadism is the amount of time spent grazing one area before moving to another as well as the amount of time allowed for plant recovery (Voisin 1988).

While Voisin (1988) advocated that overgrazing of plants was the greatest influence in land degradation and desertification, only more recently have the effects of partial-rest and total rest been more fully understood (Behnke 1999; Niamir-Fuller and Turner 1999; Cummins 2009) as factors that tend to override the influence of overgrazing and may consequently be the principle factors driving rangelands toward desertification.

The western rangelands of North America are little different than many rangelands where traditional pastoralism has been practiced for thousands of years. Both are typically arid or semiarid environments dominated by grasses and shrubs, grazed by domesticated cattle, sheep, and goats. The primary and perhaps only difference is that traditional pastoralism is a means of self-provisioning whereas ranching is a market-oriented business (Cummins 2009). As noted earlier, shifts towards market-oriented grazing leads to sedenterization (cf., partial-rest of rangelands) which in turn leads to a more rapid overgrazing of plants, loss of biodiversity, and accelerated desertification. This market-oriented shift has also changed land tenure as significant acreage is now held in "public lands" all of which are managed, by policy, under regimes of partial-rest or total rest.

Could a change be made to reduce the latency of livestock within a pasture or paddock and eliminate the negative impact of partial-rest to thereby improve rangeland ecosystems? The latter is a very large and important question and certainly some will argue that the suggested change will not yield the expected results in spite of the historical observations referenced throughout this paper indicating otherwise. This then becomes both a dilemma and a challenge for the future of rangeland ecosystems, range science, range managers, and graziers across the globe.

## **SUMMARY**

While numerous pastoral cultures have subsisted for thousands of years and continue to survive today, nearly all are facing great difficulties as the world's rangelands deteriorate. Historical observations suggest that desertification is the result of both climatic and anthropic factors with specific emphasis only recently placed upon the effect of sedenterization and the subsequent feedback cycle initiated through partial-rest and total rest prevalent across nearly all continents, societies, and grazing cultures today. As a result, the studies examined in this paper suggest that "management systems" be re-considered and supplanted by more inclusive planning processes focusing upon improving arid and semiarid rangeland ecosystems through the use of livestock as a solution to the problem of land degradation.

## **ACKNOWLEDGEMENTS**

This study was made possible by a grant from the National Aeronautics and Space Administration Goddard Space Flight Center (NNX08AO90G). Idaho State University would also like to acknowledge the Idaho Delegation for their assistance in obtaining this grant.

## **LITERATURE CITED**

Arnalds, O., 2000. Desertification: An Appeal for a Broader Perspective. Pages 5-15 in O. Arnalds and S. Archer (Eds.) Rangeland Desertification. Kluwer Academic publishers. 209 pp.

Auberville, 1949. Climats, forests et desertification de l'Afrique tropicale. Soc d'editions geographiques et coloniales. Paris

Bar-Matthews, M., A. Ayalon, A. Kaufman, and G. J. Wasserburg, 1999. The Eastern Mediterranean Paleoclimate as a Reflection of Regional Events: Soreq Cave, Israel. *Earth and Planetary Science Letters* 166:85-95

Bedell, T. E., 1998. Glossary of Terms used in Range Management. Society for Range Management. 4:32pp.

Behnke, R. H. Jr., 1999. Stock Movement and Range-management in a Himba Community in North-western Namibia. Pages 184-216 in Niamir-Fuller (Ed.) *Managing Mobility in African Rangelands: The Legitimization of Transhumance*. FAO: IT Publications. 314 pp.

Brooks, C. E. P., 1949. *Climate through the Ages: A Study of the Climatic Factors and their Variations*. London. Ernest Benn, Ltd.

Coughenour, M. B., 2008. Causes and Consequences of Herbivore Movement in Landscape Ecosystems. Pages 45-92 in K. A. Galvin, R. S. Reid, R. H. Behnke, Jr., and N. T. Hobbs (Eds.), Fragmentation in Semi-Arid and Arid Landscapes. Springer, Dordrecht, The Netherlands. 411 pp.

Cummins, B., 2009. *Bear Country: Predation, Politics, and the Changing Face of Pyrenean Pastoralism*. Carolina Academic Press, Durham, North Carolina. 355 pp.

Dougill A. and J. Cox, 1995. *Land Degradation and Grazing in the Kalahari: New Analysis and Alternative Perspectives*. Pastoral Development Network, 38pp.

Flannery, K. V., 1965. The Ecology of Early Food Production in Mesopotamia. *Science* 147(3663):1247-1256

Follett, R. F., 2001. Organic Carbon Pools in Grazing Land Soils. Pages 65-86 in R. F. Follett, J. M. Kimble, and R. Lal (Eds.) The Potential of US Grazing Lands to Sequester Carbon and Mitigate the Greenhouse Effect. Lewis publishers. 442 pp.

Geist, H. J. and E. F. Lambin, 2004. Dynamic Causal Patterns of Desertification. *Bioscience* 54(9):817-829

Goldman, M. and R. A. Schurman, 2000. Closing the Great Divide: New Social Theory on Society and nature. *Annual Review of Sociology*. 26:563-584

Gomez-Ibanez, D. A., 1975. *The Western Pyrenees: Differential Evolution of the French and Spanish Borderland*. Oxford: Clarendon Press

Gregory, J., L. Sander, and K. T. Weber, 2008. Range Vegetation Assessment in the Big Desert, Upper Snake River Plain, Idaho 2005. Pages 3-5 in K. T. Weber (Ed.), Final Report: Impact of Temporal Landcover Changes in Southeastern Idaho Rangelands (NNG05GB05G). 354pp.

Gritzner, J., 1988. *The West African Sahel. Human Agency and Environmental Change*. Geography Research paper no. 226. University of Chicago

Hellden, U., 1988. Desertification monitoring: is the desert encroaching? *Desertification Control Bulletin* UNEP, Nairobi 17:8-12

Hill, J. B., 2006. *Human Ecology in the Wadi Al-Hasa: Land Use and Abandonment through the Holocene*. The University of Arizona, Press, Tucson, Ariz. 194 pp.

Homewood, K., 2008. *Ecology of African Pastoralist Societies*. Ohio University Press, Athens, OH. 292 pp.

Huxman, T. E., M. D. Smith, P. A. Fay, A. K. Knapp, M. R. Shaw, M. E. Loik, S. D. Smith, D. T. Tissue, J. C. Zak, J. F. Weltzin, W. T. Pockman, O. E. Sala, B. M. Haddad, J. Harte, G. W. Koch, S. Schwinning, E. E. Small, and D. G. Williams, 2004. Convergence across Biomes to a Common Rain-Use Efficiency. *Nature* 429:651-654

Jahnke, H. E., 1982. *Livestock Production Systems and Livestock Development in Tropical Africa*. Kiel: Kieler Wissenschaftsverlag vauk

Keohane, A., 2008. *Bedouin: Nomads of the Desert*. Kyle Cathie Ltd. 174 pp.

Khazanov, A., 1994. *Nomads and the Outside World*. University of Wisconsin Press. 2:382 pp.

Lambin, E. F., H. Geist, J. F. Reynolds, D. M. Stafford-Smith, 2009. Coupled Human-Environment System Approaches to Desertification: Linking People to Pixels. Pages 3-14 in A. Roder and J. Hill (Eds.) Recent Advances in Remote Sensing and Geoinformation Processing for Land Degradation Assessment, CRC Press, Taylor and Francis, London. 400pp.

Lamprey, H. F., 1983. Pastoralism Yesterday and Today: The Overgrazing Problem. pp. 643-666 in F. Bourliere (Ed.) Tropical Savannas: Ecosystems of the World, Elsevier, Amsterdam

Le Houerou, H. N., 1984. Rain Use Efficiency: A Unifying Concept in Arid-land Ecology. *J. Arid Environments* 7:1-35

Lundsgaard, H. P., 1974. *Land Tenure in Oceania*. Association for Social Anthropology in Oceania Monographs #2. Honolulu: University Press of Hawaii

Mapinduzi, A. L., G. Oba, R. B. Weladji, and J. E. Colman, 2003. Use of Indigenous Ecological Knowledge of the Maasai Pastoralist for Assessing Rangeland Biodiversity in Tanzania. *African Journal of Ecology*. 41:329-336

McGovern, T. H., G. Bigelow, T. Amarosi, and D. Russell, 1988. Northern Islands, Human Error, and Environmental Degradation: A View of Social and Ecological Change in the Medieval North Atlantic. *Human Ecology* 16(3):225-270

Neeley, C., S. Bunning, and A. Wilkes, 2009. Review of Evidence on Drylands Pastoral Systems and Climate Change: Implications and Opportunities for Mitigation and Adaptation. FAO, Rome. 38 pp.

Niamir-Fuller, M. and M. D. Turner, 1999. A Review of Recent Literature on Pastoralism and Transhumance in Africa. Pages 18-46 in M. Niamir-Fuller (Eds.), Managing Mobility in African Rangelands: The Legitimization of Transhumance. FAO: IT Publications. 314 pp.

Olaizola, A., E. Manrique, and M. E. Lopez Pueyo, 1999. Organization Logics of Transhumance in Pyrenean Sheep Farming Systems. In R. Rubino and P. Mohrand-Fehr (Eds.) Systems of Sheep and Goat Production: Organization of Husbandry and Role of Extension Services. Zaragoza: CIHEAM-IAMZ

Ott, S., 1993. *The Circle of Mountains: A Basque Shepherding Community*. University of Nevada Press, Reno, NV. 242 pp.

Prince, S. D., E. Brown De Colstoun, and L. L. Kravitz, 1998. Evidence from Rain-Use Efficiencies does not indicate Sahelian Desertification. *Global Change Biology* 4:359-374

Prince, S. D., I. Becker-Reshef, and K. Rishmawi, 2009. Detection and Mapping of Long-term Land Degradation using Local Net Production Scaling: Application to Zimbabwe. *Remote Sensing of Environment* 113:1046-1057

Puigdefabregas, J., 1998. Ecological Impacts of Global Climate Change on Drylands and their Implications for Desertification. *Land Degrad. Develop.* 9: 393-406

Quirk, M., 2002. Managing Grazing. Pages 131-146 in A. C. Grice and K. C. Hodgkinson (Eds.), Global Rangelands: Progress and Prospects. CABI Publishing Oxon, UK

Reynolds, J. F., 2001. Desertification. Pages 61-78 in S. Levin (Ed.), Encyclopedia of Biodiversity. San Diego, CA: Academic Press

Salzman, P. C., 2004. *Pastoralists: Equality, Hierarchy, and the State*. Westview Press, Cambridge MA. 1993 pp.

Sandford, S., 1983. *Management of Pastoral Development in the Third World*. John Wiley and Sons, New York

- Savory, A., 1999. *Holistic Management: A New Framework for Decision Making*. Island Press, 2:616 pp.
- Seligman, N. G. and A. Perevolotsky. Has Intensive Grazing by Domestic Livestock Degraded the Old World Mediterranean Rangelands? Pages 93-103 in M Arianoutsou and R. H. Groves (Eds.) Plant-Animal Interactions in Mediterranean-Type Ecosystems. Kluwer, Dordrecht. 182 pp.
- Sheppard, E., Porter, P. W., Faust, D. R., Nagar, R., 2009. *A World of Difference: Encountering and Contesting Development*. Guilford Press, New York, NY. 2:665 pp.
- Sinclair, A. R. E., and J. M. Frywell, 1985. The Sahel of Africa: Ecology of a Disaster. *Canadian Journal of Zoology*. 63:987-994
- Smith, A. B., 1992. *Pastoralism in Africa: Origins and Development Ecology*. Ohio University Press, Athens. 305pp.
- Snyman, H. A., 1998. Dynamics and Sustainable Utilization of Rangeland Ecosystems in Arid and Semi-arid Climates of Southern Africa. *Journal of Arid Environments*. 39: 645-666
- Snyman, H. A., 2005. Rangeland Degradation in a Semi-arid South Africa- Influence on Seasonal Root Distribution, Root/shoot Ratios and Water-use Efficiency. *Journal of Arid Environments* 60: 457-481
- Stebbing, E. P., 1935. The Encroaching Sahara: The Threat to the West Africa Colonies. *Geographical Journal*. 85: 506-524
- Stock, R., 2004. *Africa South of the Sahara: A Geographical Interpretation*. Guilford Press, New York. 2:477 pp.
- Stone G. D., 1993. Agricultural Abandonment: A Comparative Study in Historical Ecology. Pages 74-84 in C. M. Cameron and S. A. Tomka (Eds.), *Abandonment of Settlements and Regions*. Cambridge: Cambridge University Press
- Thurow, T. L., 1991. Hydrology and Erosion. Pgs 141-159 in R. K. Heitschmidt and J. W. Stuth (Eds.) *Grazing Management: An Ecological Perspective*. Timber Press, Portland OR
- Thurow, T. L., 2000. Hydrologic Effects on Rangeland Degradation and Restoration Processes. Pages. 53-66 in O. Arnalds and S. Archer (Eds.), Rangeland Desertification. Kluwer Academic Publishers. Dordrecht, The Netherlands. 209 pp.
- Tucker, C.J., H. E. Dregne, and W. W. Newcomb, 1991. Expansion and Contraction of the Sahara Desert from 1980 to 1990. *Science* 253:299-301

UNCCD 1995. Down to Earth: A Simplified Guide to the Convention to Combat Desertification, Why it is Necessary and What is Important and Different about it. Bonn, Germany: Secretariat for the United Nations Convention to Combat Desertification. URL = <http://www.unccd.int/knowledge/menu.php>

Veron, S. R., J. M. Paruelo, and M. Oesterheld, 2006. Assessing Desertification. *Journal of Arid Environments*. 66:751-763

Wolfson, Z, 1990. Central Asian Environment: A Dead End. *Environmental Policy Review*. 4(1):29-46

Voisin, A, 1988. *Grass Productivity*. Island Press, Washington, DC USA. 353 pp.

Yalcin, B. C, 1986. Sheep and Goats in Turkey. FAO Animal Production and Protection Paper 60. Food and Agricultural Organization of the United Nations, Rome. 110pp.

Waller, R. D., 1985. Ecology, Migration, and Expansion in East Africa. *African Affairs*. 84: 347-370

Weber, K. T., F. Chen, B. Gokhale, C. G. Bueno, and C. L. Alados, 2009. Application of Composite-NDVI in Semiarid Rangelands. Pages 71-84 in K. T. Weber and K. Davis (Eds.), Final Report: Comparing Effects of Management Practices on Rangeland Health with Geospatial Technologies

Weber, K. T. and B. Gokhale, 2010. Effect of Grazing Treatment on Soil Moisture in Semiarid Rangelands. Pages 165-180 in K. T. Weber and K. Davis (Eds.), Final Report: Forecasting Rangeland Condition with GIS in Southeastern Idaho. 193 pp.

Wilson, E. O., 2007. Foreword. Pgs. xiii-xiv in D. J. Penn and I. Mysterud (Eds.), Evolutionary Perspectives on Environmental Problems. Aldine Transaction, New Brunswick NJ. 364pp.

**Recommended citation style:**

Weber, K.T. and S. Horst, 2011. Applying Indigenous Pastoralist Experiences to Western Range Management. Pages 197-210 in K. T. Weber and K. Davis (Eds.), Final Report: Assessing Post-Fire Recovery of Sagebrush-Steppe Rangelands in Southeastern Idaho. 252 pp.

## **Detecting Dead Shrub Patches Using Remote Sensing Techniques in Southeast Idaho**

Darci Hanson, GIS Training and Research Center, Idaho State University, Pocatello, ID 83209-8104, (<http://giscenter.isu.edu>, email: [giscenter@isu.edu](mailto:giscenter@isu.edu))

Keith T. Weber, GISP. GIS Director, Idaho State University. GIS Training and Research Center, 921 S. 8<sup>th</sup> Ave., Stop 8104, Pocatello, ID 83209-8104. [webekeit@isu.edu](mailto:webekeit@isu.edu)

### **ABSTRACT**

Five remote sensing satellite sensors (Hyperion [30m x 30m spatial resolution], Landsat 5 TM [30m x 30m spatial resolution], Satellite Pour l'Observation de la Terre (SPOT) 5 [10m x 10m spatial resolution], Quickbird [2.4m x 2.4m spatial resolution], and Worldview-2 [1.8m x 1.8m spatial resolution]) were used to determine if patches of dead-shrubs could be differentiated among a matrix of ground cover types (basalt, bare ground, grass, and live-sagebrush) using classification and regression tree analysis. Results for all image classifications were unsuccessful (overall accuracy < 75%) suggesting it may not be possible to detect dead-shrubs with the satellite-based sensors tested. However, pair-wise Analysis of Variance (ANOVA) results for *in situ* spectra collected with a handheld Analytical Spectral Devices, Inc (ASD) FieldSpec Pro field spectroradiometer, showed significant differences between dead-shrubs and all other ground cover types ( $P < 0.001$ ). To aid in the characterization of vegetation at the study site and better understand the spectral signatures of landscape features, shrub height, age, and percent water content were also compared with ANOVA results indicating a difference in percent water content between live and dead-shrubs ( $P < 0.001$ ).

**KEYWORDS:** *Shrub die-off, shrub mortality, sampling, GIS, remote sensing, sagebrush, image classification*

## INTRODUCTION

Sage-grouse (*Centrocercus urophasianus*) are a sagebrush-obligate species requiring large, contiguous expanses of habitat (Connelly et al., 2004; Aldridge et al., 2008; Knick and Connelly, 2011). Some form (particularly big sagebrush (*Artemisia tridentata*) and silver sagebrush (*Artemisia cana*)) and quantity (~15-30% canopy cover) of sagebrush within the landscape are necessary to meet seasonal food, cover, and nesting requirements of sage-grouse (Patterson 1952, Connelly et al., 2000, Connelly et al. 2011, Knick and Connelly, 2011). While the quantity, or area, of available habitat is important so is habitat quality. The National Land Cover Database (NLCD) maps typically designate sagebrush dominated areas as shrub/scrub (Figure 1) and while the entirety of the NLCD land cover classification cannot be treated as viable sage-grouse habitat, the sage-grouse conservation area (SGCA) falls within a majority these areas (Connelly et al. 2004) (Figure 2; black boundary). Similarly, sage-grouse distribution closely mirrors sagebrush distribution (Figure 3) and for this reason, land managers may treat most shrub/scrub areas as viable sage-grouse habitat.

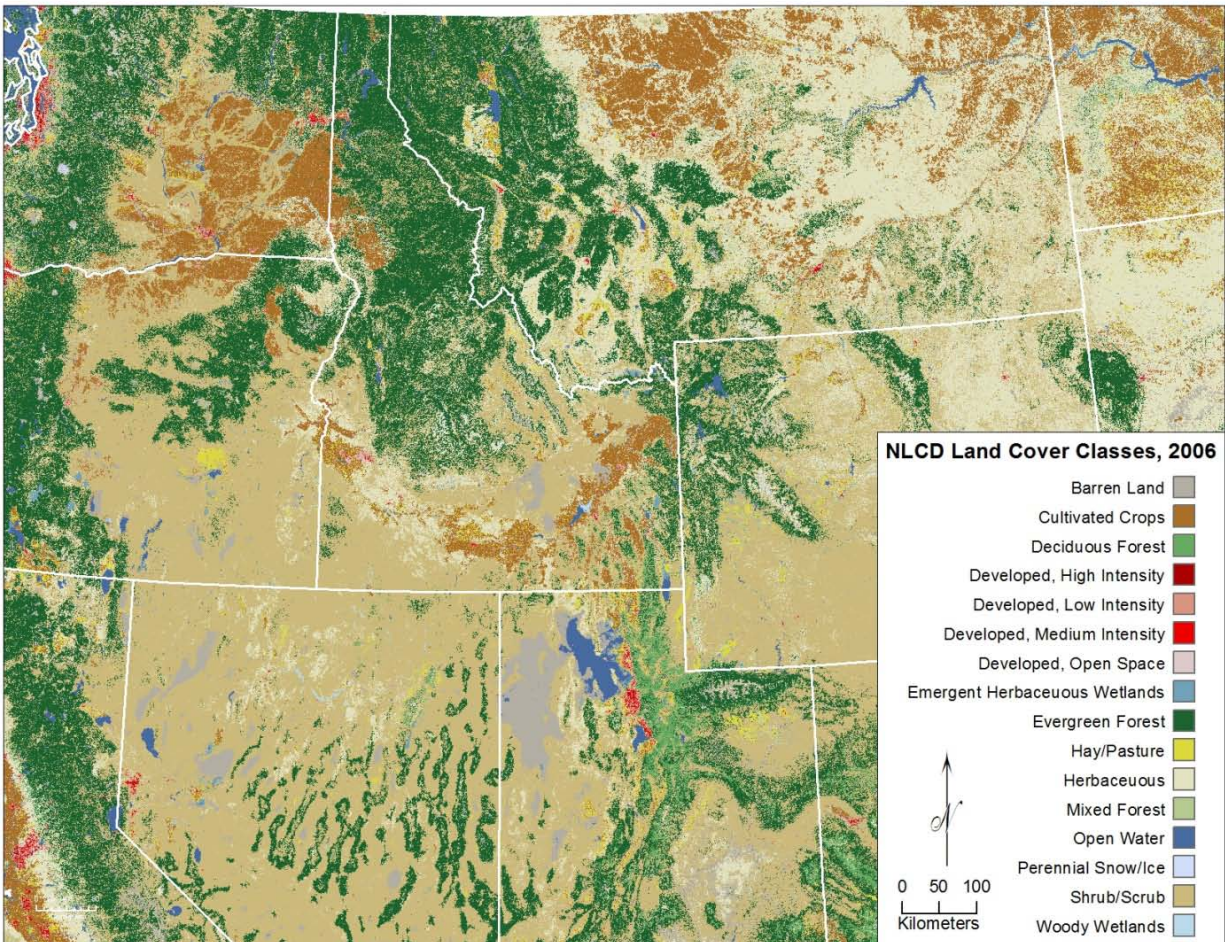


**Figure 1. Land cover based upon the National Land Cover Database (NLCD) identifying areas of shrub/scrub land cover type, which land managers often delineate as sage-grouse habitat.**

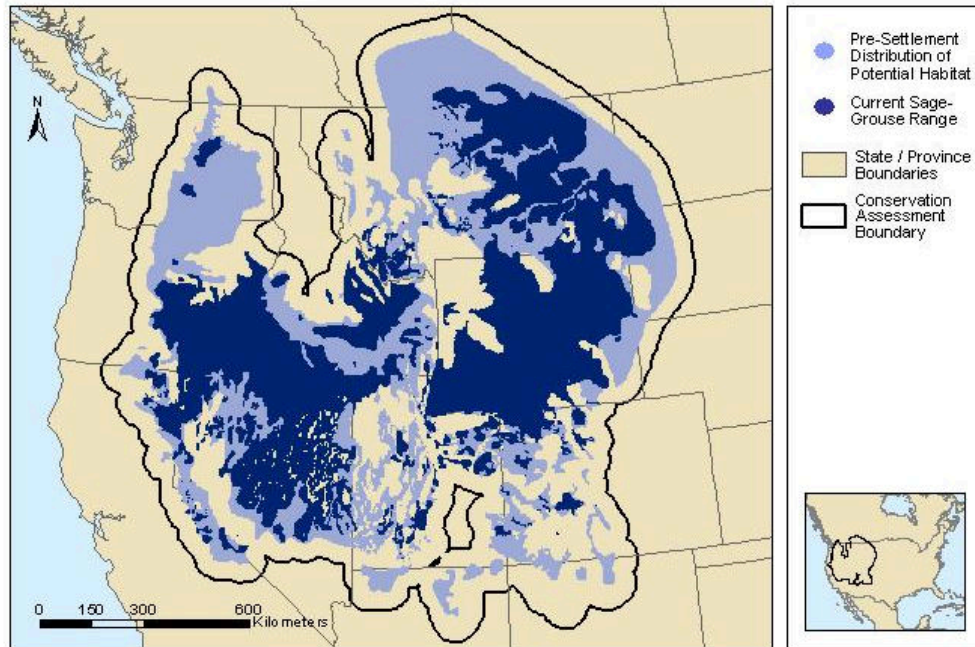


Figure 2. Sage-grouse conservation assessment boundary (SGCA) based on pre-settlement distribution of sage-grouse (source: Connelly et al. 2004).

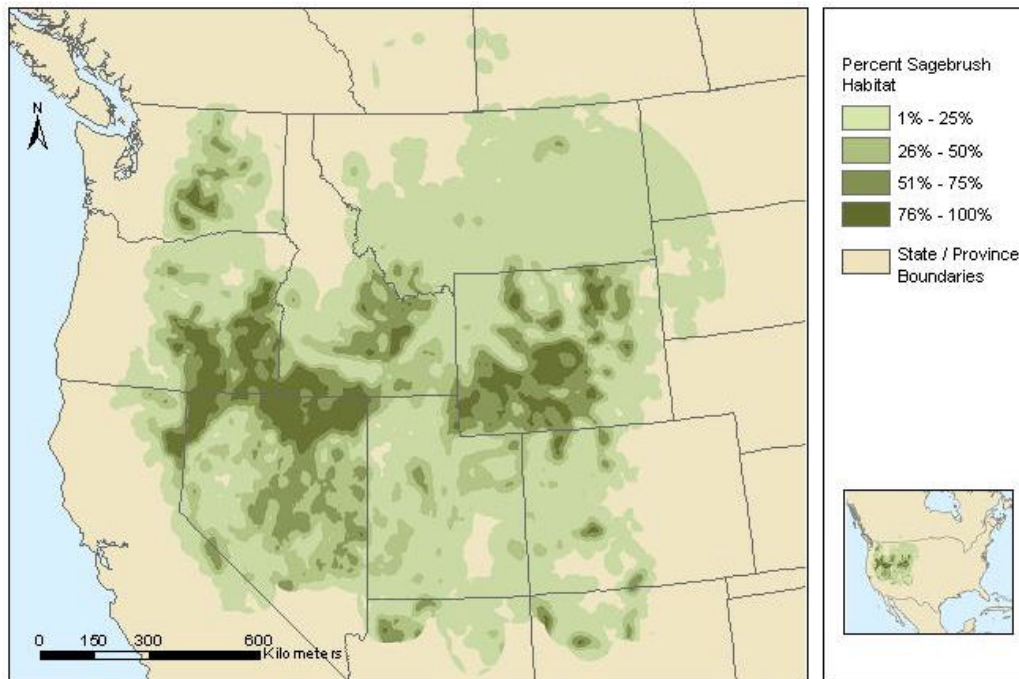


Figure 3. Estimated distribution of sagebrush density within the SGCA (source: Connelly et al. 2004).

Patches of shrub mortality can occur within otherwise healthy stands of sagebrush leading to an overestimation of total sage-grouse habitat. Sagebrush (shrub) mortality in semiarid rangelands was a widespread phenomenon in the salt-desert region of Utah between 1983 and 1988 due to persistent wet conditions (Wallace et al., 1989). In Wyoming, Colorado, and Utah snow-mold fungus was also indicated

as a possible cause of shrub mortality (Hess et al. 1985). Though this phenomenon is known to occur throughout the semiarid sagebrush-steppe for a variety of reasons including drought, wetter than normal seasons, snow-mold fungus, and insects (Hess et al. 1985, Harper et al. 1989, Haws et al. 1989, Walser et al. 1989, Wiens et al. 1991, Tilley et al. USDA NRCS, Takahashi and Huntly 2010, Hampton and Huntly 2010), published reports pertaining to this phenomenon in southeast Idaho focus primarily on shrub mortality caused by leaf defoliating insects such as the Aroga moth (*Aroga websteri*). Sagebrush is the exclusive larval host of the Aroga moth and, in high numbers larva can kill host plants and reduce the production of foliage and flowering by surviving plants (Hampton and Huntly, 2010). Takahashi and Huntly (2010) reported increases in inflorescence growth (22%), flower production (325%), and seed production (1053%) after an experimental removal of insect herbivores from big sagebrush (*Artemisia tridentata*) plants with insecticide. Regardless of the cause, shrub mortality affects sage-grouse habitat as it impacts the primary source of food and shelter.

The ability to differentiate dead-shrubs from proximal targets with remote sensing imagery would allow land managers to better assess the quality of sage-grouse habitat across their distribution. Remote sensing systems onboard satellites provide high quality yet relatively inexpensive data, and are useful for monitoring a variety of landscape characteristics (Weber et al. 2008, Weber et al. 2009, Wheeler and Glenn 2003, McMahan et al. 2003, Sankey et al. 2008). A limitation of satellite-based sensors that can impact their ability to accurately record target radiance is the signal to noise ratio (SNR) of the sensor.

Atmospheric scattering and the signal to noise ratio (SNR) of a sensor can affect the accuracy of recorded radiance of a target at the sensor. Scattering occurs when reflected light strikes other particles in the atmosphere before reaching the satellite sensor. The type of scattering (Rayleigh, Mie, or Nonselective) is dependent upon the size of particles in the atmosphere, their abundance, the wavelength of the reflected light, and the depth of the atmosphere through which the energy is traveling (Campbell, 2008). Rayleigh scattering is attributed to atmospheric gas molecules and causes visible effects such as a blue sky. Mie scattering occurs when particles have diameters that are roughly equivalent to the wavelength of the scattered radiation, and is experienced primarily in the lower atmosphere through larger particles such as dust or pollen. Nonselective scattering accounts for what we observe as a whitish haze in the atmosphere, and refers to scattering that occurs from particles larger than the wavelength of the scattered light (Campbell, 2008). The SNR of a particular sensor can also influence the ability to accurately record reflected energy of a target. The signal refers to differences in image brightness caused by actual variations in scene brightness whereas noise refers to variations unrelated to scene brightness, and more with the inherent abilities of the sensor itself. If the magnitude of noise is large relative to the signal, the resulting image will not provide a reliable representation of the target of interest (Campbell, 2008). Because of these effects, compiling a spectral library characterizing *in situ* target spectra can be useful during classification of remotely sensed imagery.

Glenn et al. (2005) successfully detected leafy spurge occurrence in Swan Valley, Idaho using HyMap hyperspectral data collected by the HyVista. *In situ* spectra of leafy spurge and other proximal vegetation were collected using an Analytical Spectral Devices, Inc (ASD) FieldSpec Pro field spectroradiometer concurrent with image acquisition to characterize *in situ* target reflectance patterns at various wavelengths across the electromagnetic (EM) spectrum. Spectral profiles were combined with known geographic locations of leafy spurge to derive endmembers within images for two data collection years.

Characterization of *in situ* target spectra enabled visual analysis of minor variations in reflectance and absorption patterns of leafy spurge across the EM spectrum, while also serving to help the authors determine if a spectral subset of image data would be necessary for successful classification.

Williams and Hunt (2004) had success detecting leafy spurge occurrence in northeast Wyoming, near Devils Tower National Monument using Airborne Visible Infrared Imaging Spectrometer (AVIRIS) and spectral mixture analysis. *In situ* spectra of leafy spurge were collected with an ASD Fieldspec UV/VNIR Spectroradiometer, and were used to verify identification of spectral endmembers of leafy spurge. These positive results further illustrate how characterizing target spectra through field collection of *in situ* spectra can help achieve positive results during image classification.

Published reports pertaining to remote detection of shrub mortality is limited. Chopping et al. (2008) describe a new method for retrieving fractional cover of large woody shrubs at the landscape scale using Earth Observation System (EOS) Multiangle Imaging SpectroRadiometer (MISR) derived imagery and a hybrid geometric-optical canopy reflectance model. Stow et al. 2007 used very high spatial resolution (1m) multispectral imagery collected with an Airborne Data Acquisition and Registration (ADAR) system with visible near infrared (V/NIR) datasets to generate shrub cover change maps for Mission Trail Regional Park in San Diego, CA. Overall accuracy and kappa statistics for classification were 83% and 0.64 respectively.

The reflectance of an object over various wavelengths of the EM spectrum is commonly referred to as a spectral signature (Chuvieco and Huete 2010). Spectral signatures are initially recorded as radiance by the sensor that has been reflected by targets from a terrain. They are then converted to reflectance values to ease interpretation and to enable cross-comparison of remote sensing image data of an area from different dates. To reliably detect a feature using remote sensing, that feature must exhibit a unique spectral signature. It was hypothesized that a difference in plant water content between dead-shrubs and live-sagebrush might be a key factor for successful classification of dead-shrub. There is a strong relationship between the reflectance in the shortwave infrared (SWIR) (1550 – 1750 nm and 2080 – 2350 nm) and the amount of water present in the leaves of a plant canopy (Jensen, 2007). Water in plants absorb incident energy in this region with increasing strength at longer wavelengths.

To detect, and thereby characterize the extent of shrub mortality within sage-grouse habitat areas of southeast Idaho, remote sensing technologies were applied. This paper describes the field sampling performed during the summer of 2010 as well as laboratory analysis of image data from five remote sensing satellite-based sensors, to determine if patches of dead-shrubs could be detected among the matrix of ground cover types at the O'Neal Ecological Reserve, Idaho. This study used random, adaptive, and directed sampling techniques to collect various sagebrush plant characteristics including field and laboratory measured weights of twig samples from dead-shrubs and live-sagebrush to calculate percent water content, along with a plot level determination of homogeneity. These data were used to classify imagery for presence/absence of dead-shrubs. Vegetation data were collected to determine if there was a statistical difference in percent water content between dead-shrubs and live-sagebrush, and likewise, if a difference in percent water content would translate to spectral differentiation in the SWIR region of the EM spectrum.

## METHODS

### Study area

The O'Neal Ecological Reserve (Figure 4) is located along the Portneuf River, approximately 30 km southeast of Pocatello, Idaho (42° 42' 25"N, 112° 13' 0" W). The O'Neal receives <0.38 m of precipitation annually with nearly 50 percent falling as snow in the winter months (October 1- March 31). An average of 0.15 m (SE = 55.4) of rainfall occurs during the growing season (April 1 – September 31). The topography is relatively flat with a mean elevation of approximately 1426 m (1400-1440 m). The site is characterized by shallow, well drained soils over basalt flows originally formed from weathered basalt, loess, and silty alluvium that remain homogenous throughout the site (USDA NRCS 1987, Weber and Gokhale 2010). Dominant plant species include big sagebrush (*Artemisia tridentata*) with various native and non-native grasses, including Indian rice grass (*Oryzopsis hymenoides*) and needle-and-thread (*Hesperostipa comata*) (Davis and Weber, 2010). The O'Neal is managed by Idaho State University (ISU) while land immediately surrounding it is managed by the USDI BLM. This area has a history of rest-rotation cattle grazing (> 20 years) at low stocking rates (300 AU/ 1467 ha [6 AUD ha<sup>-1</sup>]). The last fire to occur within the O'Neal was in 1992.

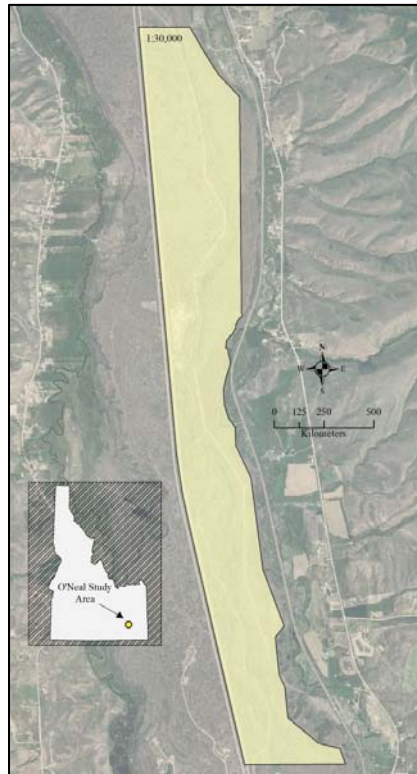


**Figure 4. Study area: The O'Neal Ecological Reserve, represented by the polygon, is located near McCammon, Idaho, 30km south of Pocatello. This was the study area was chosen as part of a research project attempting to remotely detect dead-shrub patches using five satellite-based sensors (Hyperion, Landsat 5 TM, SPOT-5, Quickbird, and Worldview-2)**

### Field data collection

Two sampling sessions were completed during the summer of 2010. The first session (14 June 2010 – 25 June 2010) consisted of 60 randomly located sample points followed with adaptive sampling applied to

stands determined to be homogeneous (> 50%) for dead-shrub based on protocols described at [http://giscenter.isu.edu/research/Techpg/nasa\\_postfire/results.htm](http://giscenter.isu.edu/research/Techpg/nasa_postfire/results.htm).

Sample points were navigated to using a Trimble GeoXH GPS receiver (< 1.0 m @ 95% CI following post-process differential correction) with each point referred to as plot center. An insufficient number of dead-shrub sites were found during the initial sampling session ( $n = 13$ ) and as a result, a directed sampling approach was used in the second sampling session (29 June 2010 – 14 July 2010). The directed sampling approach is one where field personnel use their knowledge of the study area to locate additional sample sites. While this approach introduced a bias into the sample dataset it was effective for locating uncommon targets such as homogeneous stands of dead-shrubs. When a new site was located, the same sampling protocol as described above was followed. The goal of the field collection campaign was to collect a minimum of 60 live-sagebrush and 60 dead-shrub sites.

Sagebrush and dead-shrub twig samples were collected from up to four plants at each site and weighed using a Pesola scale (+/- 1 g). Selected twigs were approximately 5 mm in diameter and approximately 250 mm in length. A total of 30 live-sagebrush twig samples were collected as well as 30 dead-shrub twig samples. These samples were placed in a bag, labeled with a unique ID consisting of the sample point ID, date, and sequence (1-4) and returned to the laboratory for drying and determination of percent water content (Davis et al. 2011).

Field spectra were collected from five *in situ* target types (basalt, bare ground, grass, dead-shrub, and live-sagebrush) during summer, 2010 ( $n = 2,565$ ). Data were collected using the ASD FieldSpec Pro and imported into Microsoft Excel for further processing. Spectra were sorted by target and wavelength.

#### *Image acquisition and processing*

Imagery for the O'Neal study area was collected during the summers of 2009-2010 to capture peak greenness of sagebrush in southeast Idaho. This was determined by viewing time-lapse video of sagebrush at the O'Neal from 12 March 2010 through 10 October 2010 (URL here for that file) (Table 1).

**Table 1. Remote sensing satellite imagery collected for the O'Neal Ecological Reserve, Idaho May - July, as part of a research project to remotely detect dead-shrub patches using five satellite-based sensors (Hyperion, Landsat 5 TM, SPOT-5, Quickbird, and Worldview-2).**

<b>Sensor</b>	<b>Collection Date</b>	<b>Spatial Resolution</b>	<b>Spectral Resolution</b>
Hyperion	16 June 2010	30m x 30m	220 bands: 400 nm to 2500 nm
Landsat 5 TM	07 May 2010	30m x 30m	7 bands: Blue, Green, Red, NIR, SWIR 1. SWIR 2
SPOT 5	20 June 2010	10m x 10m	4 bands: Green, Red, NIR, SWIR
Quickbird	06 June 2009	2.4m x 2.4m	4 bands: Blue, Green, Red, NIR
Worldview-2	16 May 2010	1.8m x 1.8m	8 bands: Blue, Green, Red, NIR1, NIR2 Coastal Blue, Yellow, Red Edge

All satellite imagery (excluding Hyperion) were atmospherically corrected using Idrisi Taiga (ver. 16.04) image processing software. Images (excluding Landsat) were co-registered for improved horizontal positional accuracy. Landsat data were delivered registered to a high degree of accuracy, however to

confirm registration accuracy, data were compared against 2004 National Agricultural Imagery Program (NAIP) imagery (1m x 1m spatial resolution) (horizontal positional accuracy within +/- 5m). WV-2 and Quickbird imagery were co-registered to known ground control points of high positional accuracy (Weber et al., 2010<sup>b</sup>). Due to coarse pixel resolution, it was not possible to co-register Hyperion, Landsat, and SPOT imagery to the same ground control points used for WV-2 and Quickbird, therefore images were co-registered to the 2004 NAIP imagery. Root mean square error (RMSE) was <50% (Table 2) of the pixel resolution for all co-registered imagery, which is suggested as the minimum necessary for reliable classification (Weber, 2006).

**Table 2. Co-registration results for remote sensing satellite imagery collected over the O’Neal Ecological Reserve, Idaho**

<b>Sensor</b>	<b>Spatial Resolution (mpp)</b>	<b>RMSE</b>	<b>% pixel size</b>
Hyperion	30.0	2.76m	9
Landsat	30.0	2.97m	10
SPOT	10.0	1.68m	17
Quickbird	2.4	0.07m	3
WV-2	1.8	0.10m	6

Spectral signatures were extracted for all images in Idrisi (Image Processing →Signature Development →SEPSIG) and spectral differentiability was tested using the Transformed Divergence Index. Transformed divergence is a commonly used measure of differentiability that calculates the statistical “distance” between classification categories. The calculated differentiability value provides a measure of potential classification accuracy. With a multiplier constant of 2,000, a calculated value of 1,500 is the suggested threshold for significant differentiability (Richards 1993, Lillesand and Kiefer 2000).

Supervised classification of imagery was performed in Idrisi to differentiate dead-shrub classes from live shrub classes using 119 field sample points acquired during the summer field sampling sessions. Sample points were separated into two classes where an attribute of 1 indicated dead-shrub and 2 indicated "other" (e.g., live-shrub, grasses, bare ground, or basalt). Using Hawth’s Tools (Beyer, 2004) in ArcMap 9.3.1, these sample points were randomly selected and divided into training and validation sites to allow for independent validation. Using Idrisi a presence/absence model for dead-shrubs was created using classification and regression tree analysis (CTA) (Image Processing →Hard Classifiers →CTA). Classification and regression tree analysis is a non-probabilistic, non-parametric statistical technique that is adept at modeling data that is non-normally distributed (Breiman et al. 1998; Friedl and Brodley 1997; Lawrence and Wright 2001; Miller and Franklin 2001). It is hypothesized that dead-shrub patches are non-normally distributed and for this reason, may be modeled more accurately with CTA relative to other supervised classification techniques such as maximum likelihood, which may be more appropriate when a dataset is known to follow a certain distribution pattern (Clark Labs, 2008). The CTA algorithms select useful spectral and ancillary data which optimally reduce divergence in a response variable (Lawrence and Wright 2001). CTA uses machine-learning to perform binary recursive splitting operations and ultimately yields a classification tree diagram that is used to produce a model of the response variable. Splitting algorithms common to CTA include entropy, gain ratio, and Gini. The entropy algorithm has a tendency to over-split, creating an unnecessarily complex tree (Zambon et al., 2006). The gain ratio

algorithm addresses the over-splitting problem through normalization while the Gini algorithm partitions the most homogeneous clusters first using a measure of impurity while isolating the largest homogeneous category from the remainder of the data (McKay and Campbell 1982; Zambon et al., 2006). As a result, classification trees developed using the Gini splitting algorithm are less complex and therefore more easily understood by the analyst. For these reasons, the Gini splitting algorithm was selected for use in this study.

A key advantage of CTA is its ability to use both spectral and non-spectral data selectively during the splitting and classification process. This allows for the use of topographic data which may be equally important in modeling dead-shrub. Such ancillary data can be used with other supervised classification techniques (Lillesand et al., 2008) but classifiers like maximum likelihood use all input data to arrive at a final classification. This is in contrast to the advantage of CTA noted above, which selectively applies input data in its classification process.

All atmospherically corrected multispectral imagery bands and an NDVI layer were used for the classification. For Hyperion, 61 image bands were selected from 220 as part of a standard data reduction technique along with three derivative slope bands for image classification. These bands were selected to correspond with wavelengths determined through visual analysis of graphed *in situ* spectra as optimal for detection of dead-shrub patches based on mean reflectance peaks of dead-shrub spectra and areas of non-overlapping variability for target spectra.

Normalized Difference Vegetation Index (NDVI) is an index of photo-synthetically active vegetation and is calculated using the red and near infrared (NIR) bands of multispectral imagery. The resulting NDVI has an interval of -1 to +1, where -1 is no vegetation and +1 is pure photo-synthetically active vegetation (Rouse et al., 1973, Tucker 1979). High reflectance of vegetation in the NIR wavelengths due to spongy mesophyll within leaf structure makes NDVI a very useful landscape productivity parameter in its ability to highlight areas of photo-synthetically active vegetation. Though there has been some evidence that NDVI is less successful a predictor variable in study areas where bare-soil exceeds 20% (Sankey et al. 2009), it is still widely accepted to be useful as a predictor variable for vegetation and is used in rangeland studies (Weber et al. 2009, Gokhale and Weber. 2009, Blanco et al. 2007, Aldridge and Boyce 2007, Zou et al. 2006). NDVI was included in this study for all multispectral imagery, as an additional separation measure of dead-shrub and was calculated in Idrisi Taiga image processing software following equation 2. The inclusion of this measure helped to isolate actively photosynthesizing vegetation from senesced vegetation.

$$NDVI = \frac{NIR\ Band - Red\ Band}{NIR\ Band + Red\ Band} \text{ (Eq. 2)}$$

#### *Laboratory and statistical analysis*

Twig samples were dried in ovens at 80° Celsius for 48 hours. Once dried, samples were re-weighed using the same Pesola scale used to weigh them in the field. Field weights were defined as “wet weight” and post-drying laboratory weights as “dry weights.” Wet and dry weights were recorded in MS Excel. Percent water content was calculated following equation 3. A single factor ANOVA test was used to determine if there was a difference in percent water content between live-sagebrush and dead-shrubs.

$$\text{Percent Water Content} = 1 - (\text{dry weight/wet weight}) \text{ (Eq. 3)}$$

Descriptive statistics for *in situ* spectra were calculated, and mean reflectance values for each target type were graphed creating a spectral profile of each target type. Variability of reflectance (@ 95% CI) within each target spectra was calculated by multiplying the standard error by 1.96 (or the z-score for a 95% confidence interval). These values were then applied to the calculated mean of each target at each wavelength and graphed. Targets were considered differentiable when separated by > 1.96 standard error. Pair-wise single factor ANOVA tests were performed (basalt, bare ground, grass, and live-sagebrush) to determine if dead-shrubs could be differentiated from the matrix of other rangeland features.

Derivative spectroscopy, or derivative analysis, is a tool commonly used in the analysis of hyperspectral remote sensing data. Derivative techniques enhance minute fluctuations in spectral reflectance and may help separate closely related absorption features (Louchard et al., 2002). Spectral derivative techniques have been applied in remote sensing and found to eliminate background signals and differentiate overlapping signatures. When applied to remote sensing, derivative analysis is a measure of the slope of the line of a portion of the spectral profile where the slope of the line appears to differ among target types. For the purpose of this research this technique was used as an additional separation measure for classification of dead-shrub using Hyperion hyperspectral imagery.

Spectral profiles were analyzed visually to locate points where the slope of the line appeared to differ from the slopes created by the other targets within the same waveband region. Derivative slopes were calculated in Idrisi using the Hyperion imagery for three spectral regions using the following equation (Tsai and Philpot 1998):

$$\text{Slope} = \frac{s(\lambda_i) - s(\lambda_j)}{\Delta\lambda} \text{ (Eq. 3)}$$

Where  $s(\lambda_i)$  is the reflectance at wavelength  $i$ ,  $s(\lambda_j)$  is the spectral reflectance at wavelength  $j$ , and  $\Delta\lambda$  refers to difference between wavelengths  $i$  and  $j$ .

#### *Classification accuracy assessment*

Resulting classification layers were independently validated in Idrisi (Image Processing → Accuracy Assessment → ERRMAT) using a standard error matrix and Kappa statistic, where predicted (modeled) target type (e.g., dead-shrub) locations were compared against known (field) target type (e.g., dead-shrub) locations (Table 3). The Kappa index of agreement served as an indicator of how well the classification performed relative to a random classification. Classifications with ≥ 75% overall accuracy were considered reliable (Goodchild et al., 1994, Weber 2006). However, classifications with overall accuracy of ~ 70% were still considered positive results. Paired error matrix tests of significance (Congalton and Green, 2008) were used to determine if any of the image classifications performed statistically better than any other, where the null hypothesis (0) indicates no difference between classifications.

## **RESULTS AND DISCUSSION**

### *Field data*

Of the sample points collected 97.7% were post-process differentially corrected to < 1m, while 0.002% were corrected at an accuracy > 1m. Sub-meter accuracy of field locations resulted in a high degree of horizontal positional accuracy which ensured that field locations were reliably located in the correct pixel during image classification. For high spatial resolution remote sensing imagery such as Quickbird (2.4m

spatial resolution) or Worldview-2 (1.8m spatial resolution) a high degree of horizontal positional accuracy (RMSE < 50%), because if the target being classified comprises one pixel of that imagery, a slight shift in the actual location relative to the measured field sites can result in lower overall accuracy (Weber 2006, Weber et al. 2007).

*Image processing*

Transformed divergence values for each of the spectral signatures developed for this study were well below the threshold (1500; Table 4) indicating low potential for differentiation of dead-shrub from the matrix of other targets during image classification.

**Table 4. Transformed divergence values for five remote sensing satellite images (Hyperion, Landsat 5 TM, SPOT 5, Quickbird, and Worldview-2) testing spectral separability of dead-shrub patches using the SEPSIG tool in Idrisi Taiga image processing software as part of a research project attempting to remotely detect dead-shrub patches at the O’Neal Ecological Reserve, Idaho.**

<b>Transformed</b>	<b>Divergence</b>	<u>Sensors</u>				
		<b>Hyperion</b>	<b>Landsat</b>	<b>SPOT</b>	<b>Quickbird</b>	<b>WV-2</b>
<b>Values</b>		840.82	563.77	826.64	952.57	605.96

*Laboratory and statistical analysis*

The mean percent water content of live-sagebrush plants was 64.6% (SE = 0.01; n = 30) and 15.6% for dead-shrubs (SE = 0.03; n = 30) and ANOVA results indicated a significant difference (P < 0.001) (Davis et al., 2010). These results suggest there is a difference in water content between dead-shrub and live-sagebrush, which means that dead-shrub patches should exhibit greater reflectance values in the SWIR region of the EM spectrum relative to live-sagebrush which would experience greater absorption at these wavelengths. These results support the hypothesis that a spectral band sensitive to the SWIR region may be important for successful classification of dead-shrubs.

Pair-wise single factor ANOVA tests for differentiability between ASD field spectra of dead-shrub and the other *in situ* targets (basalt, bare ground, grass, and live-sagebrush) revealed a statistical difference between all paired samples (P < 0.001). Calculated variability of spectra within each target class was narrow (spectral separation > 1.96 SE) further supporting evidence for differentiability among target spectra (Hanson et al., 2010). This indicates that dead-shrub patches have a unique spectral signature (the unique combination of reflected and absorbed EM radiation at varying wavelengths that uniquely identifies a target) relative to the other target types used in this study (basalt, bare ground, grass, and live-sagebrush), and therefore may be detectable via a remote sensing platform.

Three points of slope deviation were found among the mean *in situ* target spectra. These line-segments were found between 700 nm and 730 nm, 1115 nm and 1140 nm, and 1290 nm and 1330 nm (Figure 5). The resulting slopes were selected as they are considered fundamentally diagnostic (Becker et al. 2005). Slopes of these line-segments were calculated using Hyperion bands 38 and 35, 97 and 99, and 115 and 118 respectively following equation 3.

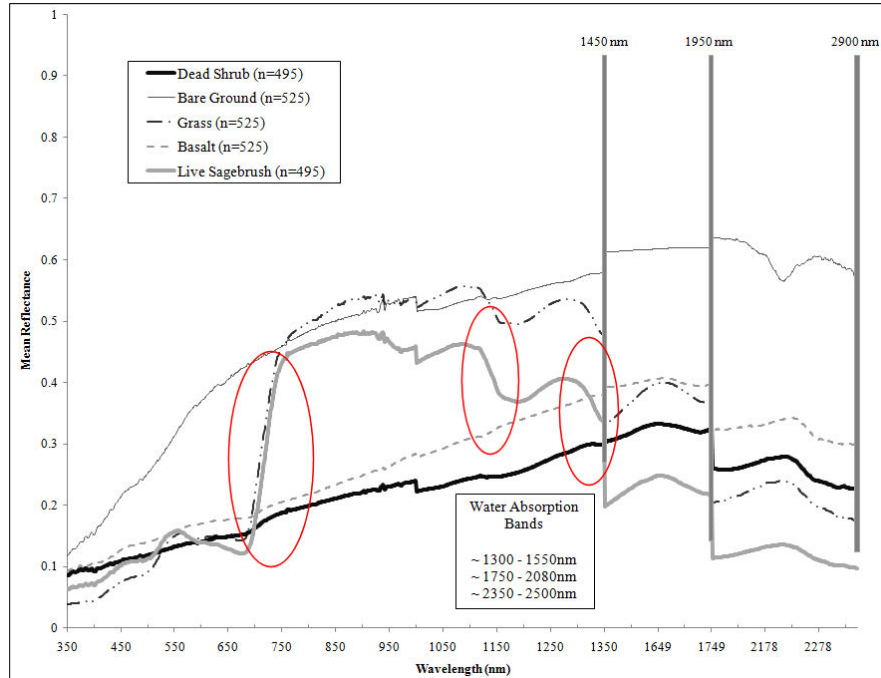


**Figure 5.** Points of slope deviation among mean *In situ* target spectra (basalt, bare ground, grass, dead-shrub, and live-sagebrush) collected at the O’Neal Ecological Reserve, Idaho.

The spectral profiles were superimposed with representations of the image bands for each sensor included in this study to gain insight as to which bands might be useful for classification (Figures 6 through 9). Visual analysis of these data revealed the reflectance peaks for dead-shrub spectra were consistently different from other target spectra between 700 nm and 2500 nm. Image bands for Hyperion were not superimposed with the spectral profiles because the excessive number of available bands (220) and narrow band widths characteristic of hyperspectral data resulting in near continuous spectral coverage. The bands that appeared to show the greatest difference between dead-shrub spectra and other targets for each of the sensors were: NIR, SWIR-1, and SWIR-2 for Landsat 5 TM (Figure 6); NIR and SWIR for SPOT 5 (Figure 7); NIR for Quickbird (Figure 8); and red edge (RE), NIR-1 and NIR-2 for WV-2 (Figure 9).

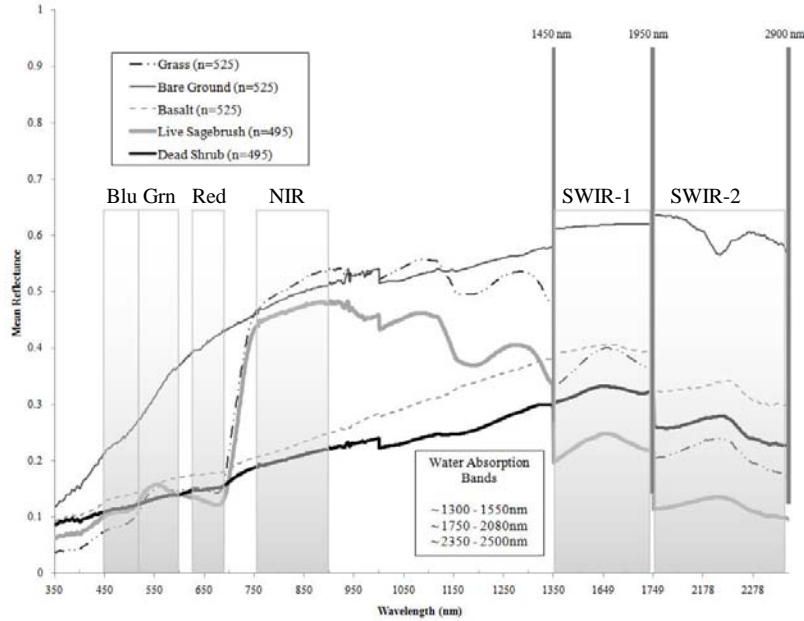


**Figure 6.** Landsat 5 TM image bands superimposed with plotted mean reflectance of *in situ* target spectra collected at the O’Neal Ecological Reserve, Idaho as part of a research project attempting to remotely detect dead-shrub patches using five satellite-based sensors (Hyperion, Landsat 5 TM, SPOT-5, Quickbird, and Worldview-2) This graph was used as a pre-analysis tool to get an idea of which bands might be useful during image classification for the successful identification of dead-shrub patches.

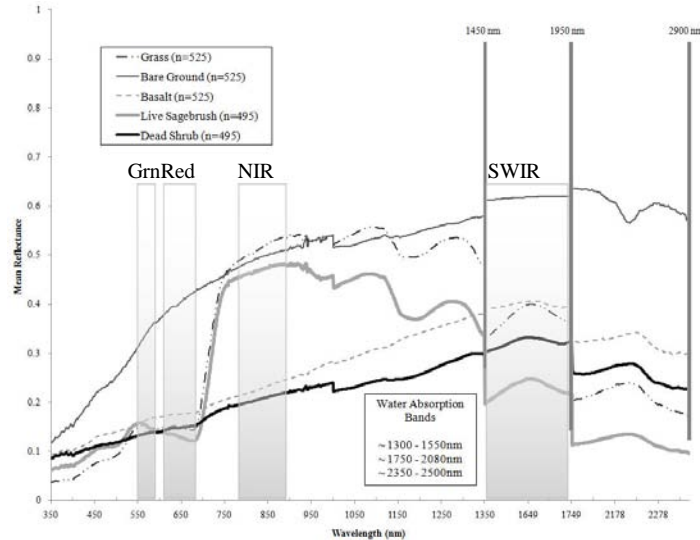


**Figure 7.** Spot 5 image bands superimposed with plotted mean reflectance of *in situ* target spectra collected at the O’Neal Ecological Reserve, Idaho as part of a research project attempting to remotely detect dead-shrub patches using five satellite-based sensors (Hyperion, Landsat 5 TM, SPOT-5, Quickbird, and Worldview-2) This graph was used as a pre-analysis tool to get an idea of which bands might be useful during image classification for the successful identification of dead-shrub patches.

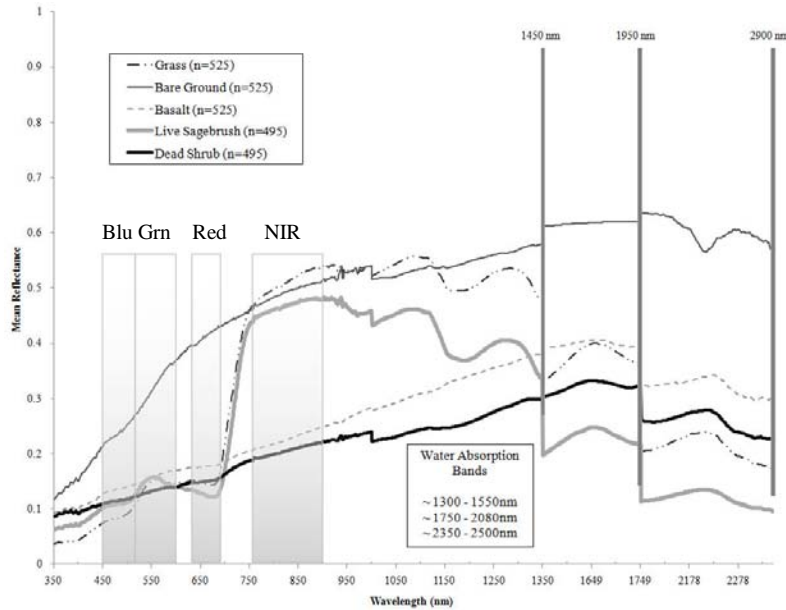


Figure 8. Quickbird image bands superimposed with plotted mean reflectance of *in situ* target spectra collected at the O’Neal Ecological Reserve, Idaho as part of a research project attempting to remotely detect dead-shrub patches using five satellite-based sensors (Hyperion, Landsat 5 TM, SPOT-5, Quickbird, and Worldview-2) This graph was used as a pre-analysis tool to get an idea of which bands might be useful during image classification for the successful identification of dead-shrub patches.

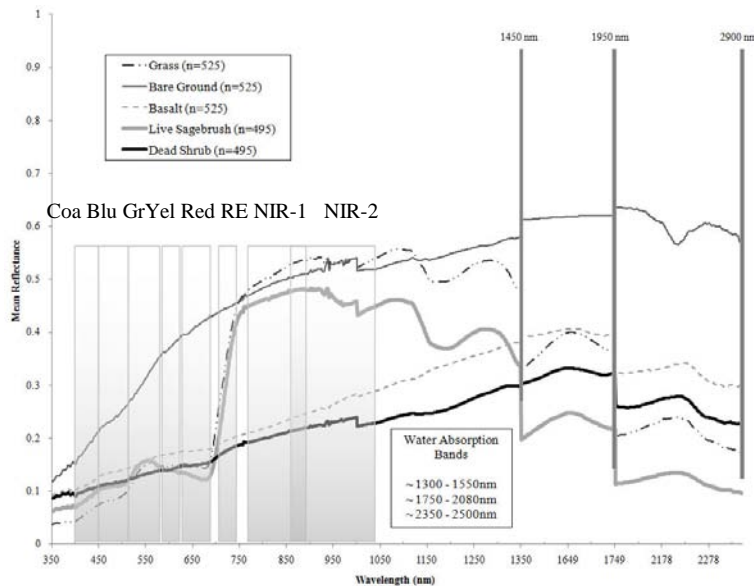


Figure 9. Worldview-2 image bands superimposed with plotted mean reflectance of *in situ* target spectra collected at the O’Neal Ecological Reserve, Idaho as part of a research project attempting to remotely detect dead-shrub patches using five satellite-based sensors (Hyperion, Landsat 5 TM, SPOT-5, Quickbird, and Worldview-2) This graph was used as a pre-analysis tool to get an idea of which bands might be useful during image classification for the successful identification of dead-shrub patches.

*Classification accuracy assessments*

Image classification of dead-shrub was unsuccessful regardless of the sensor used for classification (overall accuracy < 75%) (Table 5). This is consistent with results achieved with the transformed divergence measure of separability test. Overall Kappa statistics were also low, indicating classifications were only slightly better than random. Paired error matrix tests of significance suggest no image classification performed better than any other ( $Z < 1.96$ ). As a result, we conclude that detection of dead-shrubs is not possible with the sensors used in this study.

**Table 5. Classification accuracy assessment for the classification of five remote sensing satellite images (Hyperion, Landsat 5 TM, SPOT 5, Quickbird, and Worldview-2) of dead-shrub patches at the O’Neal Ecological Reserve, Idaho. This was part of a research project testing the abilities of satellite-based sensors to detect sage-grouse habitat quality.**

	Hyperion	Lands 5 TM	SPOT 5	Quickbird	WV-2
<b>Users Accuracy</b>	55 %	65 %	67 %	58 %	62 %
<b>Producers Accuracy</b>	60 %	65 %	60 %	64 %	66 %
<b>Overall Accuracy</b>	54 %	66 %	65 %	59 %	61 %
<b>Kappa</b>	10 %	32 %	29 %	18 %	23 %

*Assesement of error and bias*

There are several possible factors that could have contributed to the negative results for this study. Worldview-2 is the finest spatially resolved multispectral remote sensing satellite currently available. Despite its spatial resolution, this imagery may not be sufficiently spatially resolved for the type of classification attempted. Though an effort was made to record stands that represented homogenous pixels of either live-sagebrush or dead-shrubs, there likely was some pixel mixing of target spectra with adjacent or underlying targets such as exposed soil or grass which may overpower or alter the resulting dead-shrub spectra recorded at the sensor. Sagebrush is a woody shrub species and its associated spectral signature, like most vegetation in semiarid regions, lacks significant spectral contrast compared to features with strong reflectance like soil (Okin et al., 2001). Soil albedo often produces a much higher reflectance than other targets and, lacking leaves, dead-shrubs may allow underlying soil to be exposed to the sensor.

SNR of a sensor can further impact recorded radiance of a target at the sensor as it refers to the inherent abilities of the sensor to accurately record data. An SNR of approximately 100:1, as with the Hyperion imagery (Boardman, 2002) used in this study, is low, which could help explain the negative classification results observed for this sensor.

Laboratory results suggest a statistical difference in plant percent water content between dead and live shrubs ( $P < 0.001$ ). However image classifications of dead-shrub were negative for all sensors tested. These results do not support the hypothesis that a SWIR band would enable differentiation of dead-shrub patches however these results are more likely the result of the relatively coarse spatial resolution of the sensors containing SWIR image bands (Landsat, SPOT, and Hyperion). Additionally, the spectral profile produced by bare ground demonstrated nearly identical absorption and reflectance patterns as dead shrub, though with higher reflectance. It is possible that negative classification results were due to the inability of the sensor to differentiate dead shrub reflectance from the very similar yet overpowering bare ground reflectance. Future research might reexamine this hypothesis using different sensors with finer spatial resolution, as results of pair-wise ANOVA tests between *in situ* spectra of dead-shrub and proximal

targets (basalt, bare ground, grass, and live-sagebrush) indicate that differentiation was possible ( $P < 0.001$  for all sampled pairs), however while *in situ* proved that dead shrub-spectra had higher reflectance in the SWIR region than live-sagebrush, dead-shrub spectra was consistently lower than most other target types, including bare ground.

Spectral resolution of each sensor is yet another consideration. Imagery with higher spectral resolution can enable discrimination of subtle differences in spectral signatures (Aspinall et al., 2002), and provide increased species discrimination (Glenn et al., 2005). In this study, the image classification of dead-shrubs with the Hyperion hyperspectral sensor was unsuccessful despite a high spectral resolution (220 spectral bands). Although spatial resolution for Hyperion is coarse (30m x 30m) and SNR is poor ( $< 100:1$ ) (Boardman, J., 2011) which could affect the sensor's ability to accurately record target radiance even with improved spectral resolution.

## CONCLUSIONS

This project attempted to differentiate shrub mortality by classifying imagery from five satellite-based sensors (Hyperion, Landsat 5 TM, SPOT, Quickbird, and Worldview-2). Classification results were unsuccessful, with users' accuracies ranging from 55% to 67%, producers' accuracies ranging from 60% to 66%, and overall accuracies ranging from 54% to 66%. Paired error matrix tests of significance determined that no image classification performed better than any other ( $Z < 1.96$ ). These negative results were likely due to a combination of factors including coarse spatial resolution, pixel mixing, low spectral resolution, or poor SNR of the sensor. Future research should revisit this study with sensors other than the five tested here.

Analysis of *in situ* spectra, collected concurrent with the field season described in this study, confirmed differentiability of dead-shrub spectra ( $P < 0.001$ ) from the matrix of other targets (basalt, bare ground, grass, and live-sagebrush), though spectral profiles produced by dead-shrub and bare ground demonstrated nearly identical reflectance and absorption patterns, and dead-shrub spectra had consistently lower reflectance than bare ground. In addition a difference was found in plant percent water content between dead and live shrubs ( $P < 0.001$ ) suggesting that differentiation might be possible with sensors possessing SWIR band(s). Dead-shrub classifications with the imagery used in this study containing SWIR bands (Landsat, SPOT, and Hyperion) were unsuccessful and this may be due to the relatively coarse spatial resolution and resulting pixel mixing among other contributing factors. Additionally, while analysis of *in situ* spectra proved that dead-shrub spectra had higher reflectance in the SWIR region than live-sagebrush, dead-shrub spectra were consistently lower than most other target types, including bare ground.

It is hypothesized that successful classification may be possible with sensors possessing very high spatial, spectral, and radiometric resolutions. These stipulations will reduce pixel mixing, increase sensitivity of the sensor to a wider range of wavelengths across the EM spectrum, and increase the ability of the sensor to discriminate between differences in signal strengths as it records radiant flux. Currently, the required spatial resolution is only available using aerial photography. However, unlike satellite sensors where the entire image footprint is effectively acquired from a near nadir (directly underneath the sensor) perspective, with airborne sensors an increasing off-nadir angle exists for pixels at or near the edge of the imagery. Technology is constantly and rapidly evolving however, and if a satellite-based sensor is

developed incorporating very high spatial, spectral, and radiometric resolutions, results from this study suggest that positive detection of dead-shrub patches may be possible.

Globally, shrublands are one of the least protected biomes, having undergone conversion to agriculture or invasion by exotic plant species (Brooks et al., 2004, Knick and Connelly, 2011). In the west, loss of shrublands has led to population declines for shrubland obligate species, such as sage-grouse (Peterjohn and Sauer 1999, Vickery et al., 1999, Brennan and Kuvlesky 2005, Askins et al., 2007). As land managers work towards developing conservation measures for sage-grouse, any additional information regarding the quality of sage-grouse habitat could prove useful. Remote detection of shrub mortality within otherwise live and healthy stands of sagebrush could be one such piece of additional information. Though negative classification results were achieved with this study, results of *in situ* spectral analysis imply that separation is possible. Additional research using more highly resolved sensors is merited.

### **ACKNOWLEDGEMENTS**

This study was made possible by a grant from the National Aeronautics and Space Administration Goddard Space Flight Center (NNX08AO90G). Idaho State University would also like to acknowledge the Idaho Delegation for their assistance in obtaining this grant.

### **LITERATURE CITED**

- Aldridge, C.L., 2008. Range-wide Patterns of Greater Sage-grouse Persistence. *Diversity and Distributions*. 14: 983-994
- Aldridge, C.L. and M.S. Boyce, 2007. Linking Occurrence and Fitness to Persistence: Habitat-Based Approach for Endangered Greater Sage-Grouse. *Ecological Applications*. 17: 508-526
- Anderson, J., J. Tibbits, and K.T. Weber, 2008. Range Vegetation Assessment in the Big Desert, Upper Snake River Plain, Idaho 2007. Pages 16-26 in K. T. Weber (Ed.), Final Report: Impact of Temporal Landcover Changes in Southeastern Idaho Rangelands (NNG05GB05G). 345 pp.
- Aspinall, R.J., A. Marcus, and J.W. Boardman, 2002. Considerations in Collecting, Processing, and Analyzing High Spatial Resolution Hyperspectral Data for Environmental Investigations. *Journal of Geographical Systems*. 4: 15– 29
- Becker, B.L., D.P. Lusch, and J. Qi, 2005. Identifying Optimal Spectral Bands from *In Situ* Measurements of Great Lakes Coastal Wetlands using Second-derivative Analysis. *Remote Sensing of Environment*. 97: 238-248
- Beyer, H.L., 2004. Hawth's Analysis Tools for ArcGIS. URL = <http://www.spataleecology.com/htools>
- Blanco, L.J., M.O Aguilera, J.M Paruelo, and F.N. Biurrun, 2008. Grazing Effect on NDVI Across an Aridity Gradient in Argentina. *Journal of Arid Environments*. 72: 764-776
- Boardman, J., 2002. Validating Hyperion in Yellowstone National Parks Using AVIRIS, HyMap, and Ground Spectra and Validating Hyperion at Oatman, Arizona Using AVIRIS, HyMap and Ground

Spectra, EO-1 Science Validation Team Meeting, Greenbelt, Maryland. URL = [http://eo1.gsfc.nasa.gov/new/validationreport/Technology/Documents/Tech.Val.Report/Science\\_Summary\\_Boardman.pdf](http://eo1.gsfc.nasa.gov/new/validationreport/Technology/Documents/Tech.Val.Report/Science_Summary_Boardman.pdf) visited January 28, 2011

Breckenridge, R.P., 2007. Improving Rangeland Monitoring and Assessment: Integrating Remote Sensing, GIS, and Unmanned Aerial Vehicle Systems. INL/EXT-10-17983. 134pp.

Breiman, L., J. H. Friedman, R. A. Olshen, and C. J. Stone. 1998. Classification and Regression Trees. Chapman and Hall, CRC press, Boca Raton, Florida. 358 pp.

Campbell, J.B., 2008. Introduction to Remote Sensing. New York: Guilford Press, 4: 626 pp.

Canavan, L., 2009. Idrisi Taiga (ver. 16.04) Help Documentation. URL = <http://www.clarklabs.org>

Chopping, M., S. Lihong, A. Rango, J.V. Martonchik, D.P. C. Peters, and A. Laliberte, 2008. Remote Sensing of Woody Shrub Cover in Desert Grasslands Using MISR With a Geometric-Optical Canopy Reflectance Model. Remote Sensing of Environment. 112: 19-34

Chuvieco, E. and A. Huete, 2010. Fundamentals of Satellite Remote Sensing. Florida: CRC Press, 448 pp.

Clark Labs, 2008. Idrisi Focus Paper: Classification Tree Analysis. Clark University. Worcester, MA. URL = [www.clarklabs.org](http://www.clarklabs.org).

Congalton, R.G., and K. Green, 2008. Assessing the Accuracy of Remotely Sensed Data: Principles and Practices. Florida: CRC Press, 2:192 pp.

Connelly, J.W., C.A. Hagen, M.A. Schroeder, 2011. Characteristics and Dynamics of Greater Sage-Grouse Populations. In: Knick, S. T., and J. W. Connelly (Ed.). Greater Sage-grouse: Ecology and Conservation of a Landscape Species and its Habitats. Studies in Avian Biology Series. University of California Press, Berkeley, CA. 38:672 pp.

Connelly, J.W., S.T. Knick, M.A. Schroeder, and S.J. Stiver, 2004. Conservation Assessment of Greater Sage-grouse and Sagebrush Habitats. Western Association of Fish and Wildlife Agencies. Unpublished Report. Cheyenne, Wyoming. 610 pp.

Connelly, J.W., M.A. Schroeder, A.R. Sands, and C.E. Braun, 2000. Guidelines to Manage Sage Grouse Populations and their Habitats. Wildlife Society Bulletin 28:967–985

Davis, K. and K.T. Weber, 2010. 2008 Rangeland Vegetation Assessment at the O’Neal Ecological Reserve, Idaho. Pages 29-40 in K. T. Weber and K. Davis (Eds.), Final Report: Forecasting Rangeland Condition with GIS in Southeastern Idaho (NNG06GD82G). 189 pp.

Davis, K. and K.T. Weber, 2011. Wildland/Urban Interface Fire Susceptibility and Communities at Risk: A Joint Fire Modeling Project for Custer County, Idaho, bureau of Land Management, Upper Snake River

District GIS and Idaho State University GIS Training and Research Center. URL = [http://giscenter.isu.edu/research/techpg/blm\\_fire/template.htm](http://giscenter.isu.edu/research/techpg/blm_fire/template.htm) visited January 26, 2011

Davis K., K.T. Weber, and D. Hanson, 2011. 2010 Rangeland Vegetation Assessment at the O'Neal Ecological Reserve, Idaho. Field Report. Pages 21-28 in K.T. Weber and K. Davis (Eds.), Final Report: Assessing Post-Fire Recovery of Sagebrush Steppe Rangelands in Southeastern Idaho (NNX08AO90G). 252 pp.

Friedl, M.A. and C.E. Brodley, 1997. Decision Tree Classification of Land Cover from Remotely Sensed Data. *Remote Sensing of Environment* 61: 399-409

Glenn, N.F., J.T. Mundt, K.T. Weber, T.S. Prather, L.W. Lass, and J. Pettingill, 2005. Hyperspectral Data Processing for Repeat Detection of Small Infestations of Leafy Spurge. *Remote Sensing of Environment*. 95: 399-412

Gokhale, B. and K.T. Weber, 2006. Rangeland Health Modeling with Quickbird Imagery. Pages 3-16 in Weber, K. T. (Ed.), Final Report: Detection Prediction, Impact, and Management of Invasive Plants Using GIS. 196 pp.

Gokhale, B. and K.T. Weber, 2009. Spatial Pattern of NDVI in Semiarid Ecosystems of Northern Spain. Pages 149-156 in K. T. Weber and K. Davis (Eds.), Final Report: Comparing Effects of Management Practices on Rangeland Health with Geospatial Technologies (NNX06AE47G). 168 pp.

Goodchild, M.F., G.S. Biging, R.G. Congalton, P.G. Langley, N.R. Chrisman, and F.W. Davis, 1994. Final Report of the Accuracy Assessment Task Force. California Assembly bill AB1580. Santa Barbara: University of California, National Center for Geographic Information and Analysis

Hanson, D., and K. T. Weber, 2010. Data Collection Protocol: Dead and Live Sagebrush. 3pp.

Gregory, J., L. Sander, and K.T. Weber, 2008. Range Vegetation Assessment in the Big Desert, Upper Snake River Plain, Idaho, 2005. Pages 3-8 in K.T. Weber (ED), Final Report: Impact of Temporal Landcover Changes in Southeastern Idaho Rangelands (NNG05GB05G). 345 pp.

Hampton, N., and N. Huntly, 2010. Developing a Habitat Selection Model to Predict the Distribution and Abundance of the Sagebrush Defoliator Moth (*Aroga websteri* Clarke). Pages 54-56 in R.D. Blew (Ed.), Final Report: Ecological Research at the Idaho National Environmental Research Park in 2009. 89 pp.

Hanson, D., K.T. Weber, K. Davis, 2010. 2010 Field Spectrometry Collection of Sagebrush at the O'Neal Ecological Reserve, Idaho. Pages 29-36 in K. T. Weber and K. Davis (Eds.), Final Report: Assessing Post-Fire Recovery of Sagebrush –Steppe Rangelands in Southeastern Idaho (NNX08AO90G). 252 pp.

- Harper, K.T., F.J. Wagstaff and W.P. Clary. 1989. Shrub Mortality Over a 54-Year Period In Shadscale Desert West-Central Utah. *In: McArthur, E. D., E. M. Romney, S. D. Smith, and P. T. Tueller, (Eds.). Proceedings of Symposium on Cheatgrass Invasion, Shrub Die-off, and Other Aspects of Shrub Biology and Management* 119-126. Ogden, UT: US Department of Agriculture, Forest Service, Intermountain Research Station General Technical Report INT-GTR-276
- Haws, B.A., G.E. Bohart, C.R. Nelson and D.L. Nelson, 1989. Insects and Shrub Dieoff in Western States: 1986-89 Survey Results. *In: McArthur, E. D., E. M. Romney, S. D. Smith, and P. T. Tueller (Eds.), Proceedings of Symposium on Cheatgrass Invasion, Shrub Die-off, and Other Aspects of Shrub Biology and Management* 127-151. Ogden, UT: US Department of Agriculture, Forest Service, Intermountain Research Station General Technical Report INT-GTR-276. 351 pp.
- Hess, W.M., D.L. Nelson and D.L. Sturges. 1985. Morphology and Ultrastructure of a Snowmold Fungus on Sagebrush (*Artemisia tridentata*). *Mycologia* 77: 637-645
- Homer, C.G., C.L. Aldridge, D.K. Meyer, M.J. Coan and Z.H. Bowen, 2008. Multiscale Sagebrush Rangeland Habitat Modeling in Southwest Wyoming. U.S. Geological Survey Open-File Report 2008-1027
- Jensen, J.R., 2007, *Remote Sensing of the Environment: An Earth Resource Perspective*, 2nd Edition, Upper Saddle River: Prentice-Hall, 592 pp.
- Knick, S.T. and J.W. Connelly, 2011. Greater Sage-Grouse and Sagebrush: An Introduction To The Landscape. *In: Knick, S. T., and J. W. Connelly (Ed.). Greater Sage-grouse: Ecology and conservation of a landscape species and its habitats. Studies in Avian Biology Series.* University of California Press, Berkeley, CA. 38:672 pp
- Lawrence, R.L., and A. Wright, 2001. Rule-based Classification Systems using Classification and Regression Tree (CART) Analysis. *Photogrammetric Engineering and Remote Sensing.* 67: 1137-1142
- Lillesand, T.M. and R.W. Kiefer, 2000. *Remote Sensing and Imager Interpretation.* John Wiley and Sons, New York, NY. 4:724 pp.
- Louchard, E.M., R.P. Reid, C.F. Stephens, C.O. Davis, R.A. Leathers, T.V. Downes, and R. Maffione, 2002. Derivative Analysis of Absorption Features in Hyperspectral Remote Sensing Data of Carbonate Sediments. *Optical Society of America.* 10: 1573-1584
- McMahan, B, K.T. Weber, and J. Sauder, 2003. *In: K. T. Weber (Ed.). Final Report: Wildfire Effects on Rangeland Ecosystems and Livestock Grazing in Idaho.* 209 pp.
- Miller, J. and J. Franklin, 2001. Modeling the Distribution of Four Vegetation Alliances using Generalized Linear Models and Classification Trees with Spatial Dependence. *Ecological Modeling.* 157: 227-247

- Nelson, C.R., B.A. Haws, D.L. Nelson, 1989. Mealybugs and Related Hoptera of Shadscale: Possible Agents in the Dieoff Problem in the Intermountain West. *In: McArthur, E. D., E. M. Romney, S. D. Smith, and P. T. Tueller, (Eds.). Proceedings of Symposium on Cheatgrass Invasion, Shrub Die-off, and Other Aspects of Shrub Biology and Management* 152-165. Ogden, UT: US Department of Agriculture, Forest Service, Intermountain Research Station General Technical Report INT-GTR-276
- Okin, G.S., D.A. Roberts, B. Murray, and W.J. Okin, 2001. Practical Limits on Hyper Spectral Vegetation Discrimination in Arid and Semiarid Environments. *Remote Sensing of Environment*. 77: 212–225
- Patterson, R.L., 1952. *The Sage Grouse in Wyoming*. Sage Books, Inc., Denver, CO. 341 pp.
- Richards, J.A., 1993. *Remote Sensing Digital Image Analysis*, Springer-Verlag, New York, NY
- Rouse, J.W., Jr., R.H. Haas, J.A. Schell, and D.W. Deering, 1973. Monitoring the Vernal Advancement and Retrogradation (green wave effect) of Natural Vegetation. Prog. Rep. RSC 1978-1, Remote Sensing Center, Texas A&M Univ., College Station, 93pp. (NTIS No. E73-106393)
- Sankey, T.T. and K.T. Weber, 2009. Rangeland Assessments Using Remote Sensing: Is NDVI Useful? Pages 113-122 in K. T. Weber and K. Davis (Eds.), Final Report: Comparing Effects of Management Practices on Rangeland Health with Geospatial Technologies (NNX06AE47G). 168 pp.
- Sankey, T.T., C. Moffet, and K.T. Weber, 2008. Post-fire Recovery of Sagebrush Communities: Assessment using SPOT5 and Very Large-Scale Imagery. Pages 245-254 in K. T. Weber (ED), Final Report: Impact of Temporal Landcover Changes in Southeastern Idaho Rangelands (NNG05GB05G). 345pp.
- Shiojiri, K., and R. Karban, 2008. Seasonality of Herbivory and Communication between Individuals of Sagebrush. *Arthropod-Plant Interactions*. 2: 87-92
- Storch, I. 2000. Conservation Status and Threats to Grouse Worldwide: An Overview. *Wildlife Biology* 6:195–204
- Stow, D., Y. Hamada, L. Coulter, and Z. Anguelova, 2008. Monitoring Shrubland Habitat Changes through Object-oriented Change Identification with Airborne Multispectral Imagery. *Remote Sensing of Environment*. 112: 1051-1061
- Takahashi, M., and N. Huntly, 2010. Herbivorous Insects Reduce Growth and Reproduction of Big Sagebrush (*Artemisia tridentata*). *Arthropod-Plant Interactions*. 4: 257-266
- Tilley, D.J., D. Ogle, L. St. John, B. Benson, 2007. Plant Guide: Big Sagebrush. URL = [www.plant-materials.nrcs.usda.gov/pubs/idpmcpg6294.pdf](http://www.plant-materials.nrcs.usda.gov/pubs/idpmcpg6294.pdf). USDA NRCS

- Tsai, F., and W. Philpot, 1998. Derivative Analysis of Hyperspectral Data. *Remote Sensing of Environment*. 66: 41-51
- Tucker, C.J., 1979. Red and Photographic Infrared Linear Combinations for Monitoring Vegetation. *Remote Sensing of Environment*. 8: 127-150
- USDA NRC, 1987. Soil Survey of Bannock County Area, Idaho. 347 pp.
- Underwood, J., J. Tibbitts, and K.T. Weber, 2008. Range Vegetation Assessment in the Big Desert, Upper Snake River Plain, Idaho 2006. Pages 9-15 in K. T. Weber (Ed.), Final Report: Impact of Temporal Landcover Changes in Southeastern Idaho Rangelands (NNG05GB05G). 345pp.
- Wallace, A., and D.L. Nelson, 1989. Wildland Shrub Dieoffs Following Excessively Wet Periods: A Synthesis. Pages 81-83 in E. D. McArthur, E. M. Romney, S. D. Smith, and P. T. Tueller (Eds.), Proceedings--Symposium on Cheatgrass Invasion, Shrub Die-off, and Other Aspects of Shrub Biology and Management. Ogden, UT: US Department of Agriculture, Forest Service, Intermountain Research Station General Technical Report INT-GTR-276. 351 pp.
- Walser, R.H., D.J. Weber, E.D. McArthur, and S.C. Sanders, 1989. Winter Cold Hardiness of Seven Wildland Shrubs. *In*: McArthur, E.D., E.M Romney, S.D. Smith, and P.T. Tueller, (Eds.). Proceedings of Symposium on Cheatgrass Invasion, Shrub Die-off, and Other Aspects of Shrub Biology and Management 115-118. Ogden, UT: US Department of Agriculture, Forest Service, Intermountain Research Station General Technical Report INT-GTR-276
- Weber, K.T., 2006. Challenges of Integrating Geospatial Technologies into Rangeland Research and Management. *Rangeland Ecology & Management*. 59: 38-43
- Weber, K.T. and J.B. McMahan, 2003. Field Collection of Fuel Load and Vegetation Characteristics for Wildfire Risk Assessment Modeling: 2002 Field Sampling Report. *In*: K. T. Weber (Ed.). Final Report: Wildfire Effects on Rangeland Ecosystems and Livestock Grazing in Idaho. 209 pp.
- Weber, K.T. and B. Gokhale, 2010. Effect of Grazing Treatment on Soil Moisture in Semiarid Rangelands. Pages 161-174 in K. T. Weber and K. Davis (Eds.), Final Report: Forecasting Rangeland Condition with GIS in Southeastern Idaho (NNG06GD82G). 189 pp.
- Weber, K.T., N.F. Glenn, J. Tibbitts, 2010<sup>a</sup>. Investigation of Potential Bare Ground Modeling Techniques using Multispectral Satellite Imagery. Pages 101-112 in K. T. Weber and K. Davis (Eds.), Final Report: Forecasting Rangeland Condition with GIS in Southeastern Idaho (NNG06GD82G). 189 pp.
- Weber, K.T., J. Théau, and K. Serr, 2010<sup>b</sup>. Effect of Coregistration Error on Patchy Target Detection using High-Resolution Imagery. Pages 113-123 in K. T. Weber and K. Davis (Eds.), Final Report: Forecasting Rangeland Condition with GIS in Southeastern Idaho (NNG06GD82G). 189 pp.

Weber, K.T., S.S. Seefeldt, J.M. Norton, and C. Finley, 2008. Fire Severity Modeling of Sagebrush-Steppe Rangelands in Southeastern Idaho. Pages 205-217 in K. T. Weber and K. Davis (Eds), Final Report: Impact of Temporal Landcover Changes in Southeastern Idaho Rangelands. 354 pp.

Weber, K.T., C.L. Alados, C.G. Bueno, B. Gokale, B. Komac, and Y. Pueyo, 2009. Modeling Bare Ground with Classification Trees in Northern Spain. Pages 55-70 in K.T. Weber and K. Davis (Eds.), Final Report: Comparing Effects of Management Practices on Rangeland Health with Geospatial Technologies (NNX06AE47G). 168 pp.

Wheeler, D.K., N. Glenn, 2003. The Use of Remote Sensing Imagery for Evaluation of Post-Wildfire Susceptibility to Landslide and Erosion Hazards in the Salmon-Challis National Forest, Lemhi County, Idaho. In: K. T. Weber (Ed.). Final Report: Wildfire Effects on Rangeland Ecosystems and Livestock Grazing in Idaho. 209 pp.

Wiens, J.A., R.G. Cates, J.T. Rottenbury, C. Cobb, B. Van Horne, and R.A. Redak, 1991. Arthropod Dynamics on Sagebrush (*Artemisia tridentata*): Effects of Plant Chemistry and Avian Predation. *Ecological Monographs*. 61(3):299–321

Williams, A.E.P., and E.R. Hunt, 2004. Accuracy Assessment for Detection of Leafy Spurge with Hyperspectral Imagery. *Journal of Range Management*. 57: 106–112

Zou, L., S.N. Miller, and E.T Schmidtman, 2006. Mosquito Larval Habitat Mapping Using Remote Sensing and GIS: Implications of Coalbed Methane Development and West Nile Virus. *Journal of Medical Entomology*. 43: 1034-1041

**Recommended citation style:**

Hanson, D. and K. T. Weber, 2011. Detecting Dead Shrub Patches Using Remote Sensing Techniques in Southeast Idaho. Pages 211-234 in K. T. Weber and K. Davis (Eds.), Final Report: Assessing Post-Fire Recovery of Sagebrush-Steppe Rangelands in Southeastern Idaho. 252 pp.

[THIS PAGE LEFT BLANK INTENTIONALLY]

## **Quantifying Habitat Fragmentation in the Big Desert, Idaho**

Darci Hanson, GIS Training and Research Center, Idaho State University, Pocatello, ID 83209-8104, <http://giscenter.isu.edu>, email: [giscenter@isu.edu](mailto:giscenter@isu.edu)

Keith T. Weber, GISP. GIS Director, Idaho State University. GIS Training and Research Center, 921 S. 8<sup>th</sup> Ave., Stop 8104, Pocatello, ID 83209-8104. [webekeit@isu.edu](mailto:webekeit@isu.edu)

### **ABSTRACT**

Aerial imagery acquired in 1954, 1992, 2004, and 2009 for the Big Desert in southeast Idaho were used to quantify change in total area of irrigated agriculture for this region. Polygon feature classes were digitized for each year and stored in a personal geodatabase. Area was calculated and compared between years. Total area was determined after applying a 6.9 km buffer around the polygons to account for potential movements of human-subsidized (synanthropic) predation. The imagery for 1954 represented the state of sagebrush-steppe rangelands surrounding the Big Desert prior to significant conversion to irrigated agriculture, and thus was the basis for comparison between 1954 and 2009. Results indicate the Big Desert has seen an increase (>50%) in irrigated agriculture between 1954 and 2009, most of which occurred between 1954 and 1992(~50%).

*KEYWORDS: Sage-grouse, agriculture, cropland, irrigated, center pivot, GIS, aerial imagery*

## **INTRODUCTION**

The Greater Sage-Grouse (*Centrocercus urophasianus*) is a sagebrush obligate species with annual home ranges that can exceed 2700 km<sup>2</sup> (Dalke et al. 1963, Schroeder et al. 1999, Leonard et al. 2000, Knick and Connelly, 2011). Historically, sage-grouse distribution was estimated to have extended through regions of 13 US states and 3 Canadian provinces (Schroeder et al. 2004, Connelly et al. 2004). Presently, sage-grouse occupy approximately half of their estimated pre-settlement distribution (Schroeder et al. 2004). Forecasting models of potential for sage-grouse persistence indicate that 75 percent of sage-grouse populations across are likely to decline below minimum viable population of 500 individuals within 100 years if current conditions and trends persist (Garton et al. 2000).

For sage-grouse, nesting and early brood-rearing periods may be considered the bottleneck for persistence of the species as predation of adult sage-grouse is at its highest frequency during the nesting and early brood-rearing period (Connelly et al. 2000a, Naugle et al. 2004, Moynahan et al. 2006, Hagen 2011). Sage-grouse exhibit strong fidelity to previous years' nest sites even if habitat within that site is no longer viable (Fischer et al. 1993, Connelly et al., 2000, Connelly et al. 2004). The minimum recommended distance of human development from sage-grouse lekking sites is 5km for non-migratory populations, and 18km for migratory populations (Connelly et al. 2000). These distances have been recommended due to observed travel distances for population types (non-migratory and migratory), however, they are also recommended with the consideration of potential movements by synanthropic predators such as domestic dogs and cats, red fox, and corvids (Leu et al. 2008, Knick et al. 2011). Nesting hens require diverse vegetation in the form of sagebrush, succulent forbs, tall grasses, and litter, not only for sustenance during prolonged idle periods of nest incubation, but also for shelter from airborne and ground-based predators (Gregg 1991, Schroeder et al. 1999, Connelly et al. 2000<sup>a</sup>, Connelly et al. 2004, Aldridge et al. 2008). They require large areas of contiguous habitat because, though hens tend to be less mobile during the nesting period, some have been known to travel distances up to 6.2 km between nest and lek sites (Connelly et al. 2000). Sage-grouse average 51 percent nest success in relatively non-altered habitats and 37 percent in altered habitats (Connelly et al. 2011), with partial clutch loss occurring in ~50 percent of nests. This loss is partially, if not largely, due to predation during nesting and early brood-rearing periods. Predation of adults is less common during this period due to their tendency to abandon nests under predator threat (Patterson 1952, Hagen 2011). However this leaves eggs and recently hatched chicks vulnerable to predation instead. Human development such as irrigated agriculture, infrastructure such as roads, powerlines, and pipelines, and urbanization has fragmented sage-grouse habitat in sagebrush-steppe rangelands, aiding predator movements, particularly those of synanthropic predators (Tewksbury et al. 2002, Knick and Connelly 2011).

Habitat fragmentation refers to permanent or long lasting dissection of natural systems into spatially isolated parts resulting from either anthropogenic or natural influences, where they are impacted such that habitat suitability for a species or community of animals is diminished (Galvin et al. 2008). What are now coined semiarid sagebrush-steppe rangelands were once described as a "sea of sagebrush" in journals of early American explorers such as John C. Frémont and Lewis and Clark (Frémont 1845). Since that time, the "sea of sagebrush" has been divided into several discontinuous "lakes" through human development such as paved roads, fencing, urban centers, residential developments, and large-scale conversion to irrigated agriculture such as center pivot irrigation. For sage-grouse, habitat fragmentation may aid predation (Fichter and Williams 1967, Pasitschniak-Arts et al. 1998, Bunnell 2000, Connelly et al. 2000<sup>a</sup>,

Connelly et al. 2004, Leu et al. 2008, Knick et al. 2011), exacerbate the spread of invasive species such as cheatgrass (*Bromus tectorum*) (Vitousek et al. 1997, Smith et al. 2000, Browder et al. 2002, Knick et al. 2003, Connelly et al. 2004, Hansen et al. 2005), or limit the total area of contiguous, undisturbed habitat available to them (Connelly et al. 2004, Aldridge et al. 2008). The underlying cause for population declines across the entire sage-grouse distribution is loss of suitable habitat (Connelly and Braun 1997, Leonard et al. 2000, Aldridge et al. 2008, Knick and Connelly, 2011). Almost all of the Snake River Plain in southern Idaho (Figure 1) that contains deep loamy soils and once supported big sagebrush now has been converted to agriculture (particularly cropland) (Hironaka et al. 1983, Knick et al. 2011). Within this area the first private irrigation projects began on the upper Snake River near Wyoming in the 1870s. Agriculture (mostly cropland) currently covers >230,000 km<sup>2</sup> (11%) of the entire sage-grouse distribution, which translates to ~1,600,000 km<sup>2</sup> of total area influenced when a 6.9 km buffer is applied to account for potential movements of synanthropic predators (Leu et al. 2008, Knick et al. 2011). Leonard et al. (2000) correlated declining sage-grouse populations in the upper Snake River Plain of southeast Idaho with cropland area. Within their study area, cropland development was estimated to have increased from 18% to 28% between 1975 and 1985 respectively, and by 1992 reached 31% (Leonard et al. 2000, Knick et al. 2011). Center pivot irrigation (invented by the Mel Brown Company in 1957) visibly represents a large portion of irrigated agricultural development surrounding the Big Desert (Figure 2). No differentiation seems to be made in the current literature as to the impact of center pivot irrigated agriculture on sage-grouse habitat relative to other forms of irrigated agriculture. However, automated center pivot was developed to reduce labor costs, while also distributing water more efficiently and uniformly, which enabled agricultural development of lands that had previously been unsuitable for surface irrigation. This resulted in an increase in the use of center pivot irrigation by 50% from 1986 to 1996 (Evans, 2001).

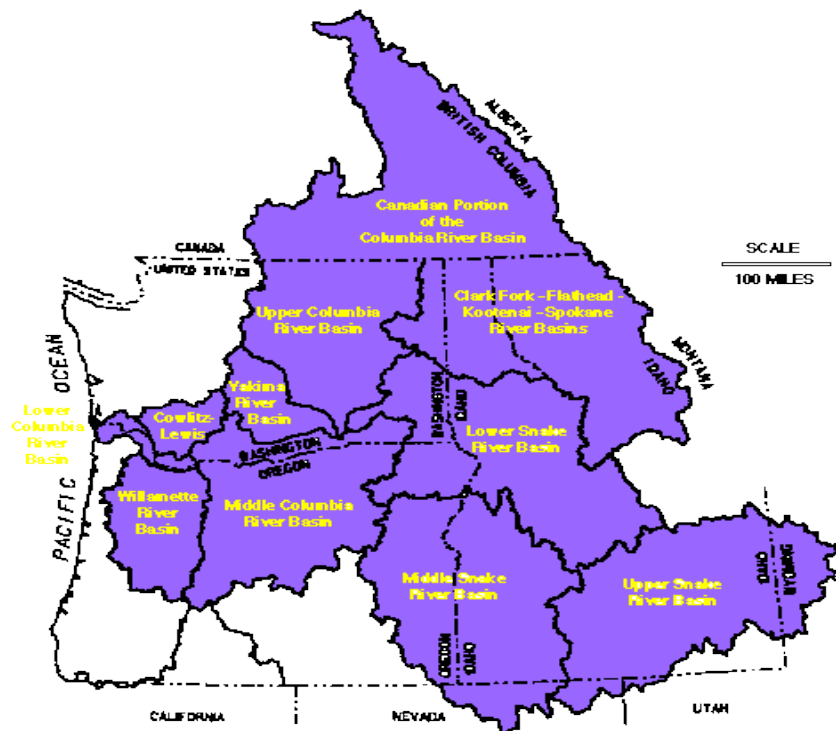
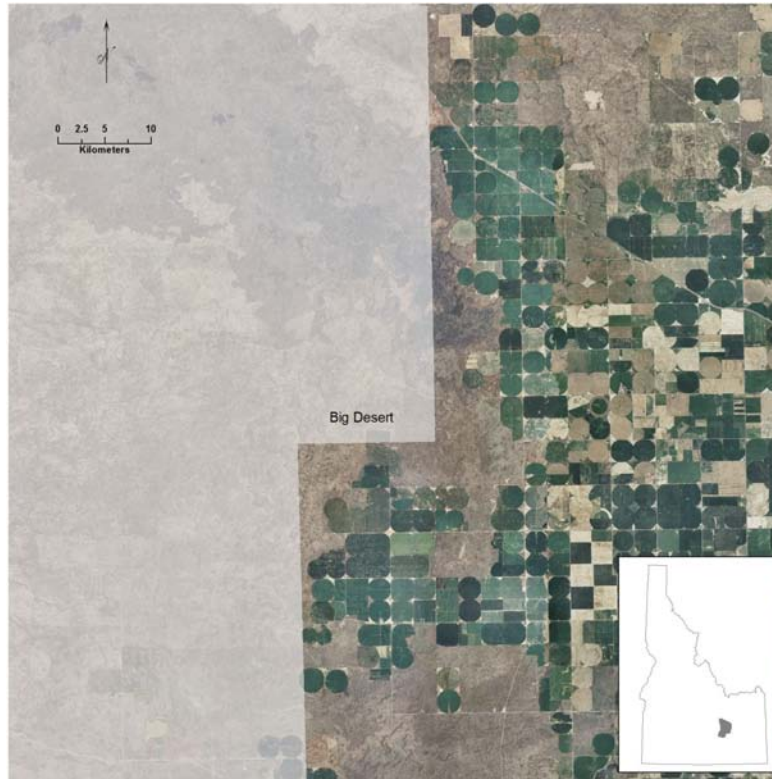


Figure 1. A map of the Columbia River Basin. The Upper Snake River plain is shown in gray (or red, or yellow) (source: US Army Corps of Engineers, North Pacific Division, CRT 69).



**Figure 2. Irrigated agricultural development for the Big Desert, southeast Idaho. This image was generated to highlight the extent of center pivot irrigation as part of a multitemporal analysis of habitat fragmentation of sage-grouse habitat in the form sagebrush-steppe rangeland conversion to agriculture.**

This paper attempts to examine habitat fragmentation in the form of irrigated agricultural development surrounding a known sage-grouse stronghold in southeast Idaho – the Big Desert. It describes the techniques used to analyze aerial image data of the Big Desert for four separate years. Image data were used to generate a multitemporal analysis of irrigated agricultural development surrounding the study area.

## **METHODS**

### *Study Area*

The Big Desert study area (Figure 3) is located in southeastern Idaho approximately 71 km northwest of Pocatello, Idaho (113° 4' 18.68" W, 43° 14' 27.88" N) (Anderson et al. 2008). The area is largely undeveloped and is characterized as semiarid sagebrush-steppe rangelands bordered by relatively recent lava formations to the west and southwest, and irrigated agricultural lands to the north, south and east (Weber and McMahan, 2003). The study area included irrigated agricultural lands adjacent to the south and east perimeter of USDI BLM Big Desert allotment. The study area is approximately 467,814 ha in size and spreads across portions of four counties including Butte, Blaine, Bingham, and Power Counties. The study area is largely managed by the Bureau of Land Management (BLM) (75 percent). The Department of Energy (DOE) manages approximately eight percent, seven percent is managed by the State of Idaho, and 10 percent is privately owned (Figure 4). Topography is generally flat to gently rolling hills with a mean elevation of 1539 m (range = 1351 m – 2297 m). Soils are comprised mostly of silicic volcanic material and Paleozoic rocks (McBride et al. 1978, Connelly et al. 2000<sup>b</sup>). Using precipitation

data relevant for 1992 to 2009, mean annual precipitation was 0.21 m (SE = 0.016 m) with about 48% falling as snow in the winter months (October 1 – March 31). Vegetation type is principally Wyoming big sagebrush (*A. tridentata wyomingensis*)-bluebunch wheatgrass (*Pseudoroegneria spicata*) with other native and non-native species found throughout such as Cheatgrass (*Bromus tectorum*) (McBride et al. 1978, Connelly et al. 1991, Gokhale and Weber, 2010). The Big Desert has a history of continuous low intensity grazing by sheep with a stocking rate of 0.051 animal units per hectare (AU/ha). According to BLM personnel, only approximately 10 percent of available AUs are utilized each year (Weber et al. 2003). In addition, the area has a history of wildfire occurrence (Weber and McMahan, 2003) and over the last 10 years there have been 14 fire occurrences within the Big Desert region.

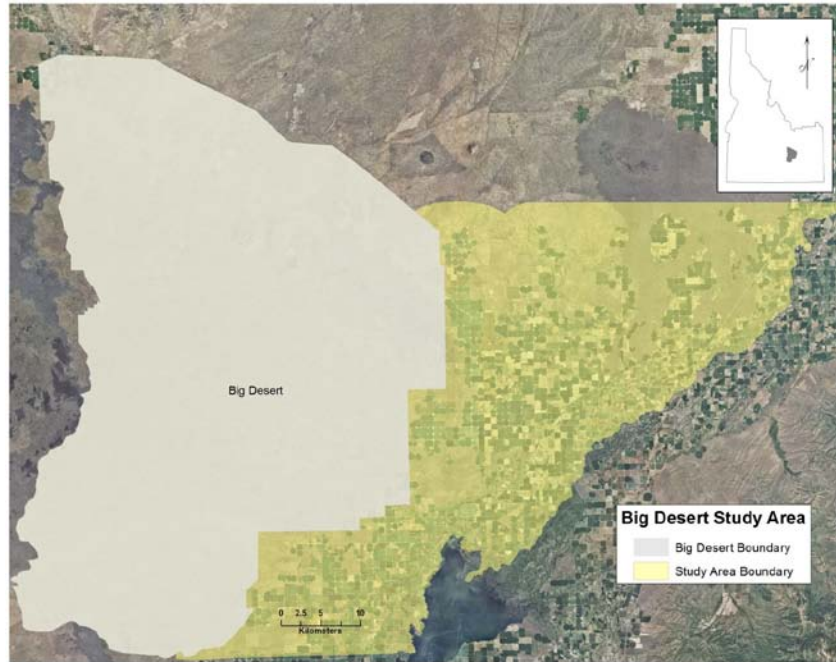


Figure 3. The Big Desert study area in southeast Idaho, ~ 71 km northwest of Pocatello. This site was chosen as the location for a multitemporal analysis of sagebrush-steppe rangeland conversion to irrigated agriculture near a sage-grouse stronghold in southeast Idaho.

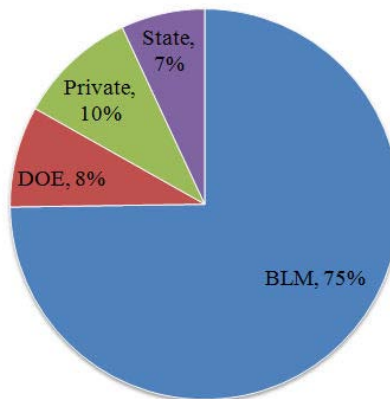
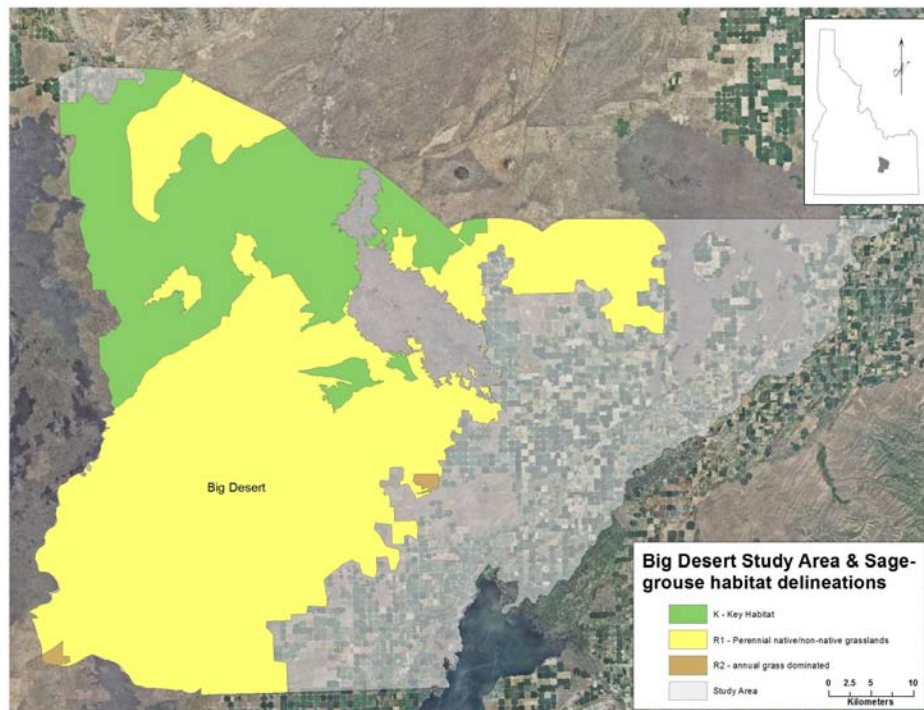


Figure 4. Management delineations for the Big Desert Study area. This study area was chosen as the site for a multi-temporal analysis of sage-grouse habitat fragmentation southeast Idaho.

There are several migratory populations of sage-grouse present in the Big Desert, which remains a region of important habitat in southeast Idaho. Big Desert sage-grouse populations have experienced gradual declines however, due to loss of habitat which has been largely attributed to wildfire (BDSGLWG, 2010). Approximately 70% of the Big Desert has been burned by wildfire since 1995, causing loss of large contiguous areas of sagebrush. Of the 70% burned, 30% has been classified as key sage-grouse habitat (BDSGLWG, 2010). In 2008, the BLM assessed habitat quality for Sage Grouse in Idaho dividing it into four classes: 1) Key delineates areas of prime habitat, 2) R1 delineates areas of perennial native and non-native grasslands with high restoration potential, 3) R2 delineates areas of annual grass dominated areas with low restoration potential, and 4) R3 delineates areas of conifer encroachment with high restoration potential. Of these classes, the Big Desert study area is considered "KEY" (28%) and "R1" (46%) habitat for sage-grouse (Figure 5).



**Figure 5. Greater Sage-Grouse habitat quality classes as developed by the Bureau of Land Management within the Big Desert, Idaho. Habitat quality class are: 1)K, which delineates areas of prime habitat, 2) R1, which delineates areas of perennial native and non-native grasslands with high restoration potential, and 3) R2, which delineates areas of annual grass dominated areas with low restoration potential.**

In 2006 the Crystal fire burned approximately 89,000 ha of the Big Desert study area (31%). Ypsilantis (BLM) indicated this area coincided with nesting and winter habitat for sage-grouse (Figure 6).

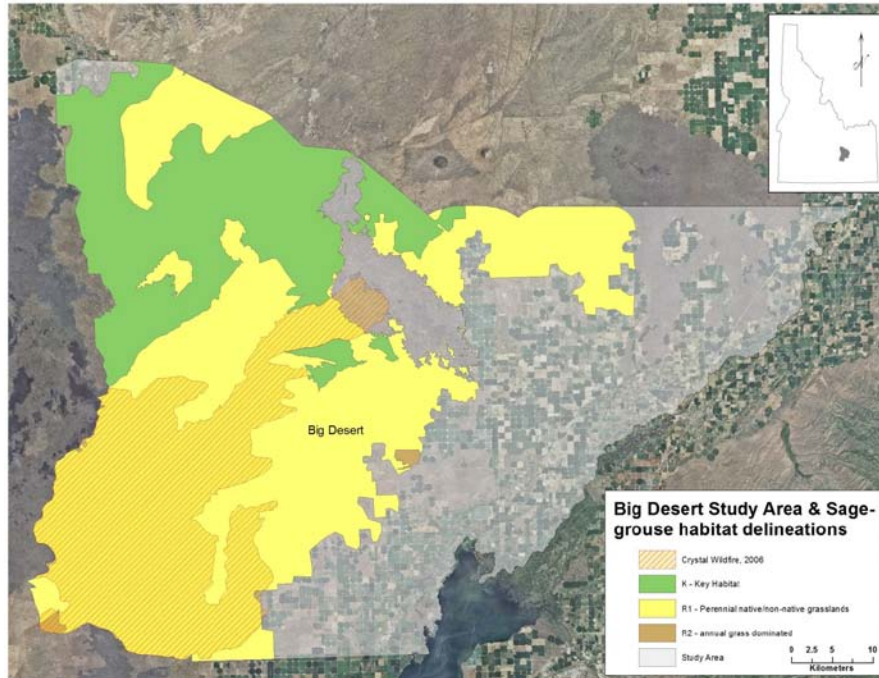


**Figure 6. Greater Sage-Grouse habitat quality classes as developed by the Bureau of Land Management within the Big Desert, Idaho superimposed with the 2006 Crystal Fire boundary. Habitat quality classes are: 1)K, which delineates areas of prime habitat, 2) R1, which delineates areas of perennial native and non-native grasslands with high restoration potential, and 3) R2, which delineates areas of annual grass dominated areas with low restoration potential.**

While wildfire has fragmented sage-grouse habitat within the Big Desert, conversion of sagebrush-steppe rangelands to cultivated agriculture on private lands (10% of the total study area) along the southern edge of the study area further fragments sage-grouse habitat. Though wildfire has an obvious impact on sage-grouse habitat in the Big Desert, it is part of the sagebrush-steppe rangeland ecosystem, and therefore does not have the same impact as fragmentation caused by anthropogenic influences such as irrigated cropland development. Habitat fragmentation of this form often permanently transforms sagebrush-steppe landscapes. Connelly et al. (2000) reported a recovery rate of approximately 14 years before a wildfire-disturbed landscape was once again considered viable for sage-grouse.

#### *Image Acquisition and processing*

Aerial imagery of the study area was collected for four separate years including 1954, 1992, 2004, and 2009. Imagery collected in 2004 and 2009 were produced through the National Agricultural Imagery Program (NAIP) (1m x 1m spatial resolution) (horizontal positional accuracy  $\pm 5$  m). Imagery collected in 1992 was a mosaic of several 3.75 minute Digital Orthophoto Quarter Quadrant (DOQQs) tiles originating from the U.S. Geological Survey (USGS) (1m x 1m spatial resolution). The imagery collected in 1954 was a mosaic of several aerial image tiles produced by the Army Map Service. Images were taken at an altitude of 8,991 m. Individual frames were arranged together manually and then scanned to a tagged image file format (TIFF) (10m x 10m spatial resolution) (Figure 7). To the author's knowledge, this aerial mosaic is the best available representation of the Big Desert prior to significant conversion of sagebrush-steppe rangelands to center pivot irrigation, and therefore served as a foundation for comparison.



**Figure 7. 1954 still frame mosaic of the Big Desert study area in southeast Idaho.**

To cover the entire study area, several tiles were mosaicked together to create a single cohesive image for each year (1954, 1992 and 2004) using LizardTech GeoExpress ver 7.0 software. NAIP imagery for 2009 covered the entire state of Idaho and was streamed into the project via the Idaho State University (ISU) GIS Training and Research Center (GIS TReC) website image service, removing the mosaic process for this image year. The imagery from 1954 was image to image co-registered to the 2004 NAIP imagery (the “gold standard” image for this study), using the ArcGIS 10.0 georectify tool. The “gold standard” image was the aerial image with the lowest root mean square error (RMSE) of horizontal positional accuracy. The remaining imagery (1992 and 2009) was tested for co-registration. Co-registration is the process by which the pixels of one image are aligned with the pixels of another so that specific geographic features appear within the correct, representative pixel. A final rectification permanently aligns the pixels of the images to the gold standard image. A first-order, or affine, transformation using nearest neighbor resampling was used as it reduces the likelihood that pixel values will change once the images are georectified. Higher order transformations may further reduce horizontal error but may also change the pixel values. Higher order transformations are typically used with images having inconsistent XY extent where greater warp/rubber sheeting is necessary for proper pixel alignment and reduced horizontal error. This process ensured good relative accuracy between images. Relative accuracy refers to the level of precision by which pixels of images are aligned relative to the “gold standard” image. Images for the later years (1992 and 2009) were tested for co-registration against the gold standard imagery (RMSE 0.03 and 0.22 respectively) and a final rectification was not necessary.

**Table 1. Root mean square error (RMSE) of all co-registered and co-registration tested imagery of the Big Desert, southeast Idaho for years 1954, 1992, 2009**

<u>Image Date</u>	<u>RMSE</u>
1954	17.3 m <sup>A</sup>
1992	0.03 m <sup>B</sup>
2009	0.22 m <sup>B</sup>

*A- imagery was rectified using nearest neighbor resampling*

*B- imagery was tested for co-registration but not rectified as the current level of co-registration was acceptable.*

*Laboratory and statistical analysis*

Heads-up digitizing was used with ArcGIS 10.0 software to create polygons around visible agricultural fields within each of the images. Polygon extents were limited to those areas visible in all images. For precise digitizing, 1992, 2004, and 2009 imagery were zoomed to an extent of 1:2,000 (where 1cm on the image is equivalent to 20m on the ground). The imagery from 1954 was digitized while zoomed to an extent of 1:60,000 (where 1cm on the image is equivalent to 600 m on the ground). The zoomed extents used (1:2,000 and 1:60,000) were chosen because they represent the extent before which imagery became too pixelated for precise digitizing while also optimizing visibility of the targets being digitized. Polygons were digitized for each year beginning with 2009 and working backward to 1954. The 2009 imagery was digitized first because it was hypothesized that, of all the imagery used for this study, it would have the greatest total area of irrigated agriculture.

Working chronologically backwards with the 2009 polygon feature class, polygons that were not fragmented in the previous year imagery (e.g., 2004) were removed so that each representative polygon layer accurately reflected irrigated agriculture present in that year. Moving backwards in time, there were instances that polygons were added rather than removed (as with the 1954 imagery) because the boundaries had faded so greatly that they were not previously visible in imagery for the more recent years (2004 and 2009). The goal for digitizing was to capture all visible boundaries within the imagery for irrigated agricultural lands, as it has been suggested that once an area has been converted from sagebrush-steppe rangelands to something else, it can never return to its original state (Seastedt et al. 2008). Polygon data were stored as feature classes in a personal geodatabase. If agricultural fields shared boundaries with neighboring fields (i.e., were only separated by a road), a single polygon was created around the outside perimeter of those fields. Patches of unconverted habitat within the extent of larger polygons were only accounted for if the area was consistent with the recommended minimum distance ( $\geq 18$ km) from lekking sites for migratory species of sage-grouse, such as those populations in the Big Desert study area (Connelly et al. 2000).

Polygons were digitized to extend only from the southeast to the east edge of the Big Desert (Figure 8), as preliminary visual analysis of the imagery suggested that the majority of conversion to irrigated agriculture surrounding the Big Desert occurred in this area. Polygons extended to the Snake River, as the purpose of the study was to examine agricultural development immediately surrounding the Big Desert.

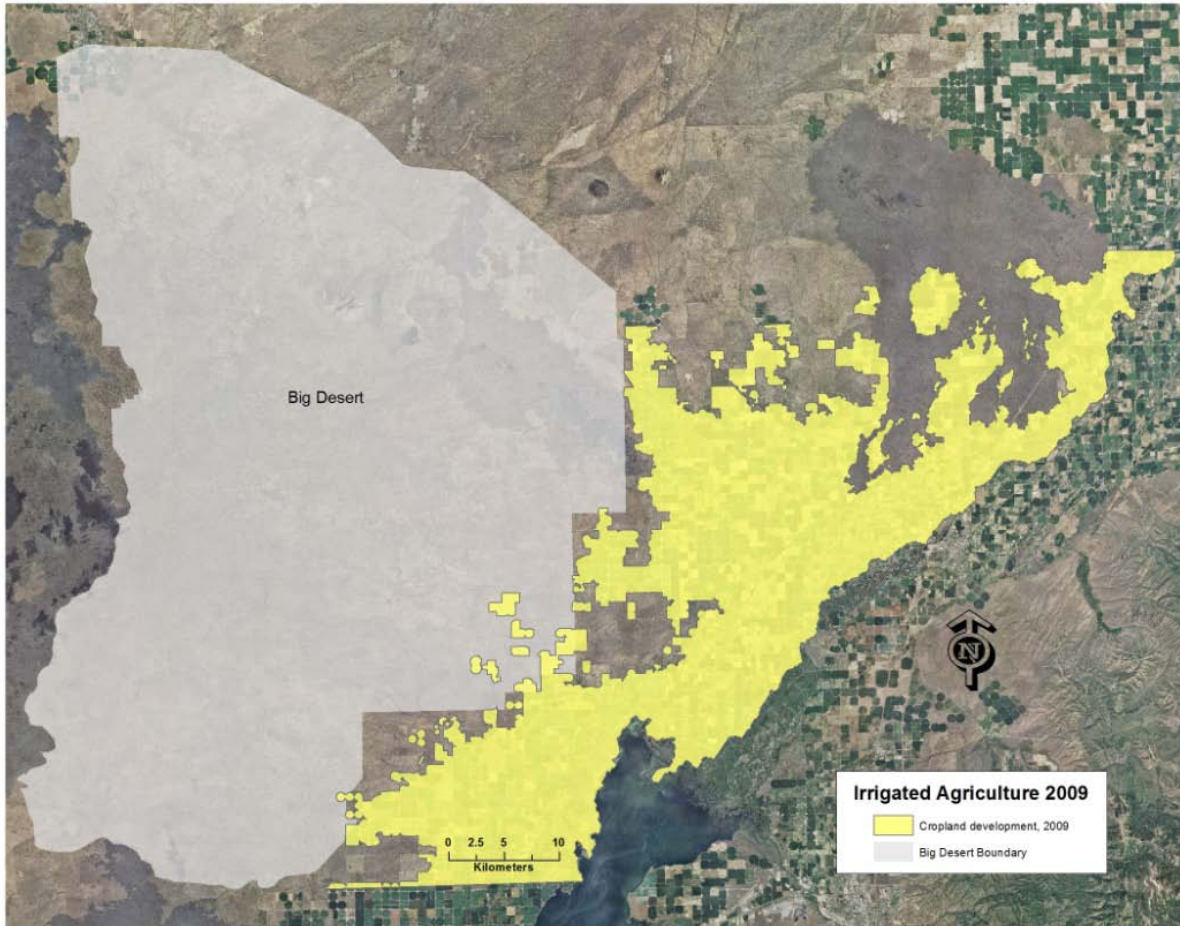


**Figure 8. Polygons of cropland development near the Big Desert, ID in 2009, extending as far north and south as the southeast boundary of the Big Desert, and to the Snake River.**

### *Geoprocessing*

A 6.9 km buffer was created around polygon extents for each year (1954, 1992, 2004, 2009) to allow for potential movements away from agricultural fields by synanthropic predators (domestic dogs and cats, red fox, and corvids) (Leu et al. 2008, Connelly et al. 2004, Knick and Connelly, 2011). Total area was calculated and compared for each year (1954, 1992, 2004, and 2009) for buffered and non-buffered polygon extents. Conversion to agriculture was recorded in hectares as well as a percent of overall change from 1954 as well as between years. Geoprocessing tasks (buffers) were documented and performed within the Model Builder application of ArcGIS 10.0 (Figure 9).

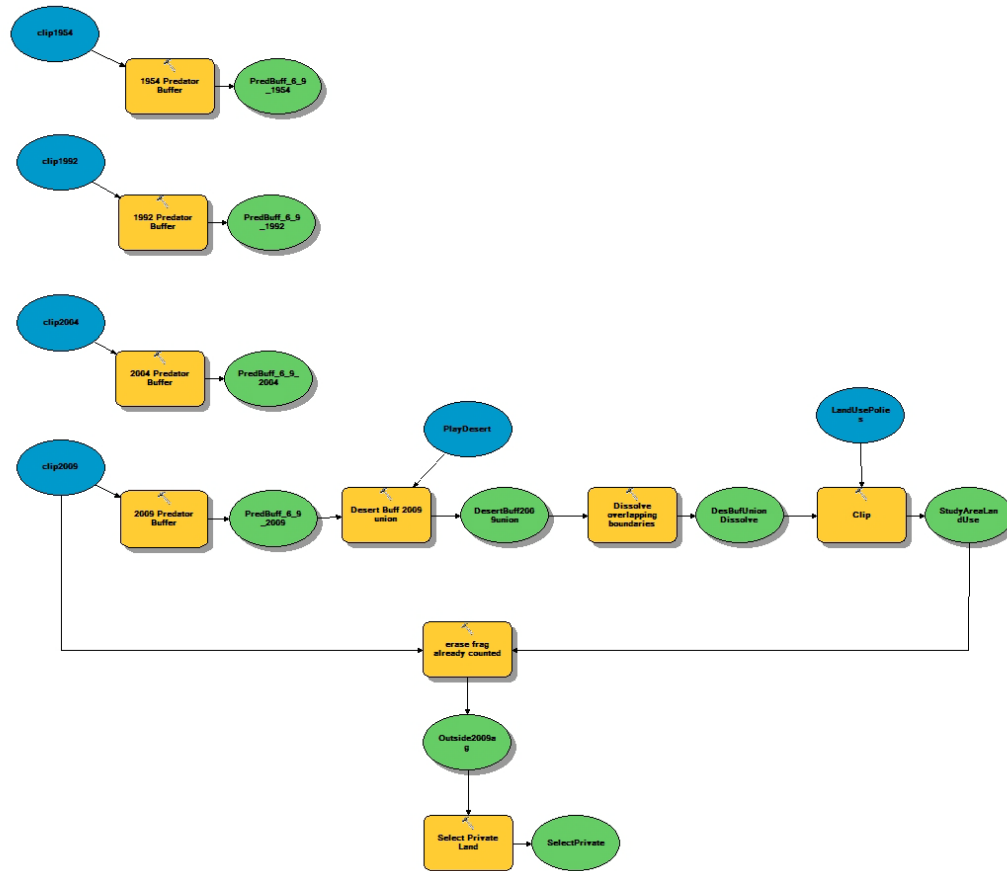


**Figure 9. Model Builder flow chart documenting geoprocessing performed in ArcGIS 10.0 to analyze total area of change between polygons representing cropland development in the Big Desert, Idaho between 1954 and 2009.**

A union was performed with the buffered polygon extent for 2009 and the Big Desert. Surface Management Agency (SMA) polygons (GIS data obtained at [www.insideidaho.org](http://www.insideidaho.org)) describing land ownership were clipped to the extent of the Big Desert study area. An erase function was performed to display those land ownership parcels within the Big Desert study area that had not been converted to irrigated agriculture as of 2009. A select function was then performed to display privately owned parcels that could be converted to irrigated agriculture. Visual analysis of the 2009 imagery was used to remove those polygons within the study area where conversion had already begun, but were not included in the study. These geoprocessing tasks were performed to indicate the potential for future habitat fragmentation through rangeland conversion to irrigated agriculture.

## RESULTS AND DISCUSSION

The year estimated to have the greatest total digitized area of irrigated agriculture was 2009 (95,210 ha or 20% of the study area). Estimated total area converted between 1954 and 2009 was 35,862 ha (Table 2), or a 60% increase from the total area present in 1954. A comparison of calculated areas between years suggested that the majority of conversion after 1954 occurred between 1954 and 1992 (51%), and much smaller percent increases from 1992 to 2004 (4%), and 2004 to 2009 (2%) equating to an approximate total increase of 6% between 1992 and 2009.

**Table 2: Total area of change in agricultural development in an area immediately adjacent to the south and east perimeter of the Big Desert, Idaho between 1954, 1992, 2004, and 2009.**

<b>Imagery</b>	<b>Total area in irrigated agriculture (ha)</b>	<b>Change in irrigated agriculture (ha)</b>	<b>Percent change relative to 1954</b>	<b>Total Estimated since 1954 (ha)</b>
<b>1954</b>	59374	59374	n/a	
<b>1992</b>	89409	30062	50 %	
<b>2004</b>	93152	3743	4 %	
<b>2009</b>	95210	2057	2 %	35862

When the 6.9 km synanthropic predation buffer was included around digitized polygon extents for each year (1954, 1992, 2004, and 2009), total area of estimated irrigated agricultural development between 1954 and 2009 increased from 35,862 ha to 42,311 ha (Table 4). This indicates that the area actually influenced is 15% greater than the area of irrigated agricultural development.

**Table 3: Total area of change in agricultural development in an area immediately adjacent to the south and east perimeter of the Big Desert, Idaho between 1954, 1992, 2004, and 2009 with a 6.9 km synanthropic predation buffer representing total area of influence.**

<b>Imagery</b>	<b>Total Area Hectares</b>	<b>Change in irrigated agriculture (ha)</b>	<b>Percent of total where total is 1954 imagery</b>	<b>Total estimated growth since 1954 (Hectares)</b>
<b>1954</b>	77305	77305	n/a	
<b>1992</b>	113660	36355	47 %	
<b>2004</b>	117511	3851	3 %	
<b>2009</b>	119616	2105	2 %	42311

To measure the potential for future fragmentation of sage-grouse habitat near the Big Desert, land use polygons were analyzed indicating an additional 27,781 ha of privately owned land could be converted to irrigated agriculture. With the current level of irrigated agricultural development, Big Desert sage-grouse populations can still use some centralized areas that are greater than 18 km away from the total area of influence (Figure 10). However, there are private lands within the study area that were not accounted for, as well as some areas that have not yet been developed (Figure 11).

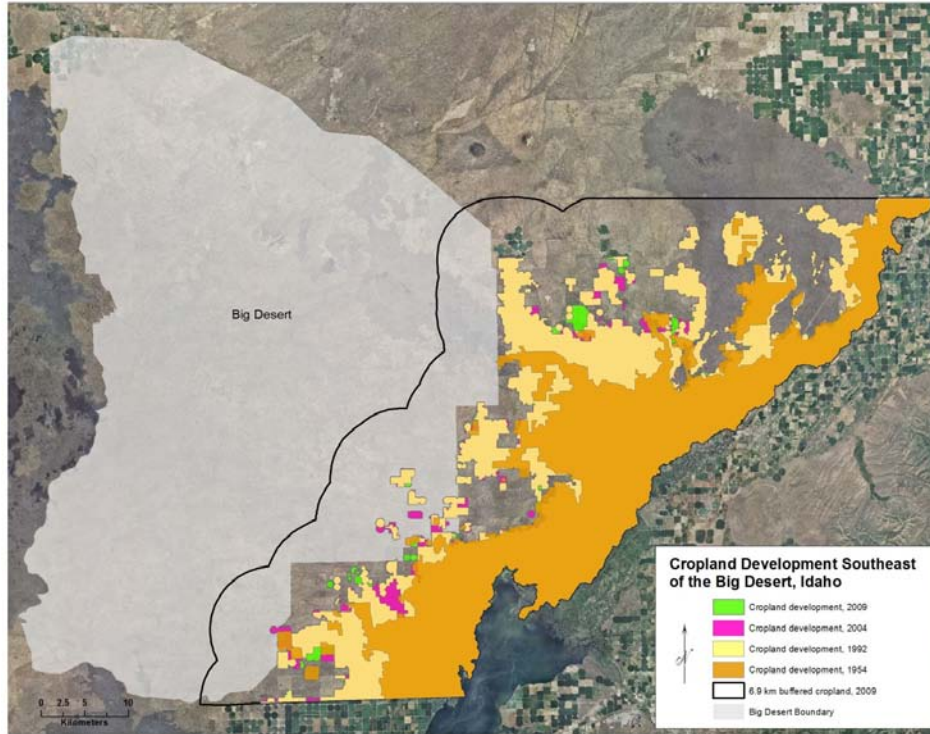


Figure 10. Irrigated agricultural development near the Big Desert, Idaho including a synanthropic predation buffer (6.9 km) showing total impact of agriculture on sage-grouse habitat.

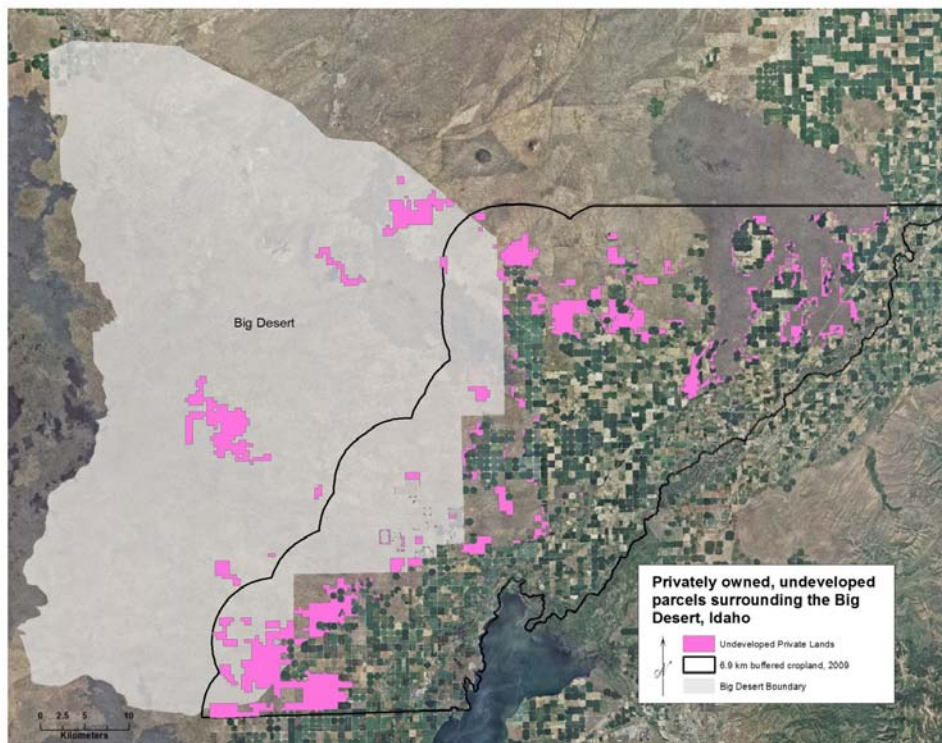


Figure 11. Potential irrigated agricultural development near the Big Desert, Idaho based on 2010 land ownership parcels ([www.insideidaho.org](http://www.insideidaho.org)) displaying privately owned lands that have not yet been converted to irrigated agriculture.

## **CONCLUSION**

The results of this study indicate the total area of land that has been converted from sagebrush-steppe rangelands to agriculture has increased since 1954. Comparison of converted areas from each year (1954, 1992, 2004, and 2009) indicate the majority of conversion occurred between 1954 and 1992 (~50%) with smaller increases in more recent years. These results correlate with agricultural development patterns along the Snake River Plain reported by Leonard et al. (2000) indicating a 10% increase in irrigated agriculture along the Snake River Plain between 1975 and 1985. Johnson et al. (2011) argued the majority of conversion of sagebrush-steppe rangelands to irrigated agriculture occurred during the first half of the 20<sup>th</sup> century. This could mean that even imagery as early as 1954 may not accurately reflect the study area prior to significant sagebrush-steppe rangeland conversion to irrigated agriculture.

Though the Big Desert Sage-Grouse Local Working Group (BDSGLWG) believes there is a limited possibility of converting sagebrush-steppe to agricultural production, there is presently an additional 27,781 ha of undeveloped, privately owned land within the Big Desert study area that, if developed, could further fragment sage-grouse habitat (Connelly et al. 2000). Current conservation measures seem to revolve around restoring sage-grouse habitat through sagebrush restoration programs such as the Conservation Reserve Program (CRP). The CRP program allows agricultural lands that have been converted from sagebrush-steppe to be planted with perennial grasses, forbs, and sagebrush (Schroeder and Vander Haegan 2011, BDSGLWG 2010, Pyke 2011). As a result, Schroeder et al. (2011) reported success in sage-grouse response to CRP lands in Washington with increases in observed nesting sites. Conclusions cannot be drawn from the results presented in this research as to the effect CRP land has had on Big Desert sage-grouse populations. However, results indicate that presently, Big Desert sage-grouse populations still have use of some centralized areas that are greater than 18 km away from the total area influenced by irrigated agricultural development.

## **ACKNOWLEDGEMENTS**

This study was made possible by a grant from the National Aeronautics and Space Administration Goddard Space Flight Center (NNX08AO90G). Idaho State University would also like to acknowledge the Idaho Delegation for their assistance in obtaining this grant.

## **LITERATURE CITED**

- Aldridge, C.L., 2008. Range-wide Patterns of Greater Sage-grouse Persistence. *Diversity and Distributions*. 14: 983-994
- Aldridge, C.L., and R.M. Brigham, 2003. Distribution, Status and Abundance of Greater Sage-Grouse, *Centrocercus urophasianus*, in Canada. *Canadian Field Naturalist*. 117: 25-34
- Anderson, J., J. Tibbits, and K.T. Weber, 2008. Range Vegetation Assessment in the Big Desert, Upper Snake River Plain, Idaho 2007. Pages 16-26 in K. T. Weber (Ed.), Final Report: Impact of Temporal Landcover Changes in Southeastern Idaho Rangelands (NNG05GB05G). 345 pp
- Beck, J.L., D.L. Mitchell, and B.D. Maxfield, 2003. Changes in the Distribution and Status of Sage-grouse in Utah. *Western North American Naturalist* 63:203-214

- Big Desert Sage-grouse Local Working Group (BDSGLWG). 2010. Sage-grouse Conservation Plan. Idaho Fish and Game. 137 pp. URL = [http://fishandgame.idaho.gov/hunt/grouse/conserves\\_plan/bigDesert.pdf](http://fishandgame.idaho.gov/hunt/grouse/conserves_plan/bigDesert.pdf). visited May 24, 2010
- Beck, T.D.I., 1977. Sage Grouse Flock Characteristics and Habitat Selection in Winter. *Journal of Wildlife Management* 41:18-26
- Braun, C.E., 1995. Distribution and Status of Sage Grouse in Colorado. *Prairie Naturalist* 27:1-9
- Browder, S.F., D.H. Johnson, and I.J. Ball, 2002. Assemblages of Breeding Birds as Indicators of Grassland Condition. *Ecological Indicators* 2: 257-270
- Bunnell, K.D., 2000. Ecological Factors Limiting Sage Grouse Recovery and Expansion in Strawberry Valley, Utah. Thesis, Brigham Young University, Provo, USA
- Connelly, J.W., and C.E. Braun, 1997. Long-term Changes in Sage Grouse *Centrocercus urophasianus* Populations in Western North America. *Wildlife Biology* 3: 229-234
- Connelly, J.W., C.A. Hagen, M.A. Schroeder, 2011. Characteristics and Dynamics of Greater Sage-Grouse Populations. In: Knick, S. T., and J. W. Connelly (Ed.). Greater Sage-grouse: Ecology and Conservation of a Landscape Species and its Habitats. Studies in Avian Biology Series, University of California Press, Berkeley, CA. 38:672 pp.
- Connelly, J.W., S.T. Knick, M.A. Schroeder, and S.J. Stiver, 2004. Conservation Assessment of Greater Sage-grouse and Sagebrush Habitats. Western Association of Fish and Wildlife Agencies. Unpublished Report. Cheyenne, Wyoming. 610 pp.
- Connelly, J.W., A.D. Apa, R.B. Smith, and K.P. Reese, 2000<sup>a</sup>. Effects of Predation and Hunting on Adult Sage-grouse *Centrocercus urophasianus* in Idaho. *Wildlife Biology* 6:227-232
- Connelly, J.W., K.P. Reese, R.A. Fischer and W.L. Wakkinen, 2000<sup>b</sup>. Response of a Sage Grouse Breeding Population to Fire in Southeastern Idaho. *Wildlife Society Bulletin* 28: 90-96
- Connelly, J.W., M.A. Schroeder, A.R. Sands and C.E. Braun, 2000: Guidelines to Manage Sage Grouse Populations and their Habitats. *Wildlife Society Bulletin* 28: 967-985
- Dalke, P.D., D.B. Pyrah, D.C. Stanton, J.E. Crawford, and E.F. Schlatterer, 1963. Ecology, Productivity, and Management of Sage Grouse in Idaho. *Journal of Wildlife Management* 27:811-841
- Evans, R.G., 2001. Center Pivot Irrigation (Draft). Agriculture Systems Research Unit, Northern Plains Agricultural Research Laboratory, USDA-Agriculture Research Service. Sidney MT 59270
- Federal Register, 2010. Endangered and Threatened Wildlife and Plants; 12-Month Findings for Petitions to List the Greater Sage-Grouse (*Centrocercus urophasianus*) as Threatened or Endangered. Department

of Interior, Fish and Wildlife Service 50 CFR Part 17. 107 pp. URL = <http://www.fws.gov/mountain-prairie/species/birds/sagegrouse/FR03052010.pdf>, visited May 12 2010

Fichter, E. and R. Williams, 1967. Distribution and Status of the Red Fox in Idaho. *Journal of Mammalogy* 48:219-230

Frémont, J.C., 1845. Report of the Exploring Expedition to the Rocky Mountains in the Year 1842, and to Oregon and Northern California in the Years 1843-44. Gales and Seaton, Washington, D.C. 20 pages  
Department of the Interior: Fish and Wildlife Service

Galvin, K.A., R.S. Reid, R.H. Behnke, N.T. Hobbs, 2008. Fragmentation of Semiarid and Arid Landscapes: Consequences for Human and Natural Systems. Dordrecht (The Netherlands): Springer. 411 pp.

Garton, E.O., J.W. Connelly, J.S. Horne, C.A. Hagen, A. Moser, and M. Schroeder, 2011. Greater Sage-Grouse Population Dynamics and Probability of Persistence In: Knick, S. T., and J. W. Connelly (Ed.). Greater Sage-grouse: Ecology and Conservation of a Landscape Species and its Habitats. Studies in Avian Biology Series, University of California Press, Berkeley, CA. 38:672 pp.

Gokhale, B. and K.T. Weber, 2010. Correlation between MODIS LAI, GPP, PsnNet, and FPAR and Vegetation Characteristics of Three Sagebrush-Steppe Sites in Southeastern Idaho. Pages 75-86 in K. T. Weber and K. Davis (Eds.), Final Report: Forecasting Rangeland Condition with GIS in Southeastern Idaho (NNG06GD82G). 189 pp

Gregg, M.A., 1991. Use and Selection of Nesting Habitat by Sage Grouse in Oregon. Thesis, Oregon State University, Corvallis, USA

Hagen, C.A., 2011. Predation on Greater Sage-Grouse: Facts, Processes, and Effects. In Knick and Connelly (Ed.). Greater Sage-grouse: Ecology and Conservation of a Landscape Species and its Habitats. Studies in Avian Biology Series, University of California Press, Berkeley, CA. 38:672 pp

Hansen, A.J., R.L. Knight, J.M. Marzluff, S. Powell, K. Brown, P.H. Gude, and K. Jones, 2005. Effects of Exurban Development on Biodiversity: Patterns, Mechanisms, and Research Needs. *Ecological Applications* 15: 1893-1905

Hironaka, M., M.A. Fosberg, and A.H. Winward, 1983. Sagebrush-grass Habitat Types of Southern Idaho. University of Idaho Forest, Wildlife, and Range Experiment Station Bulletin, Moscow, ID 35

Johnson, D.H., M.J. Holloran, J.W. Connelly, S.E. Hanser, C.L. Amundson, and S.T. Knick, 2011. Influences of Environmental and Anthropogenic Features On Greater Sage-Grouse Populations, 1997-2007. In: Knick, S. T., and J. W. Connelly (Ed.). Greater Sage-grouse: Ecology and Conservation of a Landscape Species and its Habitats. Studies in Avian Biology Series, University of California Press, Berkeley, CA. 38:672 pp

- Knick, S.T., 2011. Principal Federal Legislation and Current Management of Sagebrush Habitats: Implications for Conservation. In: Knick, S. T., and J. W. Connelly (Ed.). Greater Sage-grouse: Ecology and Conservation of a Landscape Species and its Habitats. Studies in Avian Biology Series, University of California Press, Berkeley, CA. 38:672 pp
- Knick, S.T. and J.W. Connelly, 2011. Greater Sage-Grouse and Sagebrush: An Introduction to the Landscape. In: Knick, S. T., and J. W. Connelly (Ed.). Greater Sage-grouse: Ecology and Conservation of a Landscape Species and its Habitats. Studies in Avian Biology Series, University of California Press, Berkeley, CA. 38:672 pp
- Knick, S.T., S.E. Hanser, R.F. Miller, D.A. Pyke, M.J. Wisdom, S.P. Finn, T. Rinkes, and C.J. Henny, 2011. Ecological Influence and Pathways of Land Use in Sagebrush. In: Knick, S. T., and J. W. Connelly (Ed.). Greater Sage-grouse: Ecology and Conservation of a Landscape Species and its Habitats. Studies in Avian Biology Series, University of California Press, Berkeley, CA. 38:672 pp
- Knick, S.T., D.S. Dobkin, J.T. Rotenberry, M.A. Schroeder, W.M. Vander Haegen, and C. van Riper III, 2003. Teetering on the Edge or Too Late? Conservation and Research Issues for Avifauna of Sagebrush Habitats. *The Condor* 105: 611-634
- Leonard, K.M., K.P. Reese, and J.W. Connelly, 2000. Distribution, Movements and Habitats of Sage Grouse *Centrocercus urophasianus* on the Upper Snake River Plain of Idaho. *Wildlife Biology* 6: 265-270
- Leu, M., S.E. Hanser, and S.T. Knick, 2008. The Human Footprint in the West: A Large-scale Analysis of Anthropogenic Impacts. *Ecological Applications* 18:1119–1139
- McBride, R., N.R. French, A.H. Dahl, and J.E. Detmer, 1978. Vegetation Types and Surface Soils of the Idaho National Engineering Laboratory Site. IDO-12084. National Technical Information Service, Springfield, Virginia, USA
- Moynahan, B.J., M.S. Lindberg, and J.W. Thomas, 2006. Factors Contributing to Process Variance in Annual Survival of Female Greater Sage-Grouse in Montana. *Ecological Applications* 16:1529–1538
- Naugle, D.E., C.L. Aldridge, B.L. Walker, T.E. Cornish, B.J. Moynahan, M.J. Holloran, K. Brown, G.D. Johnson, E.T. Schmidtman, R.T. Mayer, C.Y. Kato, M.R. Matchett, T.J. Christiansen, W.E. Cook, T. Creekmore, R.D. Falise, E.T. Rinkes, and M.S. Boyce, 2004. West Nile Virus: Pending Crisis for Greater Sage-Grouse. *Ecology Letters* 7: 704–713
- Psatschniak-Arts, M., R.G. Clark, and F. Messier, 1998. Duck Nesting Success in a Fragmented Prairie Landscape: Is Edge Effect Important? *Biological Conservation* 85: 55-62

Schroeder, M.A., J.R. Young, and C.E. Braun, 1999. Sage-grouse (*Centrocercus urophasianus*). A. Poole and F. Gill, editors. The Birds of North America, Number 425. The Academy of Natural Sciences, Philadelphia, Pennsylvania; The American Ornithologists' Union, Washington, D.C., USA

Schroeder, M.A., C.L. Aldridge, A.D. Apa, J.R. Bohne, C.E. Braun, S.D. Bunnell, J.W. Connelly, P.A. Deibert, S.C. Gardner, M.A. Hilliard, G.D. Kobriger, C.W. McCarthy, J.J. McCarthy, D.L. Mitchell, E.V. Rickerson, and S.J. Stiver, 2004. Distribution of Sage-grouse in North America. *Condor* 106:363-373

Seastedt, T.R., R.J. Hobbs, and K.N. Suding, 2008. Management of Novel Ecosystems: Are Novel Approaches Required? *Frontiers in Ecology and the Environment*. 6: 547-553

Smith, S.D., T.E. Huxman, S.E. Zitzer, T.N. Charlet, D.C. Housman, J.S. Coleman, L.K. Fenstermaker, J.R. Seemann and R.S. Novak, 2000. Elevated CO<sub>2</sub> Increases Productivity and Invasive Species Success in an Arid Ecosystem. *Nature* 408: 79-82

Tewksbury, J.J., A.E. Black, N. Nur, V.A. Saab, B.D. Logan, and D.S. Dobkin, 2002. Effects of Anthropogenic Fragmentation and Livestock Grazing on Western Riparian Bird Communities. *Studies in Avian Biology* 25: 158-202

Vitousek, P.M., H.A. Mooney, J. Lubchenco and J.M. Melillo, 1997. Human Domination of Earth's Ecosystem. *Science* 277: 494-499

Weber, K.T. and J.B. McMahan, 2003. Field Collection of Fuel Load and Vegetation Characteristics for Wildfire Risk Assessment Modeling: 2002 Field Sampling Report. In: K. T. Weber (Ed.). Final Report: Wildfire Effects on Rangeland Ecosystems and Livestock Grazing in Idaho. 209 pp

Weber, K.T., B.J. McMahan, and G. Russell, 2003. Effect of Livestock Grazing and Fire History on Fuel Load in Sagebrush-Steppe Rangelands. In: K. T. Weber (Ed.). Final report: Wildfire Effects on Rangeland Ecosystems and Livestock Grazing in Idaho. 209 pp.

Ypsilantis, W. USDI, Bureau of Land management, National Science & Technology Center. Crystal Fire Burn Area Rehabilitation Plan

**Recommended citation style:**

Hanson, D. and K. T. Weber, 2011. Quantifying Habitat Fragmentation in the Big Desert, Idaho. Pages 235-252 in K. T. Weber and K. Davis (Eds.), Final Report: Assessing Post-Fire Recovery of Sagebrush-Steppe Rangelands in Southeastern Idaho. 252 pp.